A Platinum Open Access Journal for Organic Chemistry

Review

Free to Authors and Readers | DOAJ Seal | *Arkivoc* **2026** (1) 202612605

Green synthesis of anticancer heterocycles: sustainable methods, SAR, and biological evaluation

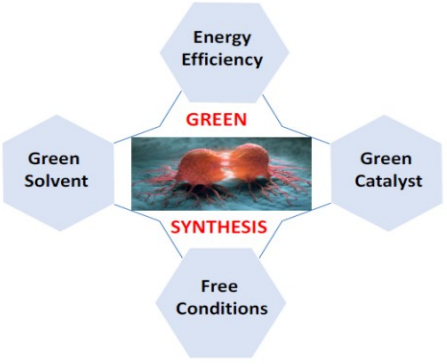
Mohamed Abd-Elmonem[a], Ramadan Ahmed Mekheimer[a], Mohamed Hisham[b], Afaf Mohamed Abdel-Hameed[a], and Kamal Usef Sadek[a]*

[a] *Department of Chemistry, Faculty of Science, Minia University, Minia 61519, Egypt*
[b] *Pharmaceutical Chemistry Department, Faculty of Pharmacy, Deraya University, New- Minia, Egypt*
Email: kusadek@yahoo.com

Received 05-07-2026 **Accepted** 09-09-2026 **Published on line** 09-21-2026

Abstract

Cancer continues to be a leading global health challenge, requiring more effective treatments with fewer side effects. Traditional chemotherapy often faces limitations due to high toxicity and emerging drug resistance. Consequently, there is a significant shift in medicinal chemistry toward utilizing green chemistry principles to synthesize heterocyclic compounds with anti-cancer potential. This approach prioritizes environmental sustainability alongside drug selectivity and efficacy. This review examines recent progress in green synthetic methodologies for anti-cancer heterocycles, emphasizing innovative technologies that reduce environmental impact while improving drug performance. Furthermore, it explores structure-activity relationships (SAR) and molecular docking studies to provide insights into optimizing drug design for better clinical outcomes. By integrating sustainable practices into drug discovery, this research aims to pave the way for safer, next-generation cancer therapies. Overall, the analysis suggests an increasing integration of sustainable synthesis and structure-guided molecular design to produce chemically efficient and biologically promising anticancer candidates.



Keywords: Anti-Cancer Heterocycles; Green Strategies; Structure-Activity Relationships; Drug Discovery; Molecular Docking; Medicinal Chemistry

Cite as *Arkivoc* **2026** (1) 202612605
DOI: https://doi.org/10.24820/ark.5550190.p012.605 ©**AUTHOR(S)**

Table of Contents

1. Introduction
2. Five-membered Nitrogen Heterocycles
    2.1. Pyrroles
    2.2. Indoles synthesis
    2.3. Spirooxindoles synthesis
    2.4. Pyrazoles synthesis
    2.5. Imidazoles synthesis
    2.6. Benzimidazoles synthesis
    2.7. Triazoles synthesis
    2.8. Benzotriazole synthesis
3. Six-membered Nitrogen Heterocycles
    3.1. Pyridines synthesis
    3.2. Quinolines synthesis
    3.3. Cinnolines synthesis
    3.4. Phthalazines synthesis
4. Oxygen, Sulphur and Nitrogen Heterocycles
    4.1. Furans
    4.2. Oxazoles
    4.3. Benzisoxazoline
    4.4. Benzothiazole synthesis
    4.5. Coumarines synthesis
5. Hybrid Heterocycles
    5.1. Hybrid molecules-based indole moiety
    5.2. Hybrid molecules-based pyrazole moiety
    5.3. Hybrid molecules-based triazole moiety
    5.4. Hybrid molecules-based oxadiazole moiety
    5.5. Hybrid molecules-based thiadiazole moiety
    5.6. Hybrid molecules-based quinoline moiety
    5.7. Hybrid molecules-based pyrimidine moiety
    5.8. Hybrid molecules-based naphthalimide moiety
    5.9. Hybrid molecules-based phthalazine moiety
6. Fused Heterocycles
    6.1. Five-five fused membered heterocycles
        6.1.1. Pyrazolo[4,3-b]indoles synthesis
        6.1.2. Imidazo-triazoles synthesis
    6.2. Five-six fused membered heterocycles
        6.2.1. Pyrrolo-phenanthroline synthesis
        6.2.2. Pyrano-pyrazoles synthesis
        6.2.3. Pyrido-carbazole synthesis
        6.2.4. Pyrido-pyrazole synthesis
        6.2.5. Imidazo-pyridines synthesis
        6.2.6. Xanthine-pyrimidines synthesis

 ©AUTHOR(S)

6.2.7. Pyrazolo-pyrimidines synthesis
6.2.8. Indeno-quinoxalines synthesis
6.2.9. Triazolo-triazines synthesis
6.2.10. Thiazolo-pyridazines synthesis
6.3. Six-six fused membered heterocycles
6.3.1. Xanthenes synthesis
6.3.2. Pyrano-pyrimidines synthesis
6.3.3. Pyrido-pyrimidines synthesis
6.3.4. Pyrido-tetrazines, Pyrido-triazepine and Pyrido-tetrazepines synthesis
Conclusions
References

1. Introduction

The synthesis of biologically important heterocycles has been a focal point in chemistry for many years. Nitrogen, oxygen, and sulfur heterocycles, whether as single or fused rings, form the structural basis for numerous bioactive compounds and pharmaceuticals. Recently, increasing concern over environmental pollution associated with organic synthesis has spurred efforts among scientists to adopt eco-friendly techniques in the synthesis of heterocycles. Green chemistry is defined as the implementation of a set of guidelines designed to reduce or eliminate the use of hazardous substances throughout the design, manufacture and application of chemical products. A specific domain of synthesizing nitrogen, oxygen and sulfur heterocycles sustainable methodologies are being crucial in the earliest stages of drug design. Developing cost-effective and environmentally friendly reaction systems has become one of the essential topics of modern synthetic chemistry.[1–4] Research focused on using green solvents, solventless reactions and green catalysts. In the context of alternative energy, sources refer to uncongenial activation methods such as microwave irradiation, ultra-sonication, mechanochemical, grinding and visible light will enhance reaction efficiency and reduce environmental footprint. To evaluate the success of these green strategies, medicinal chemistry rely on quantitate metrics as Atom-Economy, E-factor, and EcoScale.

Cancer, a highly complicated disease identified by uncontrolled cell proliferation and tumor formation caused by genetic changes and DNA damage,[5] increases worldwide dramatically. According to the World Health Organization (WHO), the overall count of cancer cases during 2022 was about 20 million, with a total number of deaths reaching 9.7 million. Importantly, the number of people alive within five years of a cancer diagnosis estimated at about 53.5 million globally. In addition, according to (WHO) one-third of three people become a victim of cancer during their lifetime, even in many highly developed countries. Moreover, higher than 13% of all fatalities globally yearly are caused by cancer, making it the second cause of death globally.[6] Lung cancer 18.7 %, is the most prevalent malignancy linked to cancer death, colon (9.2%), liver (7.8 %), stomach (6.8 %), and prostate (3.80%).

Although progress has been made in the green synthesis of anticancer heterocycles[7,8] comprehensive reviews that also examine their mode of action, cytotoxicity, and molecular docking remained limited.
Because the anticancer data summarized in this review were generated in independent studies using different cell lines, assay formats, exposure times, and experimental conditions, IC_{50} values are interpreted primarily within each original study rather than as directly interchangeable measures across studies. Where matched non-cancerous cell data are available, the selectivity index (SI) is calculated as IC_{50} in the normal cell line divided by

 ©AUTHOR(S)

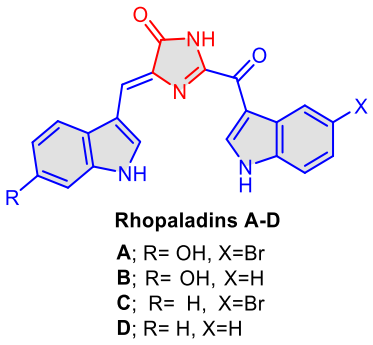
IC_{50} in the cancer cell line; values above 1 indicate preferential activity toward the cancer cells, whereas values close to 1 indicate a limited in vitro therapeutic window. Comparisons with clinically used reference agents such as cisplatin, doxorubicin, and 5-fluorouracil are emphasized only when they were evaluated under the same reported assay conditions. Such in vitro comparisons are pharmacological benchmarks and should not be interpreted as evidence of clinical equivalence, achievable human exposure, or therapeutic superiority.

2. Five-membered Nitrogen Heterocycles

2.1. Pyrroles

Pyrroles have a great deal of interest in areas linked to natural and biologically relevant heterocycles. The pyrrole ring system represents the core in scaffolds such as porphyrins, coenzymes, pigments, and alkaloids.[9–11] In spite of the several methods for the synthesis of derivatives,[12–15] the Paal-Knorr[16,17] synthesis of such scaffold remains the most reliable one.

Cervical cancer is threatening health and ranks fourth reason among women's deaths.[18] According to reports, marine alkaloids rhopaladins A-D (Figure 1) have potent cytotoxicity against human cancer cell lines.



Rhopaladins A-D

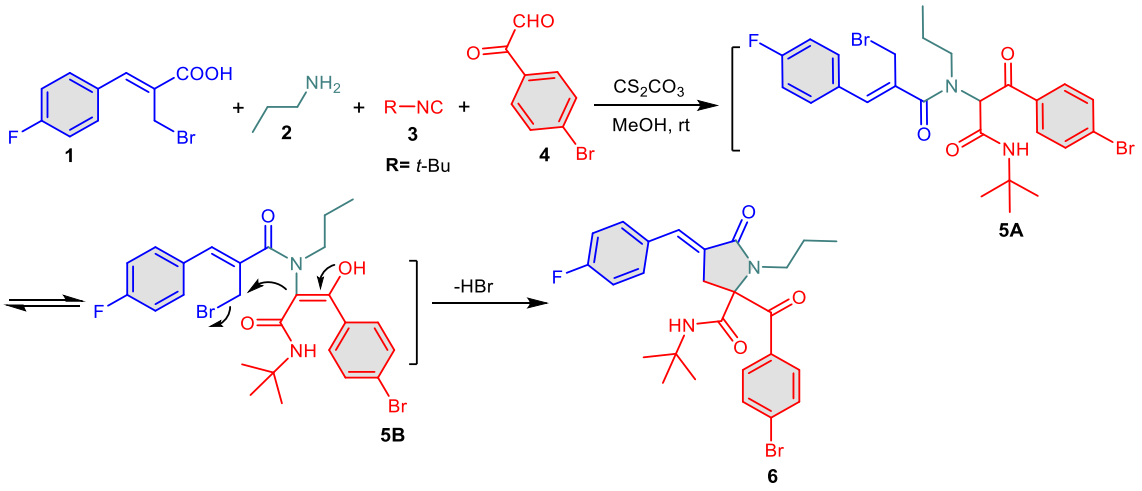
A; R= OH, X=Br
B; R= OH, X=H
C; R= H, X=Br
D; R= H, X=H

Figure 1. Structure of marine alkaloids rhopaladins **A-D**.

According to the structure-activity relationship (SAR) and because of the privileged profile of rhopaladins, Zeng and co-authors[19] have developed an efficient synthesis for new rhopaladin's analogue (*E*)-2-(4-bromobenzoyl)-*N*-(*tert*-butyl)-4-(4-fluorobenzylidene)-5-oxo-1-propylpyrrolidine-2-carboxamide (**6**) as illustrated in Scheme 1. To evaluate the greens of such reaction, its atom economy was estimated which revealed a value of 99.8 %. This indicating that almost all reactants incorporated into the product. The E-Factor calculated to be 0.16 revealing the environmental impact of the reaction.

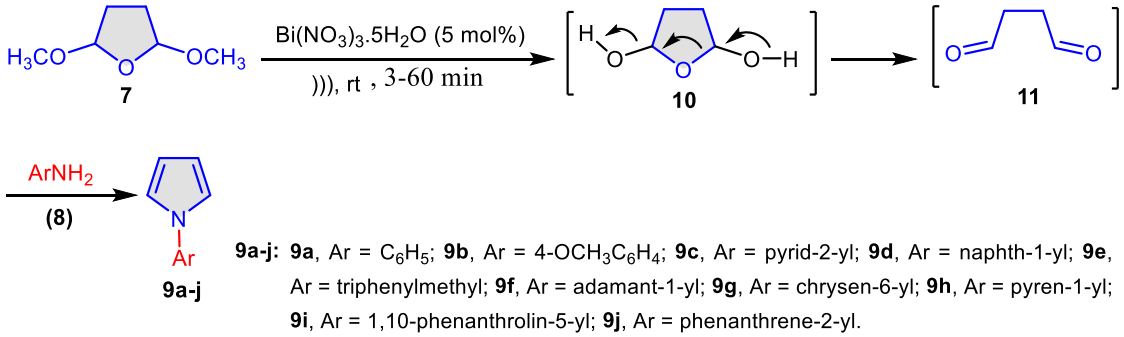
This compound was evaluated for its antiproliferative effects against HeLa cervical cancer cells and showed a time-dependent decrease in IC_{50} from 59.56 to 39.64 and 24.23 µmol/L after 24, 48, and 72 h, respectively. At the matched 24-h time point, the IC_{50} toward non-cancerous LO2 cells was 235.6 µmol/L, giving an SI of 3.96 (235.6/59.56). This approximately fourfold differential supports preferential activity toward HeLa cells under these conditions. The LO2 IC_{50} was also higher than that reported for cisplatin (21.32 µmol/L), indicating lower cytotoxicity toward this normal hepatic cell line in the same study; however, these in vitro findings should not be interpreted as evidence of clinical superiority.

 ©**AUTHOR(S)**



Scheme 1. Synthesis of (*E*)-2-(4-bromobenzoyl)-*N*-(*tert*-butyl)-4-(4-fluorobenzylidene)-5-oxo-1-propylpyrrolidine-2-carboxamide (**6**).

Less nucleophilic polyaromatic amines were used in a unique green synthesis of *N*-substituted pyrroles **9a–j**, as reported by Banik and co-authors[20] by reacting 2,5-dimethoxytetrahydrofurans (**7**) with a diversity of amines **8** following ultrasound-assisted waves utilizing bismuth nitrate pentahydrate [$Bi(NO_3)_3.5H_2O$] as eco-friendly catalyst under solvent free conditions at ambient temperature. Such reaction conditions offered excellent yields in short reaction time (Scheme 2). As well, the reaction possess estimated Atom Economy 63.56 as well as E-Factor equals 0.57. This reflects the efficiency of this protocol in the synthesis of diversity pyrrole derivatives through a green and environmentally friendly technique.



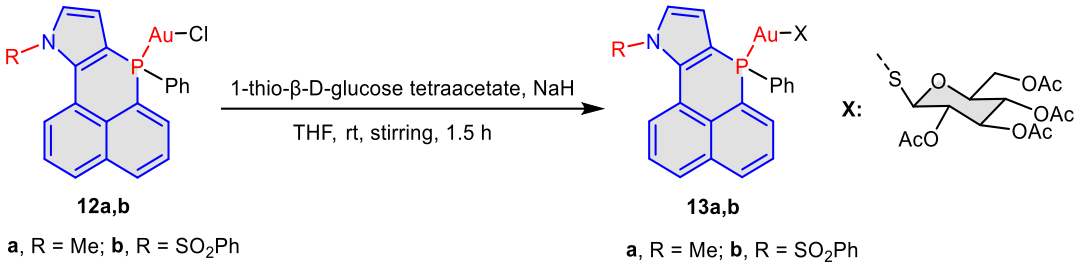
Scheme 2. Synthesis of *N*-substituted pyrroles **9a–j**.

Biological evaluation of these compounds across a panel of cancer cell lines (HepG2, HT-29, Caco-2 , Hela and NIH_3T_3) identified compounds **9h** and **9i** as highly potent, with IC_{50} values below 5 µM in specific instances, revaling the efficacy of 5-fluorouracil and cisplatin. Mechanistic investigations revealed that these pyrrole derivatives do not induce traditional apopotic characteristics like Caspase 3/7 activity or DNA fragmentation, suggesting a non-apopotic pathway for reducing cell viability.

Pyrrole-based gold complexes developed to target glioblastoma multiforme (GBM), the most aggressive adult brain tumor.[21] The synthesis of pyrrole-phosphaphenalene gold complexes bearing thio-sugar substituents **13a,b** demonstrates the potential of organometallic heterocycles. Romero-Nieto and co-authors[22] developed a synthesis of modified pyrrole-phosphaphenalene gold complexes bearing thio-sugar substituent **13a** and **13b**

 ©**AUTHOR(S)**

starting from chloro derivatives **12a** and **12b** and their activity against brain cancer (Scheme 3). Compound 13a exhibited IC_{50} values as low as 0.73 µM against NCH82 glioblastoma cells, representing a significant improvrment over traditional thiophene-based analogs **14a,b** (Figure 2). This enhanced activity is attributed to the inclusion of the thio-sugar scaffold, which improves the drug's bioactivity and perhaps its transport across biological membrane. Meanwhile the chlorine atom at the gold metal replaced by thio-sugar scaffold increases drug bioactivity remarkably.



Scheme 3. Synthesis of pyrrole-phosphaphenalene gold complexes bearing thio-sugar substituent **13a**,**b**.

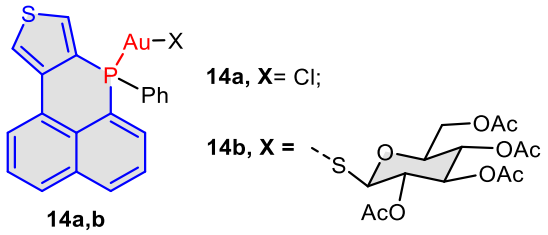
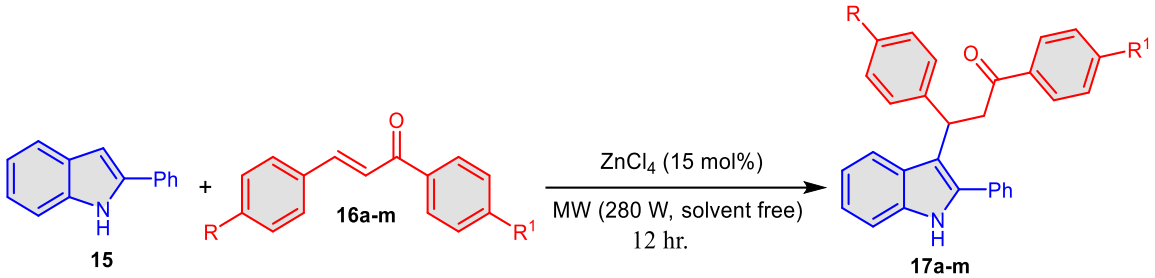


Figure 2. Thiophene-based analogs **14a,b**.

2.2. Indoles synthesis

Indoles considered a privileged scaffold in drug discovery due to their ability mimic biological indoles like tryptophan and serotonin. A recent study concerning the microwave-assisted synthesis of 3-(3-oxoaryl)indole derivatives **17a-m** through solventless reactions of 2-phenylindole (**15**) with chalcone **16a-m** catalyzed by ZnCl4 (15 mol%) under microwave-controlled heating (Scheme 4).[23] These compounds target the colchicine-binding site of tubulin, a critical protein for cell division. Molecular docking studies of the most potent analogs **17c,j** showed higher docking affinities (-10.4- 9.9 Kcal/mol.) than standard tubulin inhibitors. The binding site analysis revealed that the indole NH group forms essential hydrogen bonds with the THR 179 residue, while the phenyl rings engage in π-interactions with LEU 248 and LYS254 (Figures 3 and 4).

 ©**AUTHOR(S)**



16,17a-m: **a**, R= R^1= H; **b**, R= Br, R^1= H; **c**, R= F, R^1= H; **d**, R= Cl, R^1= H; **e**, R= CF_3, R^1= H; **f**, R= NO_2, R^1= H; **g**, R= OCH_3, R^1= H; **h**, R= CH_3, R^1= H; **i**, R= H, R^1= Cl; **j**, R= H, R^1= F; **k**, R= H, R^1=NO_2; **l**, R = H, R^1= OCH_3; **m**, R = H, R^1= CH_3.

Scheme 4. Microwave-assisted reaction for the synthesis of indole derivatives **17a-m**.

The docking protocol involves a comparison between the conformation of crystallographic and docking structure of colchicine into the tubulin receptor as presented in Figure 5.

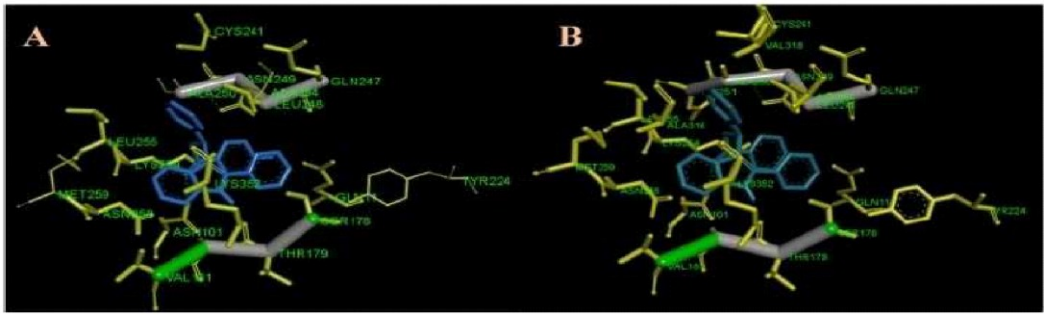


Figure 3. Docking interaction between compounds **17c** and **17j** at the tubulin receptor's colchicine binding site. Reproduced with permission from Ref.;[23] Copyright 2019; Wiley.

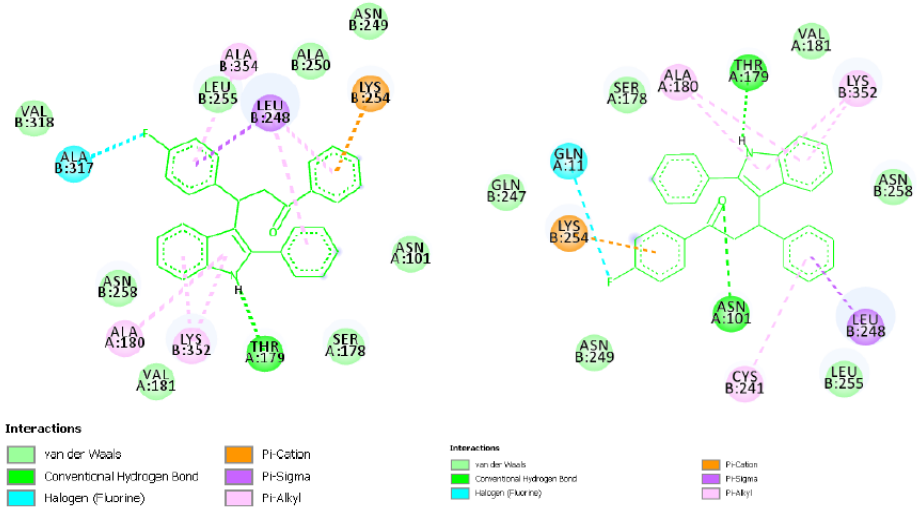


Figure 4. 2D interaction maps of compounds **17c** and **17j** with tubulin receptor. Reproduced with permission from Ref.;[23] Copyright 2019; Wiley.

 ©**AUTHOR(S)**

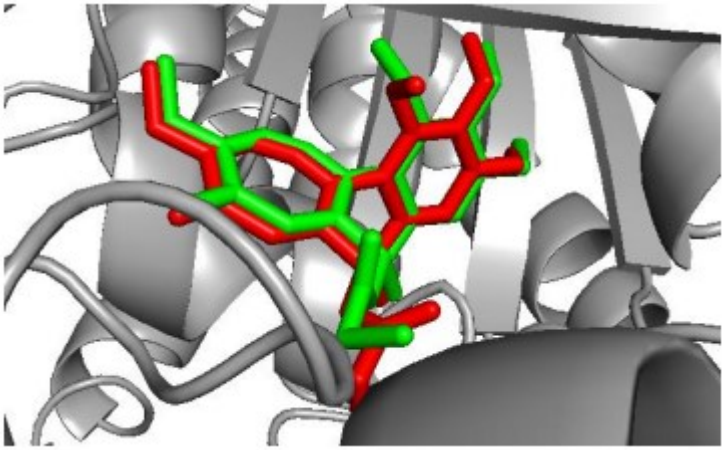
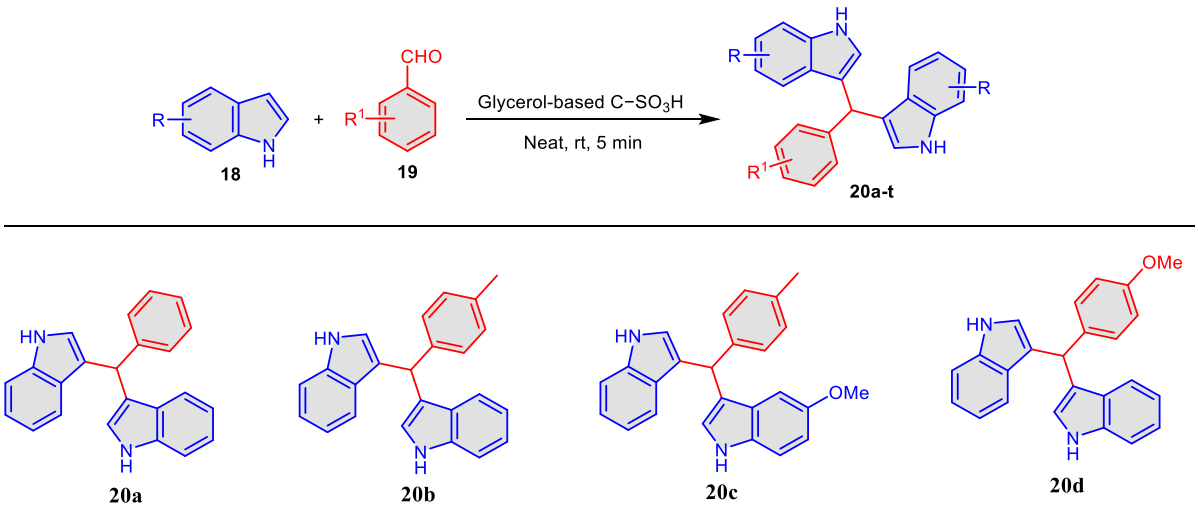
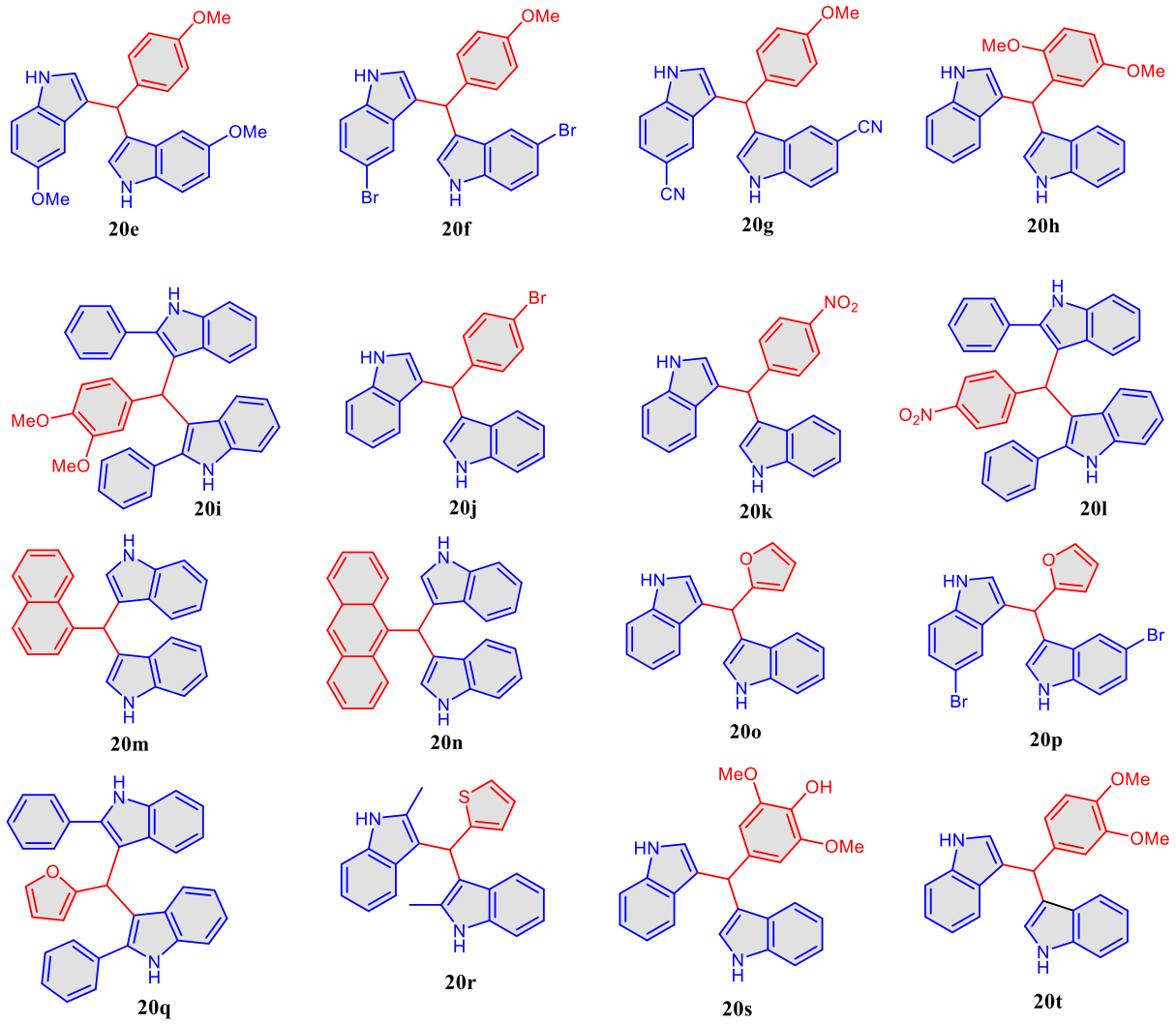


Figure 5. Crystallographic conformation (red) and docking conformation (green) of colchicine into the tubulin receptor.. Reproduced with permission from Ref.;[23] Copyright 2019; Wiley.

Indolomethanes are highly recognized as the most active N-heterocyclic scaffolds contributing to the biological function of small molecules therapeutics.[24–27] Glycerol-based carbon solid acid catalysts utilized for the green synthesis of indolomethanes **20a-t** under neat conditions. Reddy and co-authors [28] developed a green highly efficient methodology for the synthesis of 20a-t *via* reaction of indoles (**18)** with aldehydes **19** catalyzed with recyclable biodegradable glycerol-based carbon solid acid under neat reaction conditions at ambient temperature (Scheme 5). This approach aligns with the modernized principles of using renewable feedstock and avoiding hazardous mineral acids. Atom Economy and E-Factor equals 94.71 % and 0.05 respectively. The reaction under neat conditions allows removing the solvent and participate in reducing the E-Factor.



 ©**AUTHOR(S)**



Scheme 5. Synthesis of indolomethanes **20a-t** under neat conditions.

Compounds **20k** and **20c** demonstrated potent cytotoxicity against the DU145 prostate cancer cell line with IC_{50} μM values of 1.09 and 2.02 πM respectively. Molecular docking simulations with the targeted PCSK9 molecules validated these findings, showing that the indolomethanes scaffolds fit well within the active site picked, stabilized by interactions similar to those of doxorubicin (Figure 6).

©**AUTHOR(S)**

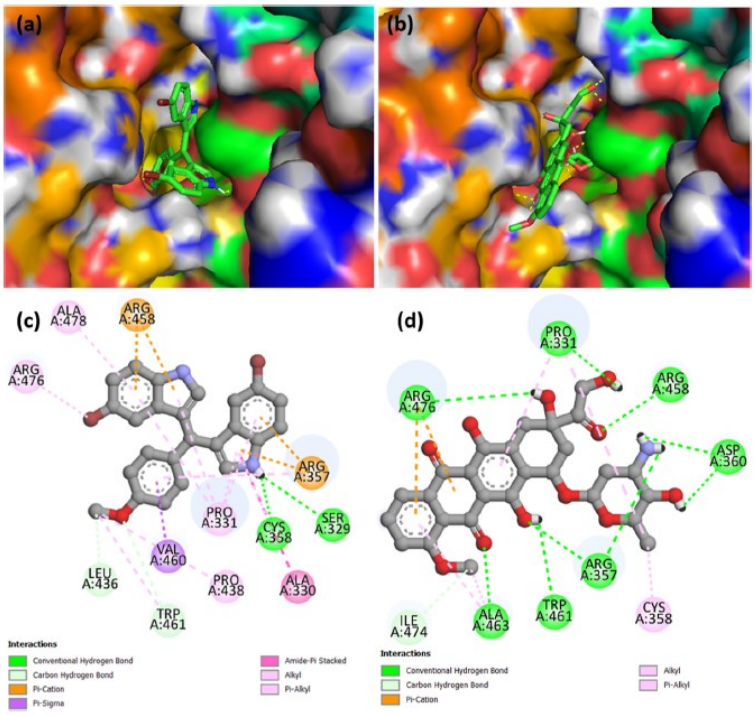
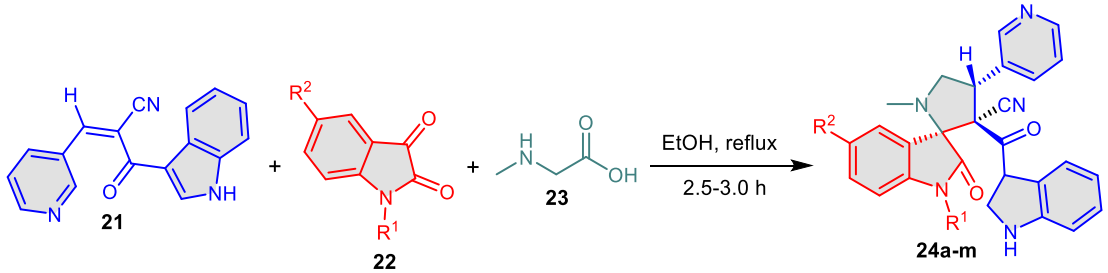


Figure 6. Docking pose of (**a**) compound **20f** and (**b**) *doxorubicin*, and binding interactions of (**c**) compound **20f** and (d) *doxorubicin* in the cavity of PCSK2. Reproduced with permission from Ref.;[28] Copyright 2023; American Chemical Society.

2.3. Spirooxindoles synthesis

Spirooxindole are characterized by a unique three-dimensional architecture allow for potent specific interactions with biological receptors.[29–31] Its synthesis often proceeds through 1,3-dipolar cycloaddition of azomethine ylides, a reaction that exhibit environmentally friendly The antitumor activity of synthesized spirooxindoles has been investigated.[32,33]

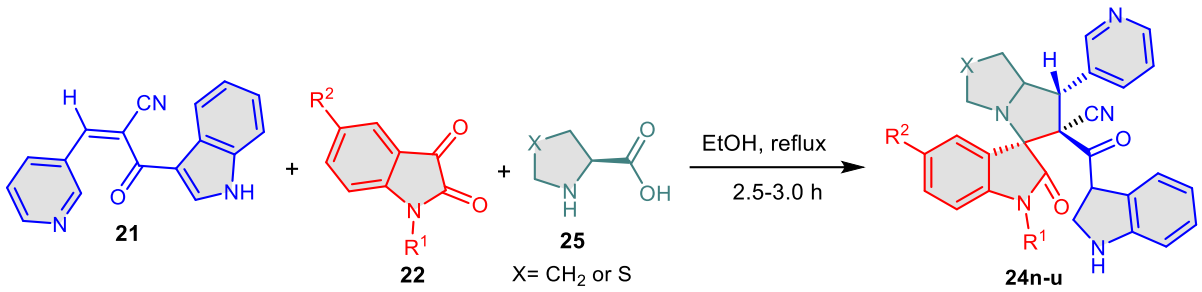
The research group of Maheswarai[34] applied 1,3-dipolar cycloaddition of (*E*)-2-(1*H*-indole-3-carbonyl)-3-(pyridin-3-yl)acrylonitrile (**21**) with isatines **22** and sarcosine (*N*-methylglycine) (**23**) or L-proline/thioproline (**25**) using ethanol under reflux as a greener solvent system for the synthesis of spirooxindole–pyrrolidine **24a-x** in good to excellent yields that target liver and lung carcinoma (Schemes 6-8).



24a-m: **a**, $R^1 = R^2 = H$; **b**, $R^1 = CH_3$, $R^2 = H$; **c**, $R^1 = C_2H_5$, $R^2 = H$; **d**, R^1 = allyl, $R^2 = H$; **e**, R^1= Benzyl, R^2= H; **f**, R^1 = H, R^2 = F; **g**, R^1 = H, R^2= Cl; **h**, R^1= H, R^2= Br; **i**, R^1= H, R^2= I; **j**, R^1= H, $R^2 = NO_2$; **k**, R^1= C_2H_5, $R^2 = NO_2$; **l**, R^1 = Benzyl, R^2 = Br; **m**, R^1 = H, $R^2 = OCF_3$.

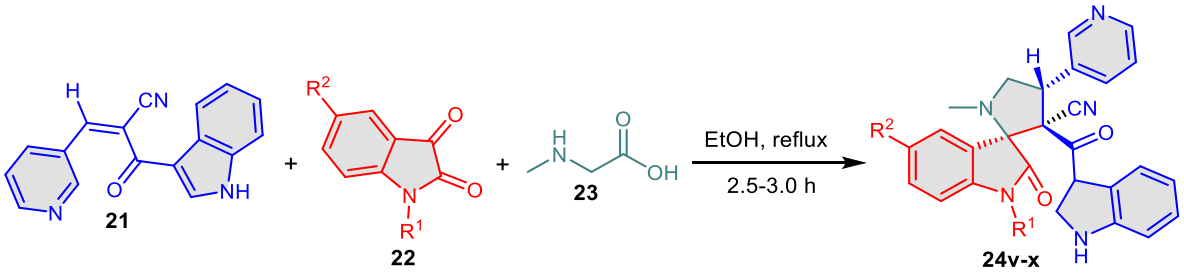
Scheme 6. Synthesis of spirooxindole–pyrrolidine derivatives **24a-m**.

 ©**AUTHOR(S)**



24n-u: **n**, $R^1 = R^2 = H$, X = CH_2; **o**, $R^1 = R^2 = H$, X = S; **p**, $R^1 = H$, $R^2 = F$, X = S; **q**, $R^1 = H$, $R^2 = Cl$, X = S; **r**, $R^1 = H$, $R^2 = Br$, X = S; **s**, $R^1 = H$, $R^2 = NO_2$, X = S; **t**, $R^1 = H$, $R^2 = Benzyl$, X = S; **u**, $R^1 = C_2H_5$, $R^2 = Br$, X = S.

Scheme 7. Synthesis of spirooxindole–pyrrolidine derivatives **24n-u**.



24v-x: **v**, $R^1 = H$, $R^2 = F$; **w**, $R^1 = H$, $R^2 = Br$; **x**, $R^1 = H$, R = I.

Scheme 8. Synthesis of spirooxindole–pyrrolidine derivatives **24v-x**.

Compounds **24u** and **24w** emerged as the most successful, withIC_{50} values against HepG2 cell lines of 9.0 and 8.0 µM/mL, respectively. Docking studies with the BCL-2 receptor (PDB code: 4lEH) highlighted the importance of pi-sigma bond anion and pi-sigma bonds with residues like ASP A:70 and MET A:74 in stabilizing the inhibitors (Figure 7).

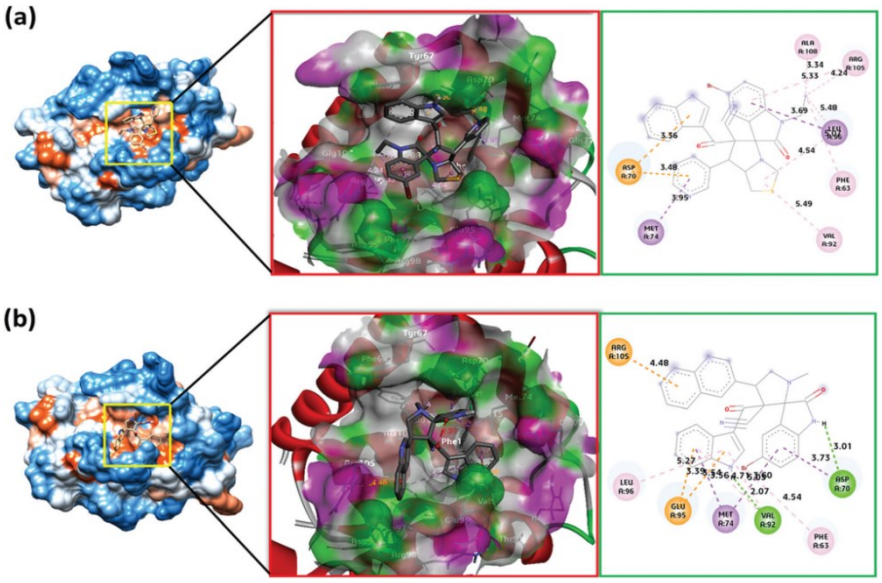
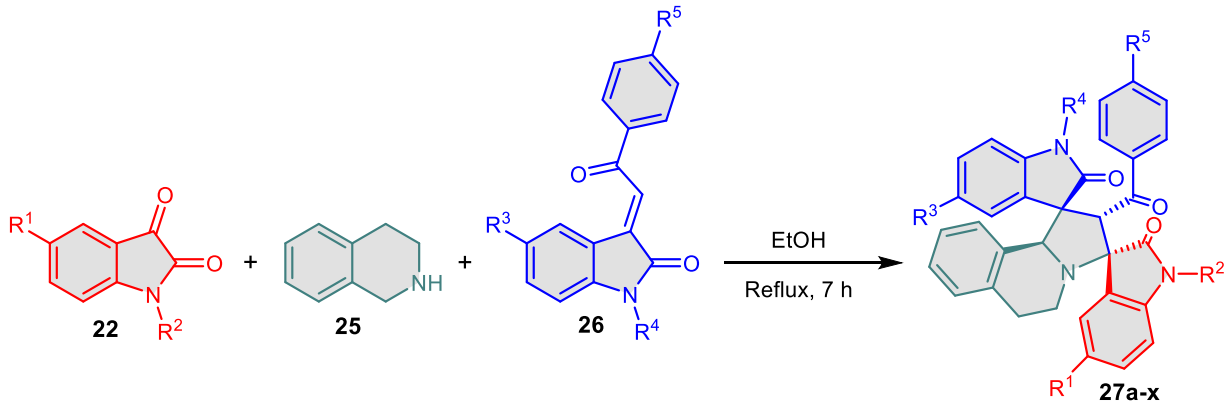


Figure 7. (**a**) Docking pose of **24u** with BCL-2 receptor, (**b**) docking pose of **24w** with BCL-2 receptor. Reproduced from Ref.;[34] Copyright 2022; Royal Society of Chemistry.

 ©**AUTHOR(S)**

The diasteroselective synthesis of dispirooxindoles **27a-x** from the reaction of isatin (**22**), 1,2,3,4-tetrahydroisoquinoline (**25**) and 3-phenacylideneoxindoles **26** in refluxing ethanol involving [3+2] cycloaddition reaction in good yields[35] (Scheme 9) further illustrate the capacity of three-component reactions to build complexity sustainably.[36] The spirooxindole core is an extremely potent and biologically active heterocycle.[37–40] These compounds were preliminary examined against mouse breast cancer (4T1) and human liver cancer (HepG2) cells. The results highlighted that polarity and substituent patterns on the nitrogen atom of isatin core significantly influenced cytotoxicity, with compound **27i** achieving a 73.50% inhibition of HepG2 cell growth.



27a-x: **a**, R^1= R^3= R^5= CH_3, R^2= R^4= H; **b**, R^1= CH_3, R^2= R^4= H, R^3= Cl, R^5= OCH_3; **c**, R^1= Cl, R^2= R^4= H, R^3, R^5 = CH_3, **d**, R^1= CH_3, R^2= R^3= R^4= R^5= H; **e**, R^1= R^3= CH_3, R^2= R^4= H, R^5= Cl; **f**, R^1= R^5= CH_3, R^2= R^4= H, R^3= Cl; **g**, R^1= R^5= Cl, R^2= R^4= H, R^3= CH_3; **h**, R^1= R^3= Cl, R^2= R^4= H, R^5= OCH_3; **i**, R^1= Cl, R^2= R^4= H, R^3= F, R^5= CH_3; **j**, R^1= CH_3, R^2= H, R^3= R^5= Cl, R^4= CH_2Ph; **k**, R^1= CH_3, R^2= R^3= R^5= H, R^4= CH_2Ph; **l**, R^1= R^3= R^5= CH_3, R^2= H, R^4= CH_2Ph; **m**, R^1= R^3= CH_3, R^2= H, R^4= CH_2Ph, R^5= Cl; **n**, R^1= R^3= R^5= CH_3, R^2= H, R^4= C_4H_9; **o**, R^1= R^3= Cl, R^2= H, R^4= C_4H_9, R^5= CH_3; **p**, R^1= R^4 = H, R^2= R^3= R^5= CH_3; **q**, R^1= R^4= H, R^2= R^5= CH_3, R^3= Cl; **r**, R^1= H, R^2= R^3= CH_3, R^4= CH_2Ph, R^5= Cl; **s**, R^1= R^3= R^5= CH_3, R^2= CH_2Ph, R^4= H; **t**, R^1= CH_3, R^2= CH_2Ph, R^3= Cl, R^4= H, R^5= OCH_3; **u**, R^1= CH_3, R^2= CH_2Ph, R^3= Cl, R^4= H, R^5= CH_3; **v**, R^1= R^3= Cl, R^2= CH_2Ph, R^4= H, R^5= CH_3; **w**, R^1= R^3= CH_3, R^2= R^4= CH_2Ph, R^5= Cl; **x**, R^1= Cl, R^2= C_4H_9, R^3= R^5= CH_3, R^4= H.

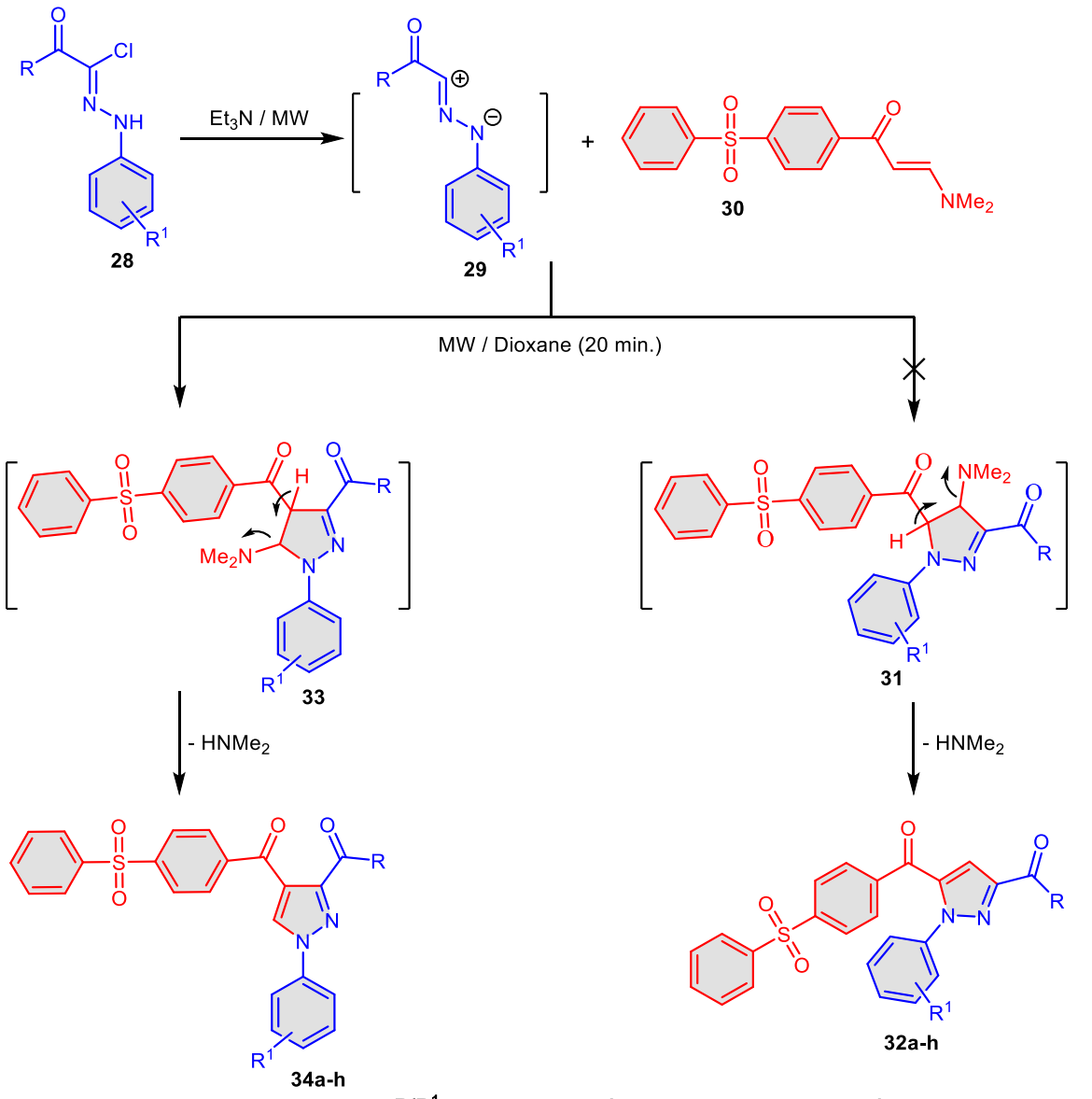
Scheme 9. Three-component synthesis of dispirooxindole derivatives **27a-x**.

2.4. Pyrazoles synthesis

Pyrazoles are among the most valuable compounds in pharmaceutical chemistry, and their utilities as synthons for the synthesis of a diversity of compounds having biological activities have received considerable attention.[41,42]

Recently regioselective synthesis[43] of novel pyrazoles **34a-h** bearing phenylsulfone moieties achieved through microwave-assisted cycloaddition of nitrileimines **28** to phenylsulfone –enamines **30** (Scheme 10).

 ©**AUTHOR(S)**



Scheme 10. Synthesis of pyrazoles **34a-h** bearing phenylsulfone moiety.

The reaction proceeds *via* cycloaddition of nitrileimine **29** to the exocyclic double bond in **30** and subsequent dimethylamine loss from intermediates **31** and **33**.

Compound **34a** showed a threefold greater potency than doxorubicin against HCT-116 cell lines, while **34b** demonstrated twofold potency against HepG-2 cells. The docking protocol was validated by redocking the co-crystallized ligand sorafenib, producing an RMSD of 1.9 Å and supporting the protocol's ability to reproduce its crystallographic pose. Docking into the VEGFR-2 tyrosine kinase active site revealed that the phenylsulphonyl moiety accommodates itself in the hydrophophobic back pocket forming crucial hydrogen bonds with Cys919 and Asn923 (Figure 8).

 ©**AUTHOR(S)**

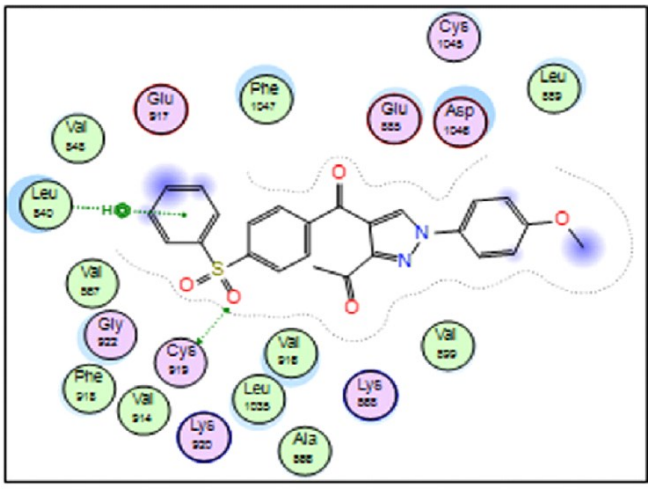


Figure 8. Compound **34a** docked onto the active site of VEGFR-2 kinase in 2D. Reproduced with permission from Ref.[43] Copyright 2022; Elsevier.

Among functionally substituted pyrazoles, 5-aminopyrazoles were extensively investigated as biologically relevant compounds.[44] Recent investigations have shown that steroidal heterocyclic compounds can effectively enhance the anticipation and treatment of hormonally-dependent cancers.[45] Moreover, it was established that a diversity of pyrazoles in the androstane series can promote anti-tumor activity rather than hormonal effect.[46–50] Microwave-induced heterocyclization of dehydroepiandrosterone (DHEA) (**43**) yielded D-ring-condensed 5-amino-1-arylpyrazoles (**48a-h**).[51] Some previously synthesized androstane-based pyrazoles with anti-cancer activities were illustrated in Figure 9.

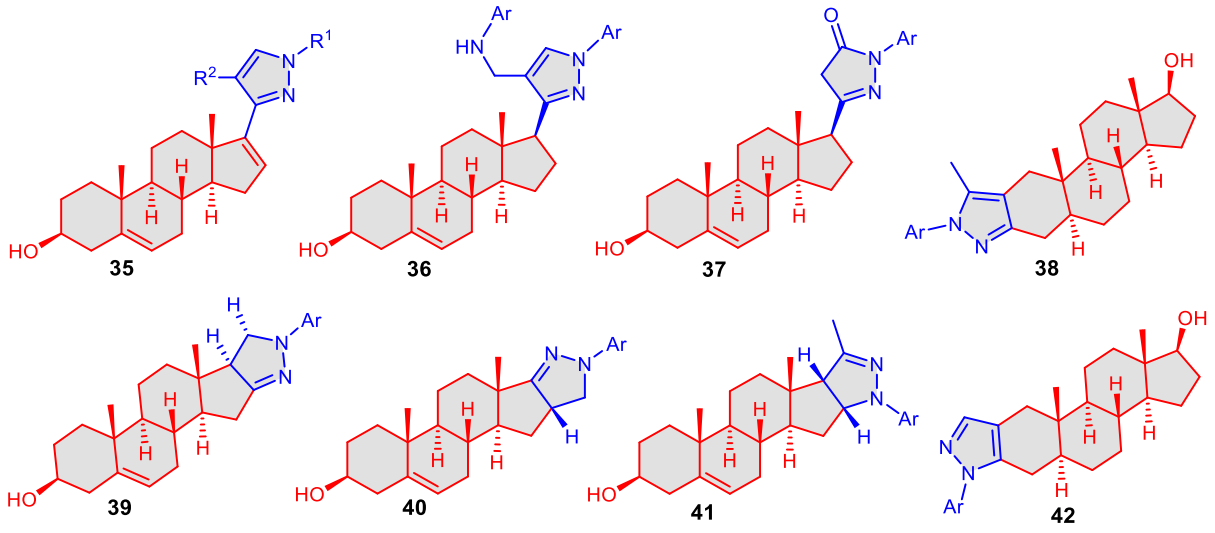
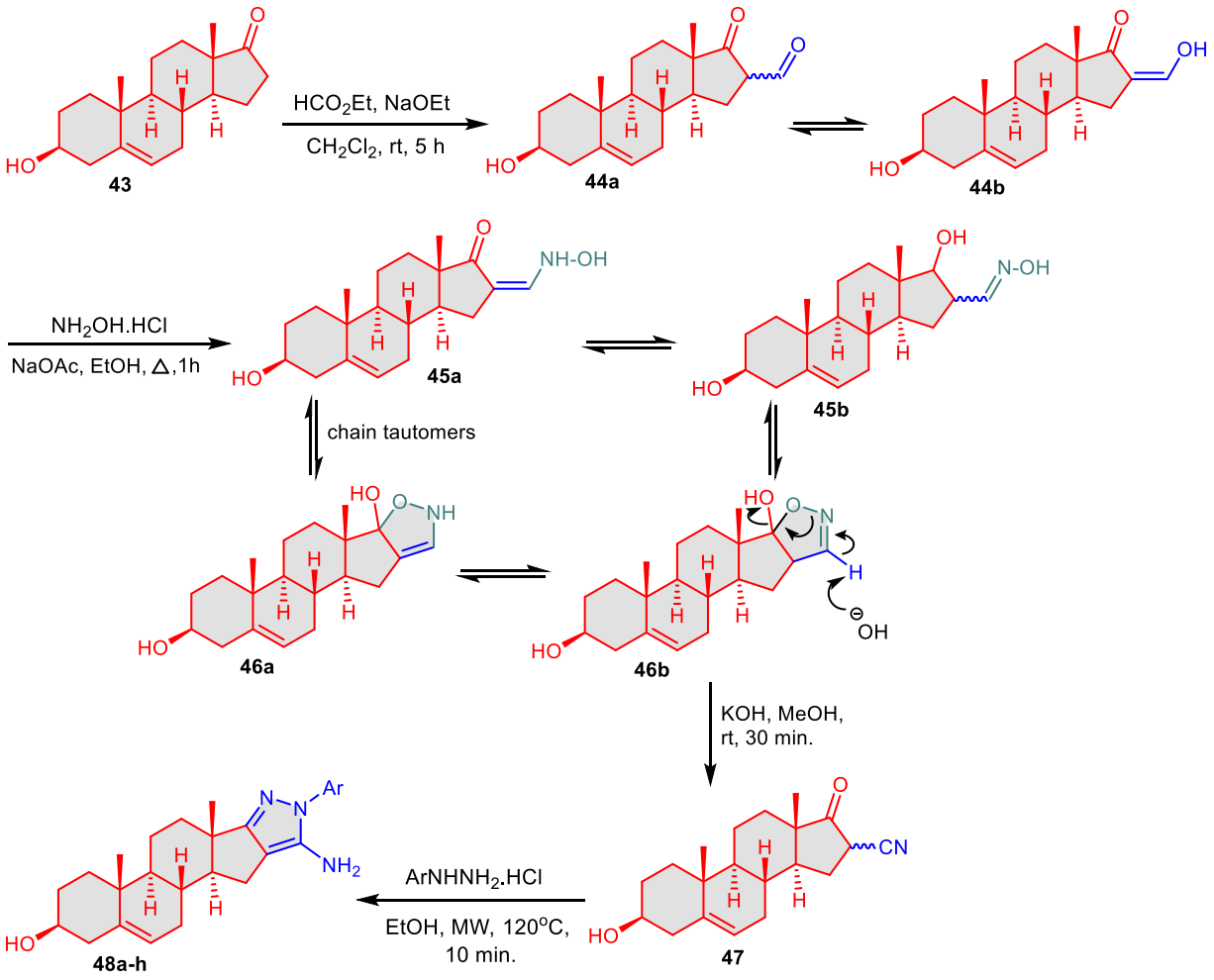


Figure 9. Androstane-based pyrazoles **35-42** as anti-cancer bioactive compounds.

 ©**AUTHOR(S)**



Scheme 11. Formation of 5-amino-1-arylpyrazoles **48a-h** based on dehydroepiandrosterone (DHEA).

Compound **48g** showed low-micromolar antiproliferative activity across the tested cancer cell lines, with IC_{50} values of 3.5-7.9 µM. On a molar basis, these values were higher than the corresponding cisplatin values reported in the same study (254.5-902 nM), indicating lower intrinsic cellular potency than cisplatin. Using the MRC-5 IC_{50} of 8.9 µM, the calculated SI values for **48g** were 1.44 (MCF-7), 1.82 (PC-3), 1.13 (A549), 2.23 (HeLa), and 2.54 (U2Os). Thus, **48g** shows only modest cancer-cell selectivity in this panel, with the greatest differential observed for U2Os and HeLa cells (Table 1).

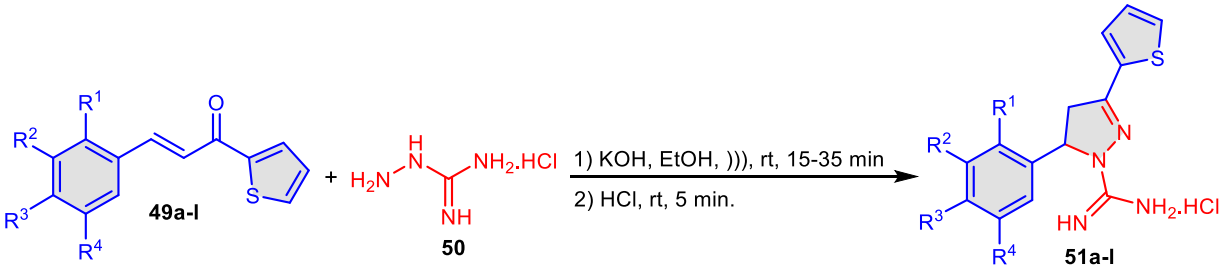
Table 1. IC_{50} values of compound **48g** and cisplatin were determined for cancer cell lines and non-cancerous MRC-5. SI = IC_{50}(MRC-5)/IC_{50}(cancer cell); SI > 1 indicates preferential cytotoxicity toward cancer cells.

Compound	IC_{50}					
	MRC-5	**MCF-7**	**PC-3**	**A549**	**HeLa**	**U2Os**
48g (µM)	8.9 ± 1.1	6.2 ± 1.0	4.9 ± 1.1	7.9 ± 1.0	4.0 ± 1.0	3.5 ± 1.0
Cisplatin (nM)	37.72 ± 1.2	338.5 ± 1.1	902 ± 1.2	369.8 ± 1.2	254.5 ± 1.2	342.8 ± 1.2
SI for 48g	—	1.44	1.82	1.13	2.23	2.54

 ©**AUTHOR(S)**

Amidines are well-known compounds, and their bioactivities have been recognized.[52–54] Pentamidine is used for the treatment of new anti-cancer agents.[55,56] Moreover, thiophene-carboxamides have shown promising inhibitory activities of neuronal nitric oxide synthesis for human melanoma treatment.[57] Pyrazoline derivatives exhibit antiproliferative activity[58] and high selectivity towards leukemia cell lines.[59]

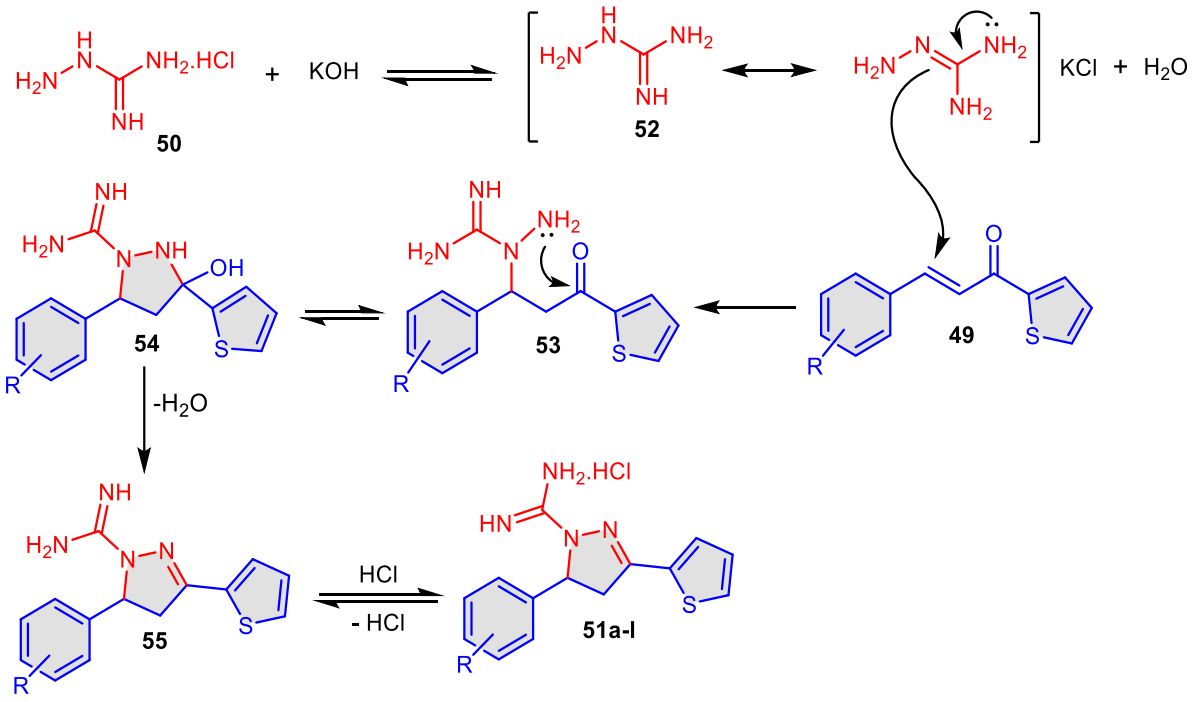
In 2017, Pizzuti and co-workers[60] described a green synthesis of the hybrid heterocycles 5-aryl-3-(thiophen-2-yl)-4,5-dihydro-1*H*-pyrazole-1-carboximidamide hydrochlorides **51a-l** through the reaction of chalcones **49a-l** with aminoguanidine hydrochloride (**50**) under ultrasound irradiation at ambient temperature as figured in Scheme 12.



49a-l; 51a-l: **a**, R^1= R^2= R^3= R^4= H; **b**, R^1= OCH_3; R^2= R^3= R^4= H; **c**, R^1= Br, R^2= R^3= R^4= H; **d**, R^1= R^3= R^4= H, R^2= NO_2; **e**, R^1= R^2= R^4= H, R^3= Me; **f**, R^1= R^2= R^4= H, R^3= CF_3; **g**, R^1= R^2= R^4= H, R^3= OMe; **h**, R^1= R^2= R^4= H, R^3= F; **i**, R^1= R^2= R^4= H, R^3= Cl; **j**, R^1= R^2= R^4= H, R^3 = Br; **k**, R^2= R^4= H, R^1= R^3= Cl; **l**, R^1= R^4= H, R^2= R^3 = OMe.

Scheme 12. Formation of 5-aryl-3-(thiophen-2-yl)-4,5-dihydro-1*H*-pyrazole-1-carboximidamide hydrochlorides **51a-l**.

The suggested mechanism for the formation of **51a-l** demonstrated in Scheme 13.



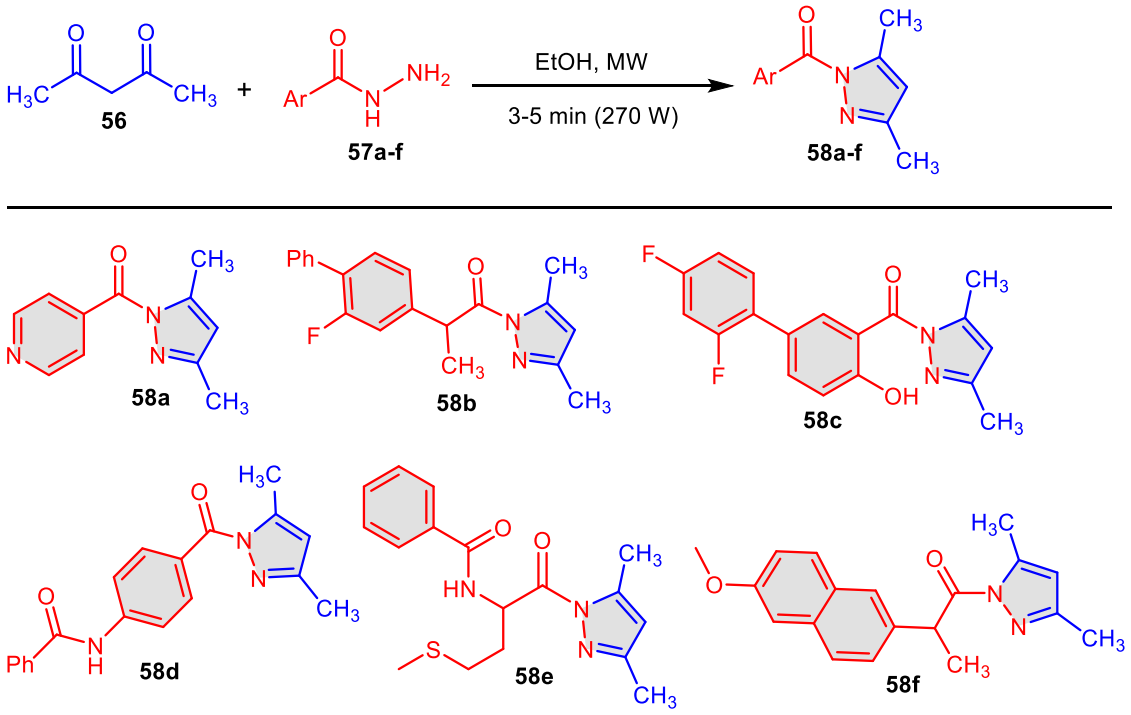
Scheme 13. Mechanism of the formation of **51a-l.**

 ©**AUTHOR(S)**

In order to evaluate the bioactivity of the formed compounds, their cytotoxicity activity against three different human leukemia cell lines estimated. The results illustrate that **51b**, **51c**, **51f**, **51i**, **51j**, and **51k** showed they are highly cytotoxic with IC_{50} ranging from 5.7-14.7 µmol L^{-1} for at least one of the tested cell lines. Compounds **51a**, **51d**, **51e**, **51g** and **51h** showed moderate cytotoxicity with IC_{50} around 40 µmol L^{-1}; however, compound **51l** has no significant activity. In addition, authors claimed that the *in vitro* cytotoxic activity of synthesized pyrazolines are in the same range as many anti-leukemia drugs named 6-mercaptopurine, 6-thioguanine, dexamethasone, and methylprednisolone.

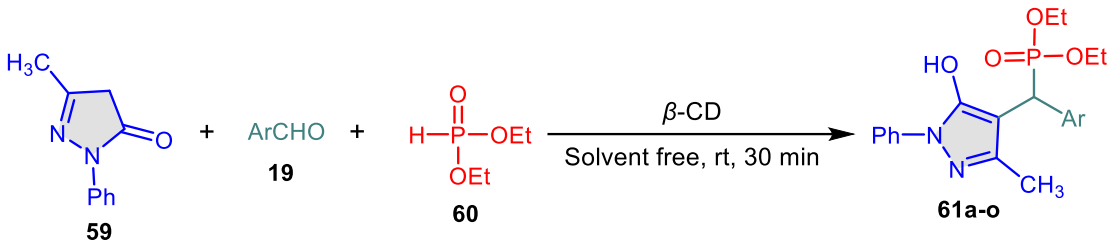
A second study utilizing pyrazole derivatives as anti-cancer reagents dates to 2014. Aydin *et al.*[61] have reported a green synthesis of diversity 1-aroyl-3,5-dimethyl-1*H*-pyrazoles **58a-f** *via* the reaction of acetylacetone (**56**) with hydrazides **57a-f** (Scheme 14) and evaluated some selected samples **58c**, **58d** and **58f** for their anti-cancer activity against 60 human tumor cell lines. Compound **58c** exhibited pronounced activity against human myelogenous leukemia (K-562) with IC_{50} value of 4.0 µM. Moreover, **58c** induced apoptosis of K-562, upon which it exploited as a potential chemo-preventive agent towards chronic myelogenous leukemia.

The rapidly growing interest of organophosphorus compounds in pharmaceutical and medicinal chemistry[62–65] inspires scientists to develop new routes for the synthesis of heterocyclic phosphonates with expected biological activity. Reddy and co-authors[66] reported efficient and green one-pot synthesis of pyrazolylphosphonates **61a-o** utilizing β-cyclodextrine as supramolecular catalyst in aqueous medium *via* reacting of 3-methyl-1-phenyl-2-pyrazoline-5-one (**59**), with various aryl aldehydes **19** and diethyl phosphite (**60**) (Scheme 15).



Scheme 14. Synthesis of 1-aroyl-3,5-dimethyl-1*H*-pyrazoles **58a-f**.

 ©**AUTHOR(S)**



61a-o: **a**, Ar = 4-$OC_2H_5C_6H_4$; **b**, Ar = 4-$CH_3C_6H_4$; **c**, Ar = 3,4-$(OCH_3)_2C_6H_3$; **d**, Ar = 3,4,5-$(OCH_3)_3C_6H_2$; **e**, Ar = 4-$N(Et)_2C_6H_4$; **f**, Ar = 3-FC_6H_4; **g**, Ar = 4-ClC_6H_4; **h**, Ar = 4-BrC_6H_4; **i**, Ar= 4-$NO_2C_6H_4$; **j**, Ar= 2-F-5-ClC_6H_3; **k**, Ar = 2-F-5-BrC_6H_3; **l**, Ar = 3-NO_2-4-Cl-C_6H_3; **m**, Ar = naphthalen-2-yl; **n**, Ar = anthracen-9-yl; **o**, Ar= pyren-1-yl.

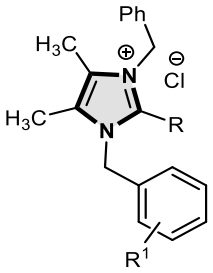
Scheme 15. Synthesis of pyrazolylphosphonates **61a-o**.

The *in vitro* anti-oxidant activity for **61a-o** encompassed free radical scavenger and cytotoxicity assays. evaluated *via* screening of their free radical scavenging activity following the DPPH and H_2O_2 methods. The activity results demonstrated that lower IC_{50} values were obtained, and a higher radical scavenging activity identified. Ascorbic acid employed as standard control. Among tested compounds **61e**, **61b,** and **61a** showed potent IC_{50} values ranging from 10.24-12.35 µg/mL, which reflects the high potency as anti- oxidants compared to IC_{50} of ascorbic acid (IC_{50} = 13.67 µg/mL). The antitumor activity of **61a-o** carried out against human breast cancer (MCF-7), prostate cancer (DU-145), and lung cancer (A-549) cell lines using sulforhodamine-B (SRB) assay and doxorubicin as standard drug. Evaluation of the cytotoxicity data revealed that compounds **61o**, **61n,** and **61m** exhibit excellent cytotoxic potential against all tested cancer cell lines, whereas products **61l**, **61f, 61h, 61g,** and **61i** possess moderate cytotoxic activity. However, compounds **61k**, **61j**, **61b**, **61c**, **61a,** and **61e** showed no cytotoxic activity to the three tested cell lines.

According to structure activity relationship The SAR analysis of these scaffolds showed significant activity with compounds bearing electron-donating groups on the phenyl ring which increases the stabilization of the produced radical intermediate. Meanwhile compounds with electron-withdrawing substituents exhibit excellent potency against (MCF-7), DU-145) and (A-549) cancer cell lines.

2.5. Imidazoles synthesis

Lepidilines A-D were accomplished imidazolium salts with 1,3-benzyl substituents exhibited potent biological activity, particularly as an anti-cancer reagent (Figure 10).[67,68]

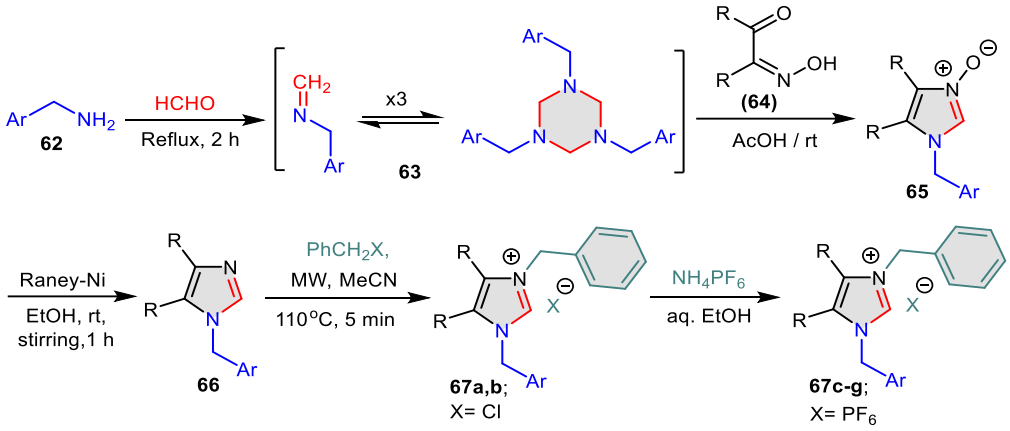


Lepidilines A-D: **A**, R = R^1 = H; **B**, R = H, R^1 = CH_3; **C**, R = H, R^1 = OCH_3; **D**, R = CH_3, R^1 = OCH_3.

Figure 10. Structure of Lepidilines A–D.

©**AUTHOR(S)**

Mlostoń and co-authors[68] described intriguing and efficient synthesis of imidazolium salts **67a-g** starting from 2-unsubstituted imidazole *N*-oxides (**65)** *via* deoxygenation followed by regioselective quaternization with benzyl chloride under controlled microwave heating as illustrated in Scheme 16. This green approach allows the synthesis of lipidiline analogues bearing a diversity of aryl substituents.



67a-g: **a**, R= CH_3, Ar= C_6H_5, X= Cl; **b**, R= CH_3, Ar= 3-$OCH_3C_6H_4$, X= Cl; **c**, R= CH_3, Ar= C_6H_5, X= PF_6; **d**, R= CH_3, Ar= 3-$OCH_3C_6H_4$, X= PF_6; **e**, R= CH_3, Ar= 3-FC_6H_4, X= PF_6; **f**, R= C_6H_5, Ar= C_6H_5, X= PF_6; **g**, R= C_6H_5, Ar= 3-$OCH_3C_6H_4$, X= PF_6.

Scheme 16. Synthesis of lepidiline analogues **67a-g**.

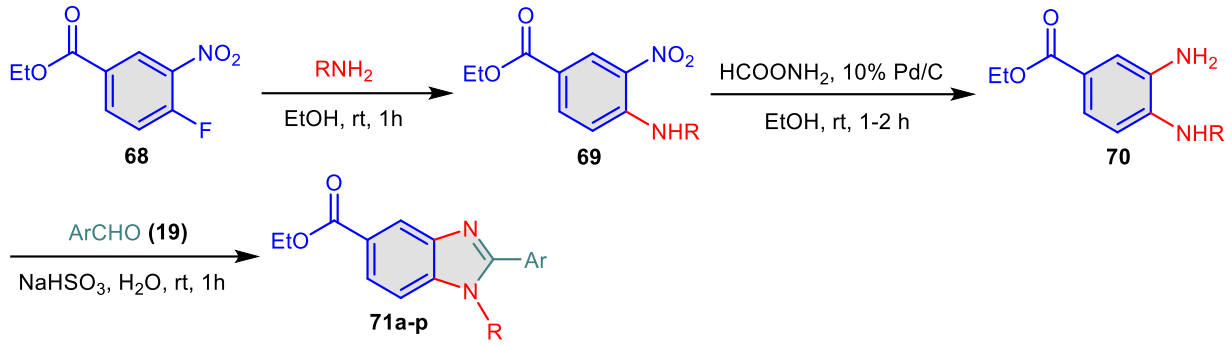
A series of compounds **67a-g** were examined for their anti-cancer potency against HepG2, A549, HeLa and normal:Vero, LLC-MK2, MRC-5 and NCTC colon 929 cell lines.

Cytotoxic studies showed that compounds **67a**, **67b**, **67c** and **67d** are the most promising against (LLC-MK2 cell line). Meanwhile, these compounds have cytotoxic concentration (CC_{50} < 80 µM) on LLC-MK2 cells. Lepidilines **67e-g** showed the most cytotoxicity on HeLa cell line with CC_{50} values below 1.0 µM.

2.6. Benzimidazoles synthesis

Benzimidazoles are a potent scaffolds in areas related to drug discovery due to their structural similarity to purine bases[69] permit their interaction with diversity of enzymes and receptors. Yoon *et al*.[70] have developed regioselective and green procedure to synthesize of ethyl 1,2-diaryl/heteroaryl-1*H*-benzo[*d*]imidazole-5-carboxylates **71a-p** employing the reaction of 4-ethoxycarbonyl-1-substituted phenylenediamine **70** and aromatic aldehydes **19** utilizing water as solvent at ambient temperature illustrated in Scheme 17.

 ©**AUTHOR(S)**



71a-p: **a**, R= 3-(2-oxopyrrolidin-1-yl)propyl, Ar= C_6H_5; **b,** R= 3-(2-oxopyrrolidin-1-yl)propyl, Ar= 4-$(NMe)_2C_6H_4$; **c**, R= 3-(2-oxopyrrolidin-1-yl)propyl, Ar= 4-OHC_6H_4; **d**, R= 3-(2-oxopyrrolidin-1-yl)propyl, Ar= 4-$CH_3C_6H_4$; **e**, R= 3-(2-oxopyrrolidin-1-yl)propyl, Ar= 4-$CF_3C_6H_4$; **f**, R= 3-(2-oxopyrrolidin-1-yl)propyl, Ar= 4-$NO_2C_6H_4$; **g**, R= 3-(2-oxopyrrolidin-1-yl)propyl, Ar= 4-ClC_6H_4; **h**, R= 3-(2-oxopyrrolidin-1-yl)propyl, Ar= 4-BrC_6H_4; **i**, R= Ar= C_6H_5; **j**, R= C_6H_5, Ar= 4-$(NMe)_2C_6H_4$; **k**, R= C_6H_5, Ar= 4-OHC_6H_4; **l,** R= C_6H_5, Ar= 4-$CH_3C_6H_4$; **m**, R= C_6H_5, Ar= 4-$CF_3C_6H_4$; **n**, R= C_6H_5, Ar= 4-$NO_2C_6H_4$; **o**, R= C_6H_5, Ar= 4-ClC_6H_4; **p**, R= C_6H_5, Ar= 4-BrC_6H_4.

Scheme 17. Synthesis of ethyl 1,2-diaryl/heteroaryl-1*H*-benzo[*d*]imidazole-5-carboxylates **71a-p.**

IC_{50} values for all synthesized compounds were evaluated using cambnol and Tenovin-6 as a standard control for both SIRT1 and SIRT2 as they displayed antitumor activities in mouse xenograft models. Results revealed that compounds **71a-p** showed higher than 50% inhibition at 50 µM for either SIRT1 or SIRT2, compounds **71b** and **71j** emerging as the most potent hits with compound **71j** showed higher potency against SIRT2 than SIRT1 with IC_{50} of 26.85 µM for **71b**.

Molecular docking studies into the SIRT2-ADpr cofactor-binding site elucidate the bonding modes of these compounds of these compounds. For compound **71j** (Figure 11), the following interactions noticed:

1- A hydrogen bonds initiated with Thr262, Leu263, Gln265, Arg97, and Gln167.

2- A π-π stacking interaction between the imidazole group of His187 and the benzene ring of Phe235 stabilizes the C-2benzene ring.

3- The C-2 NMe2 substituent improves activity through hydrophobic interactions with Val233 and Phe119

4- Lone pair interactions observed between the oxygen atoms and the phenyl ring bearing NMe2 group and Val233.

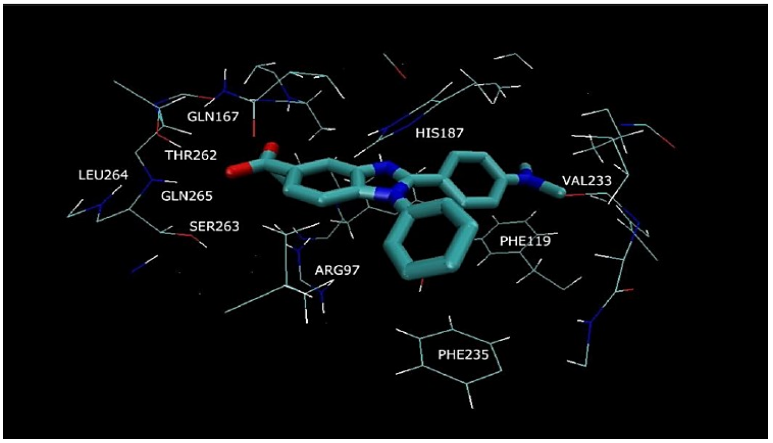


Figure 11. Molecular interactions between **71j** and SIRT2. Reproduced with permission from Ref.;[70] Copyright 2014; Elsevier.

 ©**AUTHOR(S)**

Interestingly, compound **71b** bind differently than **71j**; it binds to Lys287 through a hydrogen bond between the ketone oxygen of the pyrrolidinone moiety and receptor. Another strong hydrogen bond is that between ethyl ester oxygen with Ala85. Additionally, other hydrogen bond interactions with Asn286, Ser98, Arg97, Ser263, and Gln167 observed. Nevertheless, because the C-2 benzene ring substrate positioned outside of the receptor cavity, it had no discernible effect on the SIRT2 enzyme's ability to block sirtuin (Figure 12).

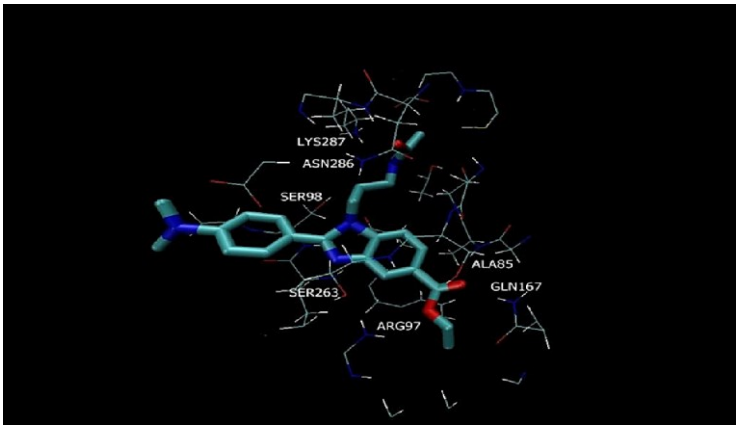
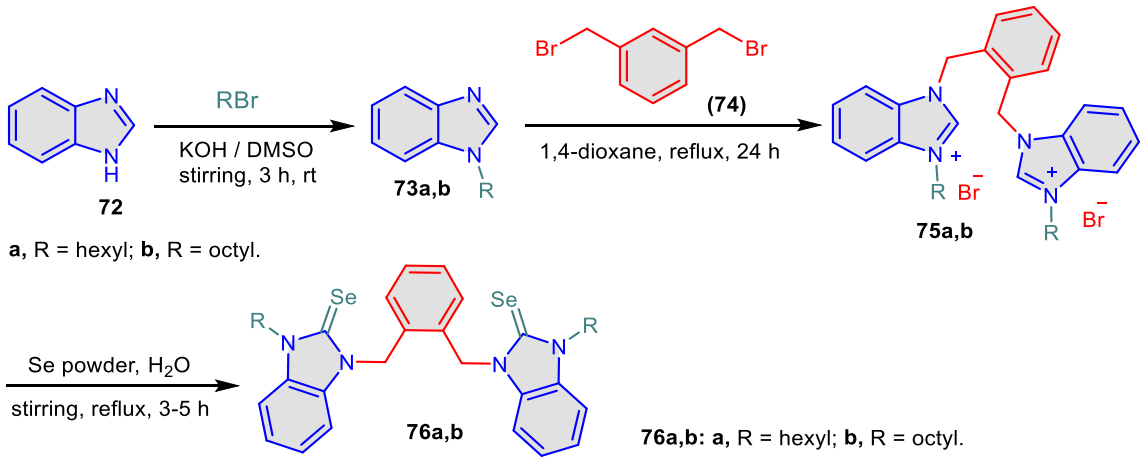


Figure 12. Molecular interactions between **71b** and SIRT2. Reproduced with permission from Ref.;[70] Copyright 2014; Elsevier.

Atif and co-authors[71] developed a green synthesis of selenium-bis-benzimidazolium compounds **76a,b** *via* the reaction sequence illustrated in Scheme 18.



Scheme 18. Synthesis of selenium-bis-benzimidazoliums **76a,b**.

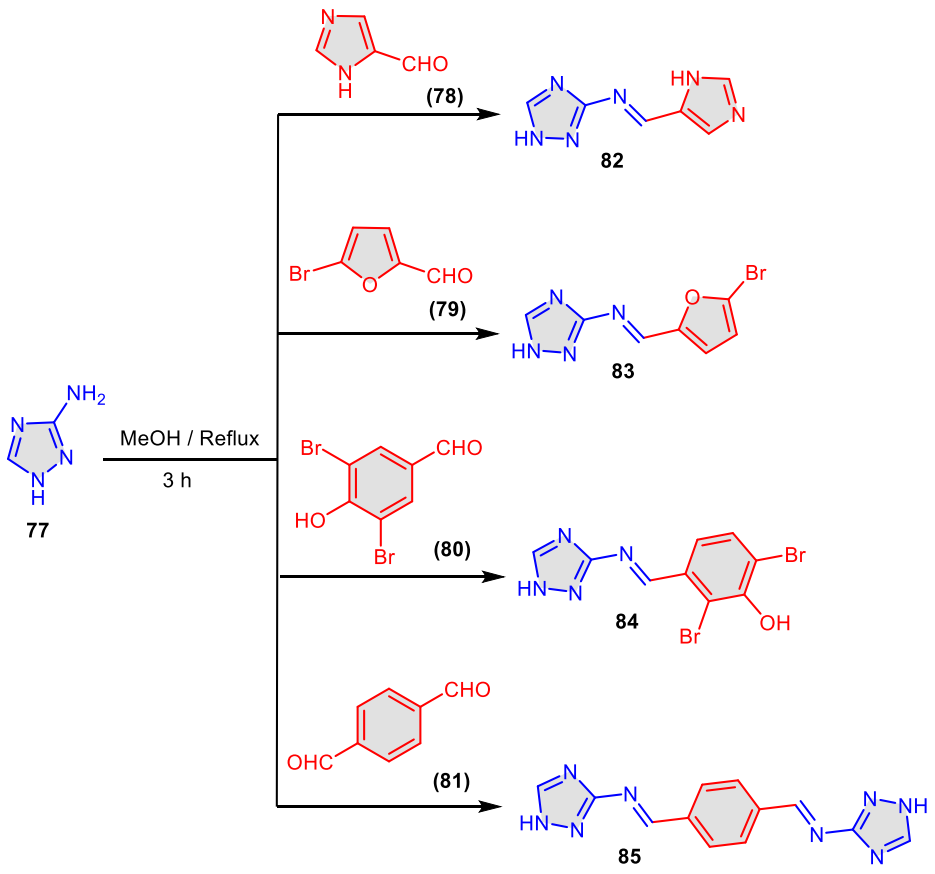
Biological screening against four human cancer cell lines MCF7, Hela, B16F10 and RGC-5 using MTT assay revealed that compound **76b** shows twice the activity of the reference drug 5-flurouracil against RGC5 cells. The results obtained revealed that compound **73b** showed equivalent activity to standard drug, meanwhile target **75b**, **76b** revealed activity higher than of reference drug against MCF-7. These phenomena established the significant incorporation of selenium in enhancing the cytotoxic potential of the benzimidazole scaffold.

 ©**AUTHOR(S)**

2.7. Triazoles synthesis

Triazole Schiff bases have gained increasing interest as precursors of several biologically relevant conjugates with different moieties. Moreover, their ability to initiate hydrogen bonds improving their toxicological, pharmacokinetic and pharmacological properties.[72–76]

A green catalyst free condensation of 3-amino-1*H*-1,2,4-triazole (**77**) with aromatic aldehydes **78-81** was developed by Abbas and co-authors,[76] yielding the corresponding Schiff bases **82-85** in good yields (Scheme 19). The structural stability of these targets estimated using quantum chemical calculations and analysis of chemical quantum descriptors. Among synthesized compounds, **82** found to exhibit the highest molecular stability.
The synthesized targets were evaluated against MCF-7 and HepG2 cancer cell lines. Compounds **84** and **85** gave IC_{50} values of 64.64 and 23.52 µg/mL, respectively. These values indicate limited activity for **84** and moderate in vitro cytotoxicity for **85**, rather than high potency. Molecular docking suggested hydrogen-bonding interactions for both compounds, with **85** showing a calculated binding affinity of -7.30 kJ/mol at the reported 3PP0 receptor model. These docking observations provide a possible binding hypothesis but do not by themselves establish anticancer efficacy or clinical relevance (Figure 13).



Scheme 19. Synthesis of the 1,2,4-triazole Schiff bases **82-85**.

 ©**AUTHOR(S)**

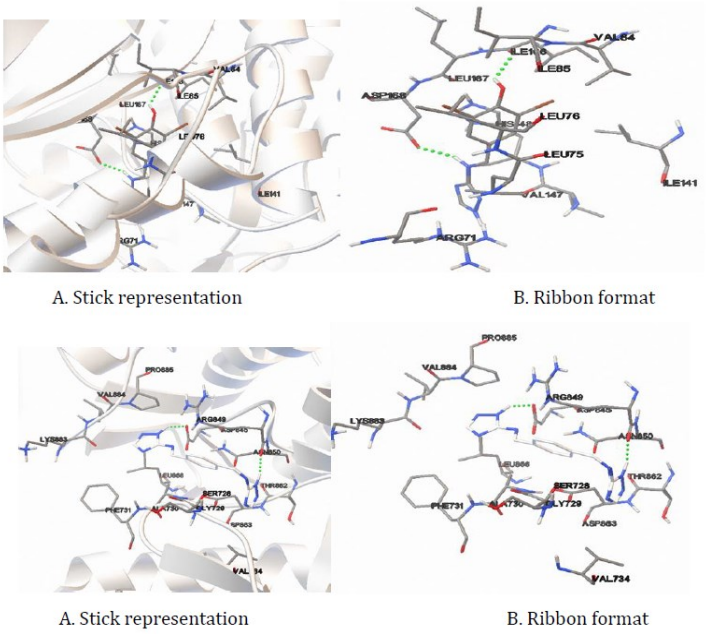


Figure 13. Orientation and position for compounds **84** and **85** with protein residue. Reproduced with permission from Ref.;[76] Copyright 2014; SPC.

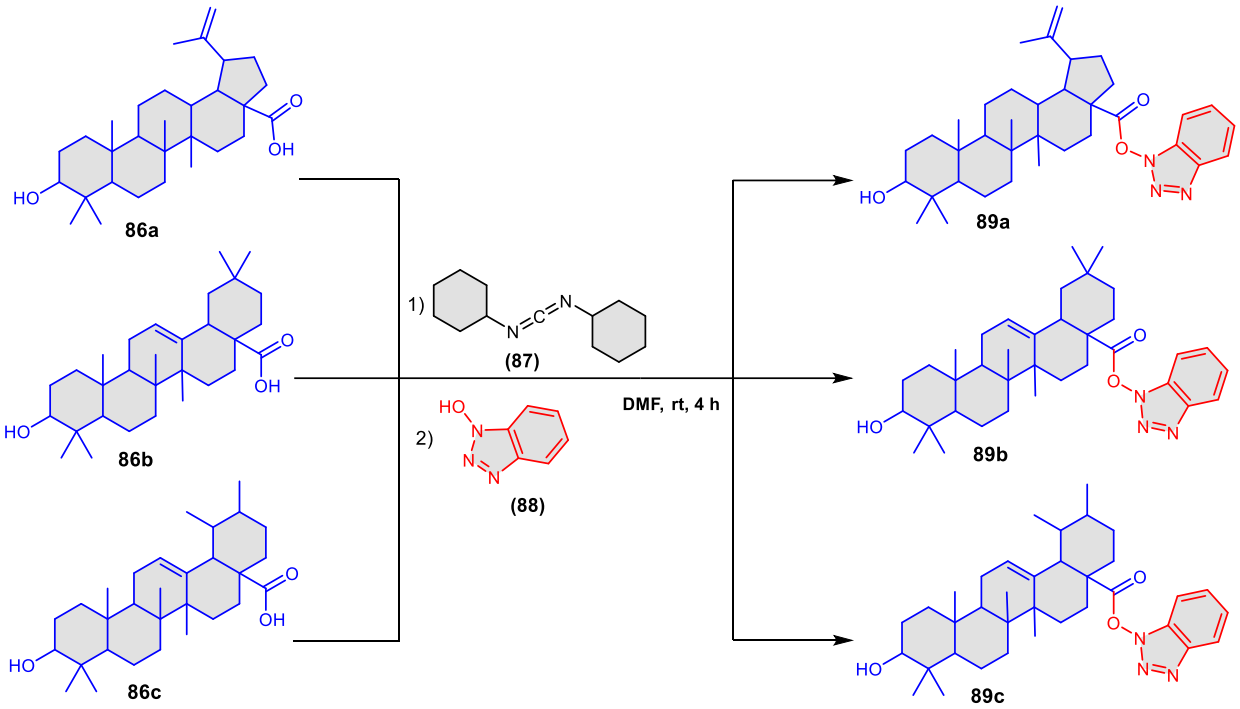
2.8. Benzotriazole synthesis

One of the challenges that lead to the identification of efficient drugs is the consequent steps from idea to product marketing. It involves time (usually 10-15 years), expenses, as well as synthetic approaches, biological activity, and toxicology.[77] In this regard, natural and synthetic drugs possess several limitations, such as unwanted side effects, low pharmacokinetic activity, and structural instability. An important breakthrough developed by establishing the possibility of adopting semisynthetic hybrid molecules that constitute biologically active natural products with *N*-containing heterocycles.

Pentacyclic triterpenoids, in particular, betulinic (BA) **86a**, oleanolic (OA) **86b,** and ursolic acids **86c** have been recognized as selective and potent anti-cancer reagents.[18]

In the year 2020,[78] Moic and co-authors reported an interesting synthesis and anti-cancer activity of novel semisynthetic benzotriazoles esters of betulinic, olenolic, and ursolic acids (**89a-c**) in moderate yields *via* reaction of parent acids with 1-hydroxybenzotrizole (**88**) in DMF at ambient temperature for 4 hours (Scheme 20).

 ©**AUTHOR(S)**



Scheme 20. Synthesis of betulinic, olenolic, and ursolic acids (**89a-c**).

The *in vitro* toxicological potency of compounds **89a-c** towards healing human keratinocytes (HaCat) and results obtained demonstrated that compounds **89a** and **89b** do not show any cytotoxic effects upon application with concentration up to 25 µM (Figure 14A, B). However, at 50 µM concentration, both compounds significantly decrease cell viability with 87.1% and 87% (Figure 14A, B). No cytotoxicity was observed on HaCaT with different concentrations of compound **89c** (Figure 14C), even at higher temperatures. For A375, a significant reduction of viability upon testing with **89a** and **89b** at 25 µM concentrations with 81.25% and 87.4%, respectively, referenced to the control sample. However, at 50-µM concentration, a more reduction of viability with 69.8% and 62% observed.

 ©**AUTHOR(S)**

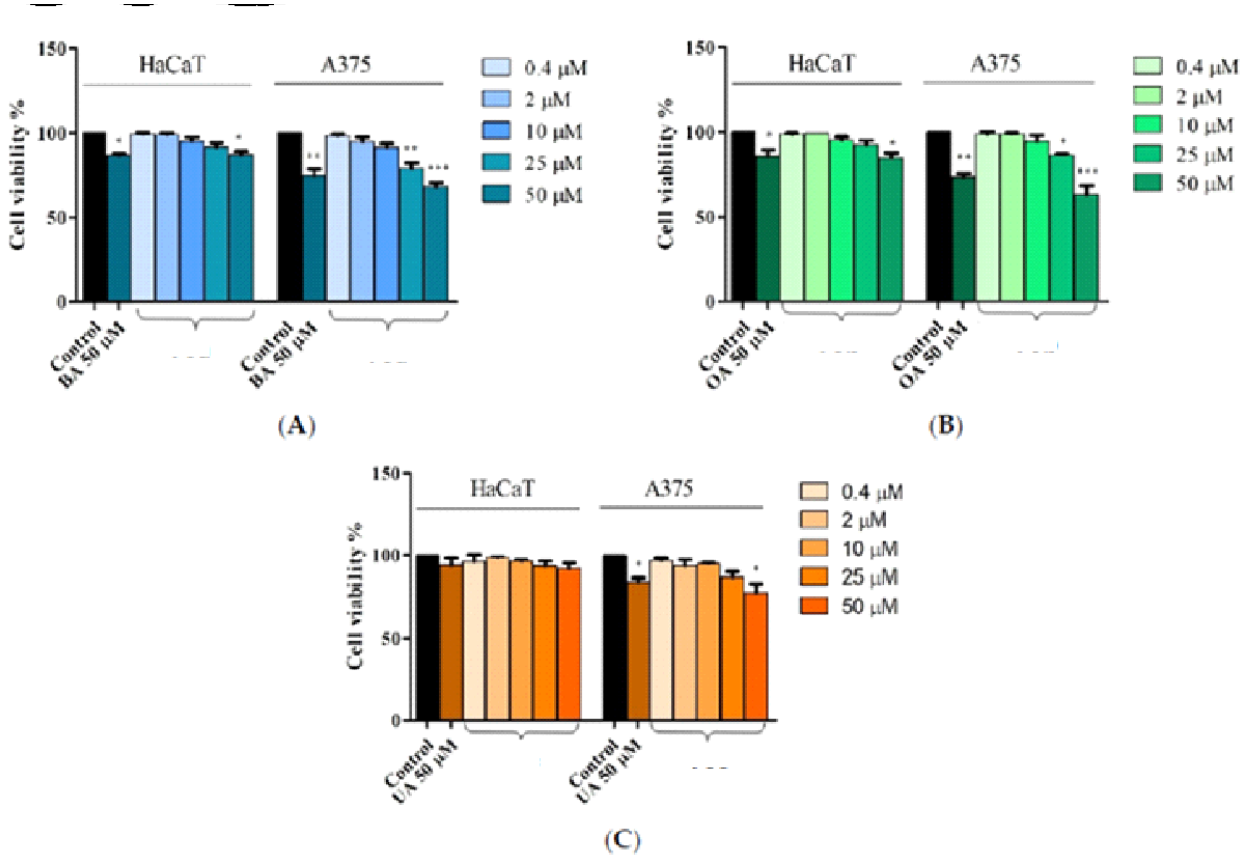


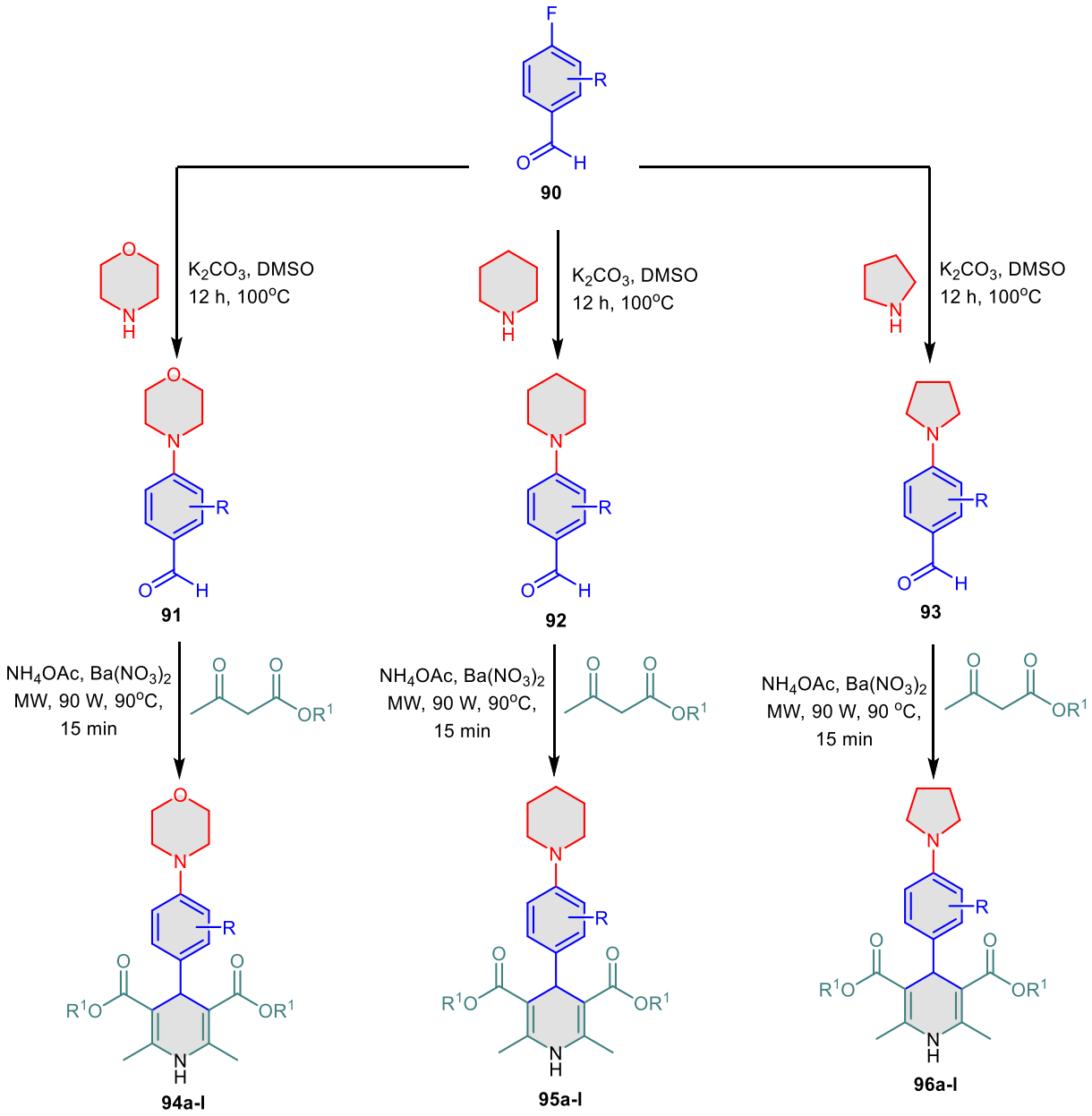
Figure 14. HaCaT and A375 cell viability after 24 hours of treatment with 0.4, 2, 10, 25, and 50 M. Compounds **89a** (**A**), **89b** (**B**), and **89c** (**C**) determined using the Alamar Blue assay. Reproduced from Ref.;[78] Copyright 2022; MDPI.

3. Six- membered Nitrogen Heterocycles

3.1. Pyridines synthesis

The anti-cancer activity of dihydropyridines has attracted increasing interest among medicinal chemists.[79,80] They are also cited for their versatile ability to reverse multidrug resistance towards human carcinoma cell lines.[81,82] Kumar *et al*.[83] developed a green synthesis of novel *N*-heterocycles linked 4-aryl-1,4-dihydropyridines **94a-l**, **95a-l**, and **96a-l** *via* Hantzsch reaction, as illustrated in (Scheme 21).

 ©**AUTHOR(S)**



R= H; 2-Cl; 3-Cl; or 3-F.

R^1= CH_3; CH_2CH_3; or $CH(CH_3)_2$.

94a-l; 95a-l; 96a-l: **a**, R= H, R^1= CH_3; **b**, R= 2-Cl, R^1= CH_3; **c**, R= 3-Cl, R^1= CH_3; **d**, R= 3-F, R^1= CH_3; **e**, R= H, R^1= CH_2CH_3;**f**, R= 2-Cl, R^1= CH_2CH_3; **g**, R= 3-Cl, R^1= CH_2CH_3; **h**, R= 3-F, R^1= CH_2CH_3; **i**, R= H, R^1= $CH_2(CH_3)_2$; **j**, R= 2-Cl, R^1= $CH_2(CH_3)_2$; **k**, R= 3-Cl, R^1= $CH_2(CH_3)_2$; **l**, R= 3-F, R^1= $CH_2(CH_3)_2$.

Scheme 21. Hantzsch reaction for the synthesis of dihydropyridines **94a-l**, **95a-l**, and **96a-l**.

The *in vitro* anti-cancer activity of compounds **94a-l**, **95a-l**, and **96a-l** against two cancer cell lines, murine mammary adenocarcinoma (EAC) and breast cancer (MCF-7), and a normal cell line (Human embryonic kidney cell line (HEK)) using doxorubicin as standard drug was evaluated. The results demonstrated that several compounds exhibited fewer toxic effects on normal cell lines reflecting their potent therapeutic activity. Meanwhile, products **95b**, **95f**, **95h,** and **95j** identified as the most active, which showed higher activity than

 ©**AUTHOR(S)**

doxorubicin. These results indicated the preference for the piperidine and pyrrolidine substituents over morpholine moiety.

The studies of molecular docking for the most active analogous **95b**, **95f**, **95h**, and **95j** performed to establish the binding affinity (Figure 15). Results demonstrated that **95h** possesses the highest binding free energy (-7.95 kcal/mol), docked energy (-9.12 kcal/mol), RMSD (0.192 Å), and inhibition constant (76.32 uM) estimated to the protein structure of 3UT5. Also, compound **95h** showed binding free energy and docked free energy equal (-7.32 kcal/mol) and (-9.25 kcal/mol), respectively, and estimated inhibition constant 95.12 uM to another protein 5TVQ.

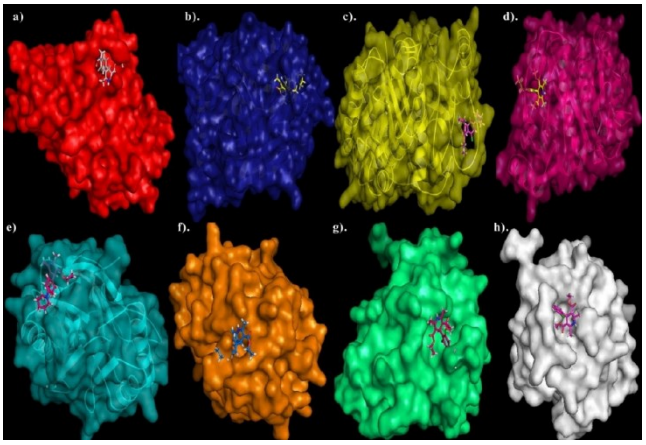
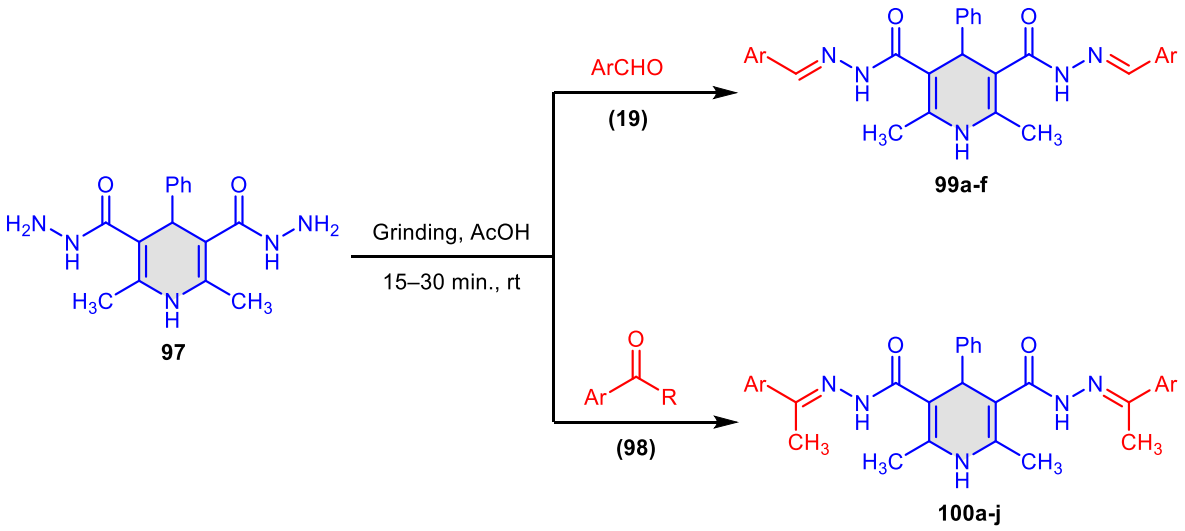


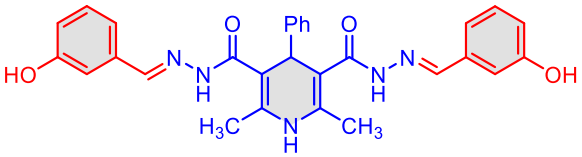
Figure 15. Docking interaction between synthesized compounds ligands **95b**, **95f**, **95h**, and **96j** and its proteins (3UT5 and 5TVQ) images produced from Pymol. **a**) 3UT5 with derivative **95b**; **b**) 3UT5 with derivative **95f**; **c**) 3UT5 with derivative **95h**; **d**) 3UT5 with derivative **96j**; **e**) 5TVQ with derivative **95b**; **f**) 5TVQ with derivative **95f**; **g**). 5TVQ with derivative **95h**; **h**). 5TVQ with derivative **96j**. Reproduced from Ref.;[83] Copyright 2022; Wiley.

The results indicated those amino acids Phe-126, 230 & 291, Leu-218& 337, Arg-247 & 331 plays a crucial roles in anchoring these ligands to their target proteins (3UT5 and 5TVQ).

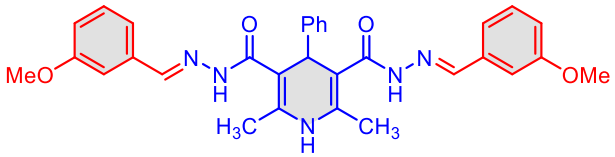
Recently 1,4-dihydropyridines proved to be highly successful multidrug agents for cancer treatment.[84] Heterocyclic hydrazones are bioactive reagents with a broad variety of biological activity.[85,86] A variety of novel 1,4-dihydropyridine-3,5-dicarbohydrazones **99a-f** and **100a-j** have been efficiently synthesized *via* a solvent-free grinding of 2,6-dimethyl-4-phenyl-1,4-dihydropyridine-3,5-dicarbohydrazides (**97**) with a diversity of carbonyl compounds without using catalyst at ambient temperature (Scheme 22).[87]

 ©AUTHOR(S)

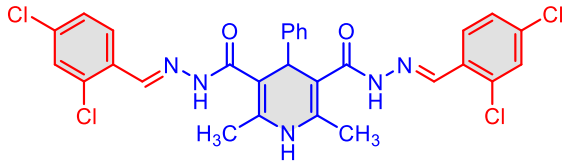




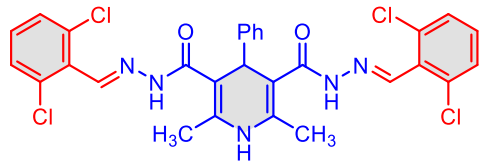
99a



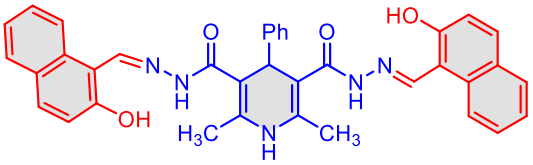
99b



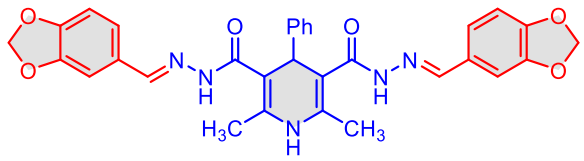
99c



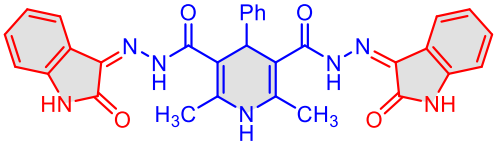
99d



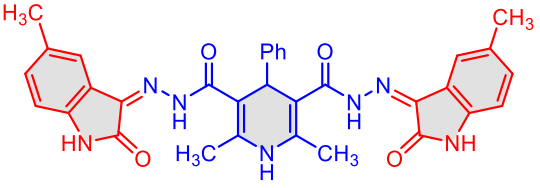
99e



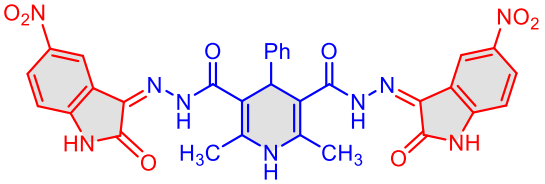
99f



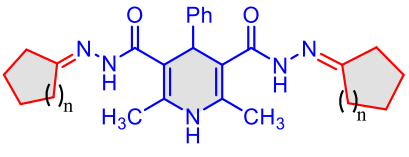
100a



100b

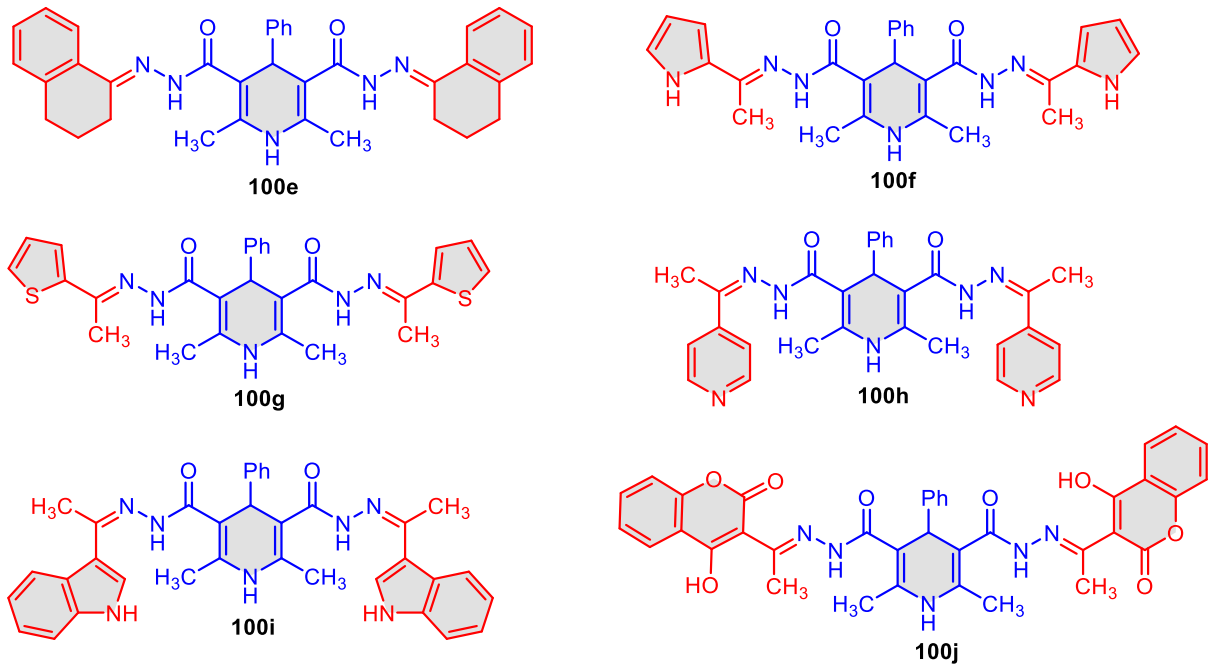


100c



100d (n= 0, 1, 2, 3)

©**AUTHOR(S)**



Scheme 22. Synthesis of *bis*-hydrazones **99a-f** and **100a-j**.

Samples **99c**, and **100g** evaluated for their *in vitro* inhibitory activity against human Hepatocellular carcinoma (HepG2) cell lines. Compounds 99c and 100g exhibited moderate in vitro cytotoxicity, with IC_{50} values of 16.67 ± 3.1 and 15.2 ± 2.1 µM, respectively. In addition, bis-pyridine **99c** that possess electron-withdrawing substituents revealed a higher cytotoxic activity than those possessing electron-donating substituents. Moreover, scaffolds with phenyl groups **99a,b** have greater activity than those with polynuclear aromatic hydrocarbons with IC_{50} values of 30.8 and 16.67 uM **99e**. Bis-pyridine with thiophene **100g** moiety with Ic50 equals 15.20 more potent than those pyrroles **100f** with Ic50 33.30 uM.

Molecular docking into DYRK1A enzyme, which often overexpressed in tumors, established the fact that these ligands compete for the ATP-binding site. The docking protocol was validated by redocking the co-crystallized inhibitor harmine, yielding RMSD values of 0.4495 Å thereby supporting its ability to reproduce the crystallographic pose. The research suggests that the drug-likeness and conformational flexibility of 100g allow it to interact effectively with catalytic Asp307 residue (Figures 16A and 16B).

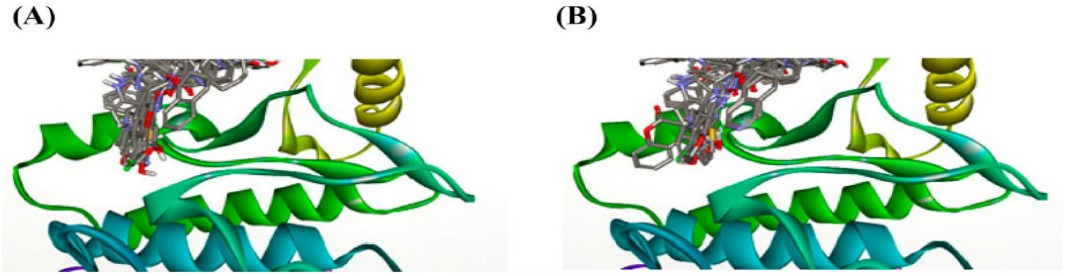


Figure 16. The ligands docked globally on the left (**A**) versus locally on the right (**B**). Reproduced with permission from Ref.;[87] Copyright 2020; Taylor & Francis.

This could be rationalized by the high drug-likeness of **100g** resulted in rendering its pharmacokinetics behavior more convenient to the cellular environment (Figures 17).

 ©**AUTHOR(S)**

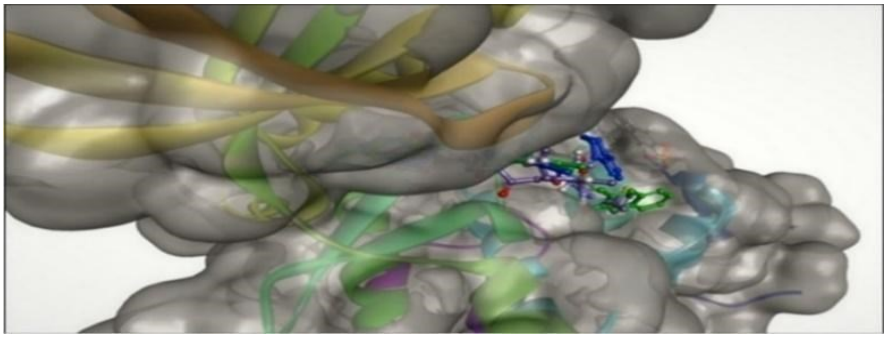


Figure 17. Compounds **99e** (green), **100e** (blue), and **100g** (purple) binding to the surface of DYRK1A and reaching to the ATP binding pocket. Reproduced with permission from Ref.;[87] Copyright 2020; Taylor & Francis.

Finally, the authors reported the interaction of **99e** within both LEU241 and the catalytic ASP307 residues; compounded **100e** exhibited interactions with the ATP anchor LYS188 as well as the catalytic ASP307, which established the interactions of **99e** with two of the important DYRK1A residues and the rendering of compound **100e** ATP binding to its pocket (Figure 18).

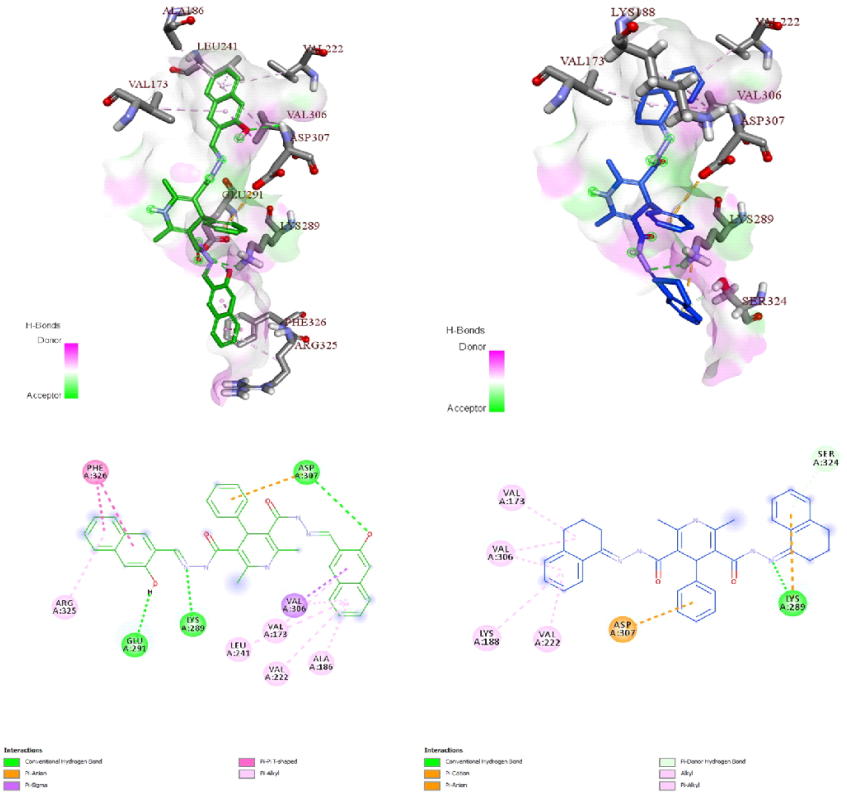


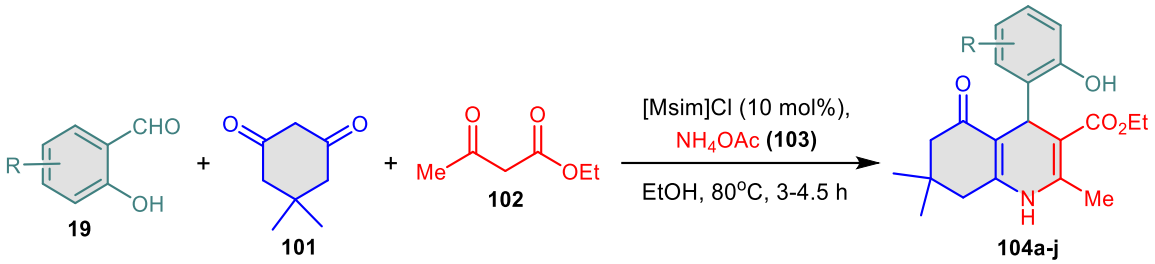
Figure 18. Compounds **99e** and **100e** interactions on the left and right sides respectively (2D over the bottom and 3D on the top). Reproduced with permission from Ref.;[87] Copyright 2020; Taylor & Francis.

3.2. Quinolines synthesis

Quinolines referred as important anti-cancer hetrocycles for their acting as topoisomerase inhibitors or sirtuin inhibitors. To elaborate the benefits of utilizing ionic liquids as green solvents than other existing protocols for the synthesis of polyhydroquinolines, Bhusare and coauthors[88] performed a green synthesis of bioactive polyhydroquinolines **104a-j**. Reported procedure involving reaction of substituted salicylaldehyde derivatives

 ©**AUTHOR(S)**

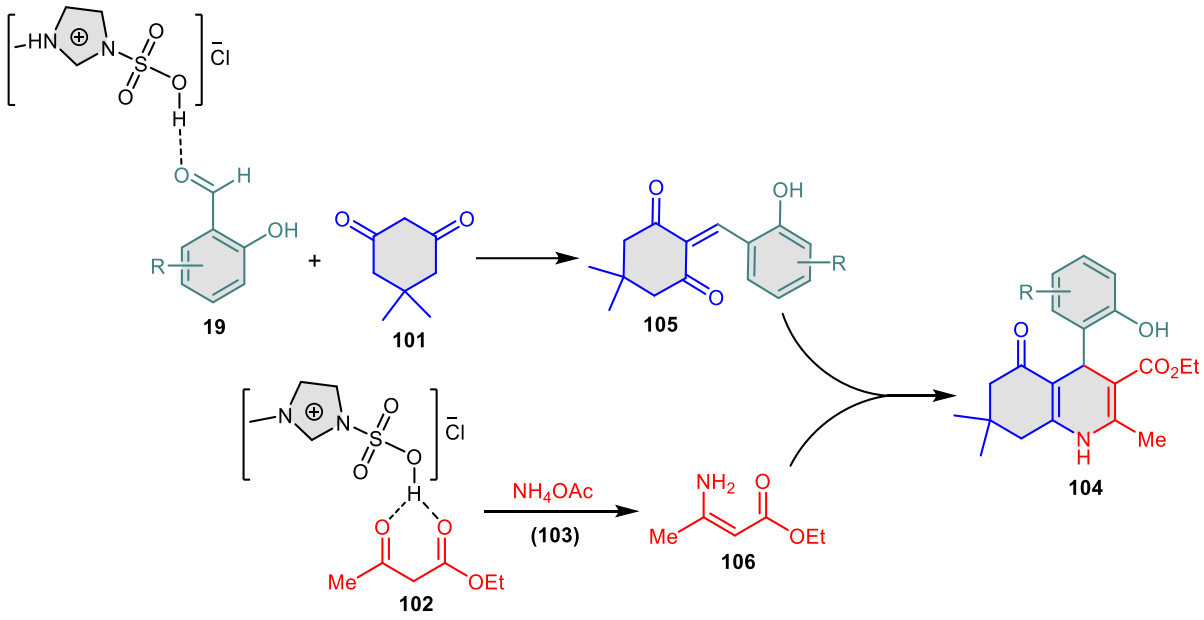
19, dimedone (**101**), ethylacetoacetate (**102**), and ammonium acetate (**103**) utilizing 3-methyl-1-sulfonic acid imidazolium chloride ([Msim]Cl) which acts as solvent and catalyst in excellent yields (Scheme 23). Atom economy of the reaction revealed a value of 75.70% indicating a good incorporation of reactants to final product. The E-factor calculated for the reaction showed a value of 4.41 conditioned by recycling of both ionic liquid and ethanol solvent.



104a-j: a, R= H; **b**, R= 3,5-$(I)_2$; **c**, R= 3,5-$(Br)_2$; **d**, R= 5-Cl; **e**, R= 5-I; **f**, R= 5-Br; **g**, R= 3-OCH_3; **h**, R= 3,5-$(Cl)_2$; **i**, R= 3-OCH_3-5-Br; **j**, R= 5-NO_2.

Scheme 23. Synthesis of polyhydroquinoline derivatives **104a-j**.

The mechanism for the formation of the reaction products depicted in Scheme 24.



Scheme 24. A plausible mechanism for the synthesis of polyhydroquinolines **104**.

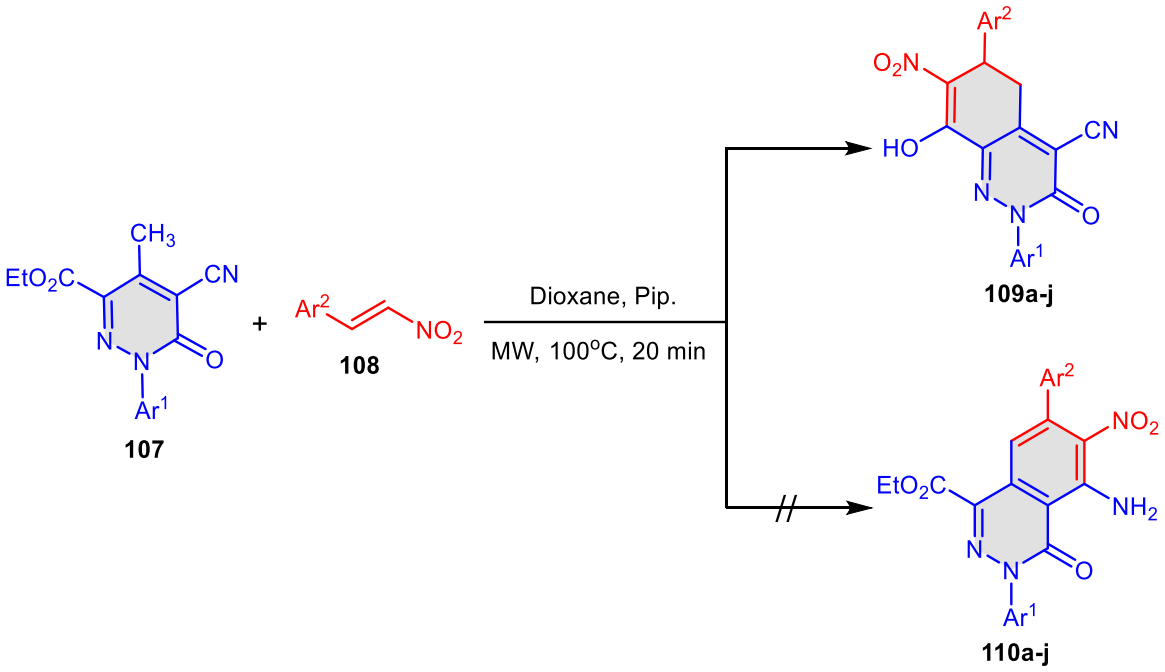
Authors reported the *in vitro* antiproliferative properties of the obtained compounds against human breast cancer line (MCF7) compared to the reference Adriamycin. Compound 104g displayed significant activity breast cancer cells (MIC= 23.66 µM), with total growth inhibition exceeding 80% indicating the possibility to be developed as novel lead structures for potential anticancer scaffolds. compounds **104b**, **104c,** and **104j** exhibit total growth inhibition (TGI) > 80%, indicating the possibility to be developed as novel lead structures for potential anticancer scaffolds.

 ©**AUTHOR(S)**

3.3. Cinnolines synthesis

Cinnolines are an important class of heterocycles and possess a remarkable interest as promising scaffolds utilized as potential anti-cancer agents.[89,90] Synthesis of cinnolines has received little attention, and most of the reported conventional methods for their synthesis suffer from drawbacks of restricted substrate scope and harsh reaction conditions.[91–95]

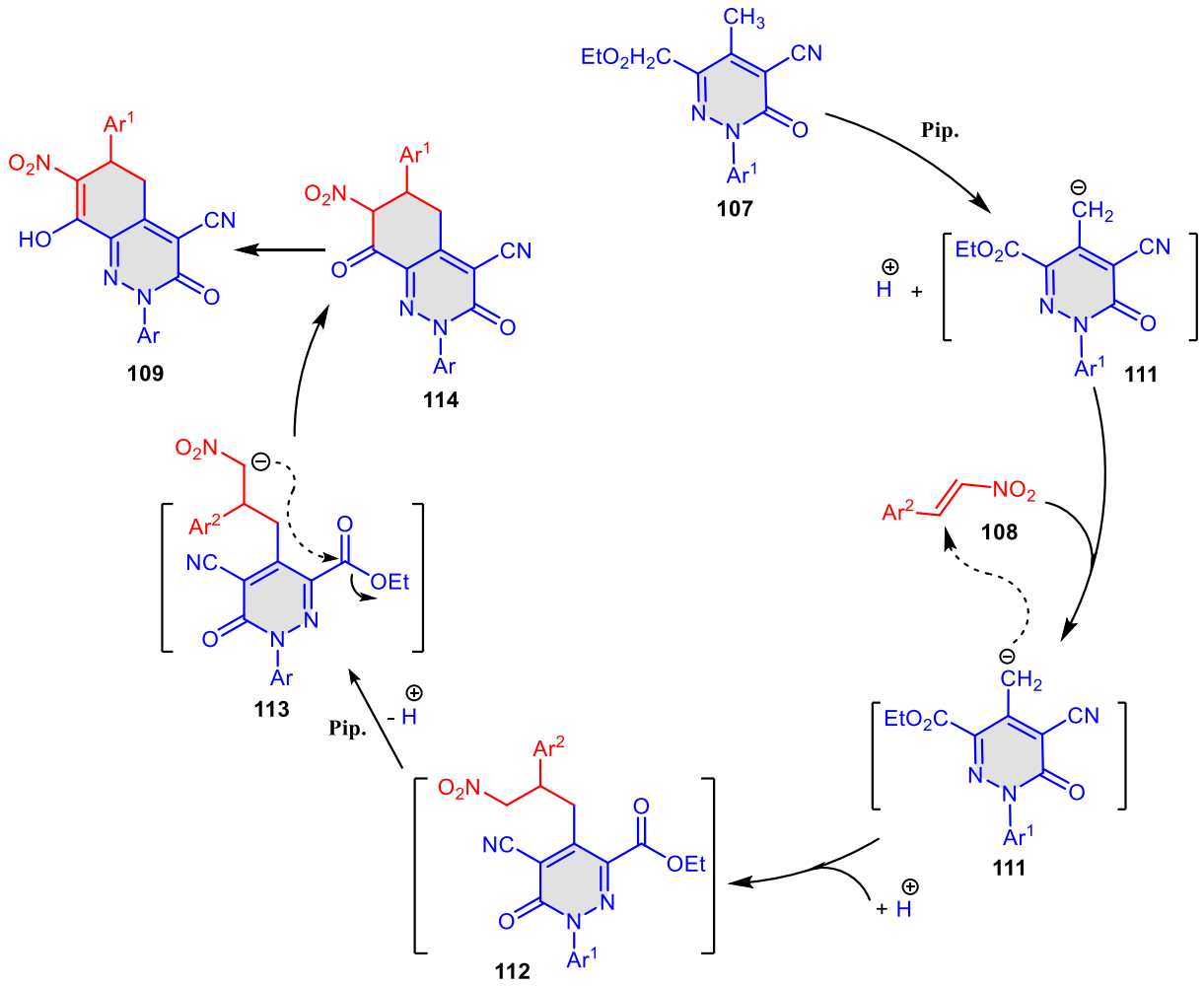
Recently, Sadek *et al.*[96] have reported an efficient and green one-pot synthesis with high-yield of polyfunctionally substituted cinnoline-4-carbonitrile derivatives **180a-j** through reaction of ethyl-5-cyano-4-methyl-1-aryl-6-oxo-1,6-dihydropyridazine-3-carboxylates **178** and nitroolefins **179** promoted by microwave irradiation (Scheme 25). Analytical and spectroscopic data ruled out the possibility of phthalazines **181** production.



109a-j: **a**, Ar^1= 4-$CH_3C_6H_4$, Ar^2= C_6H_5; **b**, Ar^1= 4-$CH_3C_6H_4$, Ar^2= 3-$NO_2C_6H_4$; **c**, Ar^1= 4-$CH_3C_6H_4$, Ar^2= 4-$OCH_3C_6H_4$; **d**, Ar^1= 4-$CH_3C_6H_4$, Ar^2= 4-ClC_6H_4; **e**, Ar^1= C_6H_5, Ar^2= 4-ClC_6H_4; **f**, Ar^1= C_6H_5, Ar^2= 4-$OCH_3C_6H_4$; **g**, Ar^1= Ar^2= C_6H_5; **h**, Ar^1= C_6H_5, Ar^2= 3-$NO_2C_6H_4$; **i**, Ar^1= 3-ClC_6H_4, Ar^2= C_6H_5; **j**, Ar^1= 4-$CH_3C_6H_4$, Ar^2= 2-furyl.

Scheme 25. Synthesis of polyfunctionally substituted cinnoline-4-carbonitrile derivatives **109a-j**.The Suggested mechanism for the formation of polyfunctionally-substituted cinnoline **109** depicted in (Scheme 26).

 ©**AUTHOR(S)**



Scheme 26. Mechanism for the formation of polyfunctionally substituted cinnoline **109**.

A unique green methodology involves conducting this synthesis inside *Lycopodium Clavatum sporopollenin* (LCS) microcapsules under microwave irradiation reported by Dyab and Sadek [97]. These natural microcapsules act as microwave microreactors, allowing for high-yield synthesis in a safe, controlled environment. Compound **109g** showed remarkable activity against leukemia (RPMI 8226) and melanoma (LOX IMVI) cell lines with IC_{50} values of 17.12 and 12.3 µM, respectively. Mechanistic studies showed that **109g** induces apoptosis through pre-G1 cell cycle arrest and the upregulation of pro-appoptotic proteins like Bax and Caspase-3. Indicating the possibility to developed as novel lead structures for potential anticancer scaffolds. The successful formation of capsulated cinnoline derivatives **109a-j** inside the LCS microcapsules without any alterations, pure cinnoline recovered from the cinn-loaded (LCS), which subjected to a diversity of biological activity studies, including anti-cancer activities (Figure 19).

 ©**AUTHOR(S)**

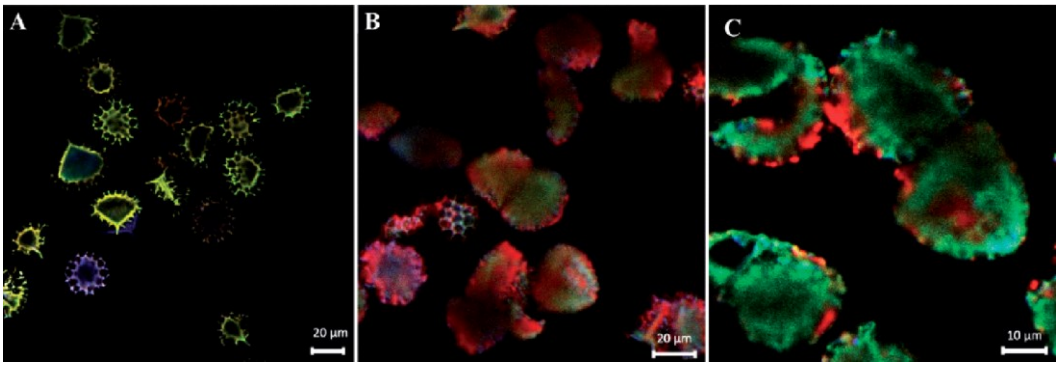
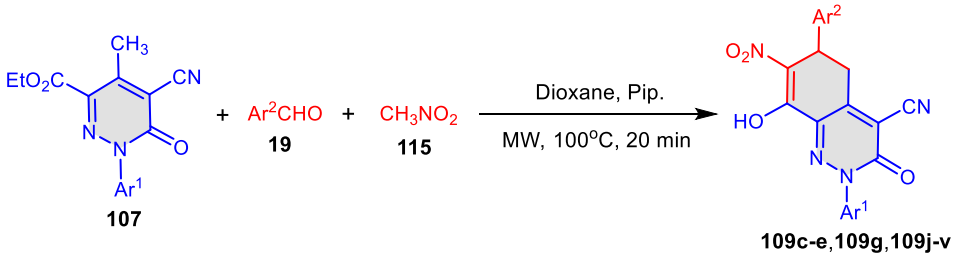


Figure 19. CLSM images of (**A**) empty LCS microcapsules, (**B**) cinn-loaded LCS microcapsules at a random focus location, and (**C**) cinn-loaded LCS at a slice depth of 14.6 µm are superimposed. Reproduced with permission from Ref.;[97] Copyright 2018; Royal Society of Chemistry.

Very recently, the multi-component one-pot reaction was successfully extended to the synthesis of **109c-e**, **109g**, and **109j-v** in high yields that included the reaction of **107** with aromatic aldehydes **19** and nitromethane (**115**) under the same reported reaction conditions (Scheme 27).[98]

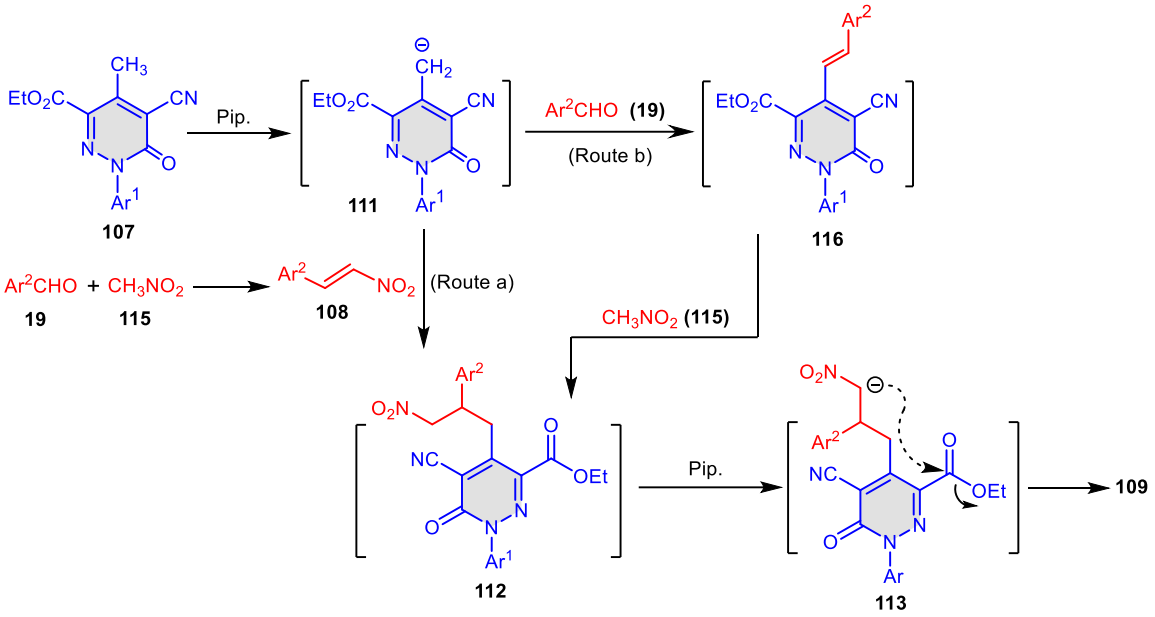


109c-e,**109g**,**109j-v**: **c**, Ar^1= 4-$CH_3C_6H_4$, Ar^2= 4-$OCH_3C_6H_4$; **d**, Ar^1= 4-$CH_3C_6H_4$, Ar^2= 4-ClC_6H_4; **e**, Ar^1= C_6H_5, Ar^2= 4-ClC_6H_4; **g**, Ar^1= Ar^2= C_6H_5; **j**, Ar^1= 4-$CH_3C_6H_4$, Ar^2= 2-furyl; **k**, Ar^1= C_6H_5, Ar^2= 2-furyl; **l**, Ar^1= C_6H_5, Ar^2= 4-$NO_2C_6H_4$; **m**, Ar^1= 4-$CH_3C_6H_4$, Ar^2= 3,4,5$(OCH_3)_3C_6H_2$; **n**, Ar^1= 4-$CH_3C_6H_4$, Ar^2= 2-ClC_6H_4; **o**, Ar^1= 4-$CH_3C_6H_4$, Ar^2= 4-$NO_2C_6H_4$; **p**, Ar^1= 4-$OCH_3C_6H_4$, Ar^2= 2-furyl; **q**, Ar^1= 4-$OCH_3C_6H_4$, Ar^2= C_6H_5; **r**, Ar^1= 4-$OCH_3C_6H_4$, Ar^2= 4-ClC_6H_4; **s**, Ar^1= 3-ClC_6H_4, Ar^2= 2-furyl; **t**, Ar^1= 3-ClC_6H_4, Ar^2= 4-ClC_6H_4; **v**, Ar^1= 3-ClC_6H_4, Ar^2= 4-$OCH_3C_6H_4$.

Scheme 27. Synthesis of cinnoline derivatives **109c-e**, **109g**, and **109j-v**.

A mechanism to account for the formation of **109c-e**, **109g,** and **109j-v** as proposed in Scheme 28. The procedure involves the formation of common intermediate **112** either *via* the reaction of Henry reaction product **108** with the carbanion **111**, which is formed by the action of base on **107** (Route a) or nucleophilic attack of **111** to aldehyde **19** which produced ylidene derivative **116** followed by reaction with nitromethane (**115**) (Route b). The final isolable product **109** formed through nucleophilic carbanion **113** at the ester carbonyl group with ethanol loss. (Route a) was preferred over (Route b) as the reactivity of the nitromethane methyl group is greater than that of the pyridazine **107**.

 ©**AUTHOR(S)**



Scheme 28. Proposed mechanism for the formation cinnolines **109** of *via* multi-component reaction.

The *in vitro* anti-cancer activity *via* apoptosis induction was evaluated for selected cinnolines **109c-e**, **109g**, and **109j-v** against sixty different cell lines of nine different panels of cancers, colon, ovarian, prostate, leukemia, melanoma, CNS, renal, breast, and lung cancer, and the results were displayed as growth inhibition percentage (GI%) caused by tested cinnolines. The interesting results highlighted remarkable patterns of selectivity and sensitivity toward the different NCI cancer cell panels. In this context, compound **109g** showed the most activity against leukemia RPMI-8226 and melanoma LOX IMVI cell lines (GI% = 106.06 and 82.1), respectively. It is noteworthy to mention that the nature of substituents on both aryl moieties affected the activity of tested cinnolines. Unsubstituted aryl groups found to be essential for higher activity. Either electron-withdrawing or electron-donating substituents in aryl group at position 6 cause a dramatic decrease in reactivity.

The IC_{50} values of **109g** against leukemia RPMI-8226 and melanoma LOX IMVI cells were 17.12 ± 1.31 and 12.32 ± 0.75 µg/mL, respectively. In the same study, the reference inhibitor staurosporine gave IC_{50} values of 24.97 ± 1.47 and 8.45 ± 0.42 µg/mL, respectively. Thus, **109g** was more active than staurosporine against RPMI-8226 but less active against LOX IMVI under the reported conditions.

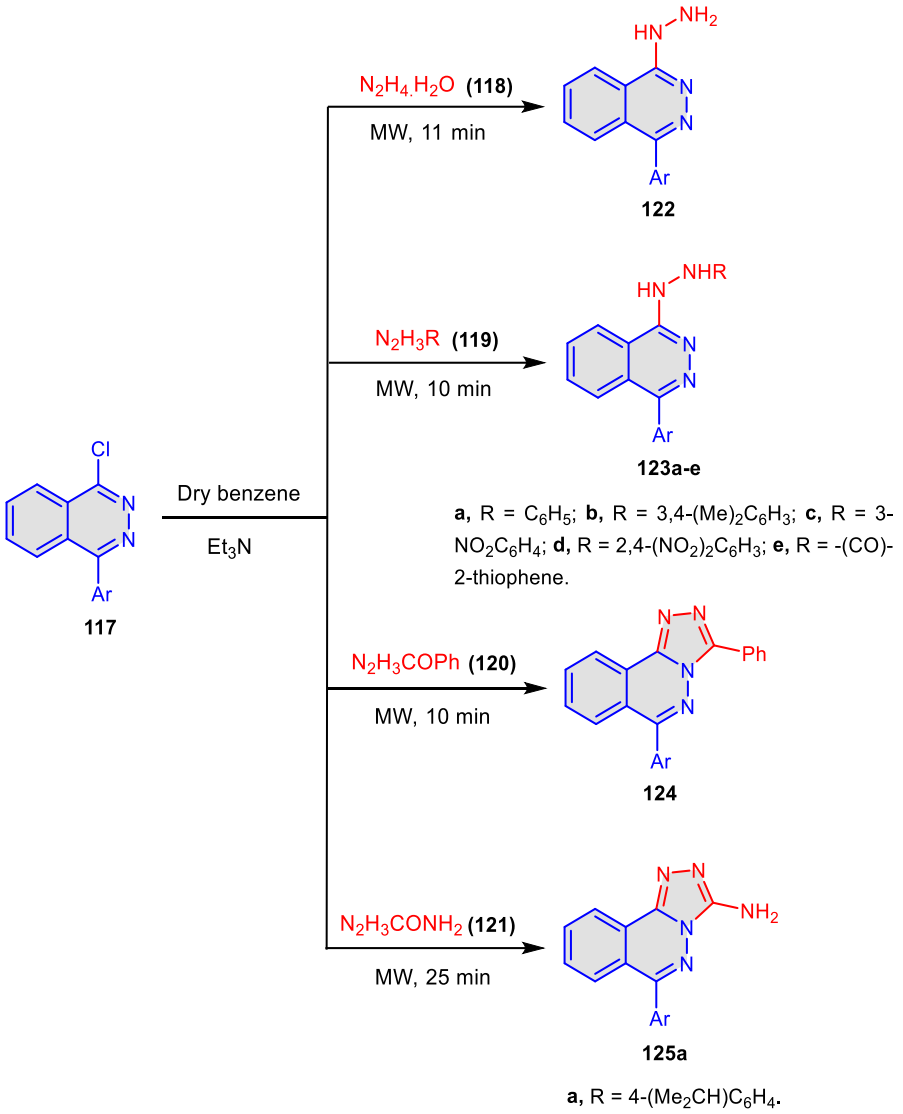
Against normal human lung fibroblast WI38 cells, **109g** showed an IC_{50} of 23.62 ± 8.57 µg/mL. The corresponding SI values were 1.38 for RPMI-8226 and 1.92 for LOX IMVI. These values indicate only modest preferential cytotoxicity toward the cancer cells and therefore do not support characterization of **109g** as highly selective.

The cell cycle distribution after treatment with **109g** in leukemia RPMI-8226 and melanoma LOX IMVI cell lines analyzed. The the results demonstrated that an increase of cell number at pre-G1 and G2/M phases and a decrease of cell number at S and G0/G1 phases was achieved and evidence by pre-G1 apoptosis and growth arrest at G2/M phase. Moreover, it induced apoptosis in both cell lines, which increases the presence of annexin V-FITC positive apoptotic cells in leukemia RPMI-8226 and melanoma LOX IMVI cell lines (from 1.09% to 12.47%) and (from 1.32% to 19.05%) respectively. In addition to lower expression levels of pro-apoptotic proteins; Bax, p53, cytochrome c, caspases 3 and 9.

©**AUTHOR(S)**

3.4. Phthalazines synthesis

In 202,4, Abdalla and co-authors[99] developed microwave assisted synthesis of diverse phthalazine derivatives **122-125** utilizing 4-chlorophthalazine precursors **117** with various hydrazine derivatives **118-121** in dry benzene with Et_3N as a catalyst (Scheme 29).



Scheme 29. Synthesis of diverse phthalazine derivatives **122-125**.

Synthesized compounds **122-125** have been tested against three-cancer cell lines (MCF-7, HCT116 and HepG2), respectively. The activity results showed that compound **123c** exhibits the best activity with IC_{50} values of 1.739 µM, 0.384 µM, and 1.52 µM utilizing Doxorubicin as a standard drug. Surface mapping and Docking into the PARP-1 active site (PDB: 7aad) confirmed the phthalazine core engaging in π-π stacking interactions while the side chains from multiple hydrogen bonds with the enzyme's residues (Figure 20).

 ©**AUTHOR(S)**

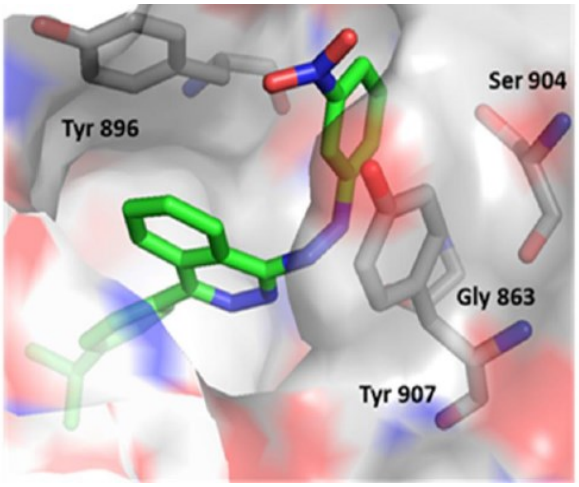


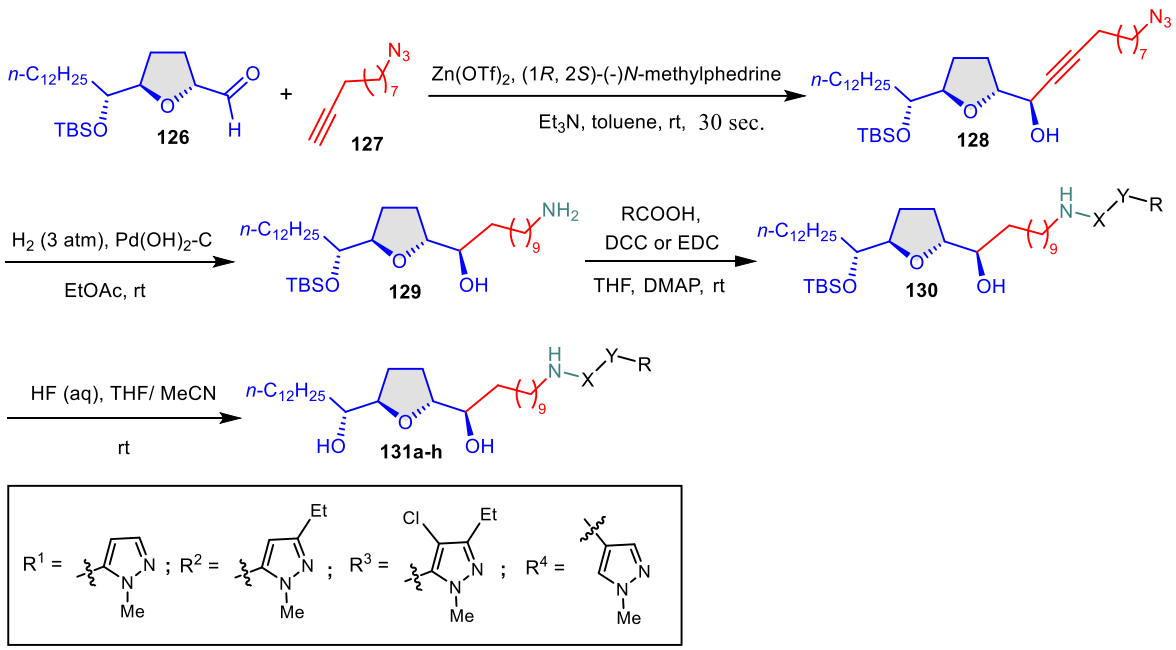
Figure 20. Surface representation of compound **123c** bound to PARP-1 (PDB code: 7aad) active site. Reproduced with permission from Ref.;[99] Copyright 2024; Taylor & Francis.

4. Oxygen, Sulphur and Nitrogen Heterocycles

4.1. Furans

Annonaceous acerogenins' are naturally occurring polyketides extracted from Annona plants that were known to reveal anti-cancer activity towards human cancer cell lines *via* mitochondrial complex I inhibition.[100] They mostly incorporate up to three tetrahydrofuran rings centered in long hydrocarbon chain and terminal α,β-unsaturated-γ-lactone ring. Kojima and co-authors[101] designed an effective synthesis of hybrid 1-methylpyrazole-linker moiety with tetrahydrofuran **131a-h** at ambient temperature as a novel anti-cancer reagent (Scheme 30).

 ©**AUTHOR(S)**



131a-h: a, X= NH, Y= C(O), R= R^1; **b,** X= NH, Y= C(O), R= R^2; **c,** X= NH, Y= C(O), R= R^3; **d**, X= NH, Y= C(O), R= R^4; **e**, X= NH, Y= SO_2, R= R^1; **f**, X= NH, Y= SO_2, R= R^4; **g**, X= NMe, Y= C(O), R= R^1; **h**, X= NH, Y= CH_2, R= R^1.

DCC = *N,N'*-dicyclohexylcarbodiimide, **EDC** = 1-(3-dimethylaminopropyl)-3-ethylcarbodiimide, **DMAP** = *N,N*-dimethylaminopyridine.

Scheme 30. Synthesis of hybrid 1-methylpyrazole-linker moiety with tetrahydrofuran **131a**–**h**.

Amide **131a** possesses highly potent and selective inhibition activities against BSY-1, HCT-116, NCI-H23, DMS114, LOX-IMVI, MKN-B, and MKN-A cell lines; however, the remaining twelve cell lines not affected. Compounds **131j**, **131k**, **131e**, **131g**, and **131h** showed similar inhibition but low selectivity against DMS114, MKNB and MKN-A. The authors concluded that the linker nitrogen atom at 2-position plays a crucial role in cancer growth inhibition.

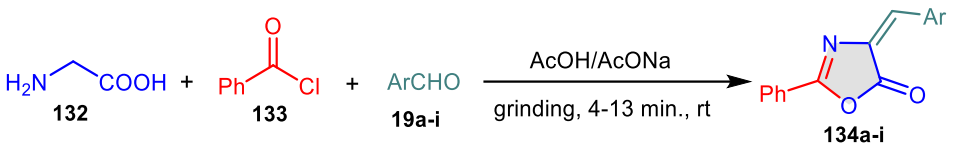
4.2. Oxazoles

Mechanochemical revealed as a green synthetic approach in terms of simplicity, operation under solvent-free conditions with high atom economy, low energy requirements, and high yields. The generation of local heat due to the collision of the crystals of two different reagents highlighted the increase in energy efficiency achieved *via* utilizing such technique.[102]

Several reports described the potential activity of oxazole as precursors in the synthesis of several small molecules and as bioactive scaffolds, particularly as anti-cancer reagents.[103,104]

El-Sayed *et al.*[105] developed a one-pot, multi-component green synthesis of 4-arylidine-2-phenyl-5(4*H*)-oxazolones (azlactones) **134a-i** in high yields through grinding glycine (**132**), benzoyl chloride (**133**) and aromatic aldehydes **19a-i** catalyzed by fused sodium acetate in drops of AcOH were present (Scheme 31). Calculated reaction Atom-Economy equals 77.3 %, which is remarkably good incorporating that most of all reactant atoms are utilized in the reaction course. E-Factor showed a value of 0.26 revealing the environmental impact of such protocol.

 ©**AUTHOR(S)**



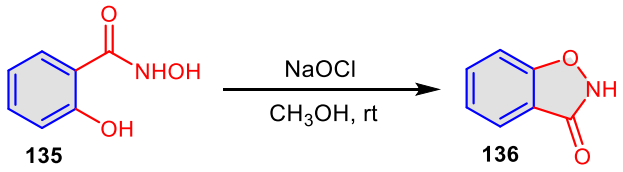
19a-i; 134a-i: **a**, Ar= C_6H_5; **b**, Ar= 4-$MeOC_6H_4$; **c**, Ar= 4-ClC_6H_4; **d**, Ar= 4-Me_2N-C_6H_4; **e**, Ar= 4-$NO_2C_6H_4$; **f**, Ar= 2-ClC_6H_4; **g**, Ar= 2-BrC_6H_4; **h**, Ar= 3,4-(OMe)-C_6H_3; **i**, Ar= -CH=CHC_6H_5.

Scheme 31. Multicomponent synthesis of 4-arylidine-2-phenyl-5(4*H*)-oxazolones **134a-i.**

4.3. Benzisoxazoline

As a reactive oxygen species (ROS), the hypochlorite ion (ClO^-) generated by living systems *via* myeloperoxidase (MPO) catalyzed peroxidation of chloride ion has received great interest due to the diversity of biological roles it plays.[106] It was demonstrated that the abnormal production of ClO^- with its high reactivity and non-selectivity can lead to cancer disease.[107] Thus, developing methods for selective and sensitive detection of ClO^- ions always desired.

A straightforward, efficient, and environmentally friendly synthesis of fluorescent 1,2-benzisoxazoline-3-one (**136**) has been devised in which hypochlorite ion was utilized as a catalyst allowing a route for its sense (Scheme 32).[108]



Scheme 32. Synthesis of 1,2-benzisoxazole-3-one (**136**).

In a preliminary study, authors evaluated the emission spectra fluorescence changes that occur when (10 mM, pH 7.4) HEPES solution of **135** was treated with (1.0 equiv) of ClO^- and other ROS (10 equiv, H_2O_2, $^1O_2$, $\cdot O^{2-}$, $ROO\cdot$, $NO\cdot$ and $\cdot OH$). Only ClO^- affords **136** associated with a large fluorescence intensity with a maximum at 415 nM (300 nM excitation).

The reaction time profile for the reaction of **135** with ClO^- estimated, which shows completion of the reaction within 30 seconds under the reaction conditions, which clearly imparts the possibility for quantitative detection of ClO^-.

In a subsequent step, the visualization of ClO^- with living cell liver hepatocellular carcinoma HepG2 evaluated. When HepG2 cells incubated with 2.5 µM of **135** at 37 °C for 30 minutes, it does not fluoresce even when excited at 300 nM. However, repeating the experiment with 2 µM of **135** then treated with 5 µM of ClO^- a blue fluorescence was displayed demonstrating that compound **135** is permeable to living cells and can be used to determine ClO^-.

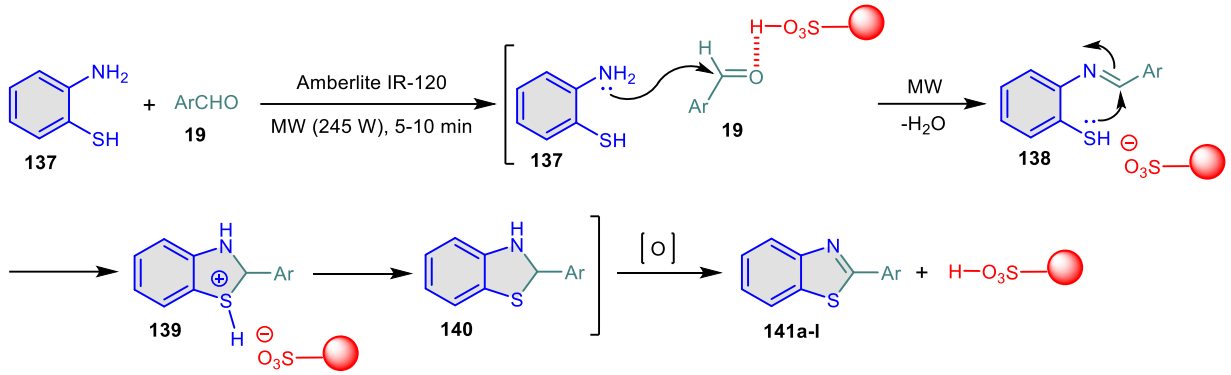
4.4. Benzothiazole synthesis

Benzothiazoles have a significant role to many therapeutic and diagnostic agents. Benzothiazole derivatives were known to be effective in treating a variety of various cancers.[109–113]

Green synthetic route utilizing reusable Amberlite IR-120 resin as a catalyst under microwave irradiation have been developed to synthesize diversity of 2-aryl/heteroaryl benzothiazoles **141a-l** in 88-92% yield (Scheme

 ©**AUTHOR(S)**

33). The atom Economy of the reaction revealed high value equals 99.34, which represents a highly effective incorporation of atoms. The E-factor further minimized by the use of MW irradiation that reduces the reaction time as well as minimizing thermal degradation. The calculated E-Factor is 0.34 reflects the efficiency and greens of the described protocol.



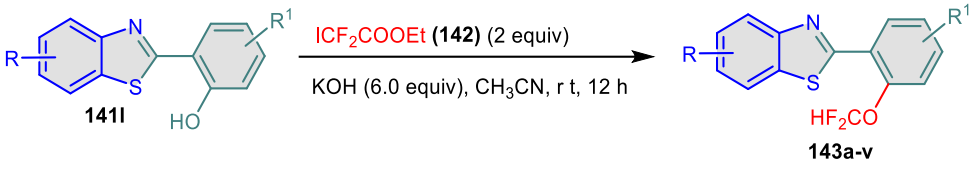
141a-l: **a**, Ar= C_6H_5; **b**, Ar= 2-ClC_6H_4; **c**, Ar= 2-$CH_3C_6H_4$; **d**, Ar= 4-FC_6H_4; **e**, Ar= 2-BrC_6H; **f**, Ar= 2-furyl; **g**, Ar= 2-indolyl; **h**, Ar= 1-naphthyl; **i**, Ar= 2-OH-3-$OCH_3C_6H_3$; **j**, Ar= 2-thienyl; **k**, Ar= 2-pyridyl; **l**, 2-OHC_6H_4.

Scheme 33. Synthesis 2-aryl/heteroaryl benzothiazoles **141a-l** using Amberlite IR-120.

These compounds exhibit IC_{50} values in the rangr of 9-32 against breast (MCF-7) and cervical (Hela) cancer cell lines. µM cell line (MCF-7) cell lines evaluated. Most of the products yielded IC_{50} values of 9-28 µM against MCF-7 cells and 15-32 µM against Hela cell lines. The introduction of electron-withdrawing groups (halogens) at the 2-aryl substituent found to increase cytotoxicity, likely by enhancing molecules interaction with DNA or cellular enzymes.

The remarkable potent pharmaceutical and biological activity of organofluorine compounds has attracted great interest in developing new synthetic routes of such scaffolds. A wide range of benzothiazoles containing (-OCF_2H) is highly desired.

Luo and Ding established a cascade green and efficient synthesis of 2-(2-(difluoromethoxy)aryl)benzo[*d*]thiazoles **143a-v** and examined their anti-cancer activity.[114] In particular, they described the fluorination of 2-(2'-hydroxyphenyl)benzothiazole **141l** with ethyl difluoroiodoacetate (**142**) promoted by KOH (6.0 equiv) in acetonitrile at ambient temperature (Scheme 34).

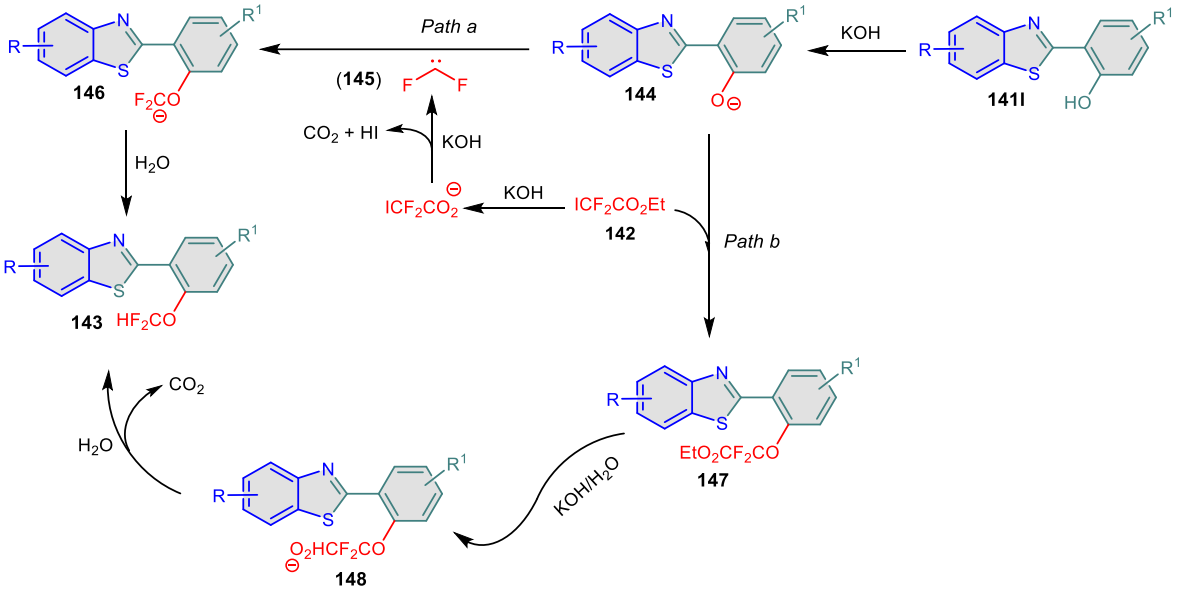


143a-v: **a**, R= R^1= H; **b,** R= H, R^1= 4-OMe; **c**, R= H, R^1= 4-NEt_2; **d**, R= H, R^1= 4-CH_3; **e**, R= H, R^1= 4-F; **f**, R= H, R^1= 5-OMe; **g**, R= H, R^1= 5-CH_3; **h**, R= H, R^1= 5-Br; **i**, R= H, R^1= 5-Cl; **j**, R= H, R^1= 5-F; **k**, R= H, R^1= 5-NO_2; **l**, R = H, R^1= 6-Br; **m**, R = H, R^1= 6-F; **n**, R= H, R^1= 6-Cl; **o**, R = H, R^1= 5,6-(–CH=CHCH=CH–); **p**, R = H, R^1= 3,5-$(Br)_2$; **q**, R= H, R^1= 3-Br,5-Cl; **r**, R= 5-OMe, R^1= H; **s**, R= 5-Cl, R^1= H, **t**, R= 5-Cl, R^1= 5-OMe; **u**, R= 5-Cl, R^1= 5-Br; **v**, R= 5-Cl, R^1= 5-NO_2.

Scheme 34. Fluorination of 2-(2'-hydroxyphenyl)benzothiazole **141l**.

 ©**AUTHOR(S)**

A plausible mechanism for this process depicted in Scheme 35 involves two different routes. The first involves *in situ* formation of difluorocarbene **145,** which is generated *via* the action of KOH on ethyl difluoroiodoacetate (**142**) and then attacked by thiazolyl phenoxide ion **144** followed by conversion to the final isolable product **143** in the presence of water (Path a). The second process is intermolecular substitution of **144** with **142** yielding **147**, followed by base hydrolysis, which formed **148**, and then decarboxylation occurred to produce the final product **143** (Path b).



Scheme 35. A plausible mechanism for the difluoromethoxylation.

Compound **143l** showed an IC_{50} of 92.0 µM against SKOV3 cells after 48 h, indicating modest cellular potency. Although the original study reported a more favorable response than cisplatin in a specific time-course comparison, the high-micromolar IC_{50} does not justify a general claim of superior anticancer potency. The biological significance of this result should therefore be considered preliminary and assay-dependent.

4.5. Coumarines synthesis

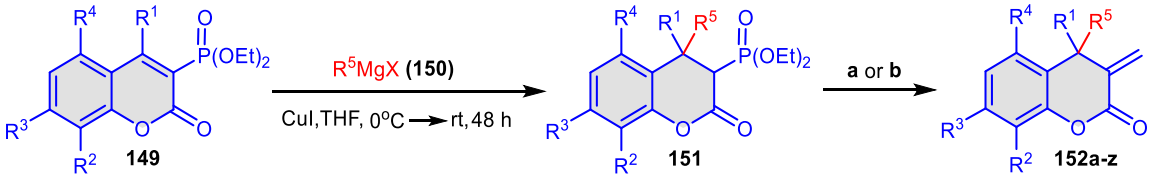
Coumarin derivatives have emerged as one of the most privileged classes of natural products, which established a track record of biological activities in which cytotoxic activity is well recognized.[115–118] The structurally related *α*-methylidene-*δ*-lactone hybrid with chroman-2-one skeleton is not present in natural compounds. Janecki and co-authors[119] introduced a convenient procedure for the synthesis of 4,4-disubstituted 3-methylidenechroman-2-ones **152a-z** from 4,4-disubstituted 3-diethoxyphosphoryl-3,4-dihydro-2*H*-chroman-2-ones **279** *via* Horner-Wadsworth-Emmons olefination. Compound **151** formed from the reaction of 4-substituted 3-diethoxyphosphorylochromen-2-ones **149** with Grignard reagents **150** and catalyzed by amounts of CuI in THF at 0 °C (Scheme 36).

Selected compounds showed submicromolar activity against HL-60 and NALM-6 leukemia cells. Compound **152j** was the most active against NALM-6 cells (IC_{50} = 0.66 µM), demonstrating strong cellular potency in that model.

The SAR analysis demonstrated that the nature of substituents at the C-4 position is the primary determinant of cytotoxicity.. Compound **152j** identified as the most active compound and rationalized for the presence of additional methoxy substituent in the aromatic ring. However, this phenomenon does not generally

 ©**AUTHOR(S)**

constitute a relationship between aromatic moiety and activity. The nature of R^1 and R^5 showed a remarkable influence on the activity. Very high cytotoxic activity demonstrated for compounds **152g-t** against NALM-6 cell lines.



a) $(CH_2O)_n$, NaH, THF, RT, 90 min; **b**) $(CH_2O)_n$, *t*-BuOK, THF, RT, 16 h.

Compound	R^1	R^2	R^3	R^4	R^5
152a	Me	H	OMe	H	Et
152b	Me	H	OMe	H	*n*-Bu
152c	Me	H	OMe	H	*i*-Pr
152d	Me	H	OMe	H	Bn
152e	Me	H	OMe	H	Cy
152f	Me	H	OMe	H	allyl
152g	Me	H	OMe	OMe	Et
152h	Me	H	OMe	OMe	*n*-Bu
152i	Me	H	OMe	OMe	*i*-Pr
152j	Me	H	OMe	OMe	Bn
152k	Me	H	OMe	OMe	Cy
152l	Me	-CH=CH-CH=CH-		H	Et
152m	Me	-CH=CH-CH=CH-		H	*n*-Bu
152n	Me	-CH=CH-CH=CH-		H	*i*-Pr
152o	Me	-CH=CH-CH=CH-		H	Bn
152p	Me	-CH=CH-CH=CH-		H	Cy
152q	Et	H	OMe	H	Et
152r	Et	H	OMe	H	*n*-Bu
152s	Et	H	OMe	H	*i*-Pr
152t	Et	H	OMe	H	Bn
152u	Et	H	OMe	OMe	Et
152v	Et	H	OMe	OMe	*n*-Bu
152w	Et	H	OMe	OMe	*i*-Pr
152x	Et	H	OMe	OMe	Bn
152y	*n*-Bu	H	OMe	H	*n*-Bu
152z	*n*-Bu	H	OMe	OMe	*n*-Bu

Scheme 36. Diverse synthesis of 4,4-disubstituted 3-methylidenechroman-2-ones **152a-z**.

The series was also tested against the non-cancerous HUVEC and MCF10A cell lines. Compounds **152g** and **152l** were reported to show up to approximately 10- and 13-fold greater cytotoxicity toward NALM-6 cells than

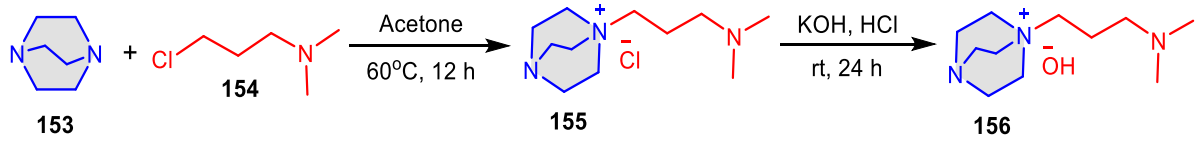
 ©**AUTHOR(S)**

toward the normal-cell models, respectively. These data provide stronger evidence of selectivity for these two analogues than potency values alone.

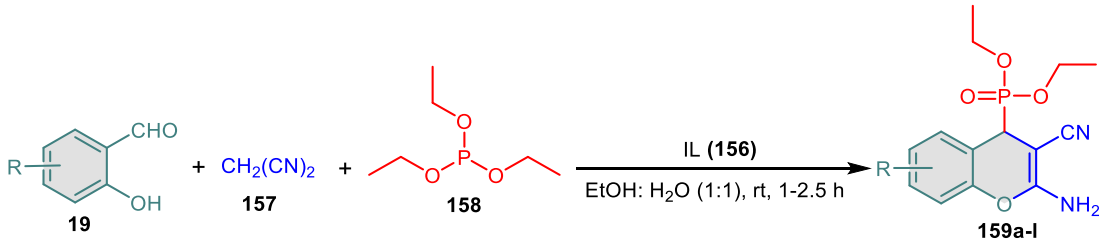
Metal chelated phosphonates have demonstrated biological and biomedical activities.[120,121] The most extensively studied protocols for their synthesis are one-pot phosphonate Michael reaction[122] and Knoevenagel condensation.[123]

Ionic liquids are highly tunable reaction medium with advantageous diversity features such as thermal stability, low vapor pressure, reusability, and environmentally friendly character.[124–128] However, they sometimes suffer from expensive producing costs and the use of toxic nonrenewable procurers for their production.[129,130] Hence, the design of low-cost ionic liquid may compensate such disadvantages, so it is important from economic viewpoint to balance between performances with production coasts. In this regard, using ionic liquids (ILs) in green chemical transformations has multi activities as solvent, catalyst, and regent. Currently, researchers are focused on the synthesis of functionalized ILs called task-specific ILs (TSIL)[131–133] in which functionalized cations and anions can act as catalyst or reagent accelerating the reaction forward.

In a further advancement, Gaikwad *et al.*[134] devised a new dual basic ionic liquid 1-[3-(dimethylamino)propyl]-1,4-diazabicyclo[2.2.2]octan-1-ium hydroxide (**156**) which prepared in Scheme 37. It has used for catalyzing the synthesis of several new (2-amino-3-cyano-4*H*-chromen-4-yl) phosphonic acid diethyl esters **159a-l** *via* one-pot reaction of salicylaldehyde derivatives **19**, malononitrile (**157**) and trimethylphosphite (**158**) in excellent yields illustrated in Scheme 38. This approach adheres to the modern green chemistry principle of using ionic liquids as solvent and catalyst. The docking results suggest possible interactions with BCL-2; however, direct BCL-2 inhibition requires experimental confirmation.



Scheme 37. Synthesis of dual basic ionic liquid **156**.



159a-l: **a**, R= H; **b**, R= 5-OCH_3; **c**, R= 5-NO_2; **d**, R= 5-Cl, **e**, R= 5-CH_3; **f,** R= 3,5-$(Cl)_2$; **g**, R= 5-Br; **h**, R= 5-(-N=N-4-$CH_3C_6H_4$); **i**, R= 5-(-N=N-4-$OCH_3C_6H_4$); **j**, R= 5-(-N=N-4-ClC_6H_4); **k**, R= 5-(-N=N-2-ClC_6H_4); **l**, R= 5-(-N=N-4-BrC_6H_4).

Scheme 38. Synthesis of substituted chromene derivatives **159a-l**.

The results revealed similar binding sites of all new compounds with binding energy ranging from -31.40 to -0.216 kcal/mol. Examples illustrated in Figure 21-23.

 ©**AUTHOR(S)**

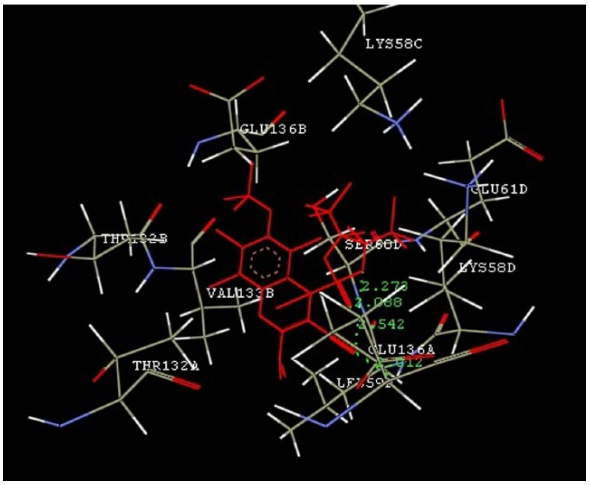


Figure 21. Binding interaction of compound **159b**. Reproduced with permission from Ref.;[134] Copyright 2019; Springer.

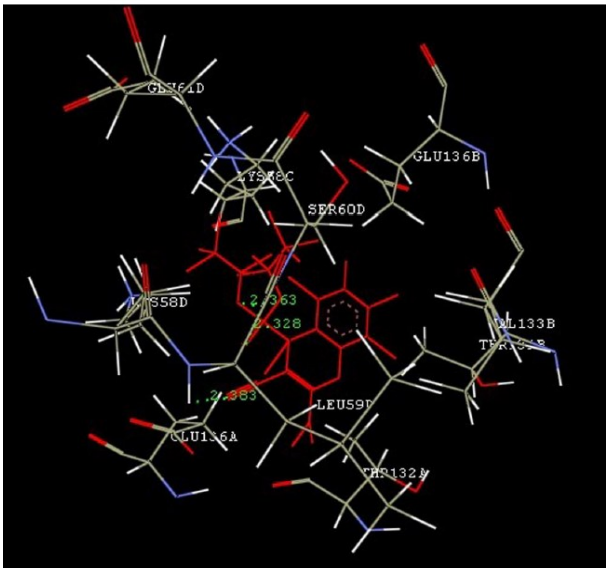


Figure 22. Binding interaction of compound **159d**. Reproduced with permission from Ref.;[134] Copyright 2019; Springer.

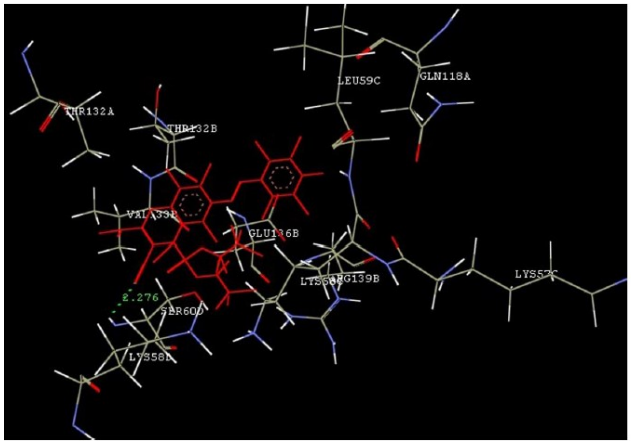


Figure 23. Binding interaction of compound **159l**. Reproduced with permission from Ref.;[134] Copyright 2019; Springer.

 ©AUTHOR(S)

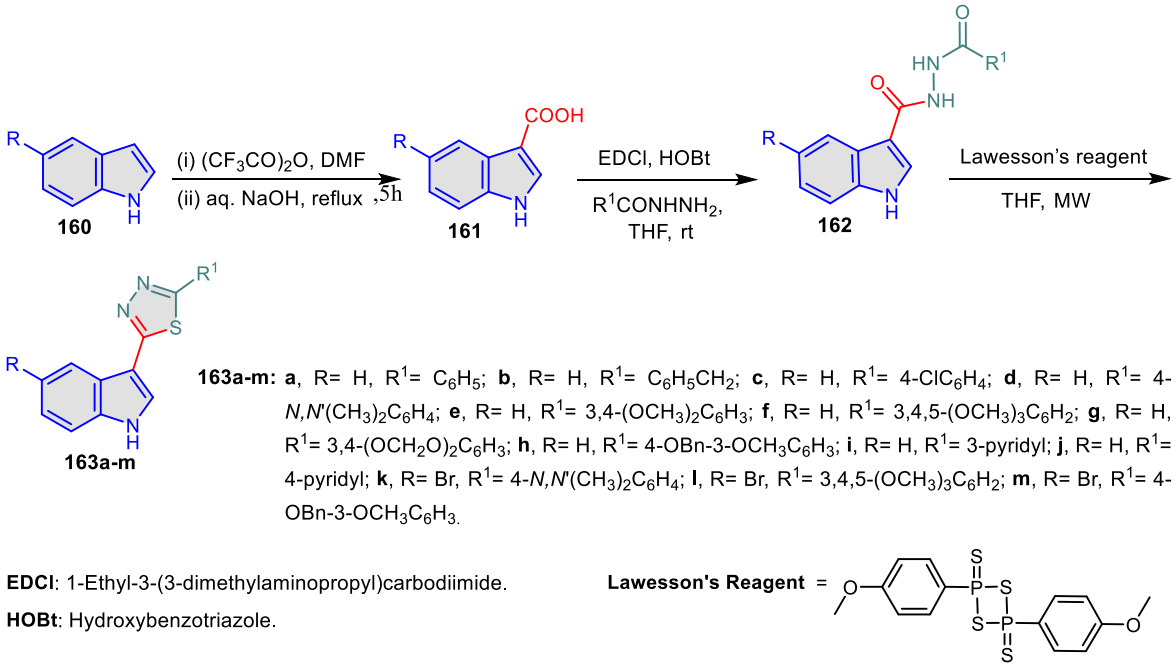
Raised challenges for the design and synthesis of anti-cancer reagents have received considerable interest over the past decades, which is driving a unique opportunity for innovation and development of new protocols in such issue. DNA binding scaffolds have the ability to bind with DNA as intercellular receptors *via* forming covalent and non-covalent adducts with minor and major grooves of DNA were mediated by changing replication of DNA, resulting in growth inhibition of tumor cells.[135–137]

5. Hybrid Heterocycles

The strategy of hybridization-combining two potent heterocycles into a single molecule – is a promising approach to overcome drug resistance and reduce toxicity.

5.1. Hybrid molecules-based indole moiety

Diversity of natural indole-based heterocycles has been reported as motif anti-cancer molecules.[138] Thiadiazole compounds considered privileged scaffolds in fields related to medicinal chemistry. Based on the fact that 1,3,4-thiadiazoles possess common structural features found in bioactive molecules,[139,140] their anti-cancer activity was widely explored.[141,142] An efficient green synthesis of 5-(3-indolyl)-1,3,4-thiadiazole derivatives 163**a-m** has been achieved *via* microwave-assisted Lawson's reagent thionation process. The reaction involves carboxylation of indole **160** to indole-3-carboxylic acid **161** and subsequent reaction with aryl hydrazides (Scheme 39).[143]
These hybrids were evaluated against prostate (PC3, DU145), breast (MCF7), and pancreatic (PaCa2) cancer cell lines. Compound **163m** showed the highest activity against PaCa2 cells (IC_{50} = 1.5 µM), whereas **163e** showed an IC_{50} of 6.8 µM against MCF7 cells. Because matched non-cancerous-cell IC_{50} values were not reported in the summarized data, these findings demonstrate differential activity among tumor cell models rather than cancer-versus-normal selectivity.



Scheme 39. Formation of 5-(3-indolyl)-1,3,4-thiadiazole derivatives **163a-m**.

 ©**AUTHOR(S)**

Compounds **163a** and **163c** revealed moderate cytotoxicity activity with IC_{50} values ranging from 41.7 to 79.6 µM. However, compounds **163d**, **163f**, **163g**, **163i**, **163j**, **163k** and **163l** revealed reduced cytotoxicity activity. Moreover, authors compared the cytotoxicity of the synthesized compounds with 5-(3-indolyl)-1,3,4-oxadiazoles and 5-(3-indolyl)-1,2,4-triazoles and concluded that 5-(3-indolyl)-2-substituted-1,3,4-thiadiazoles **163** is more potent than the aforementioned scaffolds.

Mitraphylline **164** is a natural spiro[pyrrolidin-3,3-oxindole] that showed prominent activity against breast cancer, leukemia, and sarcoma cancer.[144] To date, only spirooxindole natural products **164-168** were isolated, as illustrated in Figure 24.[145–148]

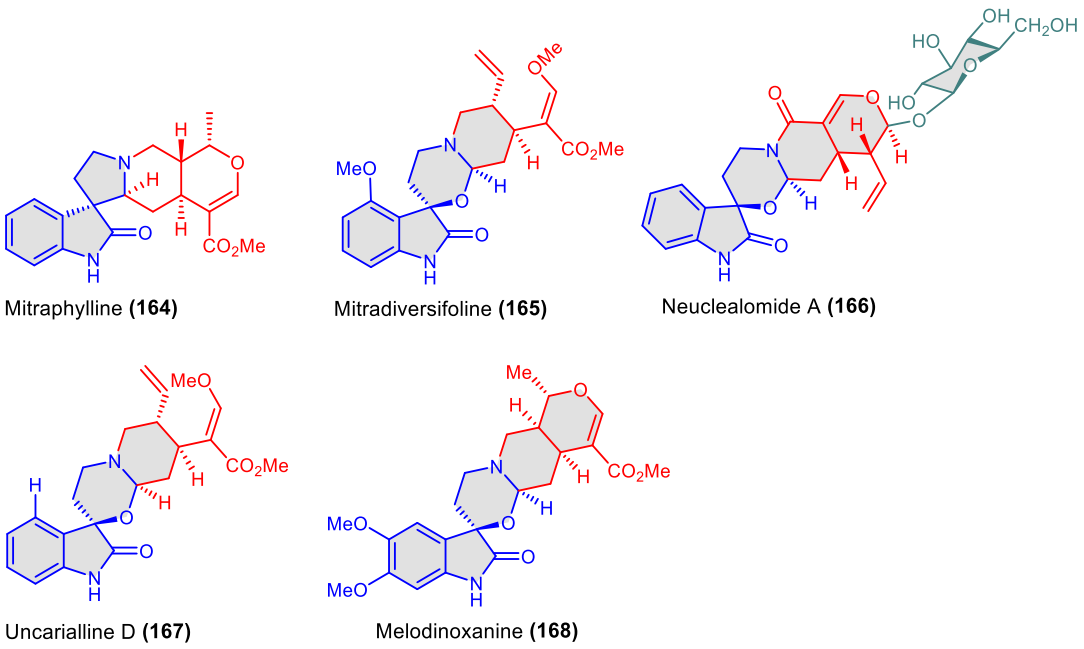
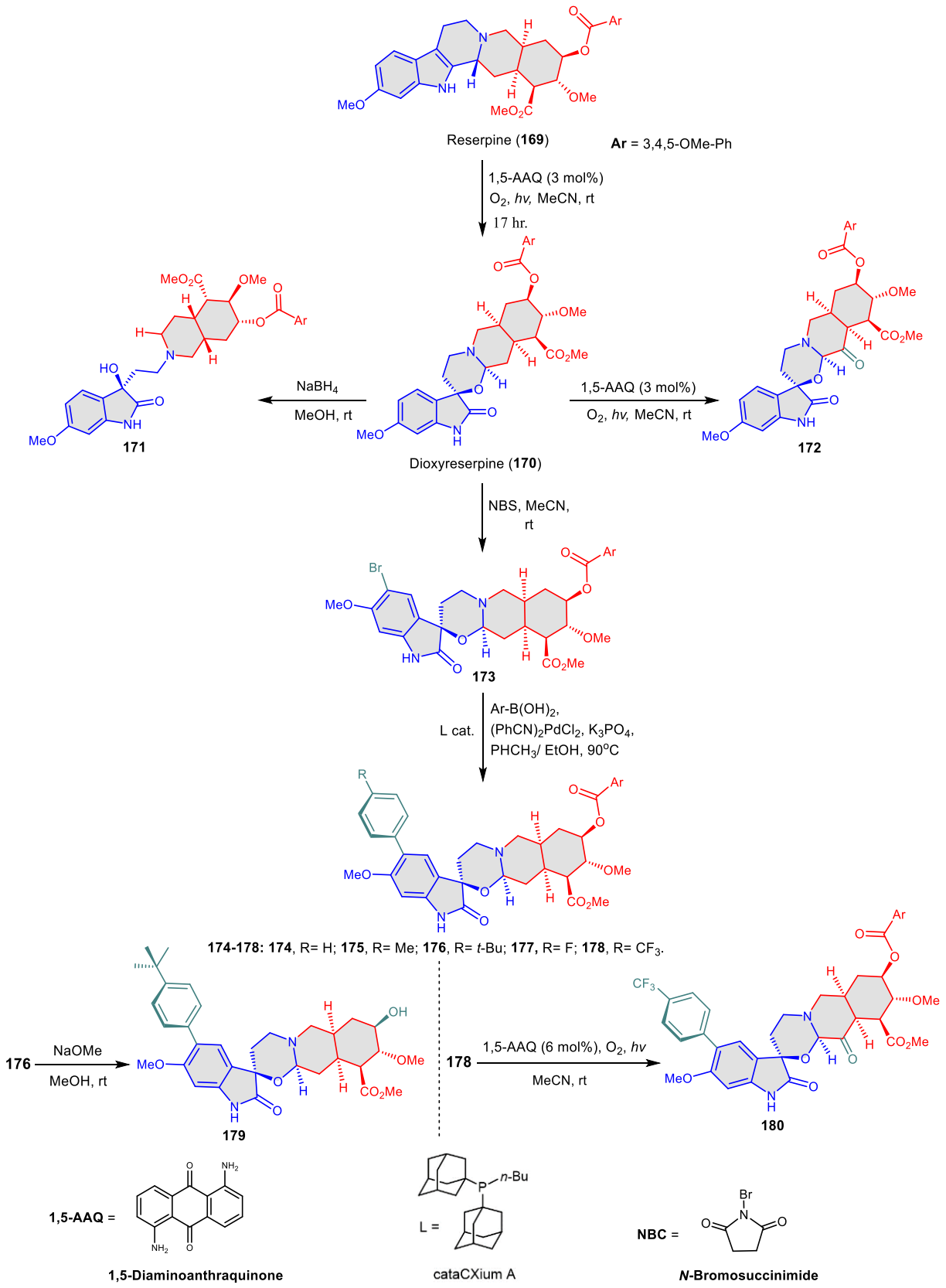


Figure 24. Structure of naturally occurring spiro-oxindoles **164**-**168**.

Brasholz and co-authors[149] developed effective synthesis of semi-synthetic analogue dioxyreserpine (**99**) from naturally occurring products reserpine (**169**). Compound **170** was transformed to analogous **171**-**180** *via* further functionalization (Scheme 40); through a catalytic photooxygenation reaction.[150,151]

 ©**AUTHOR(S)**



Scheme 40. Synthesis of dioxyreserpine (**170**), which transformed to analogous **171**-**180** *via* further functionalization.

©**AUTHOR(S)**

The newly obtained products were screened for their inhibitory activity against six human cancer cell lines, i. e. the B-ALL cell lines RS4;11 and NALM-6, the lymphoma cell lines SU-DHL-4 and SUP-T1, and the pancreatic carcinoma cell lines MIA-PaCa-2 and Capan-1. Among all tested compounds, products **172**, **175**, **178,** and **180** showed the highest inhibitory activity, with **180** being the most potent with IC_{50} illustrated in Table 2.

Table 2. Collected IC_{50} values [µM] of compounds **172**, **175**, **178**, and **180** for growth inhibition of six human carcinoma cell lines after 72 h incubation time[a]

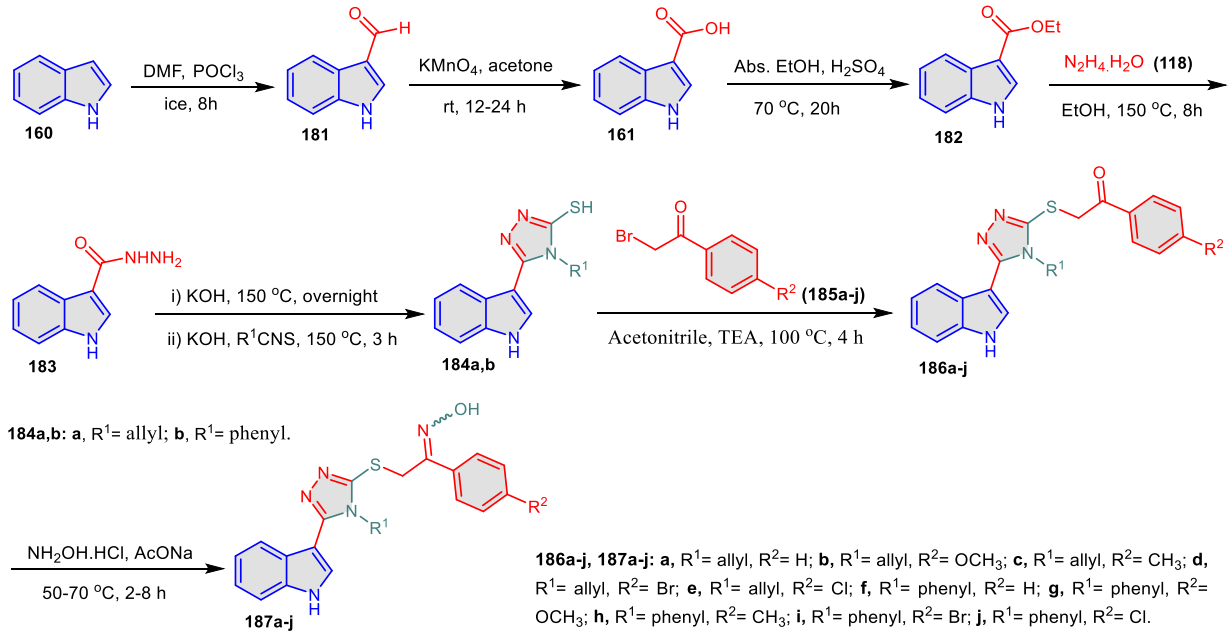
Compound	SU-DHL-4	SUP-T1	NALM-6	RS4;11	MIA-PaCa-2	Capan-1
172	2.93±0.66	2.85±1.03	3.68±1.46	2.97±1.66	3.99±0.30	23.01±12.40
175	1.39±0.07	4.72±1.52	2.38±0.10	3.71±0.87	4.18±1.32	22.15±11.01
178	1.73±0.17	3.64±3.48	1.79±0.62	1.95±0.53	6.11±2.07	n.c.
180	1.14±0.20	1.62±0.13	0.61±0.38	0.32±0.06	1.90±0.88	4.21±0.95

[a] The haematological cell lines were counted. The cell mass of the solid cell lines – measured using crystal violet staining. n.c.= not calculable.

Based on the results, the scientists concluded that adding a hydrophobic aromatic group or bromine atom at C-10 and a carbonyl group at C-14 significantly increased activity. Consequently, combination of both modifications will remarkably lead to more inhibitory activity.

In spite of several successful options for cancer treatment, a disadvantage associated with certain cancer cells concerns the development of hybrid molecules effective for resistance of medications. This inspired researchers to find alternative efficient treatments which act in alternative ways.[152,153]

Based on literature reports showing the significant biological activity of indole-based compounds,[154] recent studies revealed the potential anticancer activity of 1,2,4-triazoles which act as tubulin inhibitors.[155] Bräse and co-authors reported the synthesis of novel indole-based 1,2,4-triazole hybrids **187a-j** using indole **160** as precursor (Scheme 41).[156]



Scheme 41. Synthesis of indole-based 1,2,4-triazole hybrids **187a-j**.

 ©**AUTHOR(S)**

Analog **187j** found to be a potent lead with IC_{50} value of 3.03 ± 0.11 µM compared to CA-4 as a standard drug with IC_{50}= 833 ±0.29 µM, outperforming standard drug like combretastaain A-4 .
Molecular docking revealed that these oximes hybrids sit in the colchicine-binding pocket stabilized by hydrogen bonding between indole NH and 8.62 µM Molecular revealed that these oxime-based hybrids sit in the colchicine-binding pocket, stabilized by hydrogen bonds between the indole NH and βMet259 residue (Figure 25).

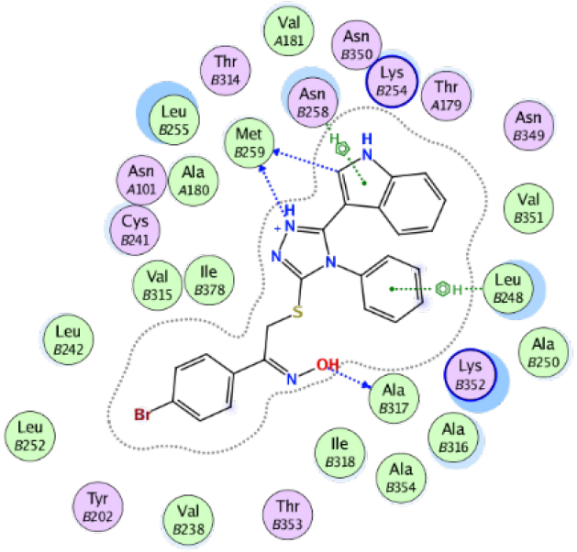


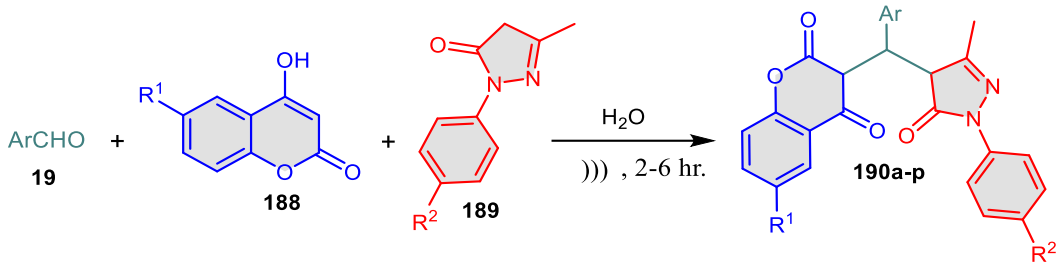
Figure 25. Ligplots at α/β-tubulin colchicine binding site: 2D-docked model of **187i**. Reproduced with permission from Ref.;[156] Copyright 2025; MDPI.

5.2. Hybrid molecules-based pyrazole moiety

Pyrazolone derivatives are a potent class exhibiting a wide range of bioactivity related to anti-cancer activity.[157] In this regard, the free radical scavenger 3-methyl-1-phenyl-2-pyrazoline-5-one (edaravone) increases the effects of murine colon cancer therapeutics *via* inhibition of nuclear factor Kappa B.[158] Additionally, the family of coumarins have a great interest in pharmaceutical and medicinal chemistry and as precursors in the synthesis of anti-tumor drugs.[159,160] Pyrazolone-based coumarine hybrid molecules possess potential against several *in vitro* and *in vivo* investigations.

Yao and co-authors reported a multi-component green synthesis of novel hybrid chroman-2,4-dione attached to edaravone moiety in water under ultrasonic irradiation. Specifically, the authors examined the reaction of 4-hydroxycoumarine **188** with aromatic aldehydes **19** and edaravone **189** in several solvents promoted with ultrasonic irradiation. The most effective solvent turned out to be water, and the corresponding 3-substituted chroman-2,4-diones **190a-p** are produced in 58-89% yield (Scheme 42).[161]

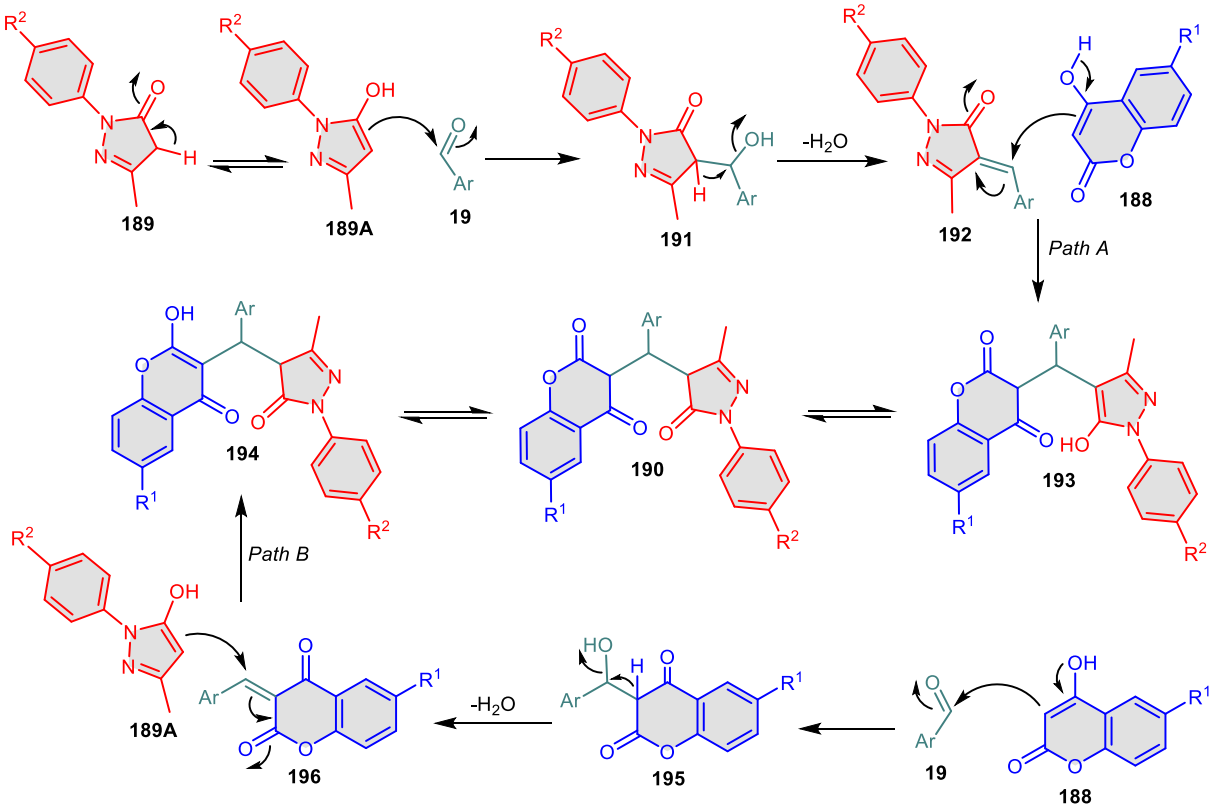
 ©AUTHOR(S)



190a-p: **a**, Ar= 3-OMe,4-OHC$_6$H$_3$, R^1= R^2= H; **b**, Ar= 3,4-(OMe)$_2$, R^1= R^2= H; **c**, Ar= 4-OMeC$_6$H$_4$, R^1= R^2= H; **d**, Ar= 3-F,4-OMeC$_6$H$_3$, R^1= R^2= H; **e**, Ar= 4-OHC$_6$H$_4$, R^1= R^2= H; **f**, Ar= 4-NO$_2$C$_6$H$_4$, R^1= R^2= H; **g**, Ar= 4-MeC$_6$H$_4$, R^1= R^2= H; **h**, Ar= C$_6$H$_5$, R^1= R^2= H; **i**, Ar= 2-furyl, R^1= R^2= H; **j**, Ar= 3-OMe-4-OHC$_6$H$_3$, R^1= Cl, R^2= H; **k**, Ar= 3-OMe-4-OHC$_6$H$_3$, R^1= F, R^2= H; **l**, Ar= 3-OMe-4-OHC$_6$H$_3$, R^1= H, R^2= Me; **m**, Ar= 3-OMe-4-OHC$_6$H$_3$, R^1= H, R^2= F; **n**, Ar= 3-OMe-4-OHC$_6$H$_3$, R^1= H, R^2= Cl; **o**, Ar= 3-OMe-4-OHC$_6$H$_3$, R^1= F, R^2= Me; **p**, Ar= 4-OMeC$_6$H$_3$, R^1= R^2= F.

Scheme 42. Synthesis of 3-substituted chroman-2,4-diones **190a-p.**

A mechanism to rationalize the formation of **190** proposed in (Scheme 43).



Scheme 43. Mechanism for the formation of 3-substituted chroman-2,4-diones **190**.

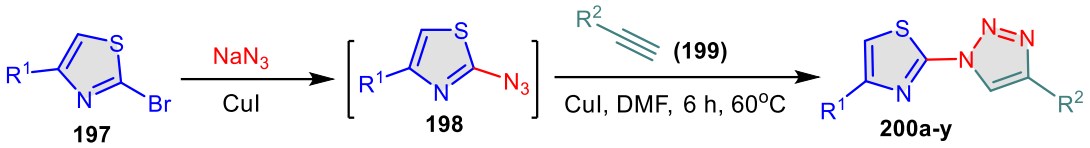
Authors evaluated the drug-likeness of synthesized 3-substituted chroman-2,4-dione applying Lipinski's rules (Rules of Five)[162,163] to determine whether particular scaffolds possess the potentiality to act as orally active drug. According to drug-like criteria, the molecular mass of synthesized compounds is less than 500 Daltons. The partition coefficient (logP) lies between 2.45-4.34, which is in agreement with good lipophilicity

 ©**AUTHOR(S)**

and solubility of estimated values. The authors concluded that all key parameters have no contradictions at all with Lipinski's rules.

5.3. Hybrid molecules-based triazole moiety

Based on the literature reports showing the high potency of 1,2,3-triazole and 2-aminothiazolyl imidazoles as anti-cancer reagents.[164] Chen and co-worker[165] developed one-pot tandem copper-catalyzed azid-alkyne cycloaddition (CuAAC) reaction for biologically relevant anti-cancer reagent, as shown in Scheme 44. The reaction show high estimated Atom-Economy equals 89.17 % reflects the greens of reaction.



200a-y: **a**, R^1= 2-furanyl, R^2= C_6H_5; **b**, R^1= 2-furanyl, R^2= 2-pyridinyl; **c**, R^1= 2-furanyl, R^2= 3-pyridinyl; **d**, R^1= 2-furanyl, R^2= 2-thiophenyl; **e**, R^1= 2-furanyl, R^2= (*E*)-C_6H_5CH=$CHCO_2CH_2$; **f**, R^1= 2-thiophenyl, R^2= C_6H_5; **g**, R^1= 2-thiophenyl, R^2= 2-pyridinyl; **h**, R^1= 2-thiophenyl, R^2= 3-pyridinyl; **i**, R^1= R^2= 2-thiophenyl; **j**, R^1= 2-thiophenyl, R^2= (*E*)-C_6H_5CH=$CHCO_2CH_2$; **k**, R^1= R^2= C_6H_5; **l**, R^1= C_6H_5, R^2= 2-pyridinyl; **m**, R^1= C_6H_5, R^2= 3-pyridinyl; **n**, R^1= C_6H_5, R^2= 2-thiophenyl; **o**, R^1= C_6H_5, R^2= (*E*)-C_6H_5CH=$CHCO_2CH_2$; **p**, R^1= 4-ClC_6H_4, R^2= C_6H_5; **q**, R^1= 4-ClC_6H_4, R^2= 2-pyridinyl; **r**, R^1= 4-ClC_6H_4, R^2= 3-pyridinyl; **s**, R^1= 4-ClC_6H_4, R^2= 2-thiophenyl, **t**, R^1= 4-ClC_6H_4, R^2= (*E*)-C_6H_5CH=$CHCO_2CH_2$; **u**, R^1= 4-FC_6H_4, R^2= C_6H_5; **v**, R^1= 4-FC_6H_4, R^2= 2-pyridinyl; **w**, R^1= 4-FC_6H_4, R^2= 3-pyridinyl, **x**, R^1= 4F-C_6H_4, R^2= 2-thiophenyl; **y**, R^1= 4-FC_6H_4, R^2= (*E*)-C_6H_5CH=$CHCO_2CH_2$.

Scheme 44. Synthesis of 1-thiazolyl-1,2,3-triazoles **200a-y**.

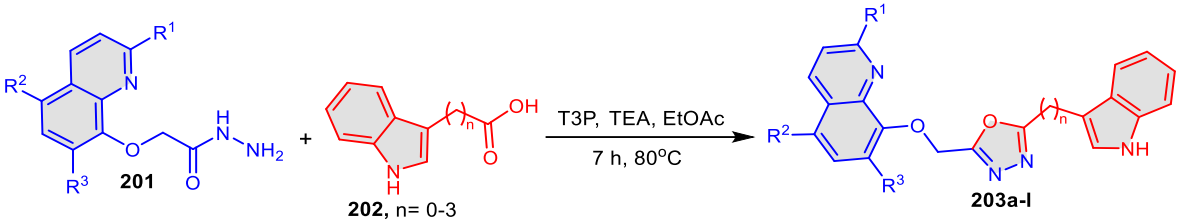
The cytotoxic activity for the synthesized compounds against MES-SA/Dx5 cancer cell lines performed using MTT assay. Almost all compounds except **200a** showed cytotoxic activity. Among them, compounds **200d**, **200c**, **200e**, **200i**, and **200f** exhibit the most potency with IC_{50} = 0.8, 1.1, 4.4, 5.1, and 5.5 µM, respectively.

Compounds with fluoro and chloro substituents attached to C-4 of phenyl group on thiazole ring found to be the more active derivatives, whereas fluoro substituents displayed a slightly increased activity. Good activities observed for compounds with aryl substituent at triazole moiety, particularly 2- and 3-pyridinyl rings. These investigations further extended to the cytotoxicity of normal Vero cell lines, and the results displayed that except **200q**, all compounds showed no cytotoxic activity. This established that these synthesized hybrid molecules possess more potent and selective effect on MES-SA/Dx5 over normal cell lines.

5.4. Hybrid molecules-based oxadiazole moiety

Indole-based hybrid molecules shown significant potential against diverse cancer types. For example in 2016, Sunil and co-authors[166] advanced a microwave-assisted synthesis of quinoline-indole-oxadiazole molecules **203a-l** *via* thionation reaction using Lawesson,s reagent applying propylphosphonic acid cyclic anhydride (T3P) as a green catalyst (Scheme 45).

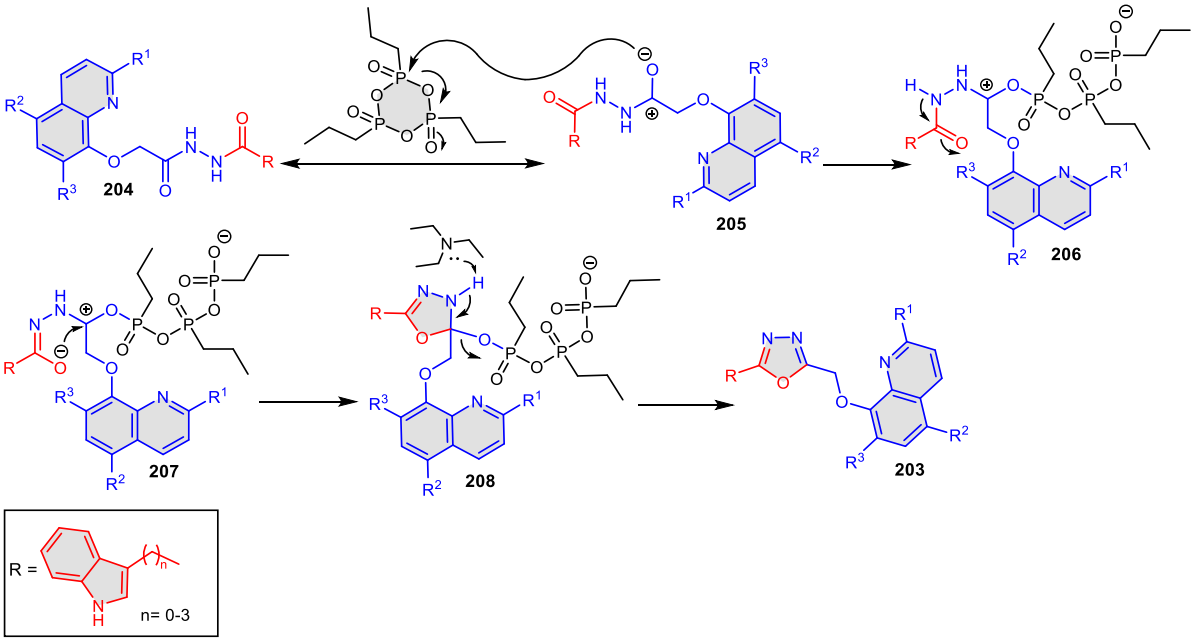
 ©**AUTHOR(S)**



203a-l: **a**, n= 0, R^1= R^2= R^3= H, **b**, n= 1, R^1= R^2= R^3= H; **c**, n= 2, R^1= R^2= R^3= H; **d**, n= 3, R^1= R^2= R^3= H; **e**, n= 0, R^1= CH_3, R^2= R^3= H; **f**, n= 1, R^1= CH_3, R^2= R^3= H; **g**, n= 2, R^1= CH_3, R^2= R^3= H; **h**, n= 3, R^1= CH_3, R^2= R^3= H; **i**, n= 0, R^1= H, R^2= R^3= Cl; **j**, n= 1, R^1= H, R^2= R^3= Cl; **k**, n= 2, R^1= H, R^2= R^3= Cl; **l**, n= 3, R^1= H, R^2= R^3= Cl.

Scheme 45. Synthesis of hybrid quinoline-indole-oxadiazole molecules **203a-l**.

The mechanism to according for the formation of the reaction production illustrated in Scheme 46.



Scheme 46. Mechanism for the formation of hybrid quinoline-indole-oxadiazole molecules **203.**

These hybrids examined for their potency against prostate (PC3, DU14) , breast (MCF7), and pancreatic (PaCa2)cancer cell lines. Compound **163m** showed the highest cytotoxic activity against PaCa2 cells, with an IC_{50} of 1.5 µM, while **163e** possess high activity against MCF7 cell lines IC_{50}=8.62 µM.

Docking studies performed for **203d** on the tubulin three binding sites in support of polymerization inhibition. Results revealed that oxadiazole **203d** established a hydrogen bonding with Asn101, Ala317, and Lys352 amino acids upon docking at the colchicine site. Moreover, **203d** also displays hydrophobic interactions with seven amino acids of tubulin due to similar orientation as colchicine (Figure 26); such orientation is crucial in allowing a hydrogen bonding of oxadiazole with hydroxyl groups of Lys353 and Ala317, and amino group of Asn101 of tubulin amino acids. The oxygen of the rather linkage binding quinoline and oxadiazole scaffolds displayed interaction with tubulin amino acids. Compounds **203d** has shown hydrogen bonds with His229 and Thr226 in the Taxol binding site, and eight hydrophobic contacts with tubulin amino acids identified.

 ©**AUTHOR(S)**

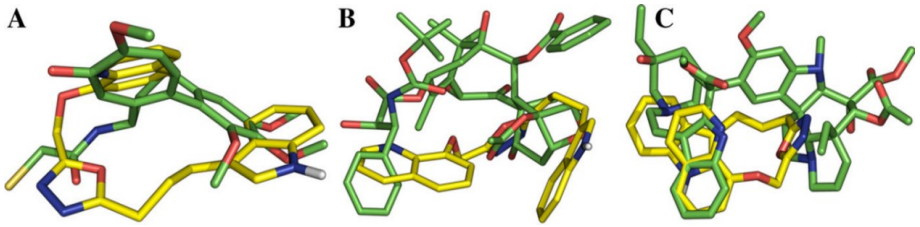


Figure 26. Models of tubulin-bound ligand **203d** superimposed on **A** colchicine, **B** pacilitaxel, and **C** vinblastine in their matching crystal structures. Carbon (yellow), oxygen (red), and nitrogen (dark blue) in Oxadiazole **203d**; carbon (green), nitrogen (blue), and oxygen (red) in CN2, TXL, and VLB. Reproduced from Ref.,[166] Copyright 2016; Springer.

The binding modes to tubulin active sites are illustrated in Figure 27. The results indicated that the nitrogens of oxadiazole and quinoline rings are essential to recognize the key amino acid residues at the binding sites of the enzyme for tubulin inhibition.

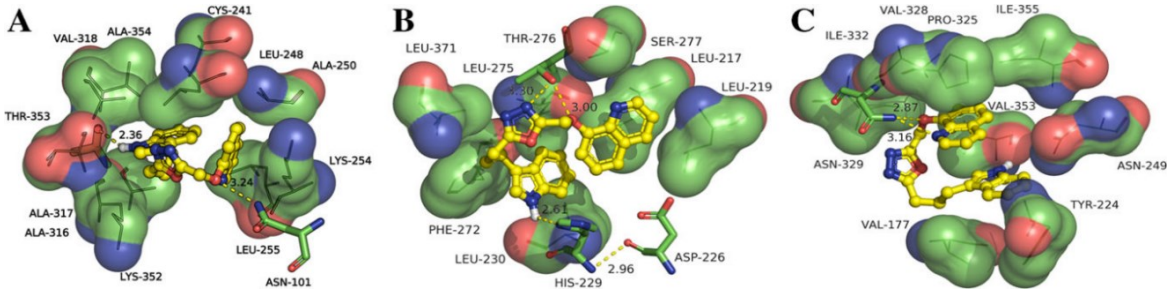


Figure 27. Computational docking models: **203d** docked at **A** colchicine, **B** pacilitaxel, and **C** vinblastine sites of tubulin. Reproduced from Ref.;[166] Copyright 2016; Springer.

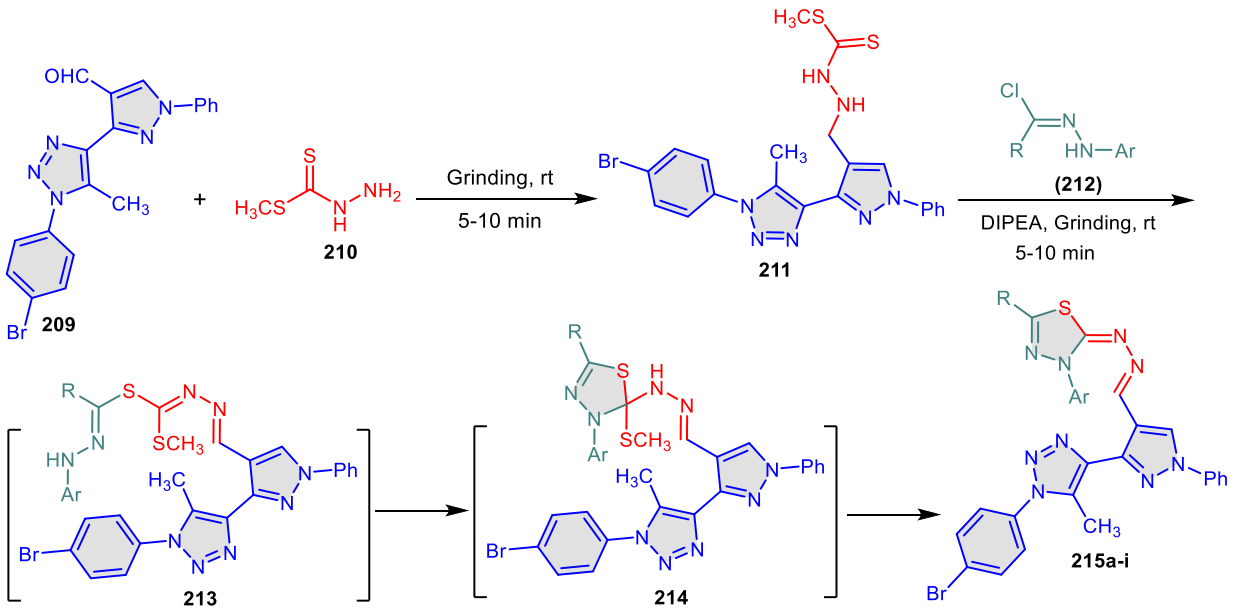
The SAR analysis demonstrated that a longer methylene-linker between indole C-3 and oxadiazole C-5 is determined to bioactivity. A longer methylene linker (n= 3) and quinoline moiety without electron donating or electron attracting substituents enhanced the activity.

5.5. Hybrid molecules-based thiadiazole moiety

Based on the literature reports showing the potential therapeutically engaging activities of 1,3,4-thiadiazole ring system and 1,2,3-triazoles as anti-tumor reagents.[167,168]

Rashdan and co-workers[169] reported a solvent and catalyst-free synthesis of hybrid 5-(substituted 1,2,3-triazole-4-yl)-1,3,4-thiadiazole derivatives **215a-i** as shown in Scheme 47. However, owing to the solubility of synthesized molecules in water is low resulted in poor bioavailability as they practically disappeared from the bloodstream without fulfilling their function; authors found an elegant solution *via* encapsulating these molecules to hydrophilic biocompatible polysaccharide such as alginate polymer to increase their bio-accessibility and chemo-sensitivity by attaching such a hydrophilic carrier.[170]

 ©AUTHOR(S)



215a-i: **a**, R= $CO_2C_2H_5$, Ar= C_6H_5; **b**, R= $CO_2C_2H_5$, Ar= 4-$CH_3C_6H_4$; **c**, R= $CO_2C_2H_5$, Ar= 4-ClC_6H_4; **d**, R= $CO_2C_2H_5$, Ar= 4-$NO_2C_6H_4$; **e**, R= $COCH_3$, Ar= C_6H_5; **f**, R= $COCH_3$, Ar= 4-$CH_3C_6H_4$; **g**, R= $COCH_3$, Ar= 4-ClC_6H_4; **h**, R= $COCH_3$, Ar= 4-$NO_2C_6H_4$; **i**, R= COPh, Ar= C_6H_5.

Scheme 47. Synthesis of hybrid 5-(substituted 1,2,3-triazole-4-yl)-1,3,4-thiadiazole derivatives **215a-i**.

Most of the synthesized compounds exhibit good anti-cancer activity against breast cells; among them, **211** and **215h**, **215d**, **215g**, **215c**, **215i**, **215e**, and **215b** revealed remarkable activity with 96.4, 92.6, 92.3, 89.2, 87.3, 83.5, 83.4, and 81.9% of cytotoxicity respectively. Moreover, Compound **211** displayed the most potent anti-cancer activity against lung cells, with 90.8% of cytotoxic activity.

The mechanism of action exemplified with **215b** and **215g,** which possess higher breast anti-tumor activity and safety. According to the IC_{50} values of compounds **215b** and **215g** against breast cells (IC_{50} = 19.8 and 26.2µg/mL), it was concluded that both compounds possessed upregulate of proapoptotic protein Bax level and downregulate of anti-apoptotic protein BCL2 level with statistically significant ($p < 0.05$). Moreover, compounds **215b** and **215g** disturb the Bax/BCL2 ratio, signaling the apoptotic cascade inside the cells (Figure 28A).

Similarly, MCF-7cells treated with 19.8 and 26.2µg/L of compounds **215b** and **215g** to determine their effect on DNA fragmentation, and the results revealed that compounds **215b** and **215g** upregulate the caspase 7-protein level compared to untreated cells with significant difference ($p < 0.05$). Meanwhile, **215b** and **215g** activate effector caspase 7 protein resulted in inducing the apoptotic cascades inside cells (Figure 28B).

©**AUTHOR(S)**

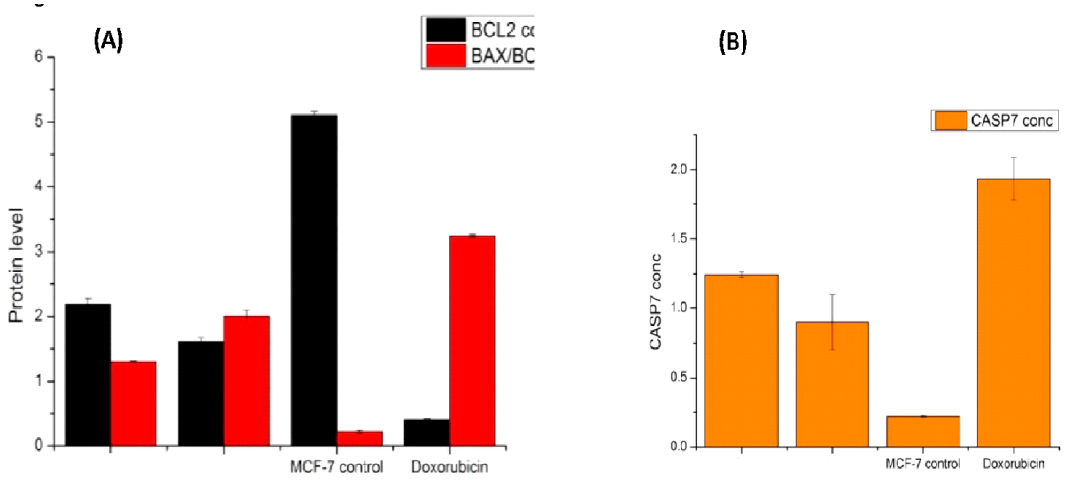


Figure 28. BCL2 protein level (ng/mL) and Bax/BCL2 ratio of MCF-7 treated with IC_{50} of compounds **215b** and **215g (A)**. Casp7 (ng/mL) quantitative estimation of MCF-7 treated with IC_{50} of compounds **215b** and **215g (B)**. Reproduced from Ref.;[169] Copyright 2019; MDPI.

5.6. Hybrid molecules-based quinoline moiety

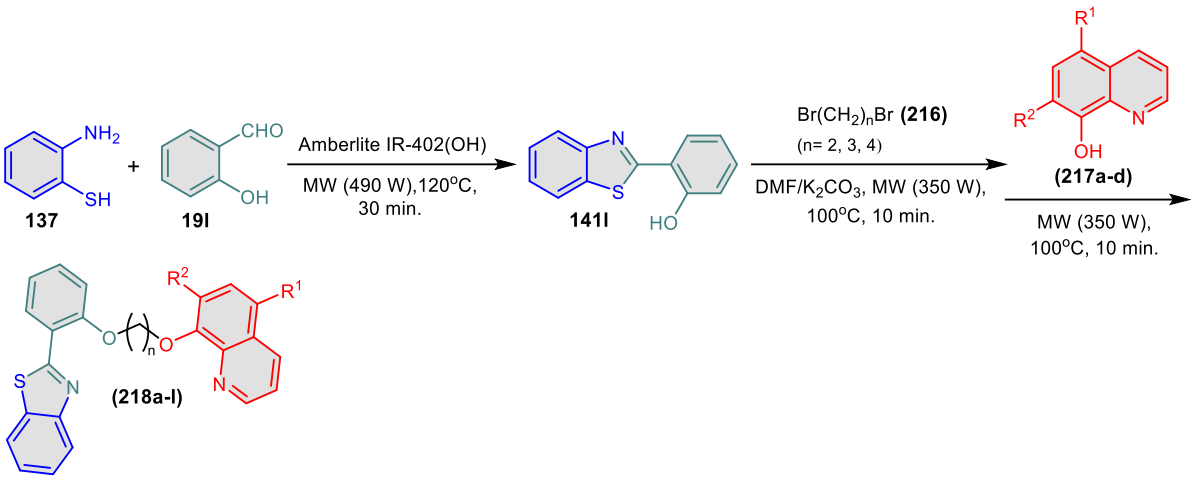
Benzothiazole derivatives are bioactive heterocycles that have received considerable interest. Moreover, 2-(2′-hydroxyphenyl)benzothiazoles have been revealed as potent amyloid markers due to their fluorescence activity.[171] 8-Hydroxyquinoline has been reported to induce cell death in leukemia cell lines [172] and suppress proteasome activity and growth in cultured human cancer cells.[173,174]

It is now well recognized that heterocycles possessing dual functions as pharmacophore and fluorophore, known as the theranostic scaffolds, have a precious ability to distinguish tumor cells from normal cells by identifying the biomarker.[175] In recent years, using fluorescently labeled pharmacophores shed significant developments in anti-cancer diagnostic approaches.

Recently a hybrid 2-(2′-hydroxyphenyl)-benzothiazole-quinoline has been synthesized and shows great efficiency for detecting Hg^{+2} in HeLa cells as well as membrane permeability.[176]

A diversity of benzothiazole-quinoline based fluorescent heterocycles **218a-l** has been developed by Paira and co-workers[177] involves Amberlite IRA-402(OH) as green catalyst under microwave irradiation (Scheme 48).

 ©**AUTHOR(S)**



217a-d: **a**, R^1= R^2= H; **b**, R^1= R^2= Br; **c**, R^1= Cl, R^2= H; **d**, R^1= Cl, R^2= I.

218a-l: **a**, R^1= R^2= H, n= 2; **b**, R^1= R^2= Br, n= 2; **c**, R^1= Cl, R^2= H, n= 2; **d**, R^1= Cl, R^2= I, n= 2; **e**, R^1= R^2= H, n= 3; **f**, R^1= R^2= Br, n= 3; **g**, R^1= Cl, R^2= H, n = 3; **h**, R^1= Cl, R^2= I, n = 3; **i**, R^1= R^2= H, n = 4; **j**, R^1= R^2= Br, n= 4; **k**, R^1=Cl, R^2= H, n= 4; **l**, R^1= Cl, R^2= I, n= 4.

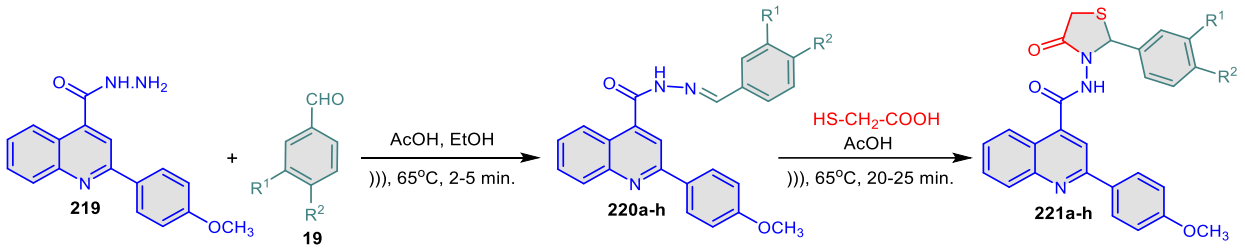
Scheme 48. Synthesis of novel benzothiazole–quinolines **218a-l**.

The present study addressed several convenient results concerning the cytotoxicity of **218a-l** and the selective potency of these heterocycles in cancer cells with respect to normal cells. Most tested compounds possess higher potency than cisplatin (reference drug) against all selected cancer cell lines. The cytotoxicity of compound **218c** revealed showed the best values with HeLa and A2780 (IC_{50} 7.45, 10.10 µM) respectively. Compound **218a** revealed the best cytotoxicity against MCF-7 and A549 (IC_{50} 5.80, 10.99 µM) cell lines. Compounds **218b**, **218e**, **218g**, **218k**, and **218l** showed IC_{50} values (7-13 µM) in MCF-7 and A549 cells. The healthy cell lines fetal lung fibroblast (MRC-5) and normal human embryonic kidney cells (HEK-293) chosen as the model normal cells to estimate the selective potency of tested scaffolds in cancer cell lines. Concerning MRC-5, compound **218a** revealed the best selectivity in MCF-7 cells, whereas the growth of HeLa, A2780, and A549 cell lines most selectively inhibited by **218g**. All compounds with respect to HEK-293 followed a similar pattern of selectivity.

Likewise, chromenes, quinoline derivatives showed great potential bioactivity as anti-cancer reagents.[178] 4-Thiazolidinones also showed diverse biological activities as anti-tumor reagents[179] and it was featured in several drugs.

With the increasing demand for the synthesis of more potent and less harmful anti-cancer drugs, novel quinoline-based thiazolidinones **221a-h** have been recently synthesized by Dofe *et al*.[180] This process involves reaction of 2-(4-methoxyphenyl)-quinoline-4-carbohydrazide (**219**) with aromatic aldehydes **19** and subsequent reaction of the produced quinoline derivative **220a-h** with mercapto acetic acid and the reaction promoted by ultrasonic irradiation (Scheme 49).

 ©**AUTHOR(S)**



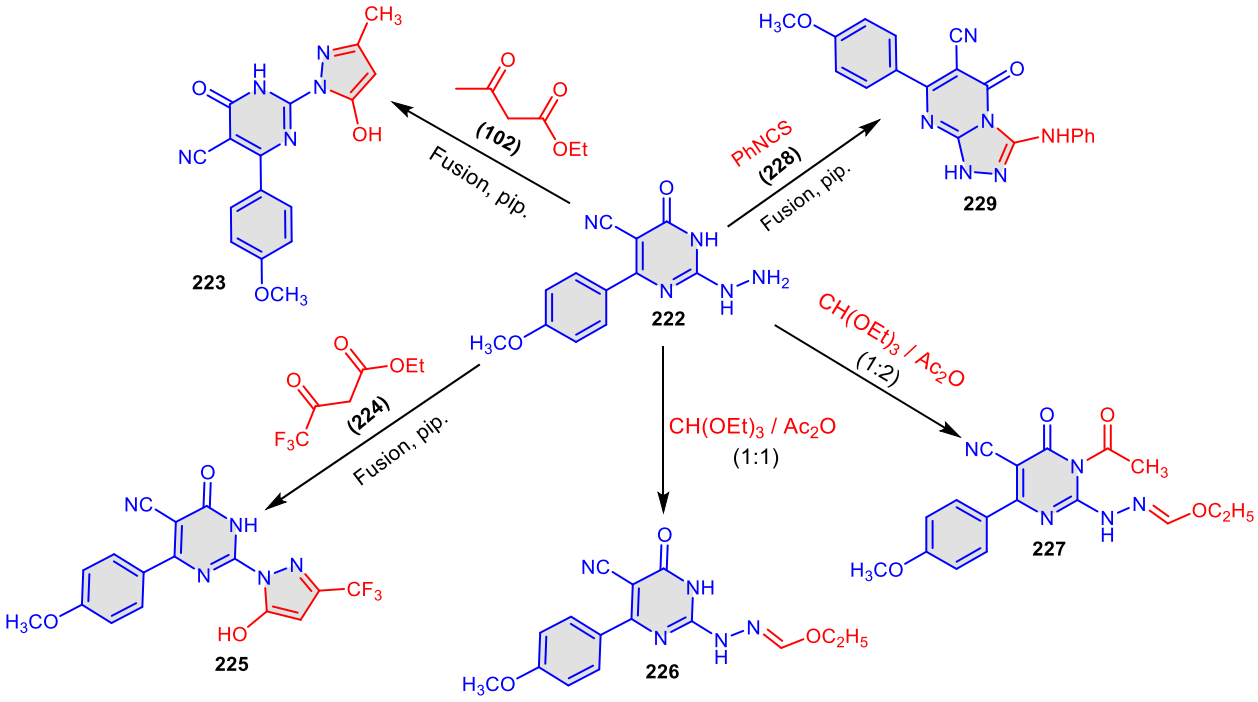
220, 221a-h: a, R^1= R^2= H; **b**, R^1= H, R^2= F; **c**, R^1= H, R^2= Cl; **d**, R^1= H, R^2= Br; **e**, R^1= H, R^2= CF_3; **f**, R^1= H, R^2= NO_2; **g**, R^1= H, R^2= CH_3; **h**, R^1= OCH_3, R^2= OH.

Scheme 49. Synthesis quinoline-based thiazolidinones **221a-h**.

In a dose-dependent mode towards breast cancer cells MCF-7, compounds **221c**, **221d**, and **221f** were shown to have significant inhibition with IC_{50} values of 5.38, 5.12, and 0.73 µM, respectively. Furthermore, the authors used flow cytometry to show that G2/M cell arrest induced within 24 hours.

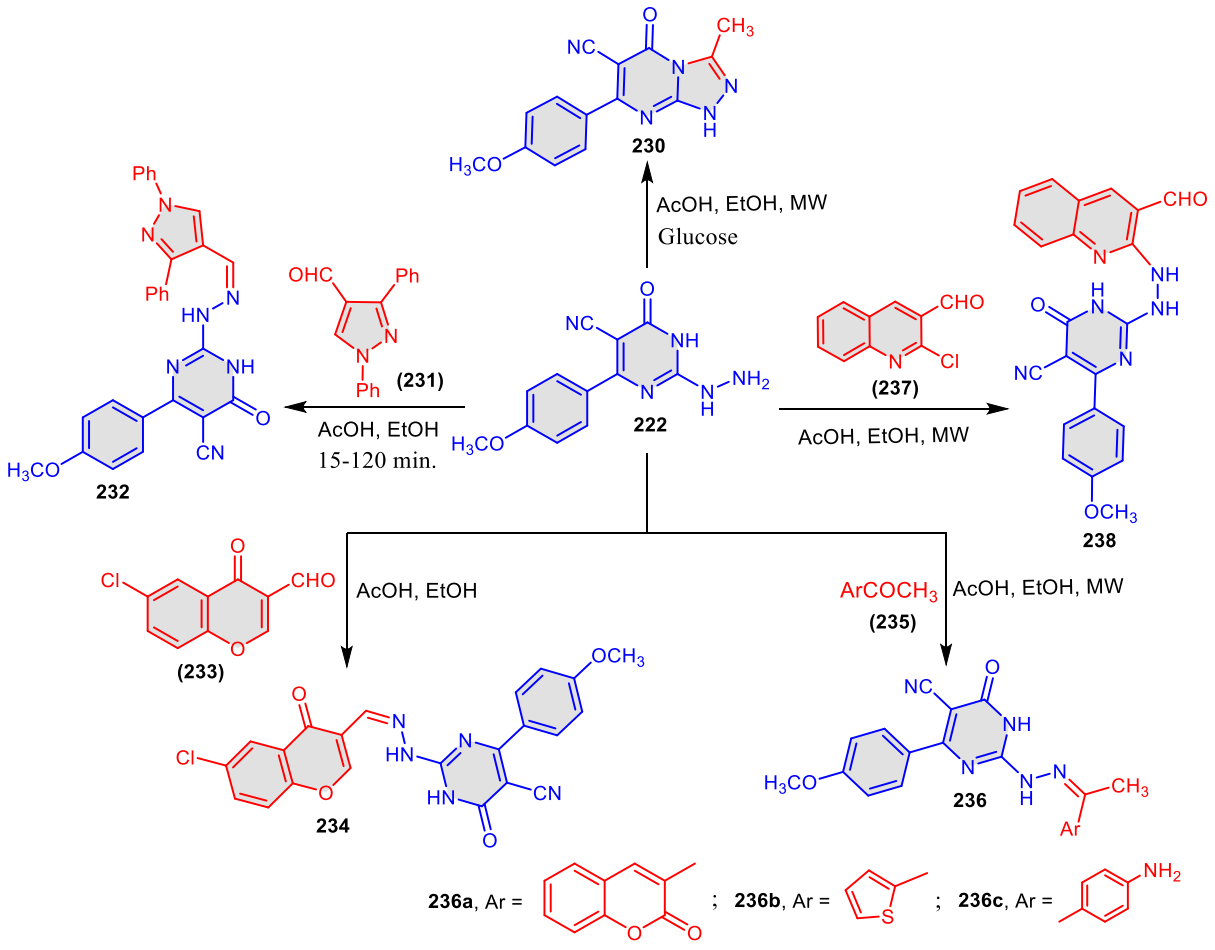
5.7. Hybrid molecules-based pyrimidine moiety

El- Naggar *et al.*[181] designed green synthesis of several new pyrimidines coupled to diversity of heterocyclic motifs using hydrazinyl pyrimidine derivative **222** as precursor (Scheme 50-52).

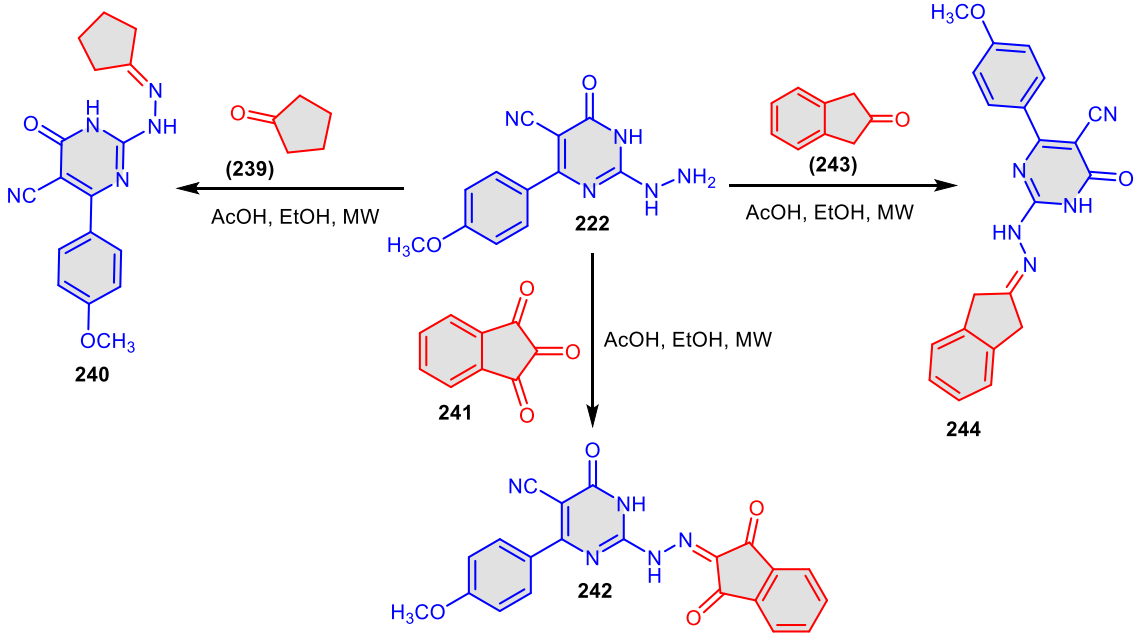


Scheme 50. Synthesis of pyrimidine derivatives **223**, **225, 226, 227** and **229**.

 ©**AUTHOR(S)**



Scheme 51. Synthesis of diversity of pyrimidine derivatives **230**, **232**, **266**, **236a-c** and **238**.



Scheme 52. Synthesis of pyrimidine derivatives **240**, **242** and **244**.

 ©**AUTHOR(S)**

In vitro antiproliferative activities of synthesized compounds revealed that **227** and **242** exhibit the best inhibitory activity with IC_{50} values of 19.04 and 15.91 µM against HePG-2 cell lines and 31.2 and 18.29 towards HCT-116 referenced to doxorubicin. Meanwhile, compounds **226**, **230,** and **236b** showed moderate activities; however, products **232**, **238**, and **236a** exhibited weak activities toward both cell lines.

The binding mode for compounds **236b** and **236c** showed values of -6.80 Kcal/mol and -7.09 Kcal/mol, respectively. The Nitrogen atom of the hydrazonyl moiety and Cys195 established one hydrogen bonding connection in compound **236b**. The phenyl group was involved in aromatic stacking interactions with Phe 225 (Figure 29).

Similarly, compound **236c** formed three hydrogen bonds, the first of them between nitrogen atom of pyrimidinone ring and Glu87, the second between pyrimidinone oxygen and His196, and the third between cyano nitrogen and Tyr 135 (Figure 30).

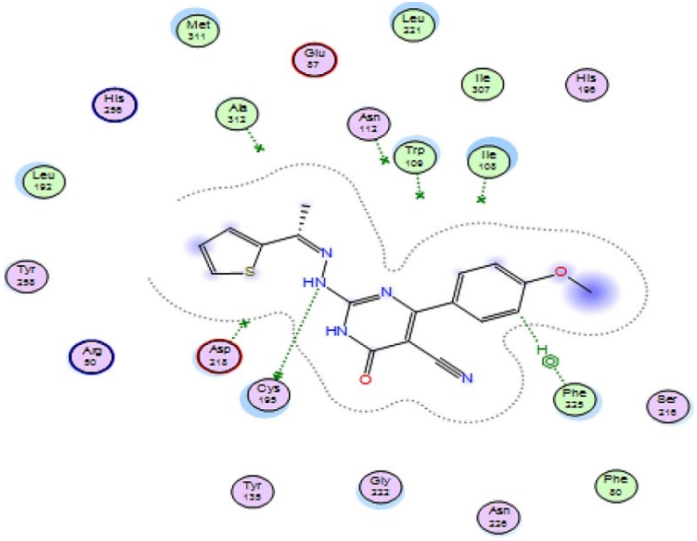


Figure 29. Mapping surface showing compound **236b** occupying the active pocket of T.S 2D. T.S., thymidylate synthase. Reproduced from Ref.;[181] Copyright 2019; Wiley.

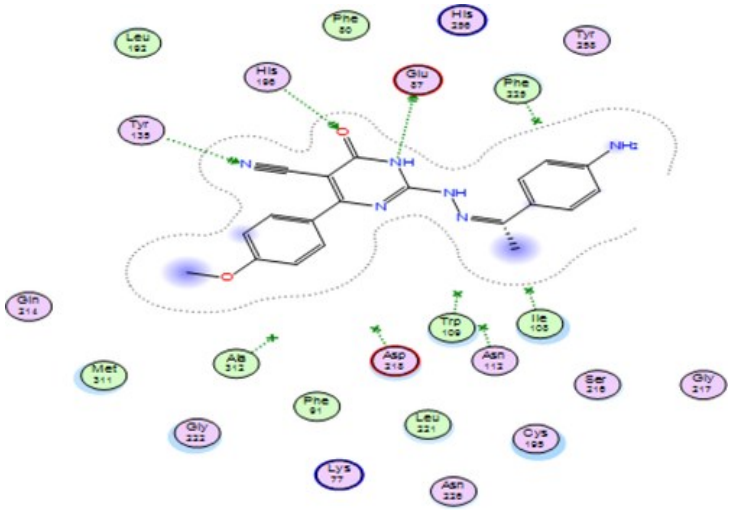


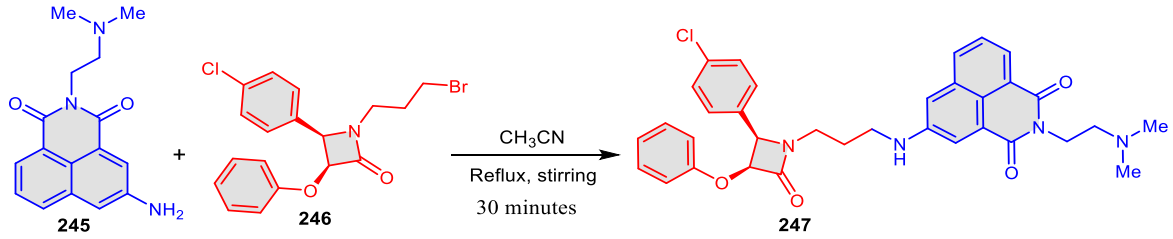
Figure 30. Mapping surface showing compound **236c** occupying the active pocket of T.S 2D. T.S., thymidylate synthase. Reproduced from Ref.;[181] Copyright 2019; Wiley.

 ©AUTHOR(S)

5.8. Hybrid molecules-based naphthalimide moiety

Amonafide as naphthalimide analogs hold tremendous promise for drug discovery. It is advanced to the clinical stage for the treatment of solid tumors, and it is now in phase III for acute myeloid leukemia treatment.[182,183] Importantly, unpleasant side effects as central neurotoxicity, low efficacy as well as hemotoxicity limit its clinical development.[184] An appealing approach to overcome such disadvantages is the synthesis of a hybrid molecule possessing lower cytotoxicity.

β-Lactams with various side chains have been widely used to treat bacterial infections.[185–187] Jarrahpour[188] and co-authors have developed an efficient synthesis of amonafide-conjugated β-lactam hybrid **247**. Coupling of amonafide (**245**) with β-lactam derivative **246** under catalyst-free conditions afforded targeted scaffold (Scheme 53). The *in vitro* activity against hepatocellular carcinoma (HepG2) cell line utilizing MTT assay evaluated at different concentration of the tested compound ranging from 100 to 5 µM for 48 and 72 hours respectively. The results revealed a moderate cytotoxic effect, and the higher values was achieved at 100 µM concentration with IC_{50} 24.5 and 17 µM respectively during 48 and 72 hours which is higher than previous values cited for amonafide scaffold. The calculated a=Atom-Economy found to be 88 % which reflects the high atom economy for simple coupling reaction. The E-Factor is 0.20 owing to the catalyst-free nature of the reaction as it removes the need for toxic heavy metals complex ligand.



Scheme 53. Coupling reaction of amonafide **245** with β-lactam derivative **246**.

Computer docking performed to evaluate the docking of **247** into DNA duplex in order to predict the binding affinity and mode considering the conformations, which is sterically acceptable. According to calculations, strong binding of docked hybrid molecule **247** to the DNA hexamer model suggested, which demonstrated that the lower the binding energy, the stronger the binding affinity between the receptor and the ligand (Figure 31). An interaction between hybrid **247** and DNA in the major groove forming a hydrogen bond to the lactam oxygen atom and result in the alternation of bond angles and bond lengths of **247**, in which some of them are increased, and others decreased.

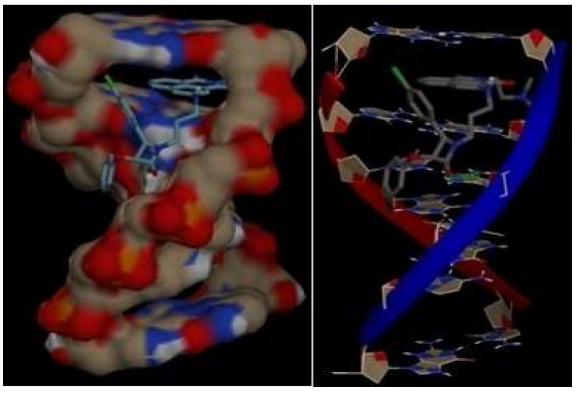
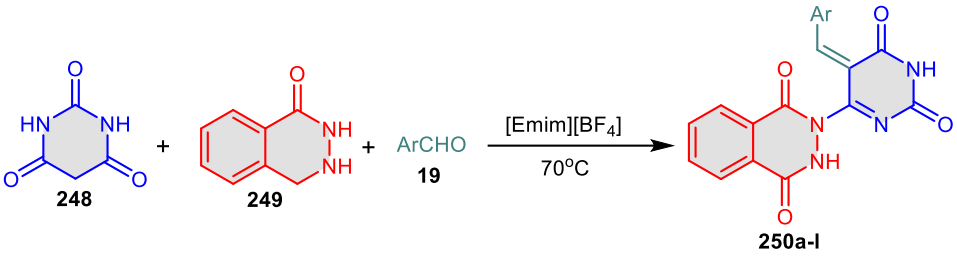


Figure 31. Molecular docking model of DNA with β-lactam **247**. Reproduced from Ref.;[188] Copyright 2019; Wiley.

 ©**AUTHOR(S)**

5.9. Hybrid molecules-based phthalazine moiety

A broad utility range has made pyrimidines privileged synthetic scaffolds.[189–192] Sreedevi and co-workers[193] introduced an efficient green, one-pot procedure for the synthesis of the hybrid 2-(5-(substituted)-2,6-dioxo-1,2,5,6-tetrahydropyrimidin-4-yl)-2,3-dihydrophthalazine-1,4-dione derivatives (**250a-l**) from aromatic aldehydes **19**, barbituric acid (**248**) and phthalhydrazide (**249**) utilizing ionic liquid [Emim][BF_4] as a green solvent and catalyst (Scheme 54).



250a-l: **a**, Ar= 2-$OCH_3C_6H_4$; **b**, Ar= 3-$OCH_3C_6H_4$; **c**, Ar= 2-$OC_2H_5C_6H_4$; **d**, Ar= 2-OHC_6H_4; **e**, Ar= 3-OHC_6H_4; **f**, Ar= 2,4-$(OH)_2C_6H_3$; **g**, Ar= 2-OH-3-$OCH_3C_6H_3$; **h**, Ar= 2-ClC_6H_4; **i**, Ar= 3-ClC_6H_4; **j**, Ar= 3-$NO_2C_6H_4$; **k**, Ar= 4-$C_2H_5C_6H_3$; **l**, Ar= 2-furyl.

Scheme 54. Synthesis of tetrahydropyrimidin-4-yl-2,3-dihydrophthalazine-1,4-diones **250a-l**.

Compounds **250l and 250j** identified as the most active for human chronic myeloid leukemia cells (K562), with IC_{50} = 21 and 24 µM and human colon carcinoma cells (Colo 205) with IC_{50} = 8 and 10 µM, whereas compounds **250c**, **250h**, **250i**, and **250k** showed moderate activity against both cell lines.

Authors extend their study to evaluate growth inhibition of products on K562 and Colo 205 cell lines. Among the products, compounds **250g** and **250j** showed the highest activity toward K562; meanwhile, compound **250a** exhibited the most potency against colon carcinoma cells (Colo 205). Moreover, all the titled compounds showed non-toxicity in normal non-cancerous cells (embryonic kidney) HEK 293.

The structure–activity relationship for obtained products investigated to establish biologically active core unit (DPD) in the synthesized scaffolds. According to the results obtained authors demonstrated that the binding mode and strength of targeted molecules depend on the diversity of structural moieties act as guest and hosting centers with proteins and enzymes (Figure 32, A-D). The effect of non-bonding delocalization of phthalazine-1,4-dione nitrogens into various parts of substituted pyrimidine-2,4-diones initiate electrophilic and nucleophilic centers, which facilitate its attack on proteins and enzymes. The structure, steric size, configuration, and nature of pyrimidine-2,4-dione substituents critically governed the accommodation in the active pockets of enzymes and proteins of living organisms, resulting in a normal metabolic biochemical process (Figure 33).

 ©**AUTHOR(S)**

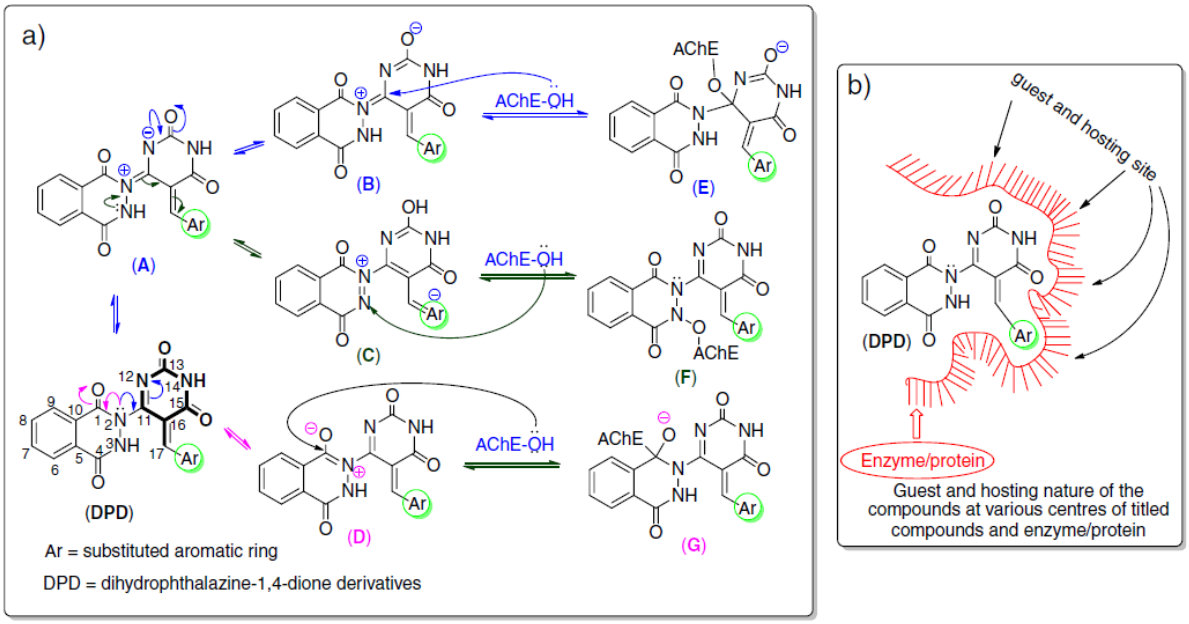


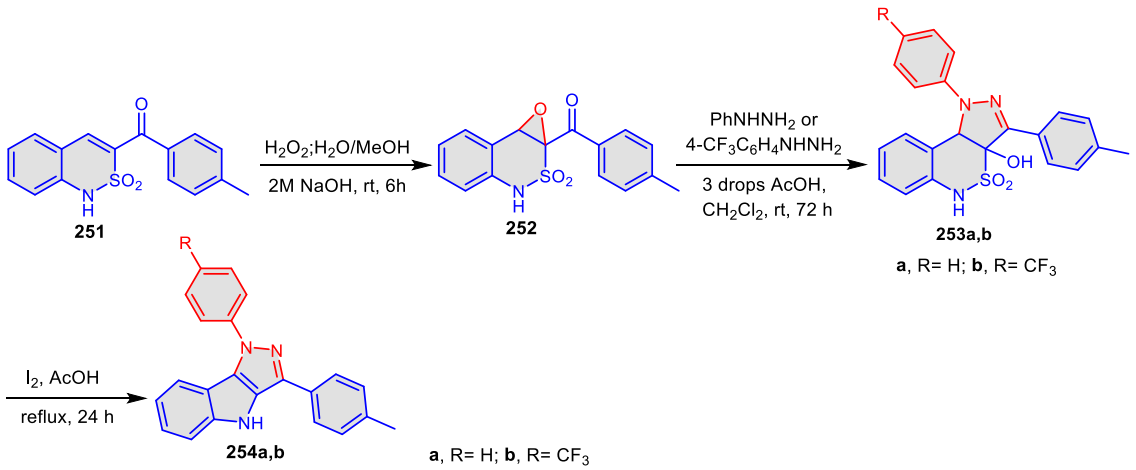
Figure 32. a) Schematic presentation of bio-active pharmacophore unit of dihydrophthalazine-1,4-dione derivatives, b) possible guest and hosting nature of the title compounds (**250a–l**): mechanistic hypothetical presentation. Reproduced from Ref.;[193] Copyright 2018; Wiley.

6. Fused Heterocycles

Fused heterocycles often revealed enhanced metabolic stability and greater ability to intercalate into DNA or bind to rigid enzyme pockets.

6.1. Five-five fused membered heterocycles

6.1.1. Pyrazolo[4,3-b]indoles synthesis. Novel 1,4-dihydropyrazolo[4,3-*b*]indoles **254a,b** synthesized *via* multistep sustainable protocol by epoxidation of 2,1-benzothiazine-2,2-dioxide **251**. Reaction of formed epoxide **252** with phenylhydrazine or 4-(trifluoromethyl)-phenylhydrazine and subsequent dehydration of the formed pyrazolo[4,3-*c*][2,1]benzothiazine-4,4-dioxides **253a,b** at ambient temperature produced the desired products[194] (Scheme 55).

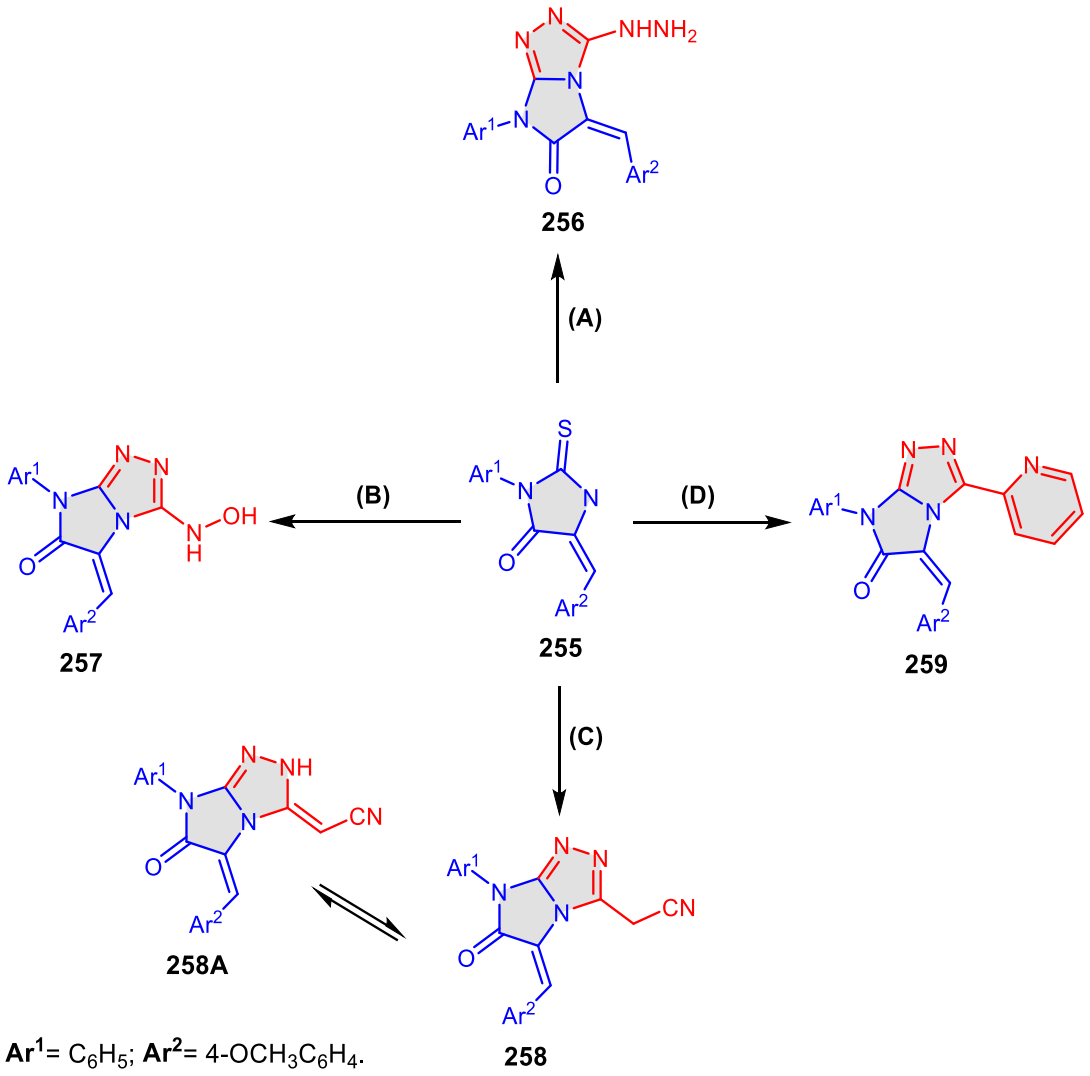


Scheme 55. Multi step reaction for the synthesis of pyrazolo[4,3-*b*]indoles **254a**,**b**.

 ©**AUTHOR(S)**

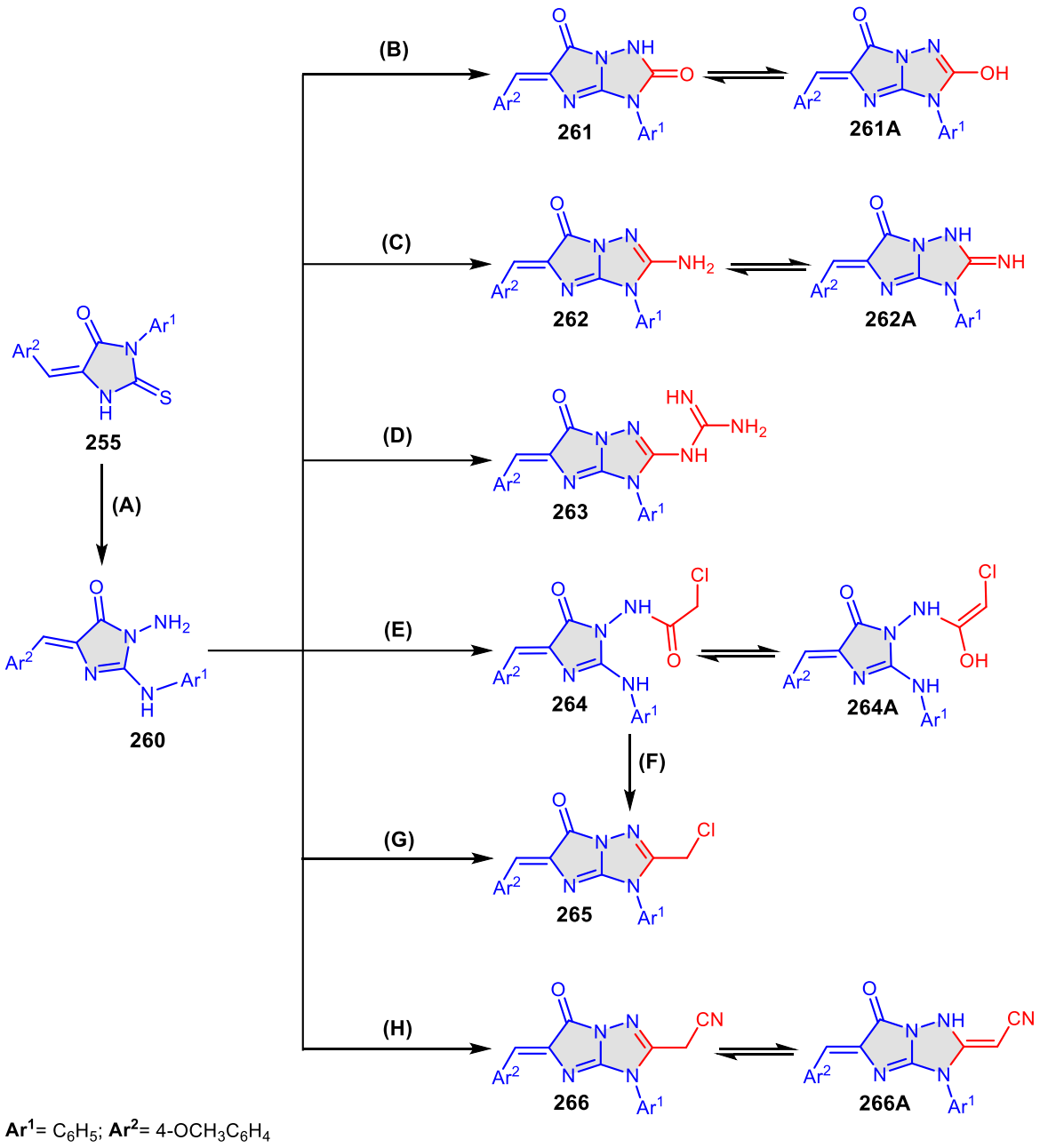
These scaffolds exhibit significant growth inhibition and induced apoptosis in acute myeloid leukemia OCI-AML3 cell lines. It show efficiency comparable to reference drugs azacitidine and decitabine with EC_{50} values (0.8 ± 0.1 and 0.7 ± 0.4 μM).

6.1.2. Imidazo-triazoles synthesis. The remarkable potent anti-cancer activity[195–197] of imidazo[1,2,4]triazole derivatives led El Deeb and co-workers to develop a green solvent-free preparation of a diversity of imidazotriazole derivatives **258-270**[198] (Scheme 56-58). It is well known that imidazo[1,2,4]triazoles were synthesized either from imidazole or triazole precursors.[196,199–202]



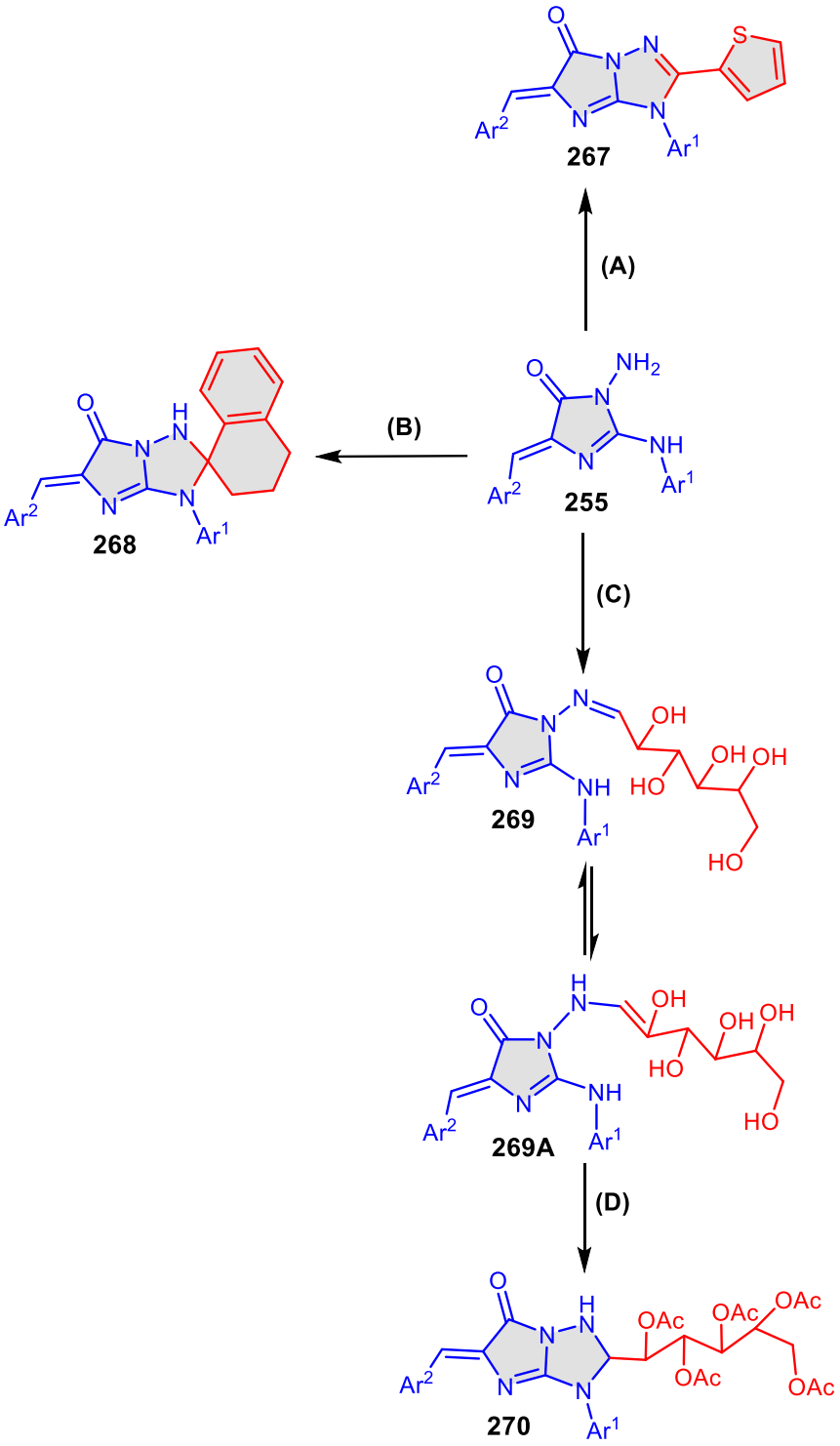
Scheme 56. Synthesis of compounds **256–259**. *Reagents and conditions*: A) thiocarbohydrazide, f
usion (**256**); B) *N*-hydroxyhydrazinecarbo-thioamide hydrochloride, fusion (**257**); C) cyanoacetohydrazide, fusion (**258**); D) picolinohydrazide, fusion, 6 h, (**259**).

 ©**AUTHOR(S)**



Scheme 57. Synthesis of compounds **260-266**. Reagents and conditions: A) hydrazine hydrate, ethanol, reflux (**260**); B) ethyl chloroformate, fusion (**261**); C) cyanamide, fusion (**262**); D) cyanoguanidine, fusion (**263**); E) chloroacetyl chloride, dioxane, reflux (**264**); F) fusion (**265**); G) chloroacetyl chloride, reflux (**265**); H) ethyl cyanoacetate, fusion (**266**).

©**AUTHOR(S)**



Scheme 58. Synthesis of compounds **267-271**. Reagents and conditions: A) thiophen-2-carbonyl chloride, pyridine, reflux (**267**); B) 1-tetralone, glacial acetic acid, reflux (**268**); C) glucose, glacial acetic acid, H_2O, ethanol, reflux (**269**); D) acetic anhydride, reflux (**270**).

The anticancer activity of the newly synthesized targeted compounds tested against collection of human cancer cell lines, and inhibition growth percent (IGP) obtained for each cell line. Compound **270** the most potent activity **270** against leukemia RPMI-8226 cell line (IGP= 54.15%), non-small cell lung cancer NCI-H522 cell line

 ©**AUTHOR(S)**

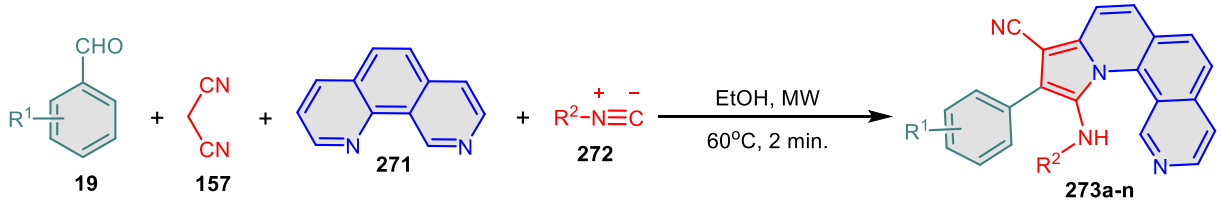
(IGP= 46.09%), melanoma UACC-62 (IGP= 41.24 %), renal cancer UO-31 cell line (IGP= 58.45%) and ovarian cancer OVCAR-8 (IGP= 48.74%). Likewise, Compounds **269** and **270** exhibit moderate to high activity against most leukemia cell lines (IGP= 20.32-67.54%). Moreover, Compound **355** was potent and selective against colon cancer SW-620 cell line (IGP= 44.13%).

Authors concluded from their results that the presence of sugar moiety in compound **269** increases the anti-cancer activity against leukemia CCRF-CEM and SR cell lines (IGP= 67.54% and 37.90%, respectively.

6.2. Five-six fused membered heterocycles

6.2.1. Pyrrolo-phenanthroline synthesis. Sustainable multi-component synthesis utilized for producing diversity of pyrrolophenathrolines **273a-n** in ethanol under microwave heating. A heterocyclic framework consists of polysubstituted pyrroles with its wide range of anti-cancer activities, and carcinostatic 1,10-phenanthrolines might exhibit biological activities for both. Only few reports discussed the synthesis of pyrrolo[1,10]phenanthrolines.

Diversity-oriented synthesis (DOS)[203–205] and biologically oriented synthesis[206,207] were utilized in a green multi-component synthesis of various pyrrolo[1,10]phenanthrolines **273a-n** in 93-98% yields through reaction of aromatic aldehydes **19**, malononitrile (**157**), 1,10-phenanthroline (**271**), and isocyanides **272** in ethanol promoted with MW heating at 60°C for 2 minutes. The nature of isocyanide substituents plays a crucial role in the reaction course. Aliphatic isocyanides have low nucleophilicity, which leads to disadvantages. However, bulky substituents like *t*-butyl moiety result in no reaction as a sequence of steric effects (Scheme 59).[208]

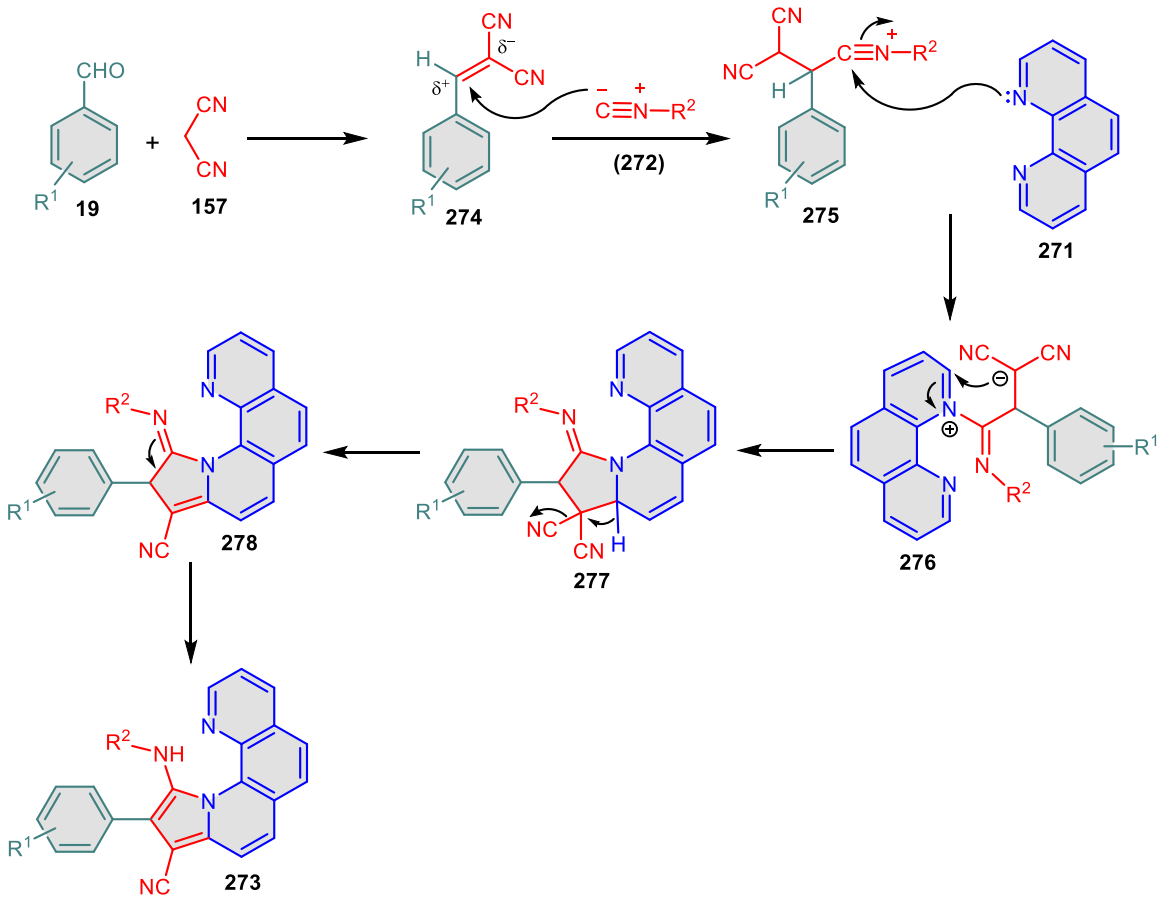


273a-n: **a**, R^1= 3,4-$(OMe)_2$, R^2= 4-$OMeC_6H_4$; **b**, R^1= 4-OC_4H_9, R^2= 4-$OMeC_6H_4$; **c**, R^1= 4-CN, R^2= 4-$OMeC_6H_4$; **d**, R^1= 4-Cl, R^2= 4-$OMeC_6H_4$; **e**, R^1= 4-NO_2, R^2= 4-$OMeC_6H_4$; **f**, R^1= 4-Me, R^2= 4-$OMeC_6H_4$; **g**, R^1= 4-OC_4H_9, R^2= cyclohexyl; **h**, R^1= 2-Cl, R^2= 4-$OMeC_6H_4$; **i**, R^1= 2,4-$(Cl)_2$, R^2= 4-$OMeC_6H_4$; **j**, R^1= H, R^2= 4-$OMeC_6H_4$; **k**, R^1= 4-$CH(CH_3)_2$, R^2= C_6H_5; **l**, R^1= 4-F, R^2= 4-$OMeC_6H_4$; **m**, R^1= 3-Br, R^2= 4-$OMeC_6H_4$, **n**, R^1= 4-CN, R^2= cyclohexyl.

Scheme 59. Synthesis of substituted pyrrolo[1,10]phenanthrolines **273a-n**.

A mechanism to account for the formation of **273** depicted in Scheme 60.

 ©**AUTHOR(S)**



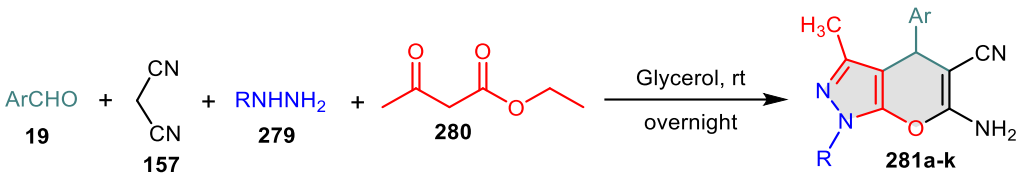
Scheme 60. A suggested mechanism for the formation pyrrolo[1,10]phenanthrolines **273**.

The nature of the N-substitution at C-11 found to be the critical determination of anti-cancer activity. Bulky or electron-withdrawing groups reducing efficiacy due to steric hindrance. The authors evaluated the cell viability and growth inhibition of synthesized compounds toward human gastric adenocarcinoma cancer cells. The results obtained exhibit dependence on the nature of *N*-substituent at C-11. Compounds **273g** and **273n** with 4-*O*-butyl and cyclohexyl *N*-substituent showed significant cytotoxicity effects compared to doxorubicin used as a standard. However, **273e** with electron-withdrawing substituents is of poor anti-cancer activity. Meanwhile, remaining scaffolds with electron-donating groups or halogen atoms showed moderate to good anti-cancer activity.

6.2.2. Pyrano-pyrazoles synthesis. Natural products play a multitude of biological properties, which used to assess the structure of novel lead compounds. Therefore, there is a need to explore area of synthetic scaffolds not occupied by natural products.[209] Pyrano[2,3-*c*]pyrazoles are privileged scaffolds that exhibit a broad variety of biological functions, particularly anti-cancer agents. Several naturally occurring pyranopyrazoles with biological activities known. Several methods were reported for their synthesis.[210–218]

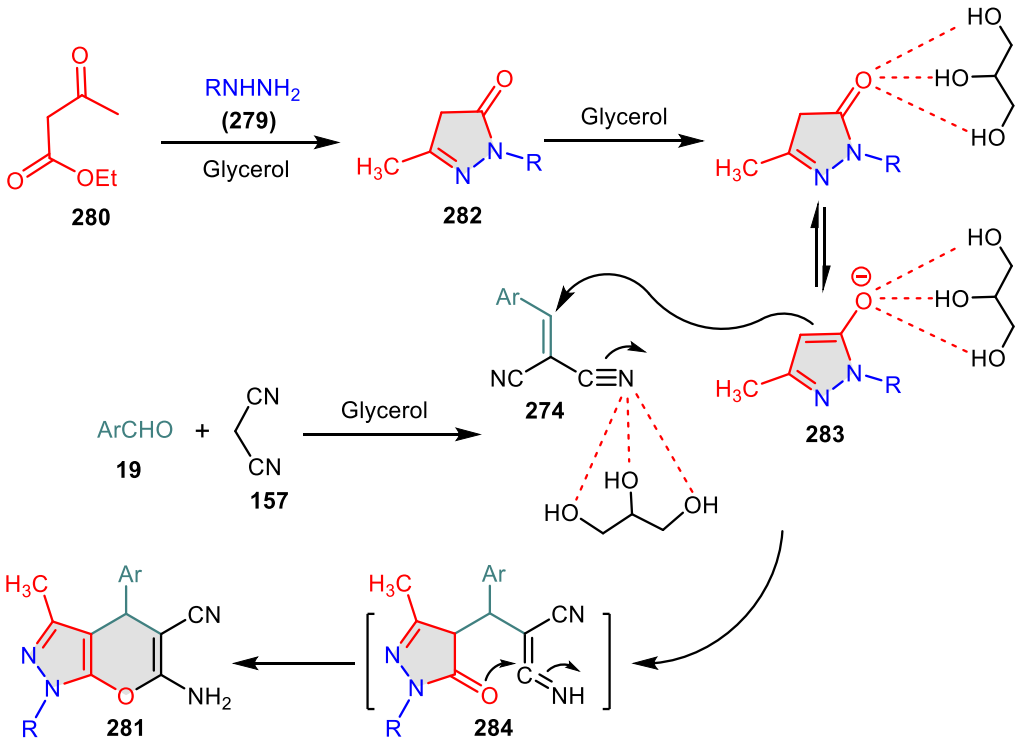
An efficient green synthesis of pyrano[2,3-*c*]-pyrazoles **281a-k** was achieved *via* a catalyst-free four-component reaction of aromatic aldehydes **19**, malononitrile (**157**), hydrazine hydrate derivatives **279** and ethyl acetoacetate (**280**) in glycerol at ambient temperature (Scheme 61).[219] A plausible mechanism to account for the formation of **161** depicted in Scheme 62. The reaction proceeds with high Atom-Economy value of 71.59 % and low E-Factor of 0.32. are foundational to high greens of the reaction.

 ©**AUTHOR(S)**



281a-k: **a**, Ar= 4-ClC_6H_4, R= H; **b**, Ar= 4-$OCH_3C_6H_4$, R= H; **c**, Ar= 2-ClC_6H_4, R= H; **d**, Ar= 2-$OCH_3C_6H_4$, R= H; **e**, Ar= C_6H_5, R= H; **f**, Ar= 2-furyl, R= H; **g**, Ar= 4-$NO_2C_6H_4$, R= H; **h**, Ar= 4-$NO_2C_6H_4$, R= C_6H_5; **i**, Ar= 2-furyl, R= C_6H_5; **j**, Ar= 2-$OCH_3C_6H_4$, R= C_6H_5; **k**, Ar= R= C_6H_5.

Scheme 61. Green synthesis of pyrano[2,3-*c*]-pyrazoles **281a-k**.



Scheme 62. Mechanism illustrate the formation of pyrano[2,3-*c*]-pyrazoles **281**.

To evaluate the greens of such approach, the EcoScale[220] for **281a** was calculated particularly when compared to other previously announced approaches and it was found to have the highest among others with a value of 95.

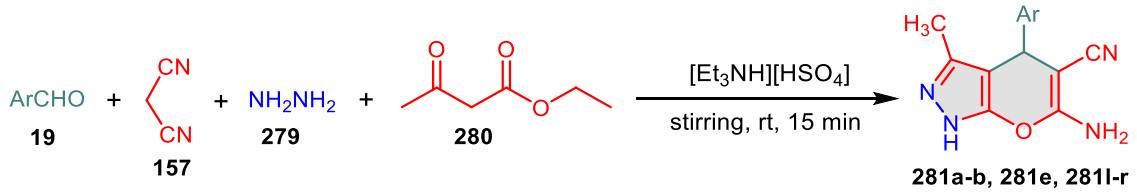
Shukla *et al.*[221,222] have recently reported that except for their study, there is no comprehensive study involving *in vitro* biological activities concerning pyranopyrazoles concerning *in silico* studies. They accomplished a similar four-component reaction as that illustrated in Scheme 61, promoted by microwave irradiation at ambient temperature.

Biological screening identified compounds **281a, 281b** as having strong cellular antiproliferative activity and proposed them as potential tubulin-targeting hits. Docking predicted favorable interactions within the tubulin binding site. with GI_{50} value of less than o.1 µM against breast (MDA-MB-231) and melanoma (SK-MEL-2) cell lines. Docking analysis into the active site of tubulin. The synthesized compounds tested for activity towards Hep3b carcinoma cell lines hepatocellular. Most of the obtained compounds exhibit moderate to good anti-

 ©**AUTHOR(S)**

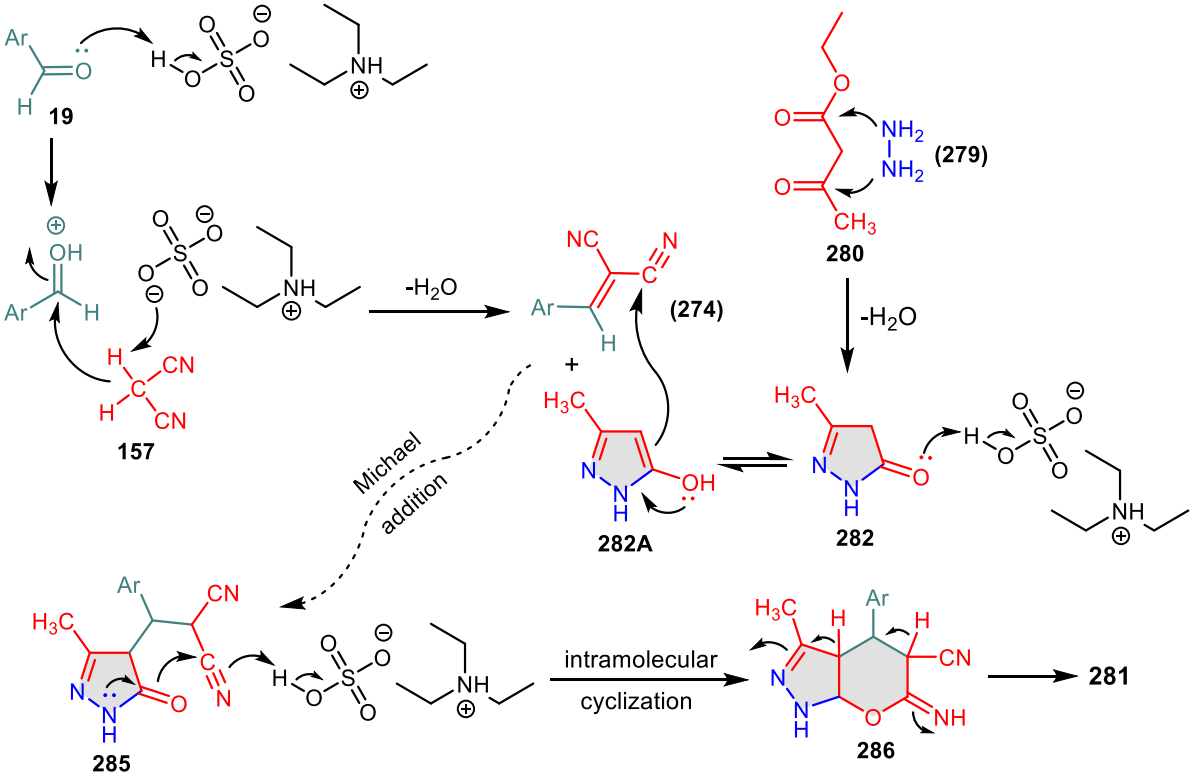
cancer activity against the MTT assay. The docking studies confirmed strong binding interactions, with **281a** establishing multiple hydrogen bonds with ASP111 and Ser153. Testing againstcompounds were K-1 protein showed that pyrano[2,3-*c*]pyrazole **281** with Ar= 4-N(Me)$_2$C$_6$H$_4$ substituent possess good binding affinities to the DNA.[221]

Owing to their significant anti-cancer activity,[223–225] Nikalje *et al*.[226] reported a green one-pot four-component process for the synthesis of dihydropyrano[2,3-*c*]pyrazoles **281** using aryl aldehydes **19**, malononitrile (**157**), hydrazine hydrate (**279**) and ethyl acetoacetate (**280**) in ionic liquid triethylammonium hydrogen sulphate [Et$_3$NH][HSO$_4$] as a solvent and catalyst at ambient temperature (Scheme 63). The reaction mechanism depicted in (Scheme 64).



281a-b, 281e, 281l-r: **a**, Ar= 4-ClC$_6$H$_4$; **b**, Ar= 4-OCH$_3$C$_6$H$_4$; **e**, Ar= C$_6$H$_5$; **l,** Ar= 4-FC$_6$H$_4$; **m,** Ar= 4-OHC$_6$H$_4$; **n**, Ar= 3-OCH$_3$-4-OHC$_6$H$_3$; **o**, Ar= 3,4-(OCH$_3$)$_2$C$_6$H$_3$; **p**, Ar= 3-NO$_2$C$_6$H$_4$; **q**, Ar= 2-thienyl; **r**, Ar= 4-(benzyloxy)C$_6$H$_5$.

Scheme 63. Four-component reaction for the synthesis of dihydropyrano[2,3-*c*]pyrazoles **281**.



Scheme 64. Mechanism describing the formation of dihydropyrano[2,3-*c*]pyrazoles **281**.

 ©**AUTHOR(S)**

Biological screening identified scaffolds 281a, 281b, as potential tubulin inhibitors with IG50 values less than 0.1 µM against breast (MDA-MB231) melanoma (SK-MEL-2) cell lines. Docking into the acive site of tubulin confirmed strong binding interactions, with scaffold 281a estabkishing multiple hydrogen bonds with ASsp 111 and Ser153.

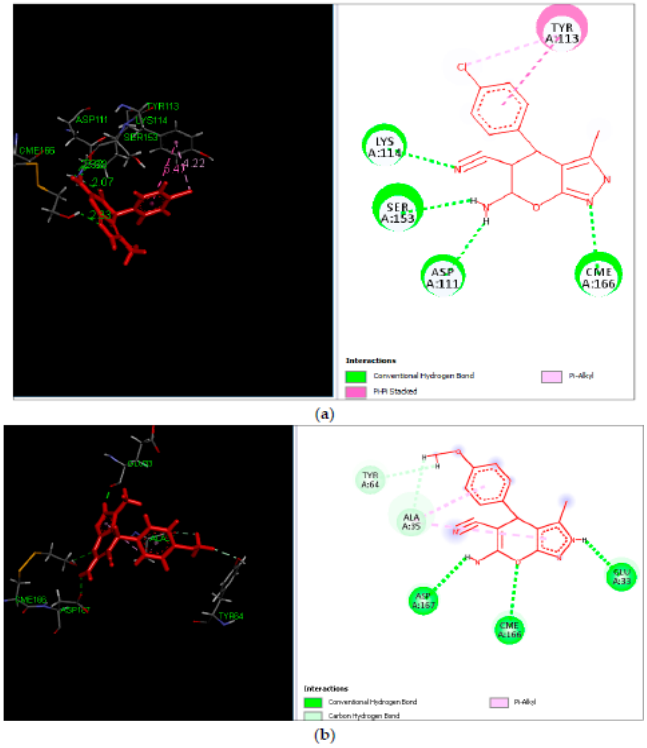
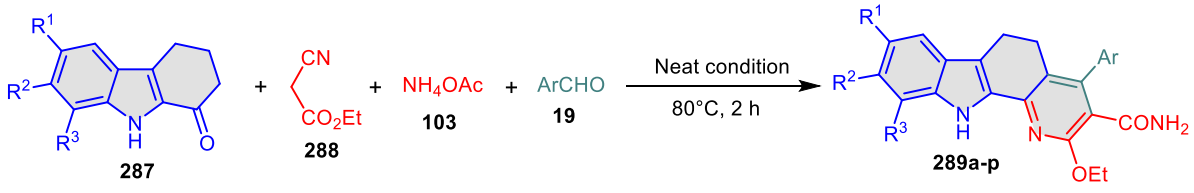


Figure 33. Binding poses and molecular interactions of (**a**) compound **281a** and (**b**) compound **281b** into the active site of tubulin. Reproduced from Ref.;[226] Copyright 2017; MDPI.

6.2.3. Pyrido-carbazole synthesis. The synthesis of 2-oxo-4-aryl-5,6-diuhydro-11H-pyrido[2,3-a]carbazol-3-carbonitriles **289a-p** through solvent-free four component reaction underscores the utility of dry-media synthesis[227] (Scheme 65). Although the previous reported methods for the synthesis of pyridocarbazoles are numerous,[228–231] the sustainable synthetic protocols are limited in the literature.

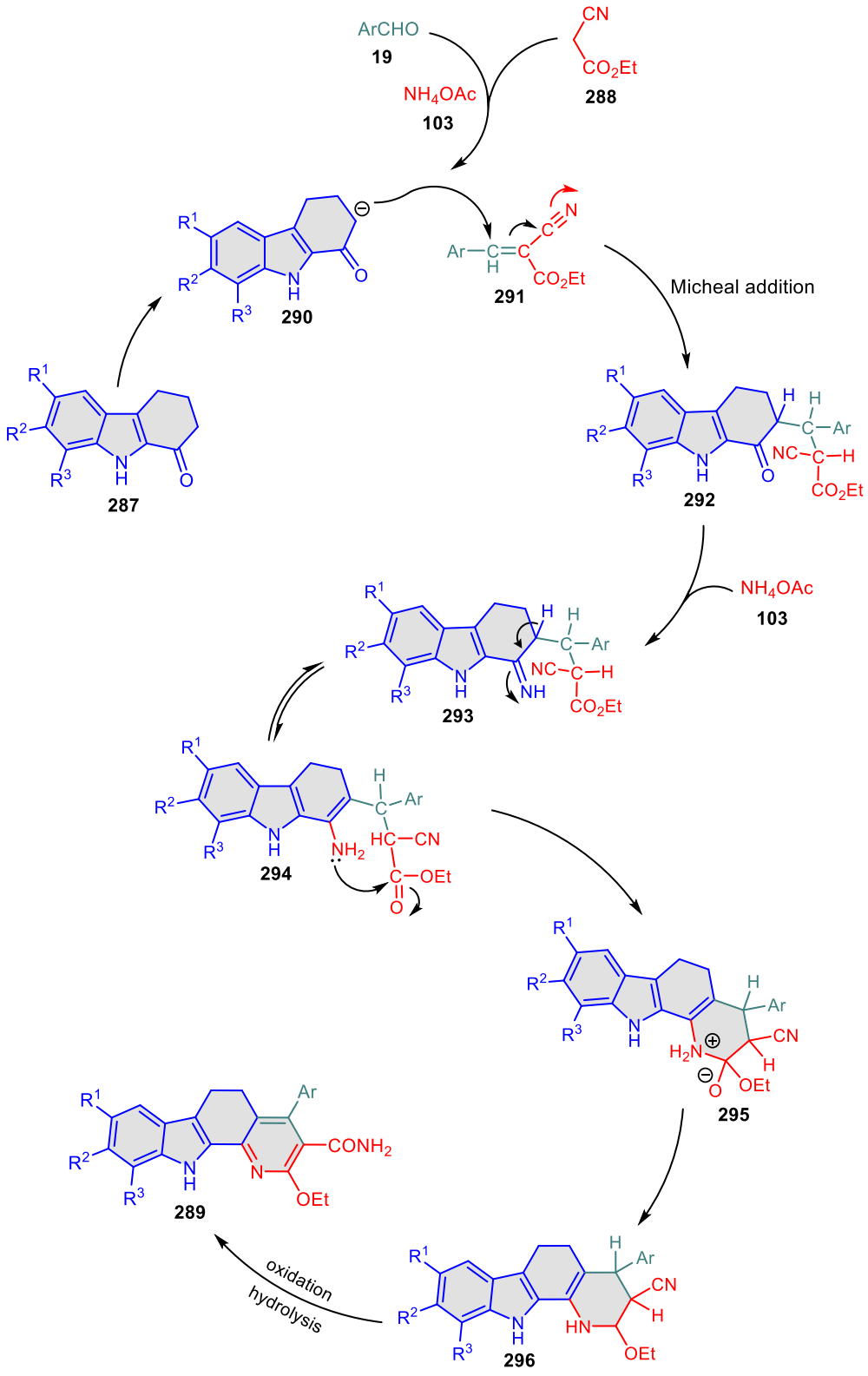


289a-p: **a**, Ar= C_6H_5, R^1= CH_3, R^2= R^3= H; **b**, Ar= C_6H_5, R^1= R^2= H, R^3= CH_3; **c**, Ar= C_6H_5, R^1= Cl, R^2= R^3= H; **d**, Ar= C_6H_5, R^1= R^2= R^3= H; **e**, Ar= 2-thienyl, R^1= CH_3, R^2= R^3= H; **f**, Ar=2-thienyl, R^1= R^2= H, R^3= CH_3; **g**, Ar= 2-thienyl, R^1= Cl, R^2= R^3= H; **h**, Ar= 4-FC_6H_4, R^1= CH_3, R^2= R^3= H; **i**, Ar= 4-FC_6H_4, R^1= R^2= H, R^3= CH_3; **j**, Ar= 4-FC_6H_4, R^1= R^2= R^3= H; **k**, Ar= 4-$CH_3C_6H_4$, R^1= CH_3, R^2= R^3= H; **l**, Ar= 4-$CH_3C_6H_4$, R^1= R^2= H, R^3= CH_3; **m**, Ar= 4-$CH_3C_6H_4$, R^1= R^2= R^3= H; **n**, Ar= 4-$OCH_3C_6H_4$, R^1= CH_3, R^2= R^3= H; **o**, Ar= 4-$OCH_3C_6H_4$, R^1= R^2= H, R^3= CH_3; **p**, Ar= 4-$OCH_3C_6H_4$, R^1= R^2= R^3= H.

Scheme 65. Synthesis of pyridocarbazoles **289a-p.**

 ©**AUTHOR(S)**

A suggested mechanism for the formation of the reaction products illustrated in Scheme 66.



Scheme 66. A plausible mechanism to for the formation of **289**.

These pyridcarbazoles tested against MCF-7 and A549 cell lines. Thiophene-containing and fluoro-substituted analogues, including **289g**, were among the more active members of the series, with IC_{50} values of approximately 45 µM.

 ©**AUTHOR(S)**

This level of activity is best described as moderate rather than highly potent. SAR studies indicated that electron-withdrawing groups and the presence of sulfur in the side chain strongly enhanced cytotoxicity.[232,233]

6.2.4. Pyrido-pyrazole synthesis. A major source in the area of cancer treatment was offered by bioactive natural products, which represent about 60% of drugs utilized as anti-cancer reagents, and the screening of derived collection of natural products is significantly higher than those resulting from screens synthesis libraries.[234,235] However, several obstacles raised in utilizing natural products as anti-cancer reagents, such as complex ring structures, large numbers of stereogenic centers as well as problems of large-scale supply.

Intriguing approaches have been initiated by Magedov *et al.*[236,237] aimed at the synthesis of bioactive natural product mimetic of podophyllotoxin drug *via* a simple one-pot reaction. In this context, an efficient synthesis of dihydropyridopyrazoles **193a-q** (Figure 34) that relied on the reaction of 5-amino-3-methylpyrazole (**191**), aromatic aldehydes **60** and tetronic acid (**192**) in ethanol and heating under reflux.[238] It is worth mentioning that the generation of podophyllotoxin *via* derivatization is inaccessible and very lengthy (Scheme 67).[239]

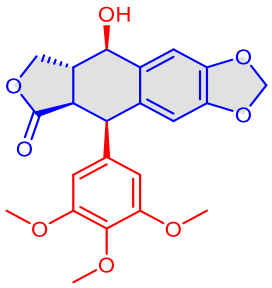
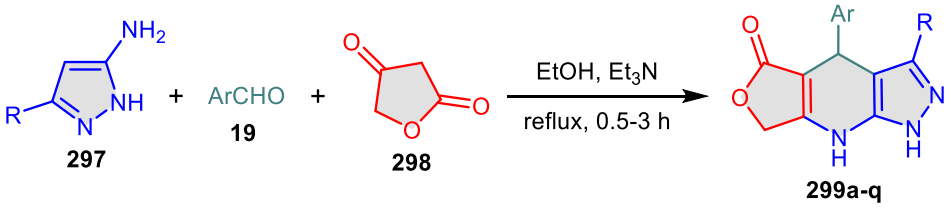


Figure 34. Structure of anti-cancer drug podophyllotoxin.



299a-q: **a**, Ar= 3,4,5-$(OCH_3)_3C_6H_2$, R= CH_3; **b**, Ar= 3,4,5-$(OCH_3)_3C_6H_2$, R= H; **c**, Ar= 3-Br-4,5-$(OCH_3)_2C_6H_2$, R= CH_3; **d**, Ar= 3-Br-4,5-$(OCH_3)_2C_6H_2$, R= H; **e**, Ar= 3-BrC_6H_4, R= CH_3; **f**, Ar= 3-BrC_6H_4, R= H; **g**, Ar= 5-Br-pyridin-3-yl, R= H; **h**, Ar= 5-Br-pyridin-3-yl, R= H; **i**, Ar= 3,5-$(Br)_2C_6H_3$, R= CH_3; **j**, Ar= 3,5-$(Br)_2C_6H_3$, R= H; **k**, Ar= 2-OH-3-OCH_3-5-BrC_6H_2, R= CH_3; **l**, Ar= 2-OH-3-OCH_3-5-BrC_6H_2, R= H; **m**, Ar= 2-OH-5-BrC_6H_3, R= CH_3; **n**, Ar= 2-OH-5-BrC_6H_3, R= H; **o**, Ar= 2-OH-3-$OCH_3C_6H_3$, R= H; **p**, Ar= 2-OH-3,5-$(Br)_2C_6H_2$, R= H; **q**, Ar= 4-Br-thien-2-yl, R= H.

Scheme 67. Synthesis of dihydropyridopyrazoles **299a-q**.

The antiproliferative activity of synthesized compounds towards human epithelioid cervix carcinoma (HeLa) and human breast carcinoma cell line (MCF-7) cell lines evaluated. Results showed that in comparison with naturally occurring podophyllotoxin, the presence of methoxy substituents in compounds **299a-q** is not important, and replacing bromo with hydroxyl substituents brings about higher potency.

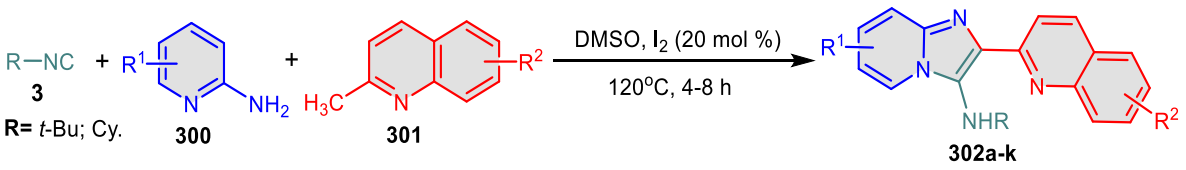
The antiproliferative activity of synthesized compounds towards human epithelioid cervix carcinoma (HeLa) and human breast carcinoma cell line (MCF-7) cell lines evaluated. Compound **299p** with aryl 2-hydroxy-3,5-

 ©**AUTHOR(S)**

dibromo-substituents is equipotent to podophyllllotoxin against HeLa and MCF-7 cell lines with GI_{50} with values 0.020 µM and 0.010 µM respectively. The apoptosis- inducing potential for the potent **299j**, GI_{50} (0.025 µM and 0.025 µM), respectively, and **299p** was compared with that of podophyllotoxin and was found to exhibit inducing at high nanomolar concentration.

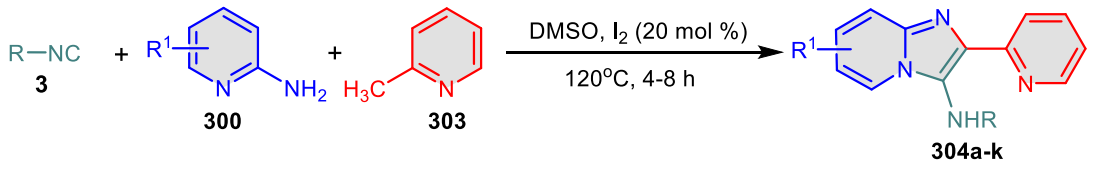
To determine their mode of action, authors performed flow cytometric cell cycle analysis, which pointed out retain of the anti-tubulin mechanism by the tested **299j** and **299p** that displayed a potent microtubule destabilizing effect like the tubulin polymerization inhibitor podophyllotoxin. This established by examination of cultured HeLa human cells treated with **299p,** which revealed both interphase and mitotic microtubule organization at low concentration (5 nM).

6.2.5. Imidazo-pyridines synthesis. A very interesting one-pot, efficient, green three-component, and metal-free synthesis of substituted imidazo[1,2-*a*]pyridines **302a-k**, **304a-k,** and **306a-d** have been developed by Kamal and co-authors.[240] Authors exploited the iodine-catalyzed oxidative amination of azaarenes benzylic C-H bonds with 2-aminoazines in DMSO. The reaction proceeds via condensation with isocyanides and heating for at 120^{0}C . This could be rationalized *via* participation of DMSO in the oxidation of benzylic C(sp^3)-H bond. Several ratios of iodine were examined, and results showed that 20 mol% was the optimum load that afforded the highest yields (Scheme 68-70). Plausible mechanism for the iodine-catalyzed oxidative condensation depicted in Scheme 71.



302a-k: **a**, R= *t*-Bu, R^1= R^2= H; **b**, R= cyclohexyl, R^1= R^2= H; **c**, R= *t*-Bu, R^1= 6-Cl, R^2= H; **d**, R= *t*-Bu, R^1= 6-Br, R^2= H; **e**, R= *t*-Bu, R^1= 6-CH_3, R^2= H; **f**, R= *t*-Bu, R^1= 7-CH_3, R^2= H; **g**, R= *t*-Bu, R^1= 8-$CONH_2$, R^2= H; **h**, R= cyclohexyl, R^1= 8-$CONH_2$, R^2= H; **i**, R= *t*-Bu, R^1= H, R^2= 7-Cl; **j**, R= *t*-Bu, R^1= H, R^2= 8-NO_2; **k**, R= *t*-Bu, R^1= H, R^2= 6-OCH_3.

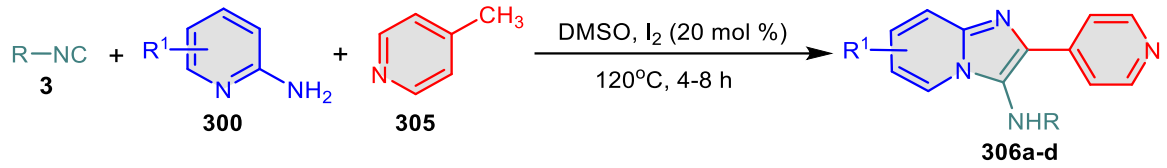
Scheme 68. Iodine-catalyzed reaction for the formation of diversity of 3-aminoimidazo[1,2-*a*]pyridines **302a-k**.



304a-k: **a**, R= *t*-Bu, R^1= H; **b**, R= cyclohexyl, R^1= H; **c**, R= *t*-Bu, R^1= 6-Cl; **d**, R= *t*-Bu, R^1= 6-Br; **e**, R= cyclohexyl, R^1= 7-CH_3; **f**, R= *t*-Bu, R^1= 6-NO_2; **g**, R= cyclohexyl, R^1= 6-NO_2; **h**, R= *t*-Bu, R^1= 8-$CONH_2$; **i**, R= cyclohexyl, R^1= 8-$CONH_2$; **j**, R= *t*-Bu, R^1= 8-CN; **k**, R= 2-Morpholinoethyl, R^1= H.

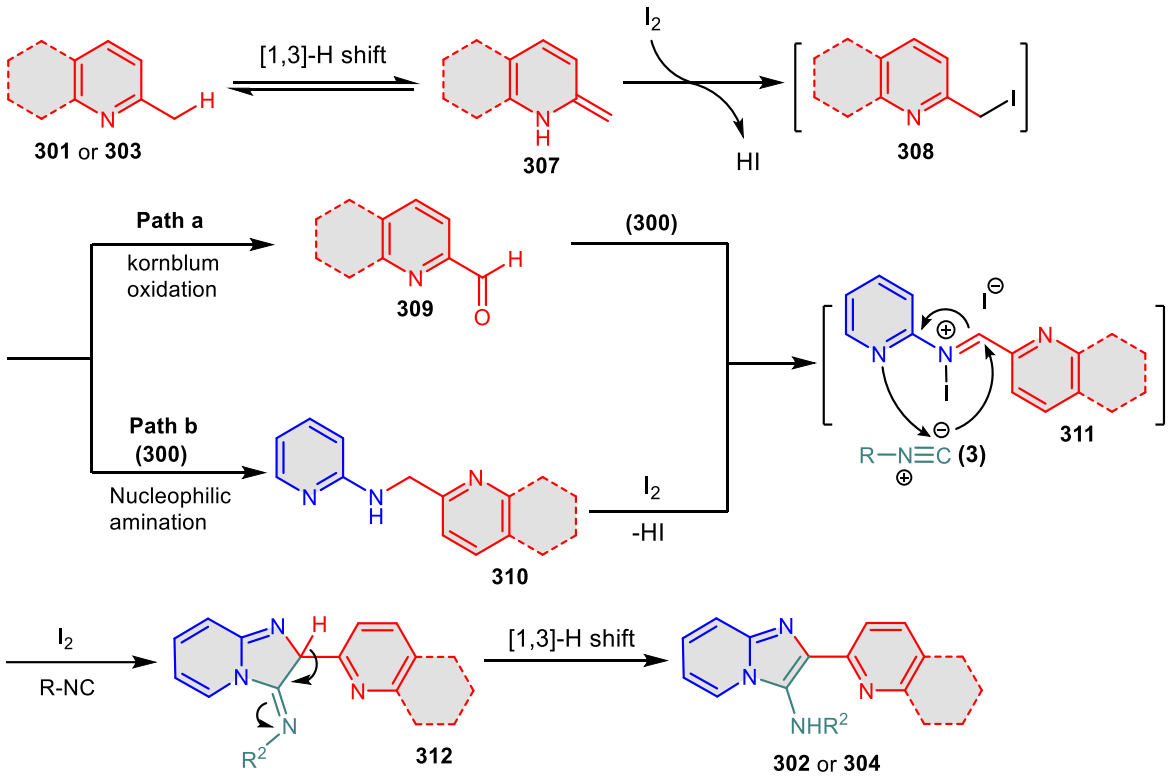
Scheme 69. Synthesis of various 3-aminoimidazo[1,2-*a*]pyridines **304a-k**.

 ©**AUTHOR(S)**



306a-d: **a**, R= *t*-Bu, R^1= H; **b**, R= cyclohexyl, R^1= 6-Cl; **c**, R= *t*-Bu, R^1= 6-Br; **d**, R= *t*-Bu, R^1= 8-CN.

Scheme 70. Synthesis of various 3-aminoimidazo[1,2-*a*]pyridines **306a-d**.



Scheme 71. Mechanism for the iodine-catalyzed oxidative condensation to produce **302** and **304**.

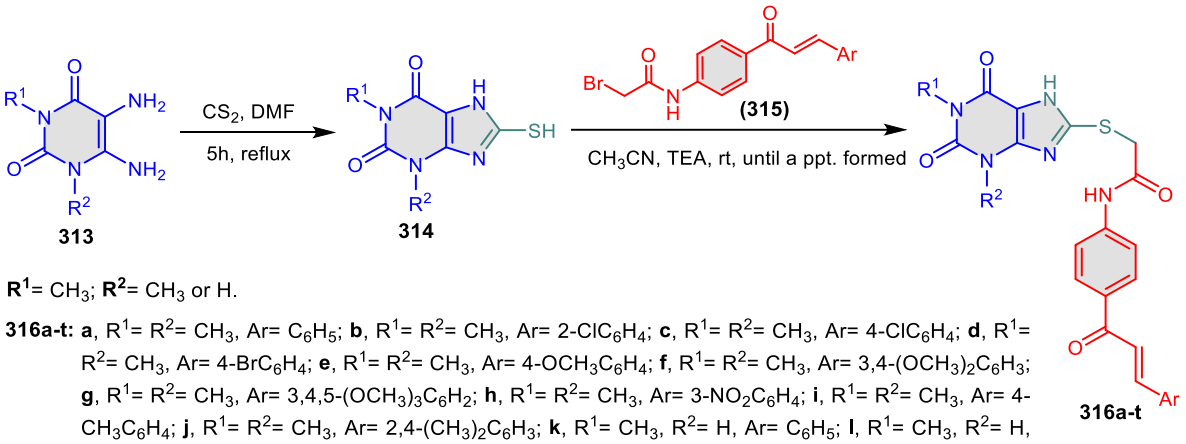
All the produced compounds screened for their cytotoxicity against five human cancer cell lines; lung cancer (A549), breast cancer (MCF-7), prostate cancer (PC-3), triple negative breast cancer (MDA-MB-231), and melanoma skin cancer (B16-F10) using MTT assay and doxorubicin as a standard drug. Compounds **302c**, **302i** and **302a** displayed the highest activity toward MDA-MB-231 with IC_{50} values of 5.01, 5.72 and 6.12 µm, respectively. Whereas **304a** is the most potent activity against MCF-7 with IC_{50} value of 4.88 µM and good results with A549 cell lines equals 7.67 µM, additionally, compounds **304b**, **304a**, and **302a** with IC_{50} 8.89, 9.7, and 11.05 µM, respectively.

The SAR of **302a**, **302c,** and **302i** was evaluated, and authors established that the presence of chlorine substituents at position-6 of imidazo[1,2-*a*]pyridine scaffold and position-7 in the quinoline ring and *N*-tertiary butyl group at the C3-position are crucial for cytotoxic activity.

 ©**AUTHOR(S)**

6.2.6. Xanthine-pyrimidines synthesis. Xanthine derivatives, such as theophylline, possess remarkable effect in lowering intracellular levels of the anti-apoptotic mediator Bcl-2. By carrying chalcone moiety, it become potent EGFR inhibitors and apoptotic inducers.[241]

Recent studies have demonstrated high bioactivity through hybridization of chalcones units with biologically active pharmacophores.[242] Inspired by this phenomenon, Youssif and co-authors[243] have reported a green synthesis of hybrid chalcone substituted xanthines **316a-t** as demonstrated in Scheme 72.



R^1= CH_3; **R**^{2}= CH_3 or H.

316a-t: **a**, R^1= R^2= CH_3, Ar= C_6H_5; **b**, R^1= R^2= CH_3, Ar= 2-ClC_6H_4; **c**, R^1= R^2= CH_3, Ar= 4-ClC_6H_4; **d**, R^1= R^2= CH_3, Ar= 4-BrC_6H_4; **e**, R^1= R^2= CH_3, Ar= 4-$OCH_3C_6H_4$; **f**, R^1= R^2= CH_3, Ar= 3,4-$(OCH_3)_2C_6H_3$; **g**, R^1= R^2= CH_3, Ar= 3,4,5-$(OCH_3)_3C_6H_2$; **h**, R^1= R^2= CH_3, Ar= 3-$NO_2C_6H_4$; **i**, R^1= R^2= CH_3, Ar= 4-$CH_3C_6H_4$; **j**, R^1= R^2= CH_3, Ar= 2,4-$(CH_3)_2C_6H_3$; **k**, R^1= CH_3, R^2= H, Ar= C_6H_5; **l**, R^1= CH_3, R^2= H, Ar= 2-ClC_6H_4; **m**, R^1= CH_3; R^2= H, Ar= 4-ClC_6H_4; **n**, R^1= CH_3, R^2= H, Ar= 4-BrC_6H_4; **o**, R^1= CH_3; R^2= H, Ar= 4-$OCH_3C_6H_4$; **p**, R^1= CH_3; R^2= H, Ar= 3,4-$(OCH_3)_2C_6H_4$; **q**, R^1= CH_3; R^2= H, Ar= 3,4,5-$(OCH_3)_3C_6H_2$; **r**, R^1= CH_3; R^2= H, Ar= 3-$NO_2C_6H_4$; **s**, R^1= CH_3; R^2= H, Ar= 4-$CH_3C_6H_4$; **t**, R^1= CH_3, R^2= H, Ar= 2,4-$(CH_3)_2C_6H_3$.

Scheme 72. Synthesis of hybrid chalcone substituted xanthines **316a-t**.

By carrying chalcone substituent, xanthine moieties showed potent EGFR and apoptotic induction. Compounds **316b, 316c** and 316h demonstrated IC50 values ranging from 1.0-1.3 1.3µM against breast (MF-7) and pancreatic (Panc1) cancer cell lines. The results demonstrated that the nature of substituent at position-4 of chalcon plays a crucial role in compound activity. Electron-withdrawing substituents showed higher inhibitory activity than those bearing electron-donating groups against almost all cell lines.

Mechanistic evaluation demonstrated that **316c** causes irreversible apoptosis and cell cycle arrest at the G2/M phase, while also inducing 8-folds higher than control and higher than that of Staurosporine (Figure 35).

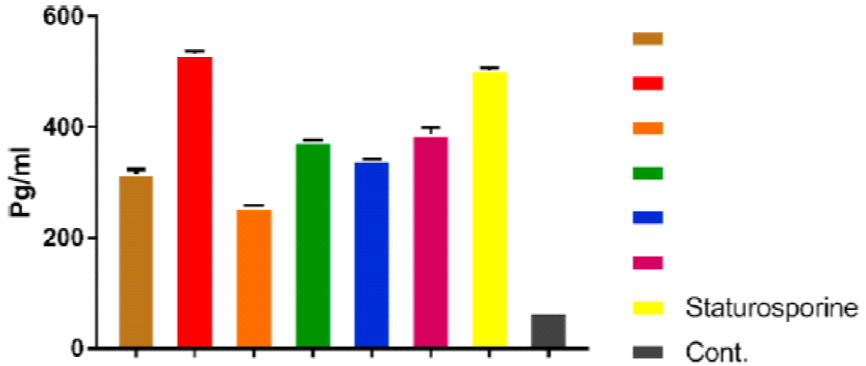


Figure 35. Caspase-3 for compounds **316b** (brown), **316c** (red), **316e** (orange), **316f** (green), **316h** (blue), **316o** (pink) and Staurosporine in (Panc-1). Reproduced with permission from Ref.;[243] Copyright 2019; Elsevier.

 ©**AUTHOR(S)**

This approach extended to evaluate the potentiality of the compounds **316c**, **316f,** and **316h** on caspase-8, Bax, and Bcl-2 levels against Panc-1. The results obtained demonstrated an impressive rise in both caspase-8 and Bax levels relative to Staurosporine, with compound **316f** showing the maximum over-expression of caspase-8 level. Compound **316c** ranked second; meanwhile, it displayed a pronounced induction of Bax referenced to doxorubicin with 25 folds higher than control unreacted Panc-1 cancer cell lines. An equipotent down-regulation of Bcl-2 protein level (1.22 ng/mL) and (1.46 ng/mL) was caused by compounds **316h** and **316c**, respectively, in Panc-1 cell line compared to Staurosporine (0.98 ng/mL) (Table 3) and (Figure 36).

Table 3. Caspase-8, Bax, and Bcl-2 levels for compounds **316c**, **316f**, **316h**, and Staurosporine on human pancreas cancer cells (Panc-1)

Compound	Caspase-8		Bax		Bcl-2	
	Conc (ng/mL)	Fold change	Conc (ng/mL)	Fold change	Conc (ng/mL)	Fold change
316c	1.21	14.33	235.20	28.46	1.46	3.48
316f	1.43	16.92	208.90	25.27	1.87	2.71
316h	1.08	12.77	188.50	22.80	1.22	4.16
Staurosporine	1.75	20.76	276.19	33.42	0.98	5.18
Control	0.084	1.0	8.26	1.0	5.08	1.0

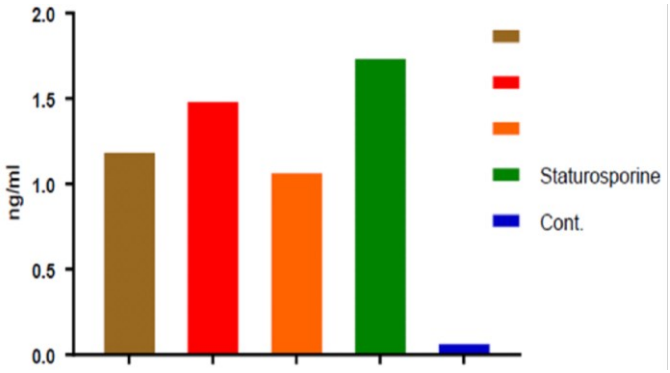


Figure 36. Caspase-8 level for compounds **316c** (brown), **316f** (red), **316h** (orange), and Staurosporine on (Panc-1). Reproduced with permission from Ref. [243]; Copyright 2019; Elsevier.

The most potent compound **316c** subjected to flow cell cycle analysis as a drug for Panc-1 cell in G0/G1 phase. A high decrease from 53.64% to 26.67% of the cell cycle in the control observed upon treatment with **316c** (Figure 36).

At the G2/M phase, this percentage notably increased to 48.56%, regarding **316c**, because of the accumulation of cells at this phase. Furthermore, the percentage of apoptotic cells increased from 1.79% in control unreacted Panc-1 cells to 27.15 and 33.57% in cells treated with 316**c** and doxorubicin, respectively, demonstrating that **316c** causes irreversible apoptosis (Figure 37).

 ©**AUTHOR(S)**

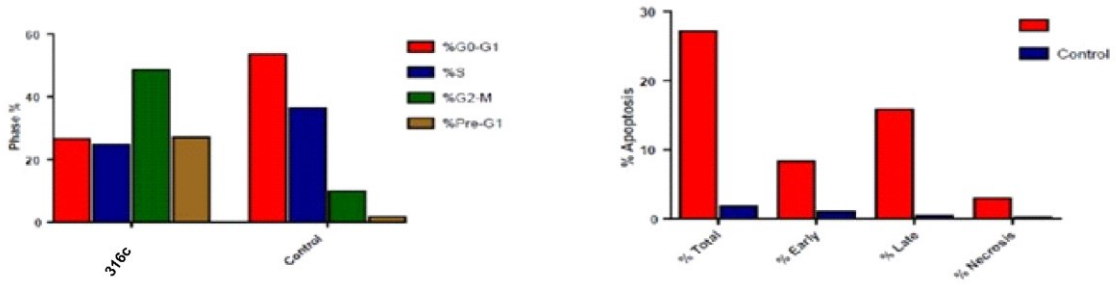
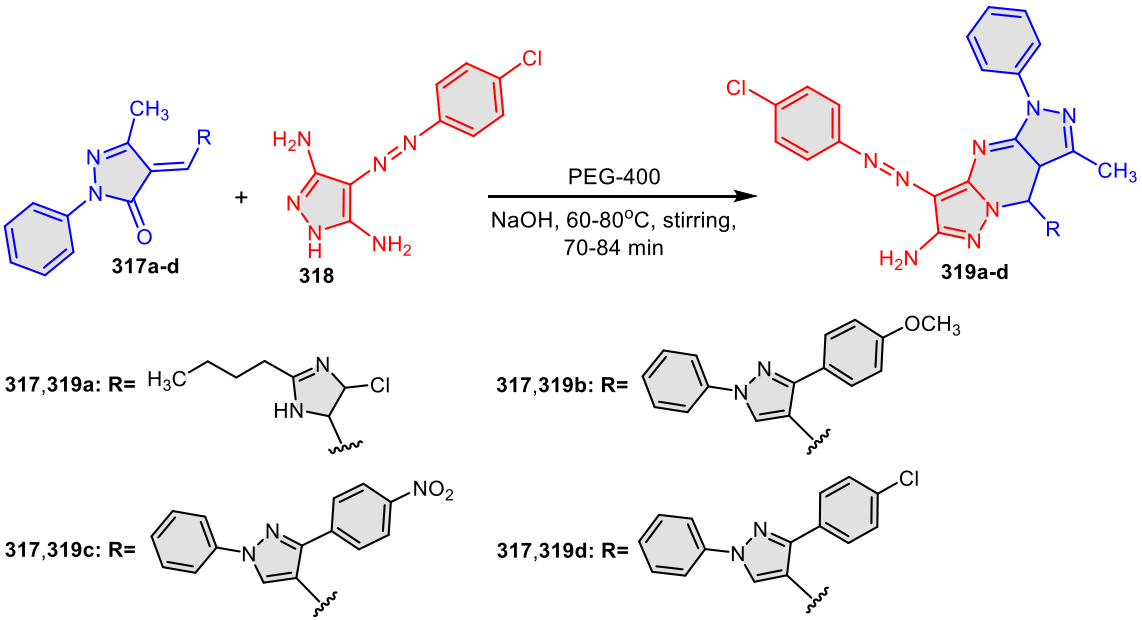


Figure 37. Cell cycle analysis on Panc-1cell line treated with compound **316c** (**A**). Compound apoptosis and necrosis percentages **316c** on Panc-1cell line (**B**). Reproduced with permission from Ref. [243]; Copyright 2019; Elsevier.

6.2.7. Pyrazolo-pyrimidines synthesis. Pyrazolo[1,5-*a*]pyrimidine derivatives as purine analogous possess significant anti-cancer and antileukemia effects, particularly those containing a number of fused bicyclic heterocycles, which are able to intercalate into base pairs. A green and efficient synthesis of pyrazolo[1,5-*a*]-pyrimidine derivatives 319**a-d** was developed by Dawane and co-authors[244] that relied on the reaction of 4-substituted benzylidene-3-methyl–1*H*-pyrazolo-5(4*H*)-one derivatives 317**a-d** with 4-arylazo-3,5-diaminopyrazole 318 in PEG-400 (polyethylene glycol) in the presence of sodium hydroxide and stirring at 60-80°C (Scheme 73).



Scheme 73. Synthesis of pyrazolo[1,5-*a*]-pyrimidine derivatives 319**a-d**.

The binding ability of Calf thymus DNA (CT-DNA) binding ability of products evaluated *via* viscosity measurements, thermal denaturation, absorption spectroscopy as well as molecular docking studies. The studies revealed that compounds **317a** and **319a** exhibited binding more affinity with base pairs of CT-DNA. The details analysis for DNA interaction with compounds **317a** and **319a** showed that they bind with pairs CT-DNA by interactions and intercalation. Moreover, the covalent binding of **317a** and **319a** with DNA resulted in

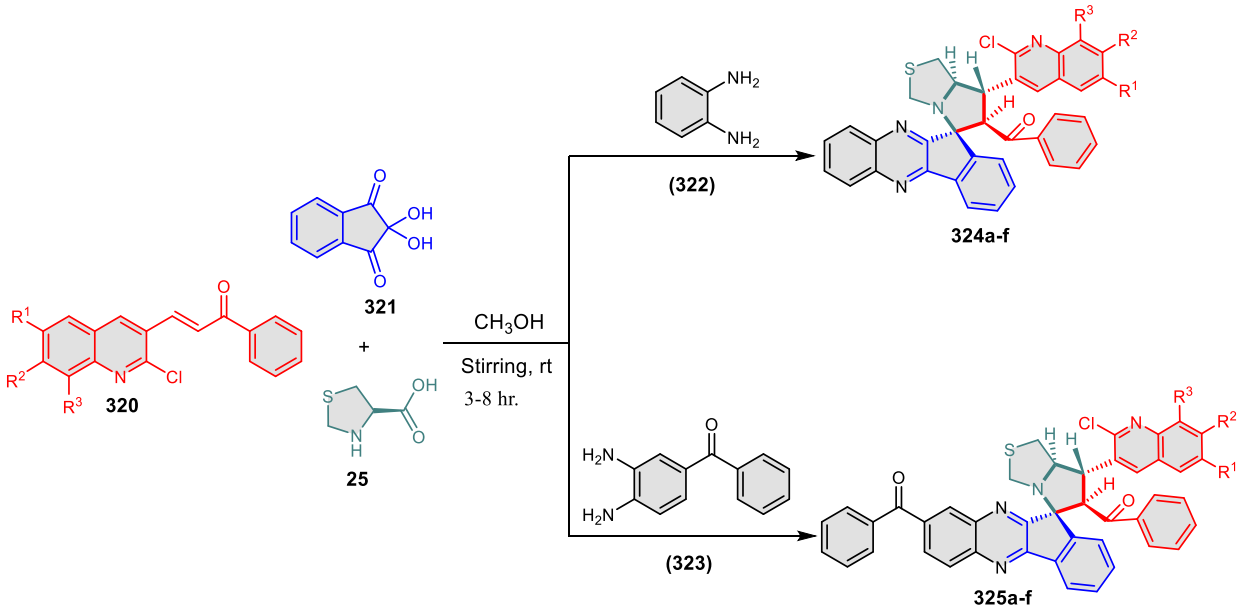
 ©**AUTHOR(S)**

conformations change of DNA resulting from increase of viscosity and intensity of spectroscopic absorption bands.

6.2.8. Indeno-quinoxalines synthesis

The creation of innovative therapeutics is crucial for enhancing the clinical prognosis of patients with tumor that operate *via* pathways distinct from those of currently available cancer treatments.[245–247]

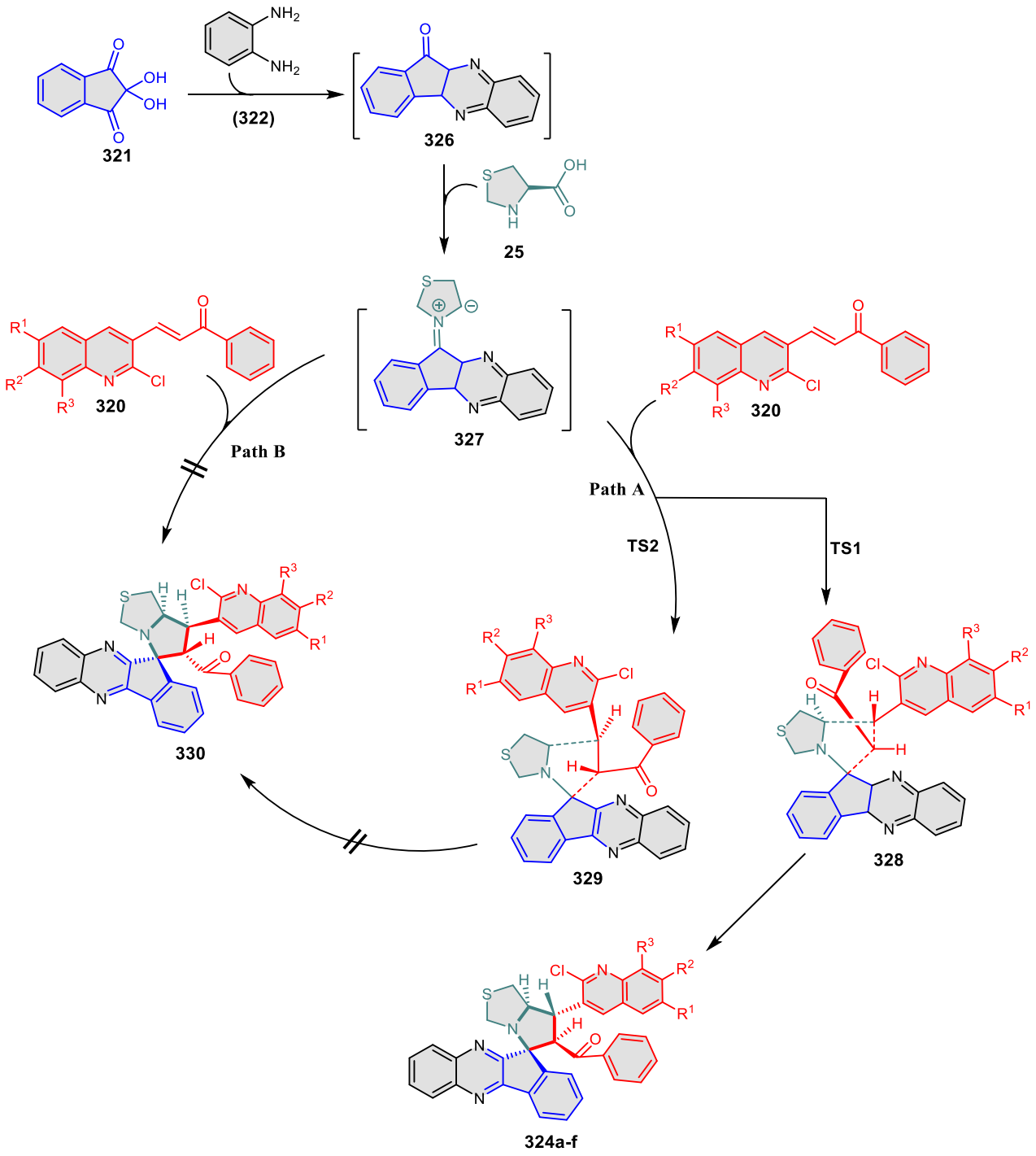
Quinolines, indeno-quinoxalines, and pyrrolizines represent a class of heterocyclic compounds of paramount significance in the field of anti-cancer drug discovery.[248–251] Recently, the research group of Rajendranan[252] introduced a new synthesis of novel spiro-indeno[1,2-*b*]quinoxaline-pyrrolothiazoles **324a-f** and **325a-f** employing a one-pot four-component reaction of quinolinyl chalcones **320**, ninhydrin (**321**), thiazolidine-2-carboxylic acid (**25**) and *o*-phenylene-diamines **322** or **323** in ethanol *via* [3+2] cycloaddition reaction (Scheme 74). The structure of products is established based on analytical and spectral data. X-ray crystallography also verified the molecular structure of synthetic compounds. A mechanism to rationalize for the formation of **324a-f** depicted in Scheme 75.



324a-f,**325a-f**: R^1= CH_3, R^2= R^3= H; **b**, R^1= R^3= H, R^2= CH_3; **c**, R^1= R^2= H, R^3= CH_3; **d**, R^1= OCH_3, R^2= R^3= H; **e**, R^1= R^3= CH_3, R^2= H; **f**, R^1= R^2= R^3= H.

Scheme 74. One-pot four-component synthesis of spiro-indeno[1,2-*b*]quinoxaline **324a-f** and **325a-f**.

 ©**AUTHOR(S)**



Scheme 75. A plausible mechanism for spiro-indeno[1,2-*b*]quinoxaline-pyrrolothiazoles **324a-f**.

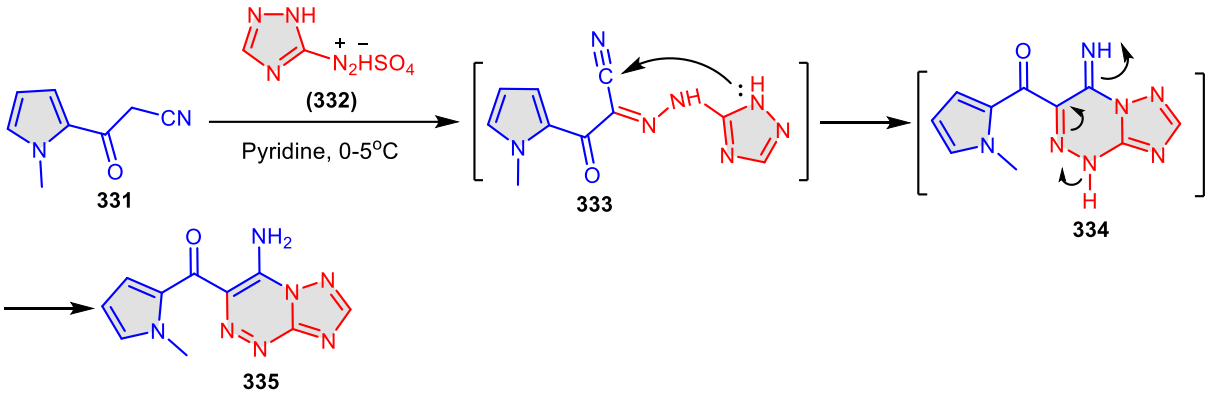
Synthesized compounds evaluated against breast cancer (MCF-7) and lung cancer (A549) cell lines *via* MTT assay method and doxorubicin as a reference drug. The results exhibited that good activity was achieved with products bearing a methyl group at position-6 and position-8 of quinoline moiety (**324e** and **325e**) with IC_{50} values of 11±1.0 and 11±1.0 µM against MCF-7 and 15±0.5 and 14±0.7 µM against A-549 compared to that of positive control doxorubicin 10±1.0 (MCF-7) and 11±1.4 (A-549) respectively. Moreover, compounds with electron-donating groups at C-6 and C-7 of quinolone moiety showed moderate potency.

A cell morphological analysis demonstrated and clearly revealed that compounds **324c**, **324e**, **325c,** and **325e** induce cell death by apoptosis and necrosis pathways.

 ©**AUTHOR(S)**

Molecular docking studies revealed that the most potent inhibitors **324c** and **325c** in using the epidermal growth factor receptor (EGFR) (PDB code: 1M17),[253,254] it is possible to investigate the binding modes at the enzyme's active site and learn more about how substances interact with its active amino acids. The protein crystal structure cleaned of the water molecules, heteroatoms, and ligands before being further prepared for docking.

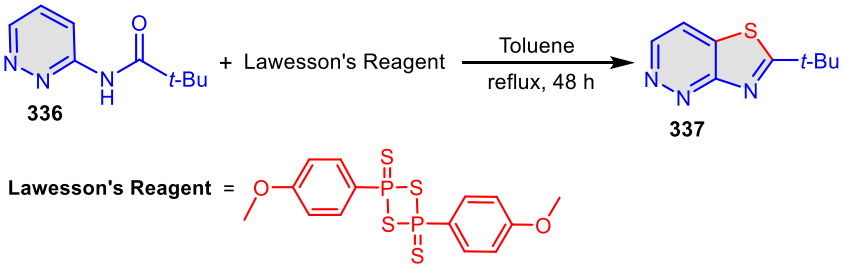
6.2.9. Triazolo-triazines synthesis. Triazolo-triazines are enormously potent and biologically relevant scaffolds.[255,256] [1,2,4]Triazolo[5,1-*c*][1,2,4]triazine (**335**) was classically synthesized *via* coupling of 2-cyanoacetyl-1-methyl-1*H*-pyrrole (**331)** with [1,2,4]triazole-3-diazonium sulfate **332** in presence of pyridine as a basic catalyst at 0-5 ºC (Scheme 76).[257]



Scheme 76. Synthesis of triazolo[5,1-*c*][1,2,4]triazine **335**.

Synthesized triazolo[5,1-c][1,2,4]triazine **335** was evaluated against HCT, Hep-2, Daoy, MCF-7, and WiDr cancer cell lines. Reported IC_{50} values were approximately 25.31-27.48 µg/mL for the responsive cell lines, indicating moderate in vitro cytotoxicity rather than high potency.

6.2.10. Thiazolo-pyridazines synthesis. Thiazolopyridazines have been widely used for several biological activities, including antimicrobial,[258] antiviral,[259] antioxidant[260] and anticancer[261] activities. Among thiazolopyridazine isomers, thiazolo[4,5-*c*]pyridazines have received much less attention, and most of their synthetic approaches suffer from major disadvantages. Only one method has been devised by Fruit and co-authors to develop their synthesis starting from pyridazine-3-carboxamide derivative **336** (Scheme 77).[262]

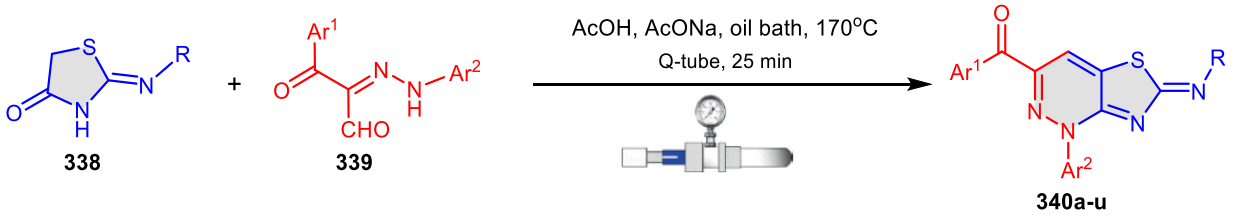


Scheme 77. Synthesis of thiazolo[4,5-*c*]pyridazine **337**.

With this background, Ibrahim and Behbehani[263] reported a straightforward, efficient, clean, short reaction times, and higher producibility environmentally friendly process using Q-tube high-pressure safe reactor to

 ©**AUTHOR(S)**

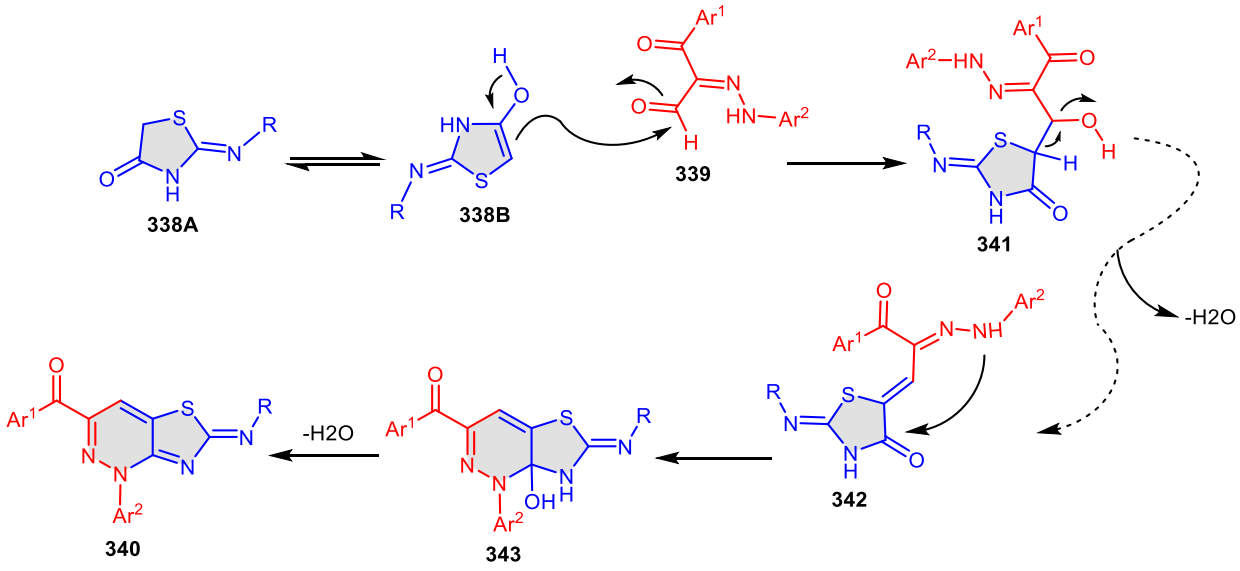
promote the synthesis of diverse thiazolo[4,5-*c*]pyridazine derivatives **340a-u** using [4+2] cyclocondensation reaction of 4-thiazolidinones **338** and 3-oxo-2-arylhydrazonopropanals **339** (Scheme 78).[264]



340a-u: **a**, R= 2-benzothiazolyl, Ar^1= Ar^2= C_6H_5; **b**, R= 2-benzothiazolyl, Ar^1= C_6H_5, Ar^2= 4-ClC_6H_4; **c**, R= 2-benzothiazolyl, Ar^1= C_6H_5, Ar^2= 4-$NO_2C_6H_4$; **d**, R= 2-benzothiazolyl, Ar^1= C_6H_5, Ar^2= 4-$OMeC_6H_4$; **e**, R= 2-benzothiazolyl, Ar^1= Ar^2= 4-ClC_6H_4; **f**, R= 2-benzothiazolyl, Ar^1= 3-ClC_6H_4, Ar^2= 2-Cl-5-$NO_2C_6H_3$; **g**, R= 2-benzothiazolyl, Ar^1= 4-BrC_6H_4, Ar^2= 2-Cl-5-$NO_2C_6H_3$; **h**, R= 2-benzothiazolyl, Ar^1= 4-BrC_6H_4, Ar^2= 2,4-$(F)_2C_6H_3$; **i**, R= 2-benzothiazolyl, Ar^1= 4-FC_6H_4, Ar^2= 4-MeC_6H_4; **j**, R= 2-benzothiazolyl, Ar^1= 1-naphthyl, Ar^2= 4-ClC_6H_4; **k**, R= 2-benzothiazolyl, Ar^1= 1-naphthyl, Ar^2= 4-$NO_2C_6H_4$; **l**, R= 2-benzothiazolyl, Ar^1= 2-naphthyl, Ar^2= 4-$NO_2C_6H_4$; **m**, R= 2-benzothiazolyl, Ar^1= 2-thienyl, Ar^2= C_6H_5; **n**, R= 2-benzothiazolyl, Ar^1= thienyl, Ar^2= 4-ClC_6H_4; **o**, R= 2-benzothiazolyl, Ar^1= 2-furyl, Ar^2= 2-Cl-5-$NO_2C_6H_3$; **p**, R= 2-benzothiazolyl, Ar^1= 1-methyl-1*H*-indol-2-yl, Ar^2= 4-$NO_2C_6H_4$; **q**, R= 4-(benzenesulfonamide), Ar^1= Ar^2= C_6H_5; **r**, R= 4-(benzenesulfonamide), Ar^1= Ar^2= 4-ClC_6H_4; **s**, R= 4-(benzenesulfonamide), Ar^1= C_6H_5, Ar^2= 4-$NO_2C_6H_4$; **t**, R= 5-(1-methyl-1*H*-indole-3-carbonyl)-2-phenyl-2*H*-[1,2,3]triazol-4-yl, Ar^1= Ar^2= C_6H_5; **u**, R= 5-(1-methyl-1*H*-indole-3-carbonyl)-2-phenyl-2*H*-[1,2,3]triazol-4-yl, Ar^1= C_6H_5, Ar^2= 4-ClC_6H_4.

Scheme 78. Synthesis thiazolo[4,5-*c*]pyridazine derivatives **340a-u**.

A plausible mechanistic pathway to account for the formation of **340** depicted in (Scheme 79).



Scheme 79. A plausible mechanism for the formation of **340**.

The cytotoxic activity of **340a-u** against three human cell lines, including colon cancer (HCT-116), breast cancer (MCF-7), and lung cancer (A549). In addition to the normal human breast cell lines (MCF-10A) using the standard [3-(4,5-dimethylthiazol-2-yl)-2,5-diphenyltetrazolium bromide] colorimetric assay and doxorubicin as

 ©**AUTHOR(S)**

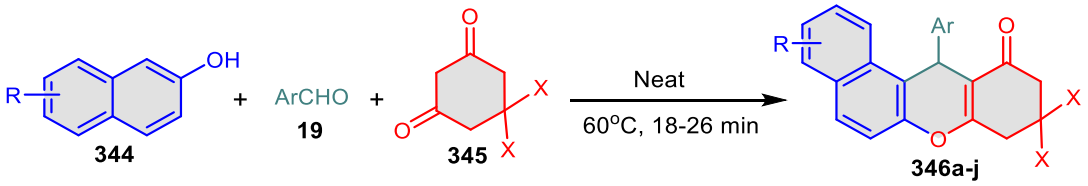
a reference anti-cancer reagent with three concentrations (12.5, 25 and 50 µM). Interestingly, **340s** p exhibits higher cytotoxicity activity (IC_{50} = 6.9 µM) compared to reference doxorubicin (IC_{50} = 11.26 µM) against colon cancer (HCT-116) cell line which indicates the crucial role of benzothiazole skeleton and two electron-withdrawing groups on the *N*-aryl moiety along with the two fluorine substituents. Meanwhile, **340c**, **340h**, **340k,** and **340p** showed the highest cytotoxic activity against breast cancer cell lines (MCF-7) with IC_{50} values 14.34, 10.39, 15.43, and 13.60 µM referenced to doxorubicin (IC_{50} = 19.35 µM).

To realize that cytotoxic characteristics of compounds **340a-u** are selective to cancer cells meanwhile have no fatal cytotoxic effect on human cells the most potent **340c**, **340h**, **340k**, **340l**, and **340s** are subjected to screening against MCF-10A cell lines (normal breast cancer cell lines). The results obtained showed comparable or higher IC_{50} values than that of doxorubicin upon applied to the same normal cell line.

6.3. Six-six fused membered heterocycles

6.3.1. Xanthenes synthesis. Xanthenes have received considerable interest due to their anti-cancer activity over the last two decades.[265–268] A diversity of synthetic modifications have been reported under different reaction conditions, which suffer from drawbacks such as harsh conditions, lower yields, and non-environmentally friendly techniques.[269–272]

Recently, Sreedevi and co-workers[273] developed a series of fluorine substituted benzo]*a*[xanthen-11-(2*H*)-ones **346a-j** *via* multi-component reaction of naphthalene-diols **344** fluoro/bromo substituted aldehydes **19** and cyclohexane-1,3-dione derivatives **345** in the absence of solvent and catalyst (Scheme 80).

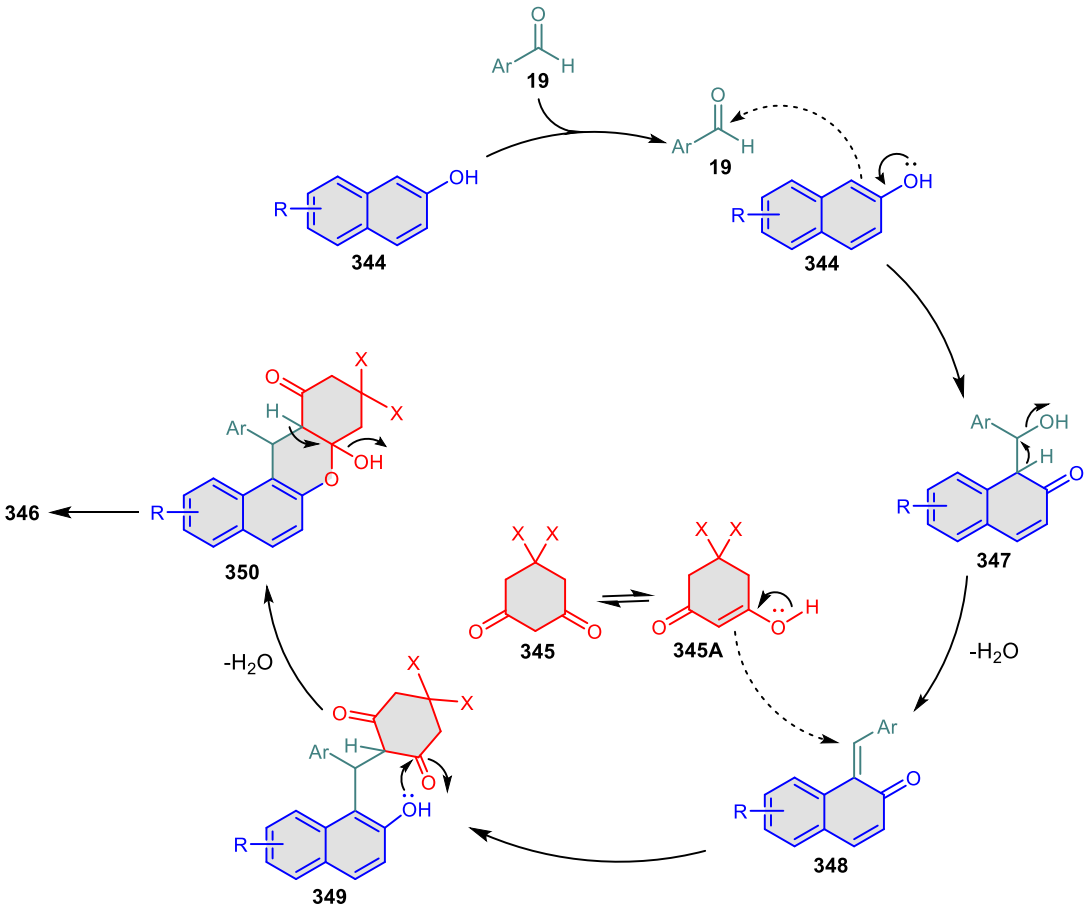


346a-j: **a**, R= 6-OH, Ar= 3-FC_6H_4, X= H; **b**, R= 2-OH, Ar= 2,4-$(F)_2C_6H_3$, X= CH_3; **c**, R= 6-OH, Ar= 2-FC_6H_4, X= H; **d**, R= 6-OH, Ar= 2-F-4-BrC_6H_3, X= H; **e**, R= 6-OH, Ar= 2,4-$(F)_2C_6H_3$, X= H; **f**, R= 6-OH, Ar= 2-FC_6H_4, X= CH_3; **g**, R= 6-OH, Ar= 3-FC_6H_4, X= CH_3; **h**, R= 2-OH, Ar= 4-FC_6H_4, X= CH_3; **i**, R= 2-OH, Ar= 2-FC_6H_4, X= H; **j**, R= 2-OH, Ar= 4-FC_6H_4, X= H.

Scheme 80. Synthesis of substituted benzo]*a*[xanthen-11-(2*H*)-ones **346a-j**.

A convenient mechanism for the formation of **346a-j** was depicted in Scheme 81.

 ©**AUTHOR(S)**



Scheme 81. A convenient mechanism for the formation of **346.**

The *in vitro* cytotoxic activity of compounds **346a-j** was investigated, and numerous compounds displayed good to excellent activity against cervical cancer cells of human (HeLa) and human hepatocellular carcinoma cell lines (HepG2) at 0.001-10 µM concentration. However, **346g** identified as the lead molecule with an IC_{50} value of 0.6 µM against HeLa cell lines and 0.8 µM towards HepG2, respectively.

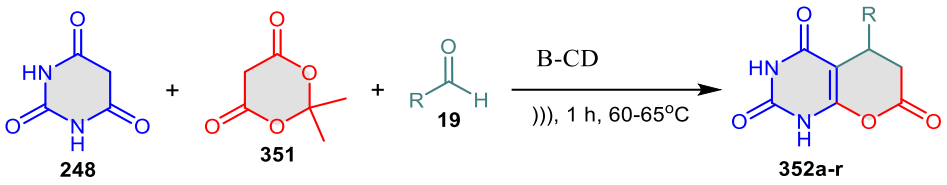
The SAR study of the titled compounds revealed that the –OH group at position-6 is essential for the activity of both cancer cell lines since they form hydrogen bonds with enzyme or protein receptors. Moreover, two oxygen and one-fluorine atom sites favor forming additional hydrogen bonds with enzymes or proteins.

The presence of electron-withdrawing fluorine at Meta position of aryl moiety at C-12, –OH group at C-6 position, and extra hydrophobic methyl groups at C-9 of **346g** rationalize for its higher *in vitro* cytotoxicity. Meanwhile, the steric factor plays a crucial role in the effectiveness of interaction with enzymes or proteins with highly sterically scaffolds abnormal cell metabolic disorders exist.

6.3.2. Pyrano-pyrimidines synthesis. Although pyrano[2,3-*d*]pyrimidine-2,4,7-triones possess remarkable anti-cancer activity in the treatment of B16 melanoma and P388 leukemia,[274] however, there have been few reports in the literature about their synthesis.[275–277] A straightforward, efficient, high-yielding green synthesis of densely functionalized 5-aryl/alkyl-5,6-dihydro-1*H*-pyrano[2,3-*d*]pyrimidine-2,4,7(3*H*)-triones (**352a-r**) have been recently reported by Bhosle and co-workers.[278] Specifically, authors developed an efficient synthesis that employed β-cyclodextrin (β-CD) cyclocondensation reaction of barbituric acid (**248**), Meldrum's acid (**351**) and aldehydes **19** in water promoted by ultrasound irradiation at 60-65°C (Scheme 82). The estimated Atom-

 ©**AUTHOR(S)**

Economy revealed value of 68.25 % significantly good established the efficient incorporating reactants in reaction course. E-factor show a value of 0.46 confirms the sustainability of the reaction.



352a-r: **a**, R= C_6H_5; **b**, R= 4-$CH_3C_6H_4$; **c**, R= 4-$OCH_3C_6H_4$; **d**, R= 4-ClC_6H_4; **e**, R= 3-ClC_6H_4; **f**, R= 2-ClC_6H_4; **g**, R= 4-BrC_6H; **h**, R= 4-OHC_6H_4; **i**, R= 2-OHC_6H_4; **j**, R= 3-OCH_3-4-OHC_6H_3; **k**, R= 3-OH-4-$OCH_3C_6H_3$; **l**, R= 3,4-$(OCH_3)_2C_6H_3$; **m**, R= 3,4,5-$(OCH_3)_3C_6H_2$; **n**, R= 4-$NO_2C_6H_4$; **o**, R= 2-$NO_2C_6H_4$; **p**, R= 4-$N(CH_3)_2C_6H_4$; **q**, R= 2-furyl; **r**, R= n-butyl.

Scheme 82. Synthesis of pyrano[2,3-*d*]pyrimidine-2,4,7-triones **352a-r**.

MTT assay used to investigate the efficiency of compounds **352a-r** as potent anti-cancer reagents against human liver cancer cell line (HePG-2) and human breast cancer (MCF-7) using 5-flurouracil (5-FU) as a reference drug. The results revealed the tremendous potential of synthesized compounds for treatments of tested anti-cancer cell lines. Compounds bearing *p*-substituents in the phenyl ring (**352c**, **352j**, **352k**, **352l**, and **352m**) showed more activity than those with *o*-substitution (**352f**, **352i,** and **352o**), and this could be rationalized for the steric hindrance effect owing to Ortho position substitution. Compound **352j** showed the most potent anti-cancer activity against HePG2 (IC_{50}= 6.8 µM) compared to standard 5-FU (IC_{50} = 7.9 µM) meanwhile **352k** ranking second with (IC_{50} = 8.8 µM). Compound **352m** possesses the most activity against MCF-7, and its IC_{50} value= 6.6 µM which is equipotent with standard drug 5-FU. Moreover, compounds **352g** and **352r** were the least active among all tested compounds.

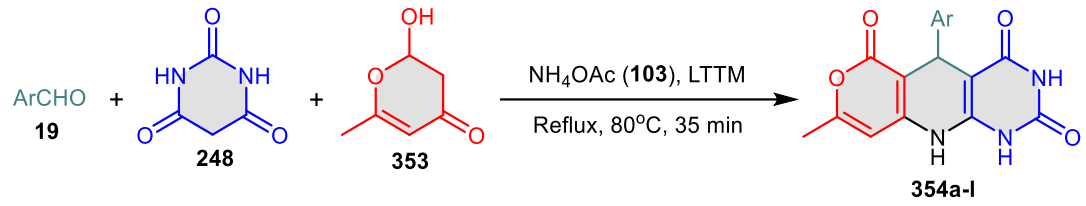
The authors concluded from their research that the presence of electron-withdrawing groups in the phenyl ring reduces its activity when compared to derivatives with electron-donating polar groups.

6.3.3. Pyrido-pyrimidines synthesis. Pyrido[2,3-*d*]pyrimidines (triazanaphthalenes) constitute an important structure of a wide range of bioactive heterocycles. They have a remarkable application in pharmaceutical and medicinal chemistry.[279–281]

Fused pyridopyrimidines with another biologically active heterocycles bring the new scaffold to become more potent as a biologically relevant heterocycle.[282,283]

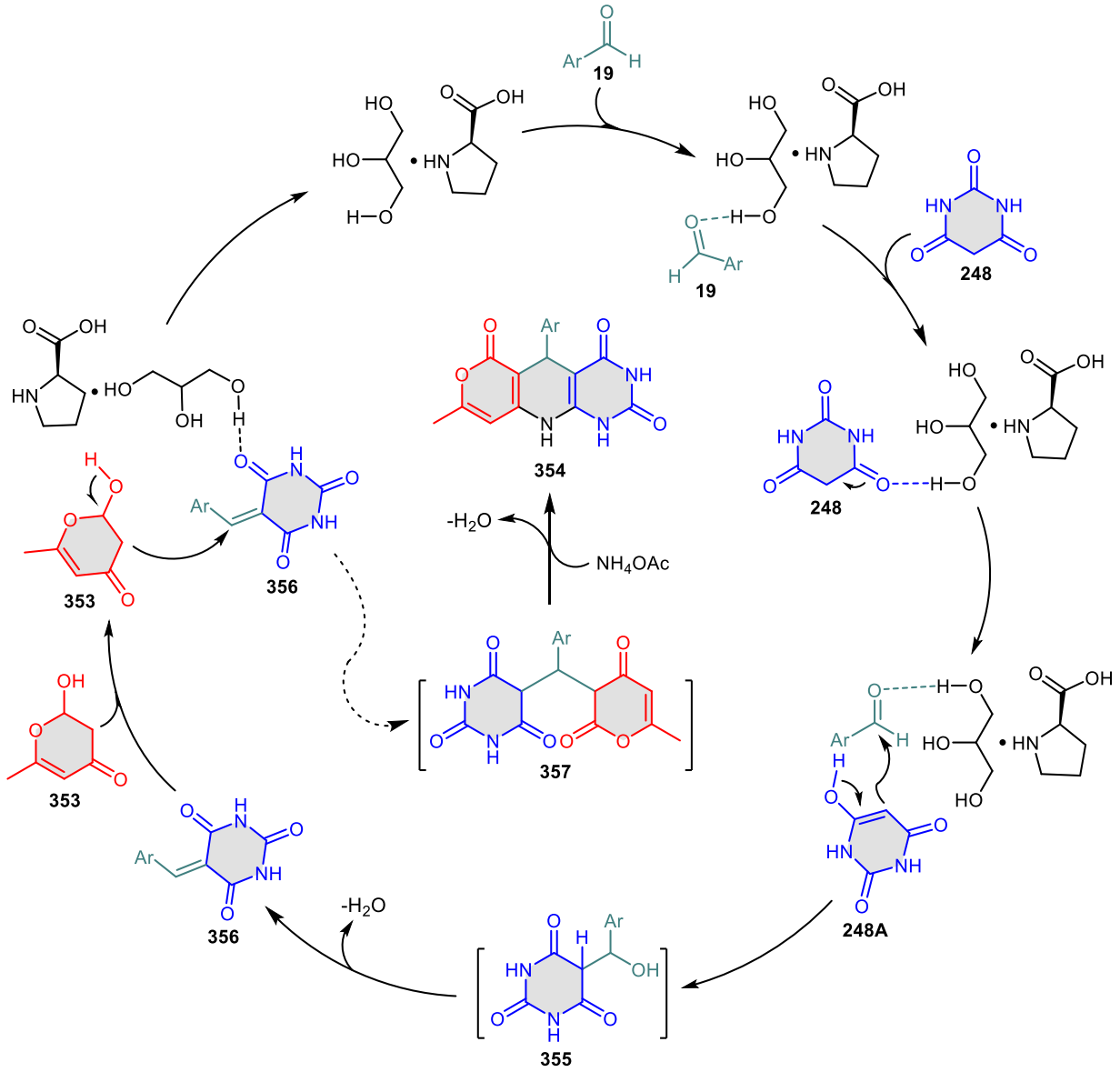
Deshmukh and his group[284] reported an efficient green four-component synthesis to access substituted pyrido-pyrimidines **354a-l** using barbituric acid (**248**), 4-hydroxy-6-methyl-2-pyrone (**353**), aromatic aldehyde **19** and ammonium acetate (**103**) utilizing low transition temperature mixture using LTTM (glycerol: proline, 1:1) as a solvent and catalyst (Scheme 83). A mechanism to account for the role of (LTTM) as a solvent and catalyst depicted in Scheme 84.

 ©**AUTHOR(S)**



354a-l: **a**, Ar= C_6H_5; **b**, Ar= 2-ClC_6H_4; **c**, Ar= 3-ClC_6H_4; **d**, Ar= 4-ClC_6H_4; **e**, Ar= 3-$NO_2C_6H_4$; **f**, Ar= 4-BrC_6H_4; **g**, Ar= 3-$OCH_3C_6H_4$; **h**, Ar= 4-$OCH_3C_6H_4$; **i**, Ar= 2-thienyl; **j**, Ar= 4*H*-chromen-3-yl; **k**, Ar= 3,4-$(F)_2C_6H_3$; **l**, Ar= 5-(benzo[*d*][1,3]dioxole).

Scheme 83. Synthesis of substituted pyrido-pyrimidines **354a-l**.



Scheme 84. Mechanistic pathway of pyrido-pyrimidines **354**.

 ©**AUTHOR(S)**

The antioxidant activity of the recently synthesized compounds assessed. The results demonstrated that compounds **354d**, **354e**, **354k,** and **354l** exhibit a significant potency at concentrations 50, 100 µg/mL.
Molecular docking carried out with myeloperoxidase enzyme (MPO), which plays a crucial role in producing reactive oxygen species, such reactive species is a critical factor in cancer disease. The binding mode of the most potent compound **354c** established hydrogen bond interactions with ALA28, PHE29, and VAL30, and Van der Waals interactions with ALA28, PHE29, VAL30, ARG31, ASN162, ASP321, and ARG323. In addition, the binding energy for **354d**, **354e**, **354k,** and **354l** ranges from -71.56 to -55.64 kcal/mol (Figure 38).

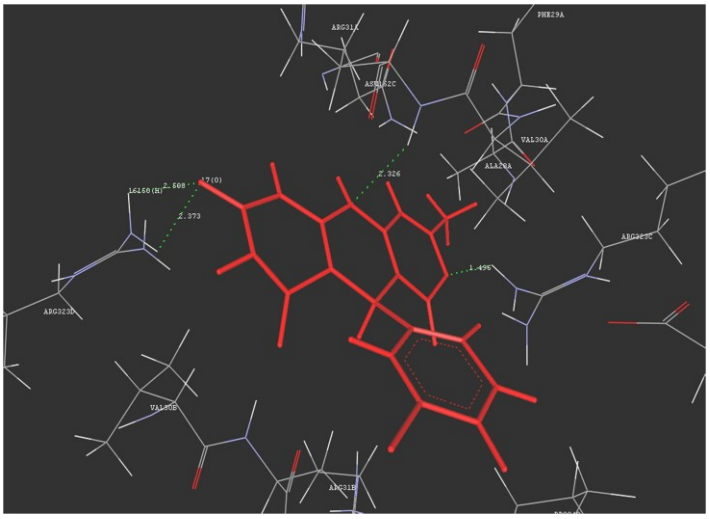
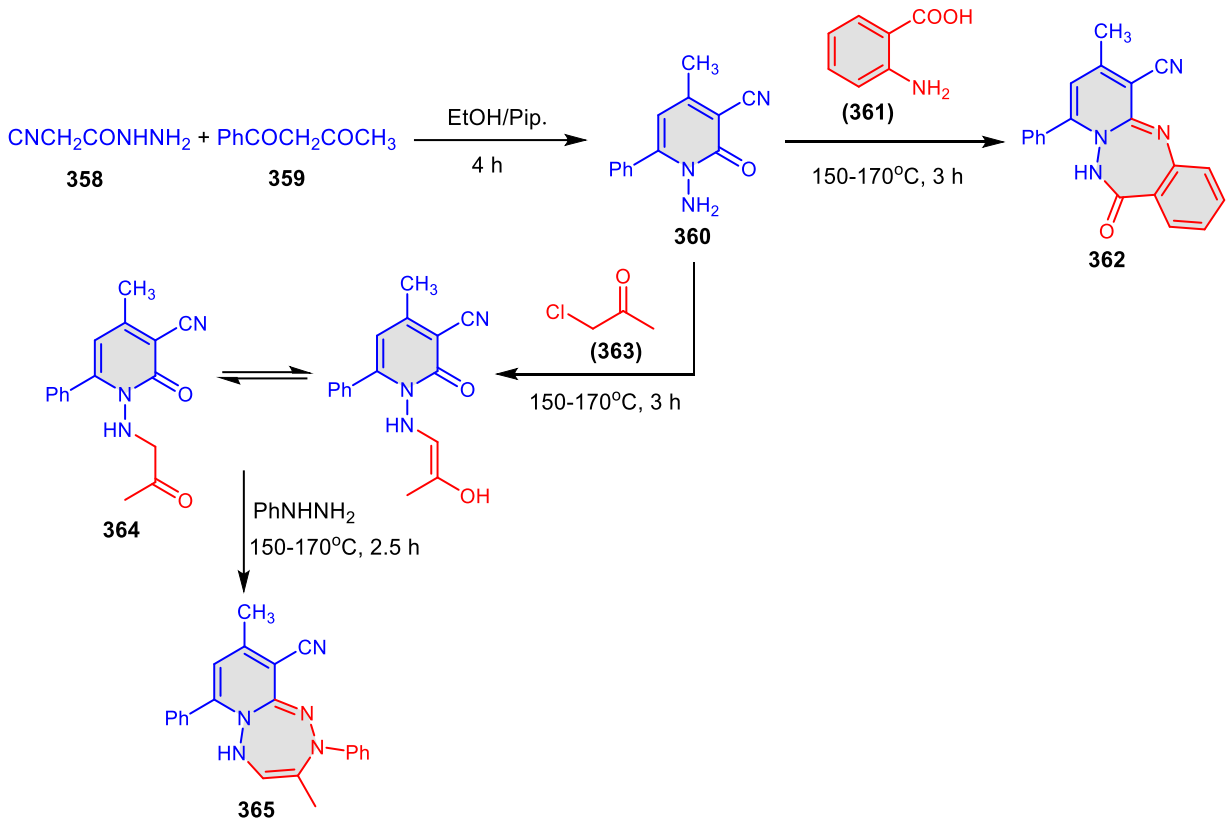


Figure 38. A significant interaction of molecule **354c** with MPO. Reproduced from Ref.;[284] Copyright 2022; Taylor & Francis.

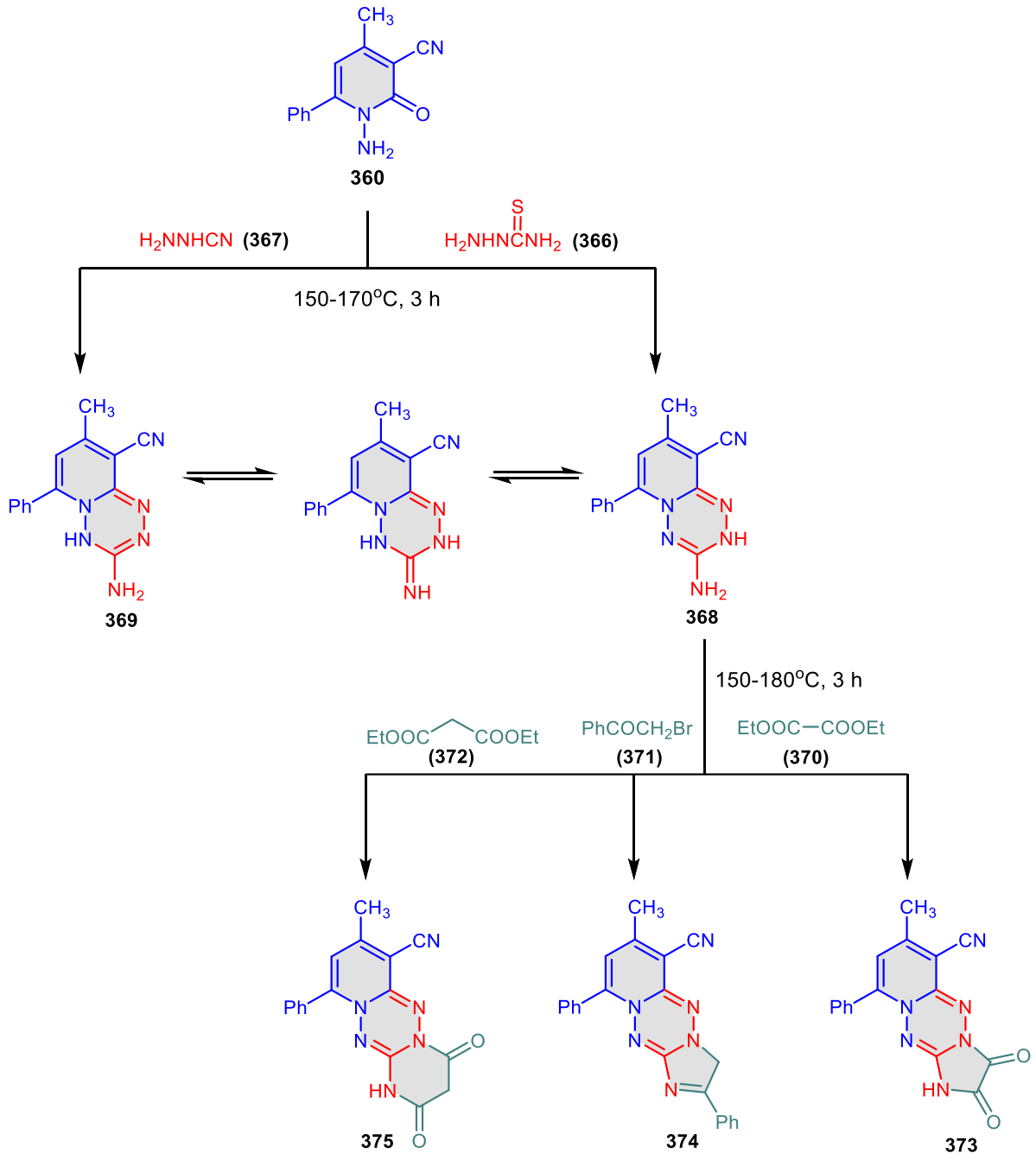
6.3.4. Pyrido-tetrazines, Pyrido-triazepine and Pyrido-tetrazepines synthesis. 1,2,4,5-Tetrazines,[285–287] 1,2,4-triazepines[288–290] and 1,2,4,5-tetrazepines [291] are classes of heterocyclic compounds having a diverse variety of biological actions. Recently, using dihydropyridine-3-carbonitrile (**360**) as a precursor,[292] Hassan *et al.*[293] developed a catalyst free synthesis of pyrido-annulated 1,2,4-triazepine **362**, 1,2,4,5-tetrazepines **365** and 1,2,4,5-tetrazines **368**, **369** and **373-375** (Schemes 85 and 86).

 ©**AUTHOR(S)**



Scheme 85. Synthesis of 1,2,4-triazepine **362** and 1,2,4,5-tetrazepines **365**.

©**AUTHOR(S)**



Scheme 86. Synthesis of 1,2,4,5-tetrazines **368**, **369** and **373-375**.

Compounds **362**, **365**, **368**, **373**, and **375** revealed moderate activity (GI% range of 21.02-36.25) against several forms of cancers, including Leukemia (RPMI-8226), non-small cell lung cancer (HOP62, NCI-H522), Melanoma (UACC-62), Prostate cancer (PC-3), Non-small cell lung cancer (HOP-62 & NCI-H522), Renal cancer (UO-31), Brest cancer (T-47D), and Ovarian Cancer (SK-OV-3). Compound **374** showed potent anticancer activity against Leukemia-RPMI-8226 (GI = 51.58) and Colon cancer-HCT116 (GI% = 77.94). Moreover, compound **374** inhibited various cell lines in moderate potency (GI = 8.07-36.84) (Figure 39).

The molecular docking studies of targets **365**, **374** and **375** with 4P7E possess a higher binding affinity *via* established several hydrogen bonds with tested enzymes.

 ©**AUTHOR(S)**

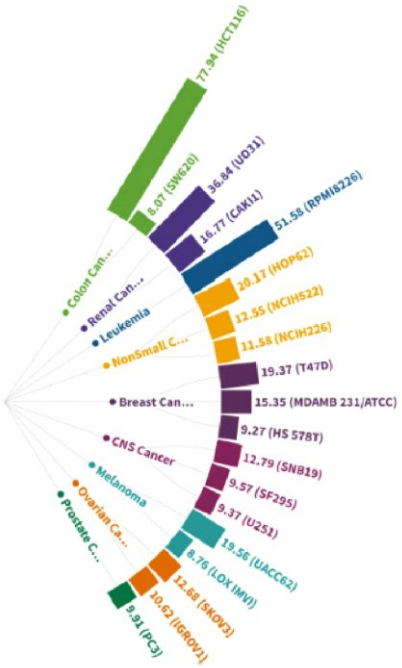


Figure 39. Radial bar chart represents: GI% of compound **374** against cancer cell lines of the nine tumor panels.

Conclusions

The dramatic increase of cancer cases nowadays crucially requires the development of green, cost-effective, and environmentally friendly reaction methodologies for synthesizing anti-cancer reagents. The development of drug candidates is highly dependent on the sustainability of synthetic protocols, and there is always a need to discover novel therapeutics. It is worth mentioning that the transition from conventional to sustainable medicinal chemistry requires evaluation of the pharmacological efficacy and environmental impact. The review demonstrated synthesized biologically relevant heterocycles *via* green methodologies often match or exceed the potency of those produced by conventional methods, while significantly reducing the environmental pollution. While conventional strategies have achieved notable success in synthesizing anti-cancer agents, there is an urgent requirement for an integrated approach to green and sustainable synthesis of these scaffolds. This review emphasizes the significance of recent advancements in the field of green synthesis of anti-cancer heterocycles. We presented a convenient and balanced overview of the green synthesis of diverse heterocyclic systems with medicinal chemistry aspects. This involves reactions proceeds with increasing energy efficiency (reactions at ambient temperature, microwave and ultrasonic promoted reactions, reaction at reduced pressure in a safe Q-tube reactor), reactions utilizing green solvents and catalysts as well as reactions at neat reaction conditions). The structural diversified heterocyclic systems exhibited a high degree of tolerance towards functional groups. Additionally, diverse biological activities comprehensively assessed. Evaluation of *in vitro* bioactivity underscored the significance of substitution patterns. SAR analysis provided valuable insights that emerged: 1- the presence of electron withdrawing groups such as halogens, nitro group or sulfonyl moieties significantly enhances anti-cancer activity in most nitrogen containing heterocycles (e.g. pyrazoles **34a**, cinnoline **109g,** xanthene **346g**) 2- the inclusion of nitrogen atoms or hydroxyl groups that can serve as hydrogen bond donors or acceptors is vital for docking in enzyme active sites (tubulin, VEGF-2, Bcl-2), 3- Fused systems and planar heterocyclic rings (pyridines and phthalazines) facilitate DNA intercalation, which is a primary

 ©**AUTHOR(S)**

mechanism for including cell cycle arrest in leukemia and colon cancer cell lines). In order to shed further light on the theme of review, we do believe that it is important for future vision in green design of biologically relevant heterocycles to focus in following different frontiers: 1-increasing the utility of enzymatic processes to perform highly stereoselective and regioselective transformations particularly in water , thus reducing the need of protective group chemistry, 2- developing diversity of heterocycles that possess potent therapeutic effect and fluorescent properties (e.g. benzothiazoles and chromenes) which allow for effective monitoring of drug delivery efficiency, 3- Utilizing AI to predict the more green possible synthetic route with the most potent pharmacophore thereby avoiding ineffective and environmentally non-friendly candidates, 4- water should be considered the standard solvent for any new chemical reaction, and organic solvents should not be used except in necessity and justification have to be provided, 5- the design of any new chemical must include a study of how to decompose it in the aquatic environment to ensure that sustainable pollutants are not left harmful to the environment.

References

1. Ameta, S. C.; Ameta, R. *Green Chemistry: Fundamentals and Applications*; 1st Ed.; Apple Academic Press: New York, **2013**.
2. Sáenz-Galindo, A.; Facio, A.; Rodriguez-Herrera, R. *"Green Chemistry and Applications";* 1st Ed.; CRC Press: Boca Raton, **2020**.
3. Prier, C. K.; Rankic, D. A.; MacMillan, D. W. C. Chem. Rev. **2013**, *113*, 5322. https://doi.org/10.1021/cr300503r
4. Iftikhar, K.; Muzammil, S.; Nadeem, H. U.; Azeem, F.; Rasul, I.; Zubair, M.; Imran, M.; Afzal, M.; Nadeem, H. U.; Siddique, M. H. Inamuddin; Boddula, R.; Asiri, A. M. B. T.-G. S. P. for C. and E. E. and S., Eds.; Elsevier, **2021**; 1. https://doi.org/10.1016/B978-0-12-821884-6.00006-1
5. Ferguson, L. R.; Chen, H.; Collins, A. R.; Connell, M.; Damia, G.; Dasgupta, S.; Malhotra, M.; *et al.* Semin. Cancer Biol. **2015**, *35*, S5. https://doi.org/10.1016/j.semcancer.2015.03.005
6. *Global Burden of Cancer, Cancer Country Profile, World Health Organization*; **2020**.
7. Brahmachari, G. B. T.-G. S. A. for B. R. H., Ed.; Elsevier: Boston, **2015**; xv. https://doi.org/10.1016/B978-0-12-800070-0.11001-1
8. Ameta, K.L.; Dandia, A. *Green Chemistry: Synthesis of Bioactive Heterocycles*; Springer New Delhi, **2014**.
9. Sundberg, R. J. *in: A.R. Katritzky, C.W. Rees, E.F.V. Scriven (Eds.), Comprehensive Heterocyclic Chemistry II, vol. 2, Pergamon Press, Oxford*; **1996**.
10. Fan, H.; Peng, J.; Hamann, M. T.; Hu, J.-F. Chem. Rev. **2008**, *108*, 264. https://doi.org/10.1021/cr078199m
11. Sundberg, R. J. *in: A.R. Katritzky, C.W. Rees (Eds.), Comprehensive Heterocyclic Chemistry, vol. 4, Pergamon Press, Oxford*; **1984**.
12. Kathriarachchi, K. K. A. D. S.; Siriwardana, A. I.; Nakamura, I.; Yamamoto, Y. Tetrahedron Lett. **2007**, *48*, 2267. https://doi.org/10.1016/j.tetlet.2007.01.170
13. Bandyopadhyay, D.; Mukherjee, S.; Banik, B. K. Molecules **2010**, *15*, 2520. https://doi.org/10.3390/molecules15042520

 ©**AUTHOR(S)**

14. Rueping, M.; Parra, A. Org. Lett. **2010**, *12*, 5281. https://doi.org/10.1021/ol102247n
15. Trost, B. M.; Osipov, M.; Dong, G. J. Am. Chem. Soc. **2010**, *132*, 15800. https://doi.org/10.1021/ja1071509
16. Ruault, P.; Pilard, J.-F.; Touaux, B.; Texier-Boulle, F.; Hamelin, J. Synlett **1994**, *1994*, 935. https://doi.org/10.1055/s-1994-23054
17. Danks, T. N. Tetrahedron Lett. **1999**, *40*, 3957. https://doi.org/10.1016/S0040-4039(99)00620-6
18. Sung, H.; Ferlay, J.; Siegel, R. L.; Laversanne, M.; Soerjomataram, I.; Jemal, A.; Bray, F. CA. Cancer J. Clin. **2021**, *71*, 209. https://doi.org/10.3322/caac.21660
19. Chen, F.; Wang, H.-M.; Kong, L.-Q.; Chen, Q.-H.; Ke, L.-N.; Dai, H.-L.; Zeng, X.-H. Front. Chem. **2022**, *10*, 921276. https://doi.org/10.3389/fchem.2022.921276
20. Bandyopadhyay, D.; Mukherjee, S.; Granados, J. C.; Short, J. D.; Banik, B. K. Eur. J. Med. Chem. **2012**, *50*, 209. https://doi.org/10.1016/j.ejmech.2012.01.055
21. Hindenberg Carlos, P. R.-N. Synlett **2016**, *27*, 2293. https://doi.org/10.1055/s-0035-1562506
22. Fermi, V.; Regulska, E.; Wolfram, A.; Wessling, P.; Rominger, F.; Herold-Mende, C.; Romero-Nieto, C. Chem. Eur. J. **2022**, *28*, e202104535. https://doi.org/10.1002/chem.202104535
23. Patel, T.; Gaikwad, R.; Jain, K.; Ganesh, R.; Bobde, Y.; Ghosh, B.; Das, K.; Gayen, S. ChemistrySelect **2019**, *4*, 4478. https://doi.org/10.1002/slct.201900088
24. Zhang, T. Y. In *Heterocyclic Chemistry in the 21st Century*; Scriven, E. F. V; Ramsden, C. A. B. T.-A. in H. C., Eds.; Academic Press, **2017**; Vol. 121, 1. https://doi.org/10.1016/bs.aihch.2016.05.001
25. Taylor, R. D.; MacCoss, M.; Lawson, A. D. G. J. Med. Chem. **2014**, *57*, 5845. https://doi.org/10.1021/jm4017625
26. Baumann, M.; Baxendale, I. R. Beilstein J. Org. Chem. **2013**, *9*, 2265. https://doi.org/10.3762/bjoc.9.265
27. Baumann, M.; Baxendale, I. R.; Ley, S. V; Nikbin, N. Beilstein J. Org. Chem. **2011**, *7*, 442. https://doi.org/10.3762/bjoc.7.57
28. Gogula, S. S.; Prasanna, D. V.; Thumma, V.; Misra, S.; Lincoln, C. A.; Reddy, P. M.; Hu, A.; Subbareddy, B. V. ACS Omega **2023**, *8*, 36401. https://doi.org/10.1021/acsomega.3c05293
29. Liu, Y.; Wang, H.; Wan, J. Asian J. Org. Chem. **2013**, *2*, 374. https://doi.org/10.1002/ajoc.201200180
30. Liu, Z.-M.; Li, N.-K.; Huang, X.-F.; Wu, B.; Li, N.; Kwok, C.-Y.; Wang, Y.; Wang, X.-W. Tetrahedron **2014**, *70*, 2406. https://doi.org/10.1016/j.tet.2014.02.023
31. Pavlovska, T. L.; Redkin, R. G.; Lipson, V. V; Atamanuk, D. V Mol. Divers. **2016**, *20*, 299. https://doi.org/10.1007/s11030-015-9629-8

 ©**AUTHOR(S)**

32. Arun, Y.; Saranraj, K.; Balachandran, C.; Perumal, P. T. Eur. J. Med. Chem. **2014**, *74*, 50. https://doi.org/10.1016/j.ejmech.2013.12.027
33. Zheng, Y.; Tice, C. M.; Singh, S. B. Bioorg. Med. Chem. Lett. **2014**, *24*, 3673. https://doi.org/10.1016/j.bmcl.2014.06.081
34. Mayakrishnan, S.; Kathirvelan, D.; Arun, Y.; Saranraj, K.; Balachandran, C.; Aoki, S.; Yuvaraj, P.; Maheswarai, N. U. New J. Chem. **2022**, *46*, 10089. https://doi.org/10.1039/D1NJ05839H
35. Huang, Y.; Huang, Y.-X.; Sun, J.; Yan, C.-G. RSC Adv. **2018**, *8*, 23990. https://doi.org/10.1039/C8RA04375B
36. Yan, L.-J.; Wang, Y.-C. ChemistrySelect **2016**, *1*, 6948. https://doi.org/10.1002/slct.201601534
37. Santos, M. M. M. Tetrahedron **2014**, *70*, 9735. https://doi.org/10.1016/j.tet.2014.08.005
38. Ye, N.; Chen, H.; Wold, E. A.; Shi, P.-Y.; Zhou, J. ACS Infect. Dis. **2016**, *2*, 382. https://doi.org/10.1021/acsinfecdis.6b00041
39. Ball-Jones, N. R.; Badillo, J. J.; Franz, A. K. Org. Biomol. Chem. **2012**, *10*, 5165. https://doi.org/10.1039/c2ob25184a
40. Singh, G. S.; Desta, Z. Y. Chem. Rev. **2012**, *112*, 6104. https://doi.org/10.1021/cr300135y
41. Ansari, A.; Ali, A.; Asif, M.; Shamsuzzaman, S. New J. Chem. **2017**, *41*, 16. https://doi.org/10.1039/C6NJ03181A
42. Karrouchi, K.; Radi, S.; Ramli, Y.; Taoufik, J.; Mabkhot, Y. N.; Al-aizari, F. A.; Ansar, M. Molecules **2018**, *23*, 134. https://doi.org/10.3390/molecules23010134
43. Shaaban, M. R.; Farghaly, T. A.; Alsaedi, A. M. R.; Abdulwahab, H. G. J. Mol. Struct. **2022**, *1249*, 131657. https://doi.org/10.1016/j.molstruc.2021.131657
44. Aggarwal, R.; Kumar, V.; Kumar, R.; Singh, S. P. Beilstein J. Org. Chem. **2011**, *7*, 179. https://doi.org/10.3762/bjoc.7.25
45. Frank, É.; Schneider, G. J. Steroid Biochem. Mol. Biol. **2013**, *137*, 301. https://doi.org/10.1016/j.jsbmb.2013.02.018
46. Baji, Á.; Kovács, F.; Mótyán, G.; Schneider, G.; Wölfling, J.; Sinka, I.; Zupkó, I.; Ocsovszki, I.; Frank, É. Steroids **2017**, *126*, 35. https://doi.org/10.1016/j.steroids.2017.08.003
47. Li, J.; Zhao, X.; Li, L.; Yuan, Z.; Tan, F.; Shi, B.; Zhang, J. Steroids **2016**, *107*, 45. https://doi.org/10.1016/j.steroids.2015.12.018
48. Mótyán, G.; Gopisetty, M. K.; Kiss-Faludy, R. E.; Kulmány, Á.; Zupkó, I.; Frank, É.; Kiricsi, M. Int. J. Mol. Sci. **2019**, *20*, 2170. https://doi.org/10.3390/ijms20092170
49. Mótyán, G.; Zupkó, I.; Minorics, R.; Schneider, G.; Wölfling, J.; Frank, É. Mol. Divers. **2015**, *19*, 511. https://doi.org/10.1007/s11030-015-9593-3
50. Kovács, D.; Wölfling, J.; Szabó, N.; Szécsi, M.; Schelz, Z.; Zupkó, I.; Frank, É. Eur. J. Med. Chem. **2016**, *120*, 284. https://doi.org/10.1016/j.ejmech.2016.05.006

 ©**AUTHOR(S)**

51. Mótyán, G.; Baji, Á.; Marć, M. A.; Gopisetty, M. K.; Adamecz, D. I.; Kiricsi, M.; Enyedy, É. A.; Frank, É. Appl. Sci. **2019**, *10*, 229. https://doi.org/10.3390/app10010229
52. Manetti, F.; Castagnolo, D.; Raffi, F.; Zizzari, A. T.; Rajamäki, S.; D'Arezzo, S.; Visca, P.; Cona, A.; Fracasso, M. E.; Doria, D.; Posteraro, B.; Sanguinetti, M.; Fadda, G.; Botta, M. J. Med. Chem. **2009**, *52*, 7376. https://doi.org/10.1021/jm900760k
53. Stolić, I.; Čipčić Paljetak, H.; Perić, M.; Matijašić, M.; Stepanić, V.; Verbanac, D.; Bajić, M. Eur. J. Med. Chem. **2015**, *90*, 68. https://doi.org/10.1016/j.ejmech.2014.11.003
54. Soeiro, M. N. C.; Werbovetz, K.; Boykin, D. W.; Wilson, W. D.; Wang, M. Z.; Hemphill, A. Parasitology **2013**, *140*, 929. https://doi.org/10.1017/S0031182013000292
55. Bhongade, B. A.; Gadad, A. K. Bioorg. Med. Chem. **2004**, *12*, 2797. https://doi.org/10.1016/j.bmc.2004.02.019
56. Özdemir, A.; Altıntop, M. D.; Kaplancıklı, Z. A.; Turan-Zitouni, G.; Çiftçi, G. A.; Yıldırım, Ş. U. J. Enzyme Inhib. Med. Chem. **2013**, *28*, 1221. https://doi.org/10.3109/14756366.2012.724682
57. Huang, H.; Li, H.; Yang, S.; Chreifi, G.; Martásek, P.; Roman, L. J.; Meyskens, F. L.; Poulos, T. L.; Silverman, R. B. J. Med. Chem. **2014**, *57*, 686. https://doi.org/10.1021/jm401252e
58. Insuasty, B.; Tigreros, A.; Orozco, F.; Quiroga, J.; Abonía, R.; Nogueras, M.; Sanchez, A.; Cobo, J. Bioorg. Med. Chem. **2010**, *18*, 4965. https://doi.org/10.1016/j.bmc.2010.06.013
59. Kumar, S.; Bawa, S.; Drabu, S.; Kumar, R.; Gupta, H. Recent Pat. Antiinfect. Drug Discov. **2009**, *4*, 154. https://doi.org/10.2174/157489109789318569
60. Santos, E. F. S. dos; Cury, N. M.; Nascimento, T. A. do; Raminelli, C.; Casagrande, G. A.; Pereira, C. M. P.; Simionatto, E.; Yunes, J. A.; Pizzuti, L. J. Braz. Chem. Soc. **2016**, *28*, 217. https://doi.org/10.5935/0103-5053.20160166
61. Aydın, S.; Kaushik-Basu, N.; Özbaş-Turan, S.; Akbuğa, J.; Mega Tiber, P.; Orun, O.; R. Gurukumar, K.; Basu, A.; Güniz Küçükgüzel, Ş. Lett. Drug Des. Discov. **2013**, *11*, 121. https://doi.org/10.2174/15701808113109990069
62. Mohan, G.; Santhisudha, S.; Reddy, N. M.; Sreekanth, T.; Murali, S.; Reddy, C. S. Monatshefte für Chemie - Chem. Mon. **2017**, *148*, 1843. https://doi.org/10.1007/s00706-017-2000-2
63. Quntar, A. A. A. Al; Gallily, R.; Katzavian, G.; Srebnik, M. Eur. J. Pharmacol. **2007**, *556*, 9. https://doi.org/10.1016/j.ejphar.2006.10.041
64. Alexander, P.; Krishnamurthy, V. V; Prisbe, E. J. J. Med. Chem. **1996**, *39*, 1321. https://doi.org/10.1021/jm950788
65. Demkowicz, S.; Rachon, J.; Daśko, M.; Kozak, W. RSC Adv. **2016**, *6*, 7101. https://doi.org/10.1039/C5RA25446A
66. Mohan, G.; Santhisudha, S.; Murali, S.; Reddy, N. B.; Sravya, G.; Zyryanov, G. V; Reddy, C. S. Res. Chem. Intermed. **2018**, *44*, 3475. https://doi.org/10.1007/s11164-018-3319-y

 ©AUTHOR(S)

67. Mlostoń, G.; Kowalczyk, M.; Celeda, M.; Gach-Janczak, K.; Janecka, A.; Jasiński, M. J. Nat. Prod. **2021**, *84*, 3071. https://doi.org/10.1021/acs.jnatprod.1c00797
68. Mlostoń, G.; Kowalczyk, M.; Celeda, M.; Jasiński, M.; Denel-Bobrowska, M.; Olejniczak, A. B. Molecules **2022**, *27*, 3524. https://doi.org/10.3390/molecules27113524
69. Horton, D. A.; Bourne, G. T.; Smythe, M. L. Chem. Rev. **2003**, *103*, 893. https://doi.org/10.1021/cr020033s
70. Yoon, Y. K.; Ali, M. A.; Wei, A. C.; Shirazi, A. N.; Parang, K.; Choon, T. S. Eur. J. Med. Chem. **2014**, *83*, 448. https://doi.org/10.1016/j.ejmech.2014.06.060
71. Atif, M.; Iqbal, M. A.; Nazari, M. V Enzym. Eng. **2020**, *12*, 1000229. https://doi.org/10.35248/2329-6674.23.12.229
72. Mironov, M. E.; Rybalova, T. V; Pokrovskii, M. A.; Emaminia, F.; Gandalipov, E. R.; Pokrovskii, A. G.; Shults, E. E. Steroids **2023**, *190*, 109133. https://doi.org/10.1016/j.steroids.2022.109133
73. Hozien, Z. A.; EL-Mahdy, A. F. M.; Abo Markeb, A.; Ali, L. S. A.; El-Sherief, H. A. H. RSC Adv. **2020**, *10*, 20184. https://doi.org/10.1039/D0RA02872J
74. Jiang, G.; Chang, Q.; Liang, D.; Zhang, Y.; Meng, Y.; Yi, Q. J. Int. Med. Res. **2020**, *48*. https://doi.org/10.1177/0300060520903874
75. Raouf, H.; Beyramabadi, S. A.; Allameh, S.; Morsali, A. J. Mol. Struct. **2019**, *1179*, 779. https://doi.org/10.1016/j.molstruc.2018.11.073
76. Azad Aghaward, S.; Abbas, L. J.; Hussein, K. A. J. Med. Chem. Sci. **2023**, *6*, 1714. https://doi.org/10.26655/JMCHEMSCI.2023.8.1
77. Hughes, J. P.; Rees, S.; Kalindjian, S. B.; Philpott, K. L. Br. J. Pharmacol. **2011**, *162*, 1239. https://doi.org/10.1111/j.1476-5381.2010.01127.x
78. Mioc, M.; Mioc, A.; Prodea, A.; Milan, A.; Balan-Porcarasu, M.; Racoviceanu, R.; Ghiulai, R.; Iovanescu, G.; Macasoi, I.; Draghici, G.; Dehelean, C.; Soica, C. Int. J. Mol. Sci. **2022**, *23*, 9992. https://doi.org/10.3390/ijms23179992
79. Mollazadeh, S.; Sahebkar, A.; Kalalinia, F.; Behravan, J.; Hadizadeh, F. Bioorg. Chem. **2019**, *91*, 103156. https://doi.org/10.1016/j.bioorg.2019.103156
80. Deswal, N.; Shrivastava, A.; Summon Hossain, M.; Gahlyan, P.; Bawa, R.; Gupta, R. D.; Kumar, R. ChemistrySelect **2021**, *6*, 717. https://doi.org/10.1002/slct.202003948
81. Morshed, S. R. M. D.; Hashimoto, K. E. N.; Murotani, Y.; Kawase, M.; Shah, A.; Satoh, K.; Kikuchi, H.; Nishikawa, H.; Maki, J. U. N.; Sakagami, H. Anticancer Res. **2005**, *25*, 2033.
82. Laupèze, B.; Amiot, L.; Bertho, N.; Grosset, J. M.; Lehne, G.; Fauchet, R.; Fardel, O. Hum. Immunol. **2001**, *62*, 1073. https://doi.org/10.1016/S0198-8859(01)00307-X
83. Kumar, R.; Yadav, N.; Jain, H.; Deswal, N.; Upadhyay, R. K.; Leekha, A.; Verma, A. K.; Kareem, A.; Chikati, R.; Kumar, L. S. ChemistrySelect **2022**, *7*, e202104129. https://doi.org/10.1002/slct.202104129
84. Zarrin, A.; Mehdipour, A. R.; Miri, R. Chem. Biol. Drug Des. **2010**, *76*, 369. https://doi.org/10.1111/j.1747-0285.2010.01025.x
85. Gökçe, M.; Utku, S.; Küpeli, E. Eur. J. Med. Chem. **2009**, *44*, 3760.

 ©**AUTHOR(S)**

https://doi.org/10.1016/j.ejmech.2009.04.048
86. Rollas, S.; Küçükgüzel, S. G. Molecules **2007**, *12*, 1910. https://doi.org/10.3390/12081910
87. Gomha, S. M.; Muhammad, Z. A.; Abdel-aziz, H. M.; Matar, I. K.; El-Sayed, A. A. Green Chem. Lett. Rev. **2020**, *13*, 6. https://doi.org/10.1080/17518253.2019.1710268
88. Jadhvar, S. C.; Kasraliker, H. M.; Goswami, S. V; Chakrawar, A. V; Bhusare, S. R. Res. Chem. Intermed. **2017**, *43*, 7211. https://doi.org/10.1007/s11164-017-3069-2
89. Stefańska, B.; Arciemiuk, M.; Bontemps-Gracz, M. M.; Dzieduszycka, M.; Kupiec, A.; Martelli, S.; Borowski, E. Bioorg. Med. Chem. **2003**, *11*, 561. https://doi.org/10.1016/S0968-0896(02)00425-X
90. Parrino, B.; Carbone, A.; Muscarella, M.; Spanò, V.; Montalbano, A.; Barraja, P.; Salvador, A.; Vedaldi, D.; Cirrincione, G.; Diana, P. J. Med. Chem. **2014**, *57*, 9495. https://doi.org/10.1021/jm501244f
91. v. Richter, V. Ber. Dtsch. Chem. Ges. **1883**, *16*, 677. https://doi.org/10.1002/cber.188301601154
92. Gewald, K.; Calderon, O.; Schäfer, H.; Hain, U. Liebigs Ann. der Chemie **1984**, *1984*, 1390. https://doi.org/10.1002/jlac.198419840715
93. Ball, C. J.; Gilmore, J.; Willis, M. C. Angew. Chemie Int. Ed. **2012**, *51*, 5718. https://doi.org/10.1002/anie.201201529
94. Zhang, G.; Miao, J.; Zhao, Y.; Ge, H. Angew. Chemie Int. Ed. **2012**, *51*, 8318. https://doi.org/10.1002/anie.201204339
95. Vinogradova, O. V; Balova, I. A. Chem. Heterocycl. Compd. **2008**, *44*, 501. https://doi.org/10.1007/s10593-008-0070-0
96. Hameed, A. A.; Ahmed, E. K.; Fattah, A. A. A.; Andrade, C. K. Z.; Sadek, K. U. Res. Chem. Intermed. **2017**, *43*, 5523. https://doi.org/10.1007/s11164-017-2944-1
97. Dyab, A. K. F.; Sadek, K. U. RSC Adv. **2018**, *8*, 23241. https://doi.org/10.1039/C8RA04195D
98. Nazmy, M. H.; Mekheimer, R. A.; Shoman, M. E.; Abo-Elsebaa, M.; Abd-Elmonem, M.; Sadek, K. U. Bioorg. Chem. **2020**, *101*, 103932. https://doi.org/10.1016/j.bioorg.2020.103932
99. Abubshait, S. A.; Almalih, R. J.; Abubshait, H. A.; Gomaa, M. S.; Abdalla, A. N. Arab J. Basic Appl. Sci. **2024**, *31*, 454. https://doi.org/10.1080/25765299.2024.2387383
100. Neske, A.; Ruiz Hidalgo, J.; Cabedo, N.; Cortes, D. Phytochemistry **2020**, *174*, 112332. https://doi.org/10.1016/j.phytochem.2020.112332
101. Ohta, K.; Fushimi, T.; Okamura, M.; Akatsuka, A.; Dan, S.; Iwasaki, H.; Yamashita, M.; Kojima, N. RSC Adv. **2022**, *12*, 15728. https://doi.org/10.1039/D2RA02399G
102. Leonardi, M.; Villacampa, M.; Menéndez, J. C. Chem. Sci. **2018**, *9*, 2042. https://doi.org/10.1039/C7SC05370C

 ©AUTHOR(S)

103. Alba, A.-N. R.; Valero, G.; Calbet, T.; Font-Bardía, M.; Moyano, A.; Rios, R. Chem. Eur. J. **2010**, *16*, 9884. https://doi.org/10.1002/chem.201000239
104. Jat, L.; Mishra, R.; Pathak, D. J. Pharm. Pharm. Sci. **2012**, *4*, 378.
105. Fahmy, A. F. M.; El-Sayed, A. A.; Hemdan, M. M. Chem. Cent. J. **2016**, *10*, 59. https://doi.org/10.1186/s13065-016-0205-9
106. Cheng, X.; Jia, H.; Long, T.; Feng, J.; Qin, J.; Li, Z. Chem. Commun. **2011**, *47*, 11978. https://doi.org/10.1039/c1cc15214a
107. Pattison, D. I.; Davies, M. J. Biochemistry **2006**, *45*, 8152. https://doi.org/10.1021/bi060348s
108. Yang, Y.; Huo, F.; Yin, C.; Xu, M.; Hu, Y.; Chao, J.; Zhang, Y.; Glass, T. E.; Yoon, J. J. Mater. Chem. B **2016**, *4*, 5101. https://doi.org/10.1039/C6TB01392A
109. Aiello, S.; Wells, G.; Stone, E. L.; Kadri, H.; Bazzi, R.; Bell, D. R.; Stevens, M. F. G.; Matthews, C. S.; Bradshaw, T. D.; Westwell, A. D. J. Med. Chem. **2008**, *51*, 5135. https://doi.org/10.1021/jm800418z
110. Leong, C.-O.; Gaskell, M.; Martin, E. A.; Heydon, R. T.; Farmer, P. B.; Bibby, M. C.; Cooper, P. A.; Double, J. A.; Bradshaw, T. D.; Stevens, M. F. G. Br. J. Cancer **2003**, *88*, 470. https://doi.org/10.1038/sj.bjc.6600719
111. Kamal, A.; Reddy, K. S.; Khan, M. N. A.; Shetti, R. V.; Ramaiah, M. J.; Pushpavalli, S.; Srinivas, C.; Pal-Bhadra, M.; Chourasia, M.; Sastry, G. N.; Juvekar, A.; Zingde, S.; Barkume, M. Bioorg. Med. Chem. **2010**, *18*, 4747. https://doi.org/10.1016/j.bmc.2010.05.007
112. Bradshaw, T. D.; Matthews, C. S.; Cookson, J.; Chew, E.-H.; Shah, M.; Bailey, K.; Monks, A.; Harris, E.; Westwell, A. D.; Wells, G.; Laughton, C. A.; Stevens, M. F. G. Cancer Res. **2005**, *65*, 3911. https://doi.org/10.1158/0008-5472.CAN-04-4141
113. Mukherjee, A.; Westwell, A. D.; Bradshaw, T. D.; Stevens, M. F. G.; Carmichael, J.; Martin, S. G. Br. J. Cancer **2005**, *92*, 350. https://doi.org/10.1038/sj.bjc.6602338
114. Zeng, H.; Luo, P.; Luo, M.; Ding, H.; Ding, Q. Tetrahedron **2019**, *75*, 130472. https://doi.org/10.1016/j.tet.2019.130472
115. Kamat, D. P.; Tilve, S. G.; Kamat, V. P.; Kirtany, J. K. Org. Prep. Proced. Int. **2015**, *47*, 1. https://doi.org/10.1080/00304948.2015.983805
116. Santos Junior, C. M.; Silva, S. M. C.; Sales, E. M.; Velozo, E. da S.; dos Santos, E. K. P.; Canuto, G. A. B.; Azeredo, F. J.; Barros, T. F.; Biegelmeyer, R. Fitoterapia **2023**, *168*, 105489. https://doi.org/10.1016/j.fitote.2023.105489
117. Kaur, M.; Kohli, S.; Sandhu, S.; Bansal, Y.; Bansal, G. Anticancer. Agents Med. Chem. **2015**, *15*, 1032. https://doi.org/10.2174/1871520615666150101125503
118. Rawat, A.; Vijaya Bhaskar Reddy, A. Eur. J. Med. Chem. Reports **2022**, *5*, 100038. https://doi.org/10.1016/j.ejmcr.2022.100038
119. Jakubowski, R.; Pomorska, D. K.; Długosz, A.; Janecka, A.; Krajewska, U.; Różalski, M.; Mirowski, M.; Bartosik, T.; Janecki, T. ChemMedChem **2017**, *12*, 599. https://doi.org/10.1002/cmdc.201700080
120. Onouchi, H.; Miyagawa, T.; Furuko, A.; Maeda, K.; Yashima, E. J. Am. Chem. Soc. **2005**, *127*, 2960. https://doi.org/10.1021/ja042806v
121. Gagnon, K. J.; Perry, H. P.; Clearfield, A. Chem. Rev. **2012**, *112*, 1034.

 ©AUTHOR(S)

https://doi.org/10.1021/cr2002257
122. Kour, P.; Kumar, A.; Sharma, R.; Chib, R.; Ali Khan, I.; Rai, V. K. Res. Chem. Intermed. **2017**, *43*, 7319. https://doi.org/10.1007/s11164-017-3077-2
123. Kour, P.; Kumar, A.; Rai, V. K. Comptes Rendus. Chim. **2016**, *20*, 140. https://doi.org/10.1016/j.crci.2016.05.013
124. Prodius, D.; Mudring, A.-V. Coord. Chem. Rev. **2018**, *363*, 1. https://doi.org/10.1016/j.ccr.2018.02.004
125. Li, J.; Yang, S.; Wu, W.; Jiang, H. European J. Org. Chem. **2018**, *2018*, 1284. https://doi.org/10.1002/ejoc.201701509
126. Zhang, X.; Pan, L.; Wang, L.; Zou, J.-J. Chem. Eng. Sci. **2018**, *180*, 95. https://doi.org/10.1016/j.ces.2017.11.044
127. Pillai, P.; Pal, N.; Mandal, A. J. Surfactants Deterg. **2017**, *20*, 1321. https://doi.org/10.1007/s11743-017-2021-1
128. Xue, Z.; Qin, L.; Jiang, J.; Mu, T.; Gao, G. Phys. Chem. Chem. Phys. **2018**, *20*, 8382. https://doi.org/10.1039/C7CP07483B
129. Hou, Y.; Gu, Y.; Zhang, S.; Yang, F.; Ding, H.; Shan, Y. J. Mol. Liq. **2008**, *143*, 154. https://doi.org/10.1016/j.molliq.2008.07.009
130. Flieger, J.; Flieger, M. Int. J. Mol. Sci. **2020**, *21*, 6267. https://doi.org/10.3390/ijms21176267
131. Rezaee Nezhad, E.; Sajjadifar, S.; Heidarizadeh, F.; Karimian, S. Arab. J. Chem. **2019**, *12*, 2098. https://doi.org/10.1016/j.arabjc.2014.12.037
132. Vekariya, R. L. J. Mol. Liq. **2017**, *227*, 44. https://doi.org/10.1016/j.molliq.2016.11.123
133. Wu, D.; Cai, P.; Zhao, X.; Kong, Y.; Pan, Y. J. Sep. Sci. **2018**, *41*, 373. https://doi.org/10.1002/jssc.201700848
134. Gaikwad, D. S.; Undale, K. A.; Patravale, A. A.; Choudhari, P. B. Res. Chem. Intermed. **2020**, *46*, 621. https://doi.org/10.1007/s11164-019-03981-3
135. Hannon, M. J. Chem. Soc. Rev. **2007**, *36*, 280. https://doi.org/10.1039/B606046N
136. MacMillan, A. M. Pure Appl. Chem. **2004**, *76*, 1521.
137. Zhang, R.; Wu, X.; Yalowich, J. C.; Hasinoff, B. B. Bioorg. Med. Chem. **2011**, *19*, 7023. https://doi.org/10.1016/j.bmc.2011.10.012
138. Diana, P.; Carbone, A.; Barraja, P.; Montalbano, A.; Martorana, A.; Dattolo, G.; Gia, O.; Via, L. D.; Cirrincione, G. Bioorg. Med. Chem. Lett. **2007**, *17*, 2342. https://doi.org/10.1016/j.bmcl.2007.01.065
139. Wu, M.; Sun, Q.; Yang, C.; Chen, D.; Ding, J.; Chen, Y.; Lin, L.; Xie, Y. Bioorg. Med. Chem. Lett. **2007**, *17*, 869. https://doi.org/10.1016/j.bmcl.2006.11.060
140. Busch, B. B.; Stevens, W. C.; Martin, R.; Ordentlich, P.; Zhou, S.; Sapp, D. W.; Horlick, R. A.; Mohan, R. J. Med. Chem. **2004**, *47*, 5593. https://doi.org/10.1021/jm049334f
141. Asbury, R.; Blessing, J. A.; Moore, D. Am. J. Clin. Oncol. **1996**, *19*, 400. https://doi.org/10.1097/00000421-199608000-00017

 ©AUTHOR(S)

142. Engstrom, P. F.; Ryan, L. M.; Falkson, G.; Haller, D. G. Am. J. Clin. Oncol. **1991**, *14*, 33. https://doi.org/10.1097/00000421-199102000-00007
143. Kumar, D.; Maruthi Kumar, N.; Chang, K.-H.; Shah, K. Eur. J. Med. Chem. **2010**, *45*, 4664. https://doi.org/10.1016/j.ejmech.2010.07.023
144. García Prado, E.; García Gimenez, M. D.; De la Puerta Vázquez, R.; Espartero Sánchez, J. L.; Sáenz Rodríguez, M. T. Phytomedicine **2007**, *14*, 280. https://doi.org/10.1016/j.phymed.2006.12.023
145. Cao, X.-F.; Wang, J.-S.; Wang, X.-B.; Luo, J.; Wang, H.-Y.; Kong, L.-Y. Phytochemistry **2013**, *96*, 389. https://doi.org/10.1016/j.phytochem.2013.10.002
146. Liang, J.-H.; Luan, Z.-L.; Tian, X.-G.; Zhao, W.-Y.; Wang, Y.-L.; Sun, C.-P.; Huo, X.-K.; Deng, S.; Zhang, B.-J.; Zhang, Z.-J.; Ma, X.-C. J. Nat. Prod. **2019**, *82*, 3302. https://doi.org/10.1021/acs.jnatprod.9b00532
147. Fan, L.; Huang, X.-J.; Fan, C.-L.; Li, G.-Q.; Wu, Z.-L.; Li, S.-G.; He, Z.-D.; Wang, Y.; Ye, W.-C. Nat. Prod. Commun. **2015**, *10*, 2087. https://doi.org/10.1177/1934578X1501001218
148. Kitajima, M.; Ohara, S.; Kogure, N.; Wu, Y.; Zhang, R.; Takayama, H. Heterocycles **2012**, *85*, 1949. https://doi.org/10.3987/COM-12-12511
149. Eichhorst, A.; Gallhof, M.; Voss, A.; Sekora, A.; Eggers, L.; Huyen, L. T.; Junghanss, C.; Murua Escobar, H.; Brasholz, M. ChemMedChem **2022**, *17*, e202200162. DOI: https://doi.org/10.1002/cmdc.202200162
150. von Drathen, T.; Hoffmann, F.; Brasholz, M. Chem. – A Eur. J. **2018**, *24*, 10253. https://doi.org/10.1002/chem.201801882
151. Frahm, M.; von Drathen, T.; Gronbach, L. M.; Voss, A.; Lorenz, F.; Bresien, J.; Villinger, A.; Hoffmann, F.; Brasholz, M. Angew. Chemie Int. Ed. **2020**, *59*, 12450. https://doi.org/10.1002/anie.202007549
152. Liu, B.; Zhou, H.; Tan, L.; Siu, K. T. H.; Guan, X.-Y. Signal Transduct. Target. Ther. **2024**, *9*, 175. https://doi.org/10.1038/s41392-024-01856-7
153. Debela, D. T.; Muzazu, S. G.; Heraro, K. D.; Ndalama, M. T.; Mesele, B. W.; Haile, D. C.; Kitui, S. K.; Manyazewal, T. SAGE Open Med. **2021**, *9*, 20503121211034370. https://doi.org/10.1177/20503121211034366
154. Al-Wahaibi, L. H.; Abou-Zied, H. A.; Abdelrahman, M. H.; Morcoss, M. M.; Trembleau, L.; Youssif, B. G. M.; Bräse, S. Front. Chem. **2024**, *12*, 1432920. https://doi.org/10.3389/fchem.2024.1432920
155. El-Sherief, H. A. M.; Youssif, B. G. M.; Abbas Bukhari, S. N.; Abdelazeem, A. H.; Abdel-Aziz, M.; Abdel-Rahman, H. M. Eur. J. Med. Chem. **2018**, *156*, 774. https://doi.org/10.1016/j.ejmech.2018.07.024
156. Mahmoud, E.; Abdelhamid, D.; Mohammed, A. F.; Almarhoon, Z. M.; Bräse, S.; Youssif, B. G. M.; Hayallah, A. M.; Abdel-Aziz, M. Pharmaceuticals **2025**, *18*, 275. https://doi.org/10.3390/ph18020275
157. Wang, X.-H.; Wang, X.; Liang, Y.; Shi, Z.; Zhang, J.; Chen, L.; Fu, L. Chin. J. Cancer **2010**, *29*, 980. https://doi.org/10.5732/cjc.010.10309
158. Kokura, S.; Yoshida, N.; Sakamoto, N.; Ishikawa, T.; Takagi, T.; Higashihara, H.; Nakabe, N.; Handa, O.; Naito, Y.; Yoshikawa, T. Cancer Lett. **2005**, *229*, 223. https://doi.org/10.1016/j.canlet.2005.06.039

 ©**AUTHOR(S)**

159. Baba, M.; Jin, Y.; Mizuno, A.; Suzuki, H.; Okada, Y.; Takasuka, N.; Tokuda, H.; Nishino, H.; Okuyama, T. Biol. Pharm. Bull. **2002**, *25*, 244. https://doi.org/10.1248/bpb.25.244
160. Murakami, A.; Kuki, W.; Takahashi, Y.; Yonei, H.; Nakamura, Y.; Ohto, Y.; Ohigashi, H.; Koshimizu, K. Japanese J. Cancer Res. **1997**, *88*, 443. https://doi.org/10.1111/j.1349-7006.1997.tb00402
161. Liang, C.; Jiang, H.; Zhou, Z.; Lei, D.; Xue, Y.; Yao, Q. Molecules **2012**, *17*, 14146. https://doi.org/10.3390/molecules171214146
162. Hopkins, A. L.; Groom, C. R. Nat. Rev. Drug Discov. **2002**, *1*, 727. https://doi.org/10.1038/nrd892
163. Lipinski, C. A. J. Pharmacol. Toxicol. Methods **2000**, *44*, 235. https://doi.org/10.1016/S1056-8719(00)00107-6
164. Reck, F.; Zhou, F.; Girardot, M.; Kern, G.; Eyermann, C. J.; Hales, N. J.; Ramsay, R. R.; Gravestock, M. B. J. Med. Chem. **2005**, *48*, 499. https://doi.org/10.1021/jm0400810
165. Li, W.-T.; Wu, W.-H.; Tang, C.-H.; Tai, R.; Chen, S.-T. ACS Comb. Sci. **2011**, *13*, 72. https://doi.org/10.1021/co1000234
166. Kamath, P. R.; Sunil, D.; Ajees, A. A. Res. Chem. Intermed. **2016**, *42*, 5899. https://doi.org/10.1007/s11164-015-2412-8
167. Yang, M.-Y.; Zhao, W.; Sun, Z.-H.; Tan, C.-X.; Weng, J.-Q.; Liu, X.-H. Lett. Drug Des. Discov. **2015**, *12*, 314. https://doi.org/10.2174/1570180811666141010000435
168. Rashdan, H. R. M.; Gomha, S. M.; El-Gendey, M. S.; El-Hashash, M. A.; Soliman, A. M. M. Green Chem. Lett. Rev. **2018**, *11*, 264. https://doi.org/10.1080/17518253.2018.1474270
169. Rashdan, H. R. M.; Farag, M. M.; El-Gendey, M. S.; Mounier, M. M. Molecules **2019**, *24*, 2371. https://doi.org/10.3390/molecules24132371
170. Merisko-Liversidge, E.; Liversidge, G. G.; Cooper, E. R. Eur. J. Pharm. Sci. **2003**, *18*, 113. https://doi.org/10.1016/S0928-0987(02)00251-8
171. Ren, Y.; Zhou, L.; Li, X. Front. Chem. **2021**, *9*, 807433. https://doi.org/10.3389/fchem.2021.807433
172. Gobec, M.; Kljun, J.; Sosič, I.; Mlinarič-Raščan, I.; Uršič, M.; Gobec, S.; Turel, I. Dalt. Trans. **2014**, *43*, 9045. https://doi.org/10.1039/C4DT00463A
173. Zhai, S.; Yang, L.; Cui, Q. C.; Sun, Y.; Dou, Q. P.; Yan, B. JBIC J. Biol. Inorg. Chem. **2010**, *15*, 259. https://doi.org/10.1007/s00775-009-0594-5
174. Chen, D.; Cui, Q. C.; Yang, H.; Barrea, R. A.; Sarkar, F. H.; Sheng, S.; Yan, B.; Reddy, G. P. V.; Dou, Q. P. Cancer Res. **2007**, *67*, 1636. https://doi.org/10.1158/0008-5472.CAN-06-3546
175. Mayeux, R. NeuroRX **2004**, *1*, 182. https://doi.org/10.1602/neurorx.1.2.182
176. Sahana, S.; Mishra, G.; Sivakumar, S.; Bharadwaj, P. K. Dalt. Trans. **2015**, *44*, 20139. https://doi.org/10.1039/C5DT03719K
177. Chhabra, M.; Babu, L. T.; Mondal, A.; Sun, H.; Paira, P. ChemistrySelect **2017**, *2*, 2480. https://doi.org/10.1002/slct.201700066
178. Dofe, V. S.; Sarkate, A. P.; Azad, R.; Gill, C. H. Res. Chem. Intermed. **2017**, *43*, 7331.

 ©**AUTHOR(S)**

https://doi.org/10.1007/s11164-017-3078-1
179. Wan, Y.; Wu, S.; Xiao, G.; Liu, T.; Hou, X.; Chen, C.; Guan, P.; Yang, X.; Fang, H. Bioorg. Med. Chem. **2015**, *23*, 1994. https://doi.org/10.1016/j.bmc.2015.03.024
180. Dofe, V. S.; Sarkate, A. P.; Azad, R.; Gill, C. H. Res. Chem. Intermed. **2018**, *44*, 1149. https://doi.org/10.1007/s11164-017-3157-3
181. Abbass, E. M.; Khalil, A. K.; El-Naggar, A. M. J. Heterocycl. Chem. **2020**, *57*, 1154. https://doi.org/10.1002/jhet.3852
182. Shao, J.; Li, Y.; Wang, Z.; Xiao, M.; Yin, P.; Lu, Y.; Qian, X.; Xu, Y.; Liu, J. Int. Immunopharmacol. **2013**, *17*, 216. https://doi.org/10.1016/j.intimp.2013.06.008
183. Wang, X.; Chen, Z.; Tong, L.; Tan, S.; Zhou, W.; Peng, T.; Han, K.; Ding, J.; Xie, H.; Xu, Y. Eur. J. Med. Chem. **2013**, *65*, 477. https://doi.org/10.1016/j.ejmech.2013.05.002
184. Wang, K.; Wang, Y.; Yan, X.; Chen, H.; Ma, G.; Zhang, P.; Li, J.; Li, X.; Zhang, J. Bioorg. Med. Chem. Lett. **2012**, *22*, 937. https://doi.org/10.1016/j.bmcl.2011.12.018
185. Kamath, A.; Ojima, I. Tetrahedron **2012**, *68*, 10640. https://doi.org/10.1016/j.tet.2012.07.090
186. Hosseyni, S.; Jarrahpour, A. Org. Biomol. Chem. **2018**, *16*, 6840. https://doi.org/10.1039/C8OB01833B
187. Mora-Ochomogo, M.; Lohans, C. T. RSC Med. Chem. **2021**, *12*, 1623. https://doi.org/10.1039/D1MD00200G
188. Rad, J. A.; Jarrahpour, A.; Aseman, M. D.; Nabavizadeh, M.; Pournejati, R.; Karbalaei-Heidari, H. R.; Turos, E. ChemistrySelect **2019**, *4*, 2741. https://doi.org/10.1002/slct.201803785
189. SONMEZ, M.; BERBER, I.; AKBAS, E. Eur. J. Med. Chem. **2006**, *41*, 101. https://doi.org/10.1016/j.ejmech.2005.10.003
190. Rizk, S. A.; El-Hashash, M. A.; Youssef, A. A.; Elgendy, A. T. Heliyon **2021**, *7*, e06220. https://doi.org/10.1016/j.heliyon.2021.e06220
191. Simijonović, D.; Petrović, Z. D.; Milovanović, V. M.; Petrović, V. P.; Bogdanović, G. A. RSC Adv. **2018**, *8*, 16663. https://doi.org/10.1039/C8RA02702A
192. Kim, J. S.; Rhee, H.-K.; Park, H. J.; Lee, S. K.; Lee, C.-O.; Park Choo, H.-Y. Bioorg. Med. Chem. **2008**, *16*, 4545. https://doi.org/10.1016/j.bmc.2008.02.049
193. Sumalatha, J.; Radha Rani, C.; Sreedevi, A. J. Heterocycl. Chem. **2018**, *55*, 593. https://doi.org/10.1002/jhet.3066
194. Ngoc Binh, V.; Adorisio, S.; Delfino, D. V; Ngo, Q. A. Nat. Prod. Commun. **2022**, *17*, 1. https://doi.org/10.1177/1934578X221105692
195. Hassan, A. Y.; Sarg, M. T.; Bayoumi, A. H.; El-Deeb, M. A. J. Heterocycl. Chem. **2018**, *55*, 1450. https://doi.org/10.1002/jhet.3184
196. Sztanke, K.; Tuzimski, T.; Rzymowska, J.; Pasternak, K.; Kandefer-Szerszeń, M. Eur. J. Med. Chem. **2008**, *43*, 404.

 ©**AUTHOR(S)**

https://doi.org/10.1016/j.ejmech.2007.03.033
197. El Rabeeb, S. I.; El Deeb, M. A.; Sarg, M. T.; Hassan, A. Y. J. Heterocycl. Chem. **2022**, *59*, 2207. https://doi.org/10.1002/jhet.4552
198. Hassan, A. Y.; Sarg, M. T.; El Deeb, M. A.; El Rabeeb, S. I. ChemistrySelect **2020**, *5*, 4755. https://doi.org/10.1002/slct.201904624
199. Fascio, M. L.; Errea, M. I.; D'Accorso, N. B. Eur. J. Med. Chem. **2015**, *90*, 666. https://doi.org/10.1016/j.ejmech.2014.12.012
200. Bunev, A. S.; Naumov, S. V; Statsyuk, V. E.; Purygin, P. P. Chem. Heterocycl. Compd. **2012**, *48*, 1415. https://doi.org/10.1007/s10593-012-1152-6
201. Aouali, M.; Allouche, F.; Zouari, I.; Mhalla, D.; Trigui, M.; Chabchoub, F. Synth. Commun. **2014**, *44*, 748. https://doi.org/10.1080/00397911.2013.804576
202. Sadek, K. U.; Abdel-Hameed, A. M.; Abdelnabi, H. A.; Meleigy, Y. Green Process. Synth. **2019**, *8*, 297. https://doi.org/10.1515/gps-2018-0093
203. Burke, M. D.; Schreiber, S. L. Angew. Chemie Int. Ed. **2004**, *43*, 46. https://doi.org/10.1002/anie.200300626
204. Spandl, R. J.; Bender, A.; Spring, D. R. Org. Biomol. Chem. **2008**, *6*, 1149. https://doi.org/10.1039/b719372f
205. Schreiber, S. L. Nature **2009**, *457*, 153. https://doi.org/10.1038/457153a
206. Bon, R. S.; Waldmann, H. Acc. Chem. Res. **2010**, *43*, 1103. https://doi.org/10.1021/ar100014h
207. Wetzel, S.; Bon, R. S.; Kumar, K.; Waldmann, H. Angew. Chem. Int. Ed. **2011**, *50*, 10800. https://doi.org/10.1002/anie.201007004
208. Dhinakaran, I.; Padmini, V.; Ganesan, K.; Selvarasu, K. ChemistrySelect **2017**, *2*, 6154. https://doi.org/10.1002/slct.201700819
209. Spring, D. R. Org. Biomol. Chem. **2003**, *1*, 3867. https://doi.org/10.1039/b310752n
210. Tu, S.-J.; Gao, Y.; Guo, C.; Shi, D.; Lu, Z. Synth. Commun. **2002**, *32*, 2137. https://doi.org/10.1081/SCC-120005420
211. Rong, L.; Li, X.; Wang, H.; Shi, D.; Tu, S.; Zhuang, Q. Synth. Commun. **2006**, *36*, 2363. https://doi.org/10.1080/00397910600640230
212. Bhaskaruni, S. V. H. S.; Maddila, S.; van Zyl, W. E.; Jonnalagadda, S. B. RSC Adv. **2018**, *8*, 16336. https://doi.org/10.1039/C8RA01994K
213. Abdollahi-Alibeik, M.; Moaddeli, A.; Masoomi, K. RSC Adv. **2015**, *5*, 74932. https://doi.org/10.1039/C5RA11343A
214. Yang, S.; Shen, L.; Kim, Y.-J.; Jeong, J.-H. Org. Biomol. Chem. **2016**, *14*, 623. https://doi.org/10.1039/C5OB01656H
215. Aliabadi, R. S.; Mahmoodi, N. O. RSC Adv. **2016**, *6*, 85877. https://doi.org/10.1039/C6RA17594E
216. Guo, R.-Y.; An, Z.-M.; Mo, L.-P.; Yang, S.-T.; Liu, H.-X.; Wang, S.-X.; Zhang, Z.-H. Tetrahedron **2013**, *69*, 9931. https://doi.org/10.1016/j.tet.2013.09.082
217. Bora, P. P.; Bihani, M.; Bez, G. J. Mol. Catal. B Enzym. **2013**, *92*, 24. https://doi.org/10.1016/j.molcatb.2013.03.015

 ©**AUTHOR(S)**

218. Tamaddon, F.; Alizadeh, M. Tetrahedron Lett. **2014**, *55*, 3588. https://doi.org/10.1016/j.tetlet.2014.04.122
219. Abdel Hamid, A.; Abd-Elmonem, M.; Hayallah, A. M.; Abo Elsoud, F. A.; Sadek, K. U. ChemistrySelect **2017**, *2*, 10689. https://doi.org/10.1002/slct.201702011
220. Van Aken, K.; Strekowski, L.; Patiny, L. Beilstein J. Org. Chem. **2006**, *2*, 1. https://doi.org/10.1186/1860-5397-2-3
221. Shukla, P.; Sharma, A.; Fageria, L.; Chowdhury, R. Curr. Bioact. Compd. **2019**, *15*, 257. https://doi.org/10.2174/1573407213666170828165512
222. Sharma, A.; Chowdhury, R.; Dash, S.; Pallavi, B.; Shukla, P. Curr. Microw. Chem. **2015**, *3*, 78. https://doi.org/10.2174/2213335602666150116233238
223. Mohamed, N. R.; Khaireldin, N. Y.; Fahmyb, A. F.; El-Sayeda, A. A. F. Der Pharma Chem **2010**, *2*, 400.
224. Parikh, P. H.; Timaniya, J. B.; Patel, M. J.; Patel, K. P. J. Mol. Struct. **2022**, *1249*, 131605. https://doi.org/10.1016/j.molstruc.2021.131605
225. Sun, X.; Zhang, L.; Gao, M.; Que, X.; Zhou, C.; Zhu, D.; Cai, Y. Molecules **2019**, *24*, 624. https://doi.org/10.3390/molecules24030624
226. Nimbalkar, U.; Seijas, J.; Vazquez-Tato, M.; Damale, M.; Sangshetti, J.; Nikalje, A. Molecules **2017**, *22*, 1628. https://doi.org/10.3390/molecules22101628
227. Arya, K. R.; Rajendra Prasad, K. J. Synth. Commun. **2018**, *48*, 1465. https://doi.org/10.1080/00397911.2018.1455211
228. Murali, K.; Sparkes, H. A.; Pandiyan, B. V.; Rajendra Prasad, K. J. New J. Chem. **2017**, *41*, 8242. https://doi.org/10.1039/C7NJ00643H
229. Indumathi, T.; Rajendra Prasad, K. J. Med. Chem. Res. **2014**, *23*, 4345. https://doi.org/10.1007/s00044-014-0999-8
230. Li, B.; Yue, Z.-Z.; Feng, J.-M.; He, Q.; Miao, Z.-H.; Yang, C.-H. Eur. J. Med. Chem. **2013**, *66*, 531. https://doi.org/10.1016/j.ejmech.2013.05.045
231. Saravanabhavan, M.; Murugesan, V.; Sekar, M. J. Photochem. Photobiol. B Biol. **2014**, *133*, 145. https://doi.org/10.1016/j.jphotobiol.2014.02.020
232. Starčević, K.; Kralj, M.; Piantanida, I.; Šuman, L.; Pavelić, K.; Karminski-Zamola, G. Eur. J. Med. Chem. **2006**, *41*, 925. https://doi.org/10.1016/j.ejmech.2006.03.012
233. Wang, Y. D.; Johnson, S.; Powell, D.; McGinnis, J. P.; Miranda, M.; Rabindran, S. K. Bioorg. Med. Chem. Lett. **2005**, *15*, 3763. https://doi.org/10.1016/j.bmcl.2005.05.127
234. Newman, D. J.; Cragg, G. M.; Snader, K. M. J. Nat. Prod. **2003**, *66*, 1022. https://doi.org/10.1021/np030096l
235. Breinbauer, R.; Vetter, I. R.; Waldmann, H. Angew. Chem. Int. Ed. **2002**, *41*, 2878. https://doi.org/10.1002/1521-3773(20020816)41:16<2878::AID-ANIE2878>3.0.CO;2-B
236. Magedov, I. V; Manpadi, M.; Rozhkova, E.; Przheval'skii, N. M.; Rogelj, S.; Shors, S. T.; Steelant, W. F. A.; Slambrouck, S. Van; Kornienko, A. Bioorg. Med. Chem. Lett. **2007**, *17*, 1381. https://doi.org/10.1016/j.bmcl.2006.11.095
237. Magedov, I. V; Manpadi, M.; Van slambrouck, S.; Steelant, W. F. A.; Rozhkova, E.; Przheval'skii, N. M.; Rogelj, S.; Kornienko, A. J. Med. Chem. **2007**, *50*, 5183.

 ©**AUTHOR(S)**

https://doi.org/10.1021/jm070528f
238. Magedov, I. V; Frolova, L.; Manpadi, M.; Bhoga, U. devi; Tang, H.; Evdokimov, N. M.; George, O.; Hadje Georgiou, K.; Renner, S.; Getlik, M.; Kinnibrugh, T. L.; Fernandes, M. A.; Van slambrouck, S.; Steelant, W. F. A.; Shuster, C. B.; Rogelj, S.; van Otterlo, W. A. L.; Kornienko, A. J. Med. Chem. **2011**, *54*, 4234. https://doi.org/10.1021/jm200410r
239. Berkowitz, D. B.; Maeng, J.-H.; Dantzig, A. H.; Shepard, R. L.; Norman, B. H. J. Am. Chem. Soc. **1996**, *118*, 9426. https://doi.org/10.1021/ja961489s
240. Mani, G. S.; Shaik, S. P.; Tangella, Y.; Bale, S.; Godugu, C.; Kamal, A. Org. Biomol. Chem. **2017**, *15*, 6780. https://doi.org/10.1039/C7OB01384A
241. Voynikov, Y.; Momekov, G.; Peikov, P.; Stavrakov, G. Pharmacia **2014**, *61*, 12.
242. Ahmed, F. F.; Abd El-Hafeez, A. A.; Abbas, S. H.; Abdelhamid, D.; Abdel-Aziz, M. Eur. J. Med. Chem. **2018**, *151*, 705. https://doi.org/10.1016/j.ejmech.2018.03.073
243. Abou-Zied, H. A.; Youssif, B. G. M.; Mohamed, M. F. A.; Hayallah, A. M.; Abdel-Aziz, M. Bioorg. Chem. **2019**, *89*, 102997. https://doi.org/10.1016/j.bioorg.2019.102997
244. Chobe, S. S.; Dawane, B. S.; Tumbi, K. M.; Nandekar, P. P.; Sangamwar, A. T. Bioorg. Med. Chem. Lett. **2012**, *22*, 7566. https://doi.org/10.1016/j.bmcl.2012.10.027
245. Singh, S. K.; Clarke, I. D.; Terasaki, M.; Bonn, V. E.; Hawkins, C.; Squire, J.; Dirks, P. B. Cancer Res. **2003**, *63*, 5821.
246. Ricci-Vitiani, L.; Lombardi, D. G.; Pilozzi, E.; Biffoni, M.; Todaro, M.; Peschle, C.; De Maria, R. Nature **2007**, *445*, 111. https://doi.org/10.1038/nature05384
247. Bomken, S.; Fišer, K.; Heidenreich, O.; Vormoor, J. Br. J. Cancer **2010**, *103*, 439. https://doi.org/10.1038/sj.bjc.6605821
248. Afzal, O.; Kumar, S.; Haider, M. R.; Ali, M. R.; Kumar, R.; Jaggi, M.; Bawa, S. Eur. J. Med. Chem. **2015**, *97*, 871. https://doi.org/10.1016/j.ejmech.2014.07.044
249. Belal, A.; El-Gendy, B. E.-D. M. Bioorg. Med. Chem. **2014**, *22*, 46. https://doi.org/10.1016/j.bmc.2013.11.040
250. Ikhiri, K.; Ahond, A.; Poupat, C.; Potier, P.; Pusset, J.; Sévenet, T. J. Nat. Prod. **1987**, *50*, 626. https://doi.org/10.1021/np50052a008
251. Tseng, C.-H.; Chen, Y.-R.; Tzeng, C.-C.; Liu, W.; Chou, C.-K.; Chiu, C.-C.; Chen, Y.-L. Eur. J. Med. Chem. **2016**, *108*, 258. https://doi.org/10.1016/j.ejmech.2015.11.031
252. Saravana Mani, K.; Murugesapandian, B.; Kaminsky, W.; Rajendran, S. P. Tetrahedron Lett. **2018**, *59*, 2921. https://doi.org/10.1016/j.tetlet.2018.06.035
253. Arasakumar, T.; Mathusalini, S.; Gopalan, S.; Shyamsivappan, S.; Ata, A.; Mohan, P. S. Bioorg. Med. Chem. Lett. **2017**, *27*, 1538. https://doi.org/10.1016/j.bmcl.2017.02.042
254. Stamos, J.; Sliwkowski, M. X.; Eigenbrot, C. J. Biol. Chem. **2002**, *277*, 46265. https://doi.org/10.1074/jbc.m207135200

 ©**AUTHOR(S)**

255. Grieco, I.; Bassani, D.; Trevisan, L.; Salmaso, V.; Cescon, E.; Prencipe, F.; Da Ros, T.; Martinez-Gonzalez, L.; Martinez, A.; Spalluto, G.; Moro, S.; Federico, S. Bioorg. Chem. **2024**, *151*, 107659. https://doi.org/10.1016/j.bioorg.2024.107659
256. Grieco, I.; Bissaro, M.; Tiz, D. B.; Perez, D. I.; Perez, C.; Martinez, A.; Redenti, S.; Mariotto, E.; Bortolozzi, R.; Viola, G.; Cozza, G.; Spalluto, G.; Moro, S.; Federico, S. Eur. J. Med. Chem. **2021**, *216*, 113331. https://doi.org/10.1016/j.ejmech.2021.113331
257. Gomha, S. M.; Khalil, K. D.; El-Zanaty, A. M.; Riyadh, S. M. Heterocycles **2013**, *87*, 1109. https://doi.org/10.3987/COM-13-12696
258. Faidallah, H. M.; Rostom, S. A. F.; Basaif, S. A.; Makki, M. S. T.; Khan, K. A. Arch. Pharm. Res. **2013**, *36*, 1354. https://doi.org/10.1007/s12272-013-0144-0
259. Demchenko, S. A.; Lozinskii, M. O. Farm. Zh. **2019**, *6*, 20.
260. Hashem, H. E.; Haneen, D. S. A.; Saied, K. F.; Youssef, A. S. A. Synth. Commun. **2019**, *49*, 3169. https://doi.org/10.1080/00397911.2019.1658786
261. Ewida, M. A.; Abou El Ella, D. A.; Lasheen, D. S.; Ewida, H. A.; El-Gazzar, Y. I.; El-Subbagh, H. I. Bioorg. Chem. **2017**, *74*, 228. https://doi.org/10.1016/j.bioorg.2017.08.010
262. Fruit, C.; Turck, A.; Plé, N.; Quéguiner, G. J. Heterocycl. Chem. **2002**, *39*, 1077. https://doi.org/10.1002/jhet.5570390536
263. Ibrahim, H. M.; Behbehani, H. Sci. Rep. **2020**, *10*, 6492. https://doi.org/10.1038/s41598-020-63453-2
264. Behbehani, H.; Ibrahim, H. M. Molecules **2012**, *17*, 6362. https://doi.org/10.3390/molecules17066362
265. Kumar, A.; Sharma, S.; Maurya, R. A.; Sarkar, J. J. Comb. Chem. **2010**, *12*, 20. https://doi.org/10.1021/cc900143h
266. Song, Y.; Yang, Y.; Wu, L.; Dong, N.; Gao, S.; Ji, H.; Du, X.; Liu, B.; Chen, G. Molecules **2017**, *22*, 517. https://doi.org/10.3390/molecules22040517
267. Giri, R.; Goodell, J. R.; Xing, C.; Benoit, A.; Kaur, H.; Hiasa, H.; Ferguson, D. M. Bioorg. Med. Chem. **2010**, *18*, 1456. https://doi.org/10.1016/j.bmc.2010.01.018
268. Shagufta; Ahmad, I. Eur. J. Med. Chem. **2016**, *116*, 267. https://doi.org/10.1016/j.ejmech.2016.03.058
269. Heydari, R.; Shahrekipour, F. Res. Chem. Intermed. **2015**, *41*, 4581. https://doi.org/10.1007/s11164-014-1553-5
270. M. Heravi, M.; Alinejhad, H.; Bakhtiari, K.; Saeedi, M.; A. Oskooie, H.; F. Bamoharram, F. Bull. Chem. Soc. Ethiop. **2011**, *25*, 399. https://doi.org/10.4314/bcse.v25i3.68592
271. Nandi, G. C.; Samai, S.; Kumar, R.; Singh, M. S. Tetrahedron **2009**, *65*, 7129. https://doi.org/10.1016/j.tet.2009.06.024
272. Khurana, J. M.; Magoo, D. Tetrahedron Lett. **2009**, *50*, 4777. https://doi.org/10.1016/j.tetlet.2009.06.029
273. Sumalatha, J.; Sreedevi, A.; Rani, C. R. Asian J. Chem. **2020**, *32*, 923. https://doi.org/10.14233/ajchem.2020.22503
274. Li, L. H.; Wallace, T. L.; Richard, K. A.; Tracey, D. E. Cancer Res. **1985**, *45*, 532.

 ©**AUTHOR(S)**

275. Dandia, A.; Gupta, S. L.; Bhaskaran, S. Eur. Chem. Bull. **2013**, *2*, 836.
276. Sharma, A. K.; Jayakumar, S.; Hundal, M. S.; Mahajan, M. P. J. Chem. Soc. Perkin Trans. 1 **2002**, 774. https://doi.org/10.1039/b109922c
277. Azzam, S. H. S.; Pasha, M. A. Tetrahedron Lett. **2012**, *53*, 7056. https://doi.org/10.1016/j.tetlet.2012.10.056
278. Bhosle, M. R.; Andil, P.; Wahul, D.; Bondle, G. M.; Sarkate, A.; Tiwari, S. V J. Iran. Chem. Soc. **2019**, *16*, 1553. https://doi.org/10.1007/s13738-019-01633-2
279. Palopa, J. A.; Planoa, D.; Morenoa, E.; Sanmartín, C. Arkivoc **2013**, *2014*, 187. https://doi.org/10.3998/ark.5550190.p008.244
280. Guo, X.-N.; Zhong, L.; Tan, J.-Z.; Li, J.; Luo, X.-M.; Jiang, H.-L.; Nan, F.-J.; Lin, L.-P.; Zhang, X.-W.; Ding, J. Cancer Biol. Ther. **2005**, *4*, 1125. https://doi.org/10.4161/cbt.4.10.2024
281. Fares, M.; Abou-Seri, S. M.; Abdel-Aziz, H. A.; Abbas, S. E.-S.; Youssef, M. M.; Eladwy, R. A. Eur. J. Med. Chem. **2014**, *83*, 155. https://doi.org/10.1016/j.ejmech.2014.06.027
282. Kammasud, N.; Boonyarat, C.; Sanphanya, K.; Utsintong, M.; Tsunoda, S.; Sakurai, H.; Saiki, I.; André, I.; Grierson, D. S.; Vajragupta, O. Bioorg. Med. Chem. Lett. **2009**, *19*, 745. https://doi.org/10.1016/j.bmcl.2008.12.023
283. Hayallah, A. M.; Abdel-Hamid, M. K. Der Pharm Chem **2014**, *6*, 45.
284. Mohire, P. P.; Chandam, D. R.; Patravale, A. A.; Choudhari, P.; Karande, V.; Ghosh, J. S.; Deshmukh, M. B. Polycycl. Aromat. Compd. **2022**, *42*, 137. https://doi.org/10.1080/10406638.2020.1720749
285. Xia, J.; Chen, S.-F.; Lv, Y.-P.; Lu, L.-N.; Hu, W.-X.; Zhou, Y.-L. Mol. Med. Rep. **2015**, *11*, 3398. https://doi.org/10.3892/mmr.2015.3160
286. Chen, S.-F.; Xia, J.; Lv, Y.-P.; Liu, J.-L.; LI, W.-X.; YU, X.-P.; HU, W.-X.; Zhou, Y.-L. Oncol. Rep. **2015**, *33*, 1915. https://doi.org/10.3892/or.2015.3803
287. Xu, F.; Yang, Z.; Jiang, J.; Pan, W.; Yang, X.; Wu, J.; Zhu, Y.; Wang, J.; Shou, Q.-Y.; Wu, H. Bioorg. Med. Chem. Lett. **2016**, *26*, 3042. https://doi.org/10.1016/j.bmcl.2016.05.007
288. Serrar, H.; Marmouzi, I.; Benzekri, Z.; Boukhris, S.; Hassikou, A.; Faouzi, M. E. A.; Souizi, A. Lett. Org. Chem. **2017**, *14*, 267. https://doi.org/10.2174/1570178614666170227124523
289. Elattar, K. M.; Abozeid, M. A.; Mousa, I. A.; El-Mekabaty, A. RSC Adv. **2015**, *5*, 106710. https://doi.org/10.1039/C5RA21108E
290. Wagner, E.; Wietrzyk, J.; Psurski, M.; Becan, L.; Turlej, E. ACS Omega **2021**, *6*, 119. https://doi.org/10.1021/acsomega.0c03801
291. Darehkordi, A.; Khorasani, F. N.; Mohammadi, M.; Kazemi, E. Monatshefte für Chemie - Chem. Mon. **2020**, *151*, 1835. https://doi.org/10.1007/s00706-020-02703-5
292. Elgemeie, G. E. H.; Hussain, B. A. W. J. Chem. Res. Synopses **1993**, *3*, 87.
293. Hassan, A. Y.; Shabaan, S. N.; El-Sebaey, S. A.; Abou-Amra, E. S. Sci. Rep. **2023**, *13*, 5585. https://doi.org/10.1038/s41598-023-32421-x

 ©**AUTHOR(S)**

Authors' Biographies



Mohamed Abd-Elmonem was born in *Ghazala*-Dakahlia, Egypt, in 1986. He studied Chemistry at the Faculty of Science- Mansoura University, where he obtained his B.Sc. degree in 2007. He has been entitled as an Ideal Student throughout the faculty of Science- Mansoura University. He received his M.Sc. degree from Faculty of Science, Minia University in 2017 under the supervision of Prof. Dr. Kamal Usef Sadek, working in the field of green organic synthesis for bioactive heterocyclic compounds. In 2023, he received his Ph.D. degree in Green Organic Synthesis for anti-cancer and antimicrobial heterocycles. In addition to his postdoctoral research, he currently serves as Optomization Section Head - Amreyah Cement Company.



Ramadan Ahmed Mekheimer was born in El-Minia, Egypt, on March 9, 1960 and graduated in chemistry with distinction degree at the University of Minia. He received his B.Sc. (1982) degree from Minia University. In 1987-1989, the University of Minia awarded him a channel system program to complete his Ph.D. thesis under the supervision of Prof. Dr. Thomas Kappe in Institute of Organic Chemistry, Karl-Franzens University, Graz, Austria, and he received his Ph.D. (1990) degree from Chemistry Department, Faculty of Science, Minia University. After his Ph.D. degree he take time in establishing his organic synthesis lab. In 1994, the University of Minia awarded him the University Prize designated for the outstanding organic researcher scientist. In 1995, he became Assistant Professor. During a postdoctoral stay in 1997-1998 at the University of Connecticut, Storrs, USA, he joined the group of Professor M. Smith. In 2000, the Academy of Science and Technology, Cairo, Egypt awarded him 'The State's Encouragement National Prize in Organic Chemistry'. Since 2001, he has been a Full Professor of Organic Chemistry at the University of Minia. At the beginning of his career, he was interested in the development of new methodologies for the synthesis of new nitrones, heterocyclic azides and studying their chemical behavior, synthesis of aminoquinolines as antimalaria, and the synthesis of novel fused heterocyclic ring systems, especially those containing pyridine or quinoline nucleus, of biological and pharmacological

 ©AUTHOR(S)

interest. His current research interests include the design of efficient environmentally benign synthetic approaches for the synthesis of potentially bioactive heterocyclic compounds utilizing microwave and ultrasound irradiations and solar energy as energy sources, besides the use of eco-friendly catalysts and solvents (particularly water) in organic synthesis. To date, he has synthesized with his research group more than 600 new organic substances, mainly heterocyclic structures.



Mohamed Hisham Mohamed received his B.Sc. degree in pharmaceutical sciences from Faculty of Pharmacy at Minia University, Egypt (2012). He obtained his M.Sc. (2018) and Ph.D. degrees (2023) in pharmaceutical medicinal chemistry from Faculty of Pharmacy at Minia University, Egypt. He was appointed as an Assistant Professor of pharmaceutical medicinal chemistry at the Faculty of Pharmacy, Deraya University. His research is mainly focused on the design and synthesis of novel organic compounds and testing them for their biological applications. His primary research areas include the development of anti-inflammatory, anticancer, and antimicrobial drug candidates. On the other hand, he is interested in computational chemistry and its medicinal applications to support rational drug design. His ORCID iD is 0000-0002-5467-8939. Currently, he is focused on the design and synthesis of biologically relevant organic compounds and their computational studies.



Afaf Mohamed Abdel Hameed graduated from the Faculty of Science at Minia University (Egypt) in 1995. She received her Ph.D. degree in Organic Chemistry from the Faculty of Science, Minia University (2005). In 2012, she was promoted to Associate Professor of Organic Chemistry at the Faculty of Science, Minia University. Since 2018, she has been a Full Professor of Organic Chemistry at the Faculty of Science, Minia University. Her current research interests include the design of green and environmentally friendly techniques for the synthesis of bioactive heterocyclic compounds.

 ©**AUTHOR(S)**



Kamal Usef Sadek received his B.Sc. degree (honor) in applied chemistry from Assiut University in (1969). He obtained his M.Sc. (1975) and Ph.D. (1978) degrees from Cairo University under the supervision of Prof. Dr. M.H. Elnagdi. He was appointed as a demonstrator of organic chemistry at Minia University (1975), then he was appointed as a lecturer (1980), associate Professor (1985), and Full Professor (1990). In 1987, he was awarded the Alexander von Humboldt fellowship with Prof. Dr. W. Weigrebe in Regensburg University, and he had several study leaves with Prof. M. Rgitz at Kaiserslautern University and Prf. H.H. Otto at Freiburg and Gerifswald Universities. Since 1985 he established his independent research work on heterocyclic synthesis. In 2016, he received Minia University's Appreciation Award in Natural Sciences. Currently, he is focused on green synthesis of biologically relevant heterocycles.

This paper is an open access article distributed under the terms of the Creative Commons Attribution (CC BY) license (http://creativecommons.org/licenses/by/4.0/)